Engineering and biocatalytic applications of methylaspartate ammonia lyase

Raj, Hans

ENGINEERING AND BIOCATALYTIC APPLICATIONS OF METHYLASPARTATE AMMONIA LYASE

Asymmetric synthesis of aspartic acid derivatives

Hans Raj

2013

The research described in this thesis was carried out in the Department of Pharmaceutical Biology (Groningen Research Institute of Pharmacy, University of Groningen, The Netherlands) and was financially supported by the Netherlands Organization of Scientific Research (VENI grant 700.54.401, VIDI grant 700.56.421, ECHO grant 700.59.042), and by the Netherlands Ministry of Economic Affairs and the B-Basic partner organizations (www.b-basic.nl) through B-Basic, a public-private NWO-ACTS programme (ACTS = Advanced Chemical Technologies for Sustainability).

The research work was carried out according to the requirements of the Graduate School of Science, Faculty of Mathematics and Natural Sciences, University of Groningen, The Netherlands.

Printing of this thesis was financially supported by the University Library and the Graduate School of Science, Faculty of Mathematics and Natural Sciences, University of Groningen, The Netherlands.

ISBN: 978-90-367-6455-1 (printed version)

ISBN: 978-90-367-6454-4 (electronic version)

Layout, Cover Design and Printing: Off Page, www.offpage.nl

RIJKSUNIVERSITEIT GRONINGEN

ENGINEERING AND BIOCATALYTIC APPLICATIONS OF METHYLASPARTATE AMMONIA LYASE

Asymmetric synthesis of aspartic acid derivatives

Proefschrift

ter verkrijging van het doctoraat in de
Wiskunde en Natuurwetenschappen
aan de Rijksuniversiteit Groningen
op gezag van de
Rector Magnificus, dr. E. Sterken,
in het openbaar te verdedigen op
vrijdag 11 oktober 2013
om 14:30 uur

door

Hans Raj

geboren op 23 augustus 1980

te Bani, India

Promotores:	Prof. dr. G.J. Poelarends Prof. dr. W.J. Quax
Beoordelingscommissie:	Prof. dr. ir. A.J. Minnaard Prof. dr. A.S.S. Dömling Prof. dr. ir. M.W. Fraaije

"It must be remembered that the purpose of education is not to fill the minds of students with facts…it is to teach them to think."

Robert M. Hutchins

Paranimfen: Naveen Mehta

Harshwardhan Poddar

Table of Contents

Aim and outline of this thesis

Optically pure aspartic acid derivatives are highly valuable as tools for biological research and as chiral building blocks for pharmaceuticals, nutraceuticals, and peptidomimetics. The preparation of these amino acids remains a difficult and laborious task with conventional organic synthesis, and the use of a biocatalytic methodology can be an important and highly competitive alternative option. In recent years, the enzyme methylaspartate ammonia lyase (MAL), which in nature catalyzes the conversion of 3-methylaspartate to ammonia and mesaconate, has gained a lot of interest because of its potential for application in the asymmetric synthesis of substituted aspartic acids. However, the biocatalytic applicability of MAL is limited by its poor diastereoselectivity and narrow substrate scope. Therefore, the aim of the work described in this thesis was to engineer MAL, guided by the crystal structure of the enzyme in complex with its natural substrate, in order to enhance its diastereoselectivity and to broaden its substrate scope, making this lyase more suitable for biocatalytic applications.

In **Chapter 1**, we review the current knowledge on aspartate ammonia lyases and methylaspartate ammonia lyases. The main focus of this chapter is on the three-dimensional structures of these lyases in complex with their natural substrates, their catalytic mechanisms, and the recent progress in the engineering and application of these enzymes to prepare enantiopure L-aspartic acid derivatives.

In **Chapter 2**, we describe the engineering of MAL with the aim to alter its diastereoselectivity. Based on the crystal structure of the enzyme complexed with substrate, the residues Lys-331, His-194 and Gln-329 are suggested to be involved in the formation and stabilization of the enolate anion intermediate. The roles of these active site residues in the diastereoselectivity of the MAL-catalyzed reaction were investigated by using site-directed mutagenesis. Substitutions at these positions resulted in mutant enzymes that show strongly enhanced diastereoselectivity in the amination of mesaconate. It is suggested that the high diastereo- and enantioselectivity of the most active mutant

(H194A) can be exploited for the selective synthesis of the desired *threo* isomers of various 3-substituted aspartic acids.

In **Chapter 3**, we describe the engineering of MAL for the asymmetric synthesis of valuable aspartic acid derivatives. The engineering strategy was based on saturation mutagenesis at carefully chosen sites lining the binding pocket for the substrate's amino or methyl group, with a view to expanding both the nucleophile and electrophile spectrum of MAL. Engineering of the amine-binding pocket yielded a mutant enzyme (Q73A) that exhibits a very broad nucleophile scope in the addition reaction to mesaconate. Engineering of the methyl-binding pocket resulted in a mutant enzyme (L384A) that has a very broad electrophile scope in the ammonia addition reaction. These engineered MALs have exciting potential as biocatalysts for the asymmetric synthesis of a large variety of substituted aspartic acids.

In **Chapter 4**, we report the synthesis of a large variety of *N*-substituted aspartic acids by the addition of structurally diverse amines to fumaric acid, using the Q73A mutant enzyme as biocatalyst. The enzyme-catalyzed addition reactions are highly enantioselective, only yielding the L-enantiomers of the corresponding amino acid products.

In **Chapter 5**, we describe kinetic resolutions and asymmetric synthesis of various 3-substituted aspartic acids using the H194A and H194A\L384A mutant enzymes as biocatalysts. The enzyme-catalyzed reactions are highly stereoselective, which allows the preparation of various 3-substituted aspartic acids with a high diastereo- and enantiomeric excess.

In **Chapter 6**, we describe the roles of active site residues in the catalytic mechanism of MAL. Based on the crystal structure of the enzyme in complex with the natural substrate, the residues that contribute towards substrate binding were selected and subjected to site-directed mutagenesis. The mutant enzymes were characterized for their structural integrity and ability to catalyze the amination of mesaconate. On the basis of the observed properties of the mutant enzymes, we propose a detailed catalytic mechanism for the MAL-catalyzed reaction.

In **Chapter 7**, we report the cloning, recombinant expression and purification of methylaspartate ammonia lyase from the thermophilic bacterium *Carboxydothermus hydrogenoformans* Z-2901. Heat-inactivation assays showed that the purified enzyme is stable at 50°C for several hours. The enzyme shows a broad substrate scope, accepting various substituted amines and fumarates, and displays high regio- and stereoselectivity. This makes this newly identified thermostable MAL an attractive biocatalyst for the asymmetric synthesis of aspartic acid derivatives and a promising target for future engineering experiments.

In **Chapter 8**, the work described in this thesis is summarized, final conclusions are drawn, and suggestions for future work are presented.

Chapter 1

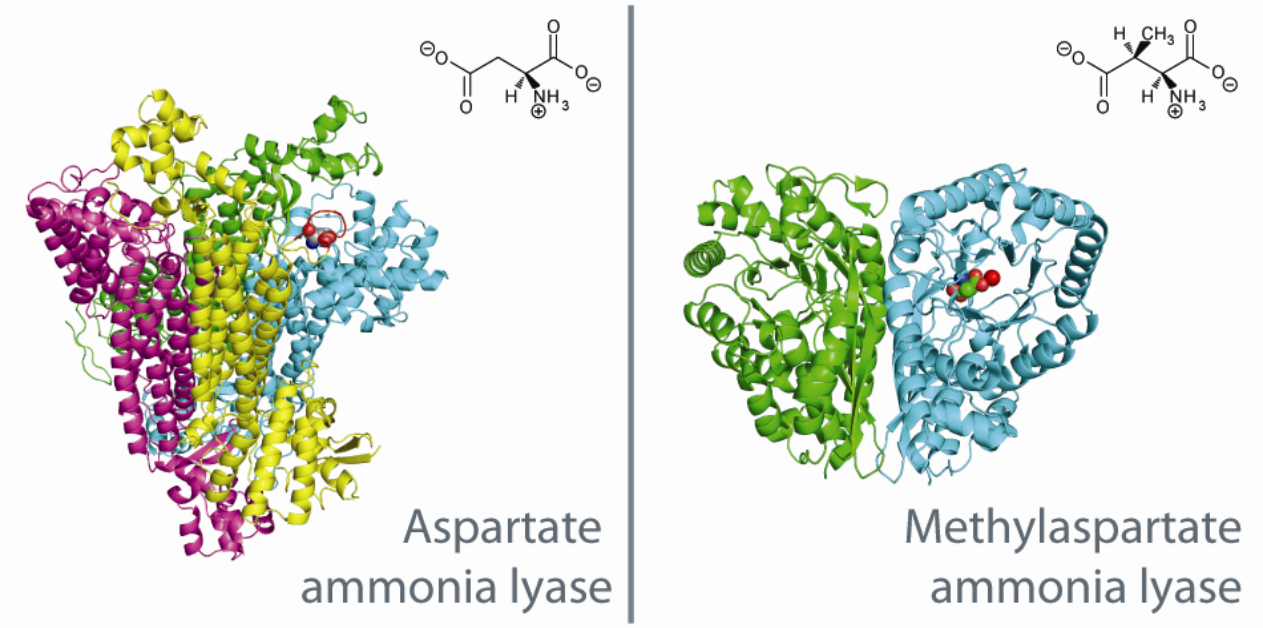

Catalytic mechanisms and biocatalytic applications of aspartate and methylaspartate ammonia lyases

Marianne de Villiers, Vinod Puthan Veetil, **Hans Raj**, Jandré de Villiers, and Gerrit J. Poelarends

Department of Pharmaceutical Biology, Groningen Research Institute of Pharmacy, University of Groningen, Antonius Deusinglaan 1, 9713 AV Groningen, The Netherlands.

Published in *ACS Chemical Biology* (2012) 7, 1618-1628.

ABSTRACT

Ammonia lyases catalyze the formation of α,β-unsaturated bonds by the elimination of ammonia from their substrates. This conceptually straightforward reaction has been the emphasis of many studies, with the main focus on the catalytic mechanism of these enzymes and/or the use of these enzymes as catalysts for the synthesis of enantiomerically pure α-amino acids. In this review aspartate ammonia lyase and 3-methylaspartate ammonia lyase, which represent two different enzyme superfamilies, are discussed in detail. In the last few years, the three-dimensional structures of these lyases in complex with their natural substrates have revealed the details of two elegant catalytic strategies. These strategies exploit similar deamination mechanisms that involve general-base catalyzed formation of an enzyme-stabilized enolate anion (*aci*-carboxylate) intermediate. Recent progress in the engineering and application of these enzymes to prepare enantiopure L-aspartic acid derivatives, which are highly valuable as tools for biological research and as chiral building blocks for pharmaceuticals and food additives, is also discussed.

INTRODUCTION

Ammonia lyases are capable of cleaving carbon-nitrogen bonds without employing hydrolysis or oxidation mechanisms.[1] Various ammonia lyases exist in nature, with three types of lyases specific for aspartate or its derivatives as substrates: aspartate ammonia lyase (aspartase), 3-methylaspartate ammonia lyase (MAL) and 3-hydroxyaspartate ammonia lyase.[1]

Aspartate ammonia lyase (aspartase; EC 4.3.1.1) plays an important role in microbial nitrogen metabolism by catalyzing the reversible deamination of L-aspartate (**1**) to yield fumarate (**2**) and ammonia (Scheme 1A). This enzyme was discovered in the early twentieth century after it was established that bacteria could transform aspartate to succinate.[2, 3] It was shown in 1926 that an equilibrium between L-aspartate, fumarate and ammonia exists in the presence of resting bacterial cells, and further investigation indicated that a deaminase was responsible for the reversible elimination of ammonia from L-aspartate to give fumarate.[4] Since then, extensive investigations have resulted in the identification and characterization of aspartase from various organisms, including *Escherichia coli*, *Pseudomonas fluorescens*, *Hafnia alvei* (formerly known as *Bacterium cadaveris*), *Bacillus subtilis*, and *Bacillus* sp. YM55-1.[5-13]

3-Methylaspartate ammonia lyase (MAL; EC 4.3.1.2) catalyzes the reversible α,β-elimination of ammonia from L-*threo*-3-methylaspartate (**3**) and L-*erythro*-3-methylaspartate (**4**) to yield mesaconate (**5**) (Scheme 1B). MAL activity was first detected by Barker *et al.*[14] in cell-free extracts of the anaerobic bacterium *Clostridium tetanomorphum* H1. In this bacterium, the MAL-catalyzed deamination reaction forms the second step in the catabolic pathway in which L-glutamate is metabolized via L-*threo*-3-methylaspartate to finally yield acetyl-coenzyme A.[14, 15] MAL has subsequently been identified in several other facultative anaerobic organisms, including *Morganella morganii*, *Citrobacter amolonaticus*, *Fusobacterium varium* and *Hafnia alvei*, which form part of the *Enterobacteriaceae* family.[15-19] MAL also forms part of the anabolic methylaspartate cycle in haloarchaea, in which acetyl-CoA is converted to glyoxylate via L-*threo*-3-

methylaspartate.[20] In addition to the MALs that have been isolated and characterized from these sources, there are more than hundred putative MAL sequences available in various databases. Raj *et al*. used one of these sequences to study a MAL from the thermophilic bacterium *Carboxydothermus hydrogenoformans* Z-2901.[21]

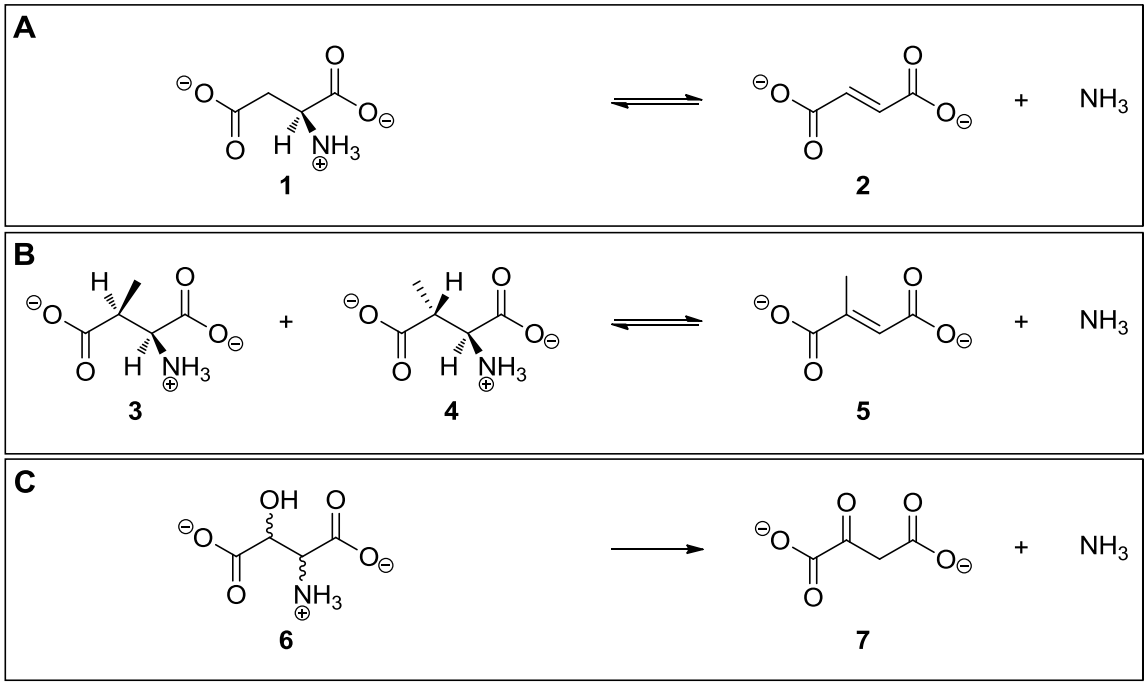

Scheme 1. Reactions catalyzed by ammonia lyases specific for aspartate and its derivatives. (A) Aspartate ammonia lyase catalyzes the reversible deamination of L-aspartate (**1**) to yield fumarate (**2**) and ammonia. (B) 3-Methylaspartate ammonia lyase catalyzes the reversible deamination of L-3-methylaspartate (*threo* isomer **3** and *erythro* isomer **4**) to yield mesaconate (**5**) and ammonia. (C) 3-Hydroxyaspartate ammonia lyases catalyze the deamination of *threo*- or *erythro*-3-hydroxyaspartate (**6**) to yield oxaloacetate (**7**) and ammonia.

Two other enzymes, which are classically known as hydratases, have been classified as ammonia lyases by NC-IUBMB: *threo*-3-hydroxyaspartate ammonia lyase (or *threo*-3-hydroxyaspartate dehydratase, EC 4.3.1.16) and *erythro*-3-hydroxyaspartate ammonia lyase (or *erythro*-3-hydroxyaspartate dehydratase, EC 4.3.1.20).[1] As indicated by their names, these enzymes catalyze the deamination of different epimers (*threo* or *erythro*) of 3-hydroxyaspartate (**6**) to yield oxaloacetate (**7**) and ammonia (Scheme 1C). Furthermore, there are two distinct *threo*-3-

hydroxyaspartate ammonia lyases known which exhibit specificity toward either the D- or L-enantiomer of *threo*-3-hydroxyaspartate. These pyridoxal-phosphate- and divalent cation-dependent enzymes were first identified in the 1960s and are involved in the glycolate and glyoxylate degradative pathways.[22, 23] The first enzyme to be identified was *erythro*-3-hydroxyaspartate dehydratase from *Micrococcus denitrificans* (*Paracoccus denitrificans*).[23, 24] Almost 35 years later L-*threo*-3-hydroxyaspartate dehydratase was identified in *Pseudomonas sp.* T62 and a few years later in *Saccharomyces cerevisiae*.[25, 26] Recently, enzyme activity towards D-*threo*-3-hydroxyaspartate was identified in *Delftia sp.* HT23 and the enzyme was named D-*threo*-3-hydroxyaspartate dehydratase.[27] As these enzymes are classically characterized as hydratases and since limited information is available for them, they will not be further discussed in this review.

ASPARTATE AMMONIA LYASE (ASPARTASE)

Properties and catalytic mechanism

Aspartases have been isolated and characterized from different Gram-negative and Gram-positive bacteria, with the aspartase from *E. coli* (AspA) being the focus of most studies. Originally AspA was isolated in a seven-step purification process from *E. coli* with an overall yield of 20%.[5] As science evolved, the isolation of AspA became easier with the enzyme being overexpressed and purified to homogeneity with a yield of ~100 mg per 10 g of cell pellet.[2] This 52 kDa protein is allosterically activated by L-aspartate and Mg^{2+} ions, which are essential for catalytic activity at alkaline pH.[28-30] AspA shows maximum activity at 55°C and pH 8.0, but prolonged incubation of the enzyme at this temperature resulted in total loss of activity after 30 minutes.[2, 12]

In recent years, aspartase from the thermophilic bacterium *Bacillus* sp. YM55-1 (AspB) has also been in the spotlight due to its possible use as a biocatalyst for amino acid synthesis. The purification of AspB was reported in 1999, and it was the first thermostable aspartase identified and characterized.[12] AspB has similar subunit molecular weight (51 kDa) and oligomeric state as other aspartases from mesophilic organisms, however it is structurally more stable at elevated

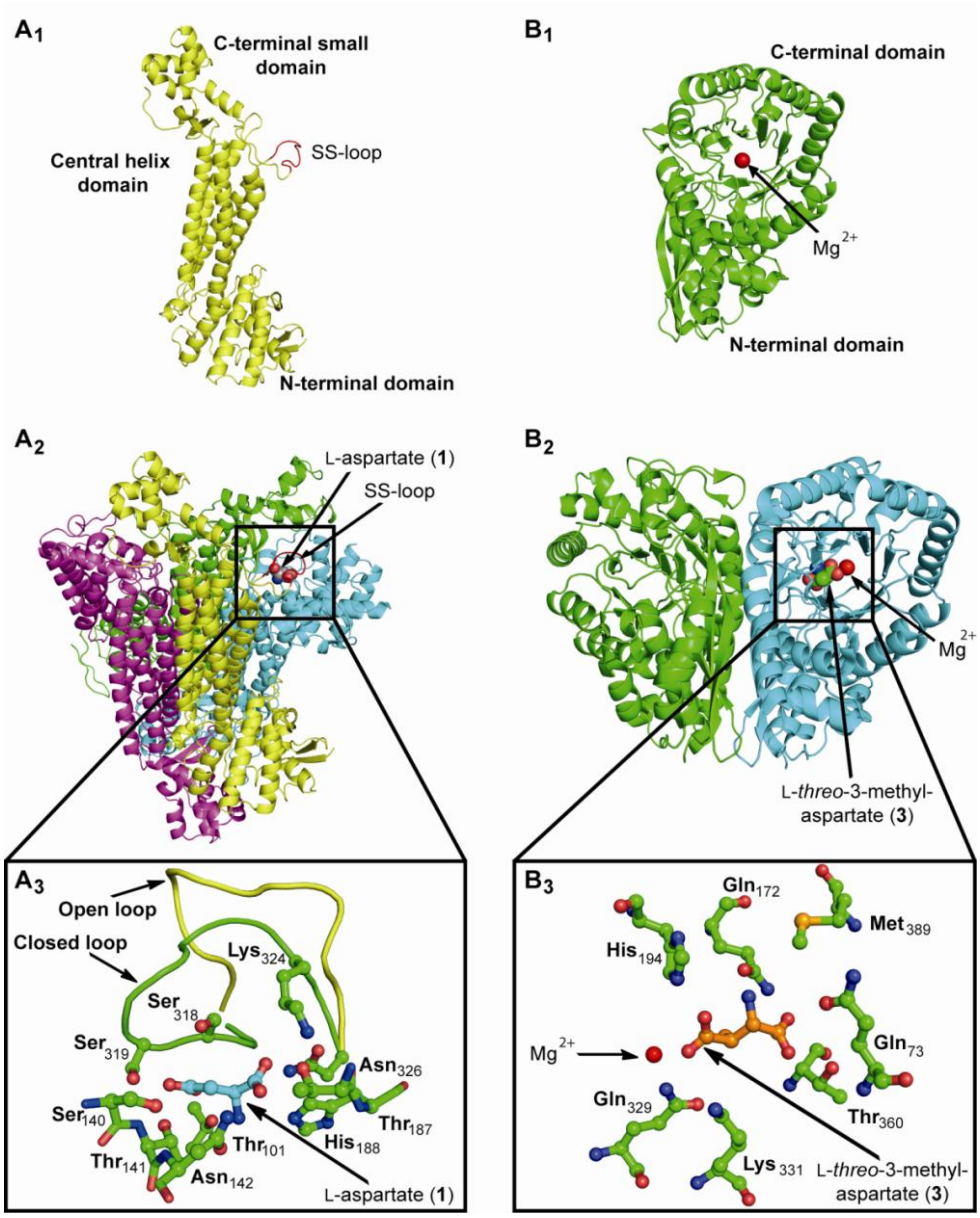

Figure 1. Crystal structures of aspartate and methylaspartate ammonia lyases. A_1) The structure of the AspB monomer.[39] The three domains are labeled and the SS-loop is indicated in red. AspA has a similar structure as shown here for AspB.[31] A_2) Structure of the functional AspB tetramer.[39] The four monomers forming the homotetramer are indicated in magenta, yellow, cyan and green. The location of one of four active sites is indicated by the bound L-aspartate (**1**) molecule, with the SS-loop indicated in red. A_3) A close-up of the active site of AspB in complex with L-aspartate (**1**). The different conformations of the SS-loop are shown, with the closed conformation in green and the open conformation in yellow. The amino acid residues which are most important for substrate binding and catalysis are shown. B_1) Structure of the MAL monomer.[60] The bound Mg^{2+} ion is shown as a red ball. B_2) Structure of the functional MAL homodimer, in complex with Mg^{2+} (red ball) and L-*threo*-3-methylaspartate (**3**).[60] The two monomers are indicated in green and cyan. The location of one of the two active sites is indicated by the bound ligand. B_3) A close-up of the active site of *Ca*MAL in complex with Mg^{2+} (red ball) and L-*threo*-3-methylaspartate (**3**).[60] The amino acid residues which are most important for substrate binding and catalysis are shown.

temperatures as well as in the presence of guanidine hydrochloride.[12] AspB shows maximum activity at 65°C and at pH 8.0.[12] In contrast to its *E. coli* and *P. fluorescence* counterparts, AspB is not allosterically activated by substrate and does not require Mg^{2+} ions for activity at alkaline pH.[12]

The crystal structure of unliganded AspA was elucidated in 1997 to 2.8 Å resolution,[31] and showed that each monomer of AspA contains three structurally distinct domains (Figure $1A_1$). The C-terminal domain is the smallest domain in the subunit and consists mainly of two helix-turn-helix motifs which are orientated approximately 90° relative to each other. The central helix domain is formed from five long α-helices and contains more than half of the total residues of the subunit. Finally, the N-terminal domain consists of a short, two stranded anti-parallel β-sheet followed by five α-helices.[31] AspA belongs to the aspartase/fumarase superfamily, which also includes fumarase C, adenylosuccinate lyase, argininosuccinate lyase, δ-crystallin and 3-carboxy-*cis*-*cis*-muconate lactonizing enzyme.[32-37] The members of the aspartase/fumarase superfamily have a similar active site architecture and share a common tertiary and quaternary fold, although they can show pairwise sequence identities as low as 15%. AspA functions as a homotetramer, which contains four composite active sites, each of which is generated by conserved motifs from three monomers (Figure $1A_2$). A flexible loop of ~10 amino acid residues forms part of one of these conserved motifs with a signature sequence of GSSxxPxKxN. This specific loop, also called the SS-loop, has been shown to be important for substrate binding and catalysis in some of the enzymes of this superfamily.[32, 33, 38, 39]

Kinetic studies have shown that AspA displays non-Michaelis-Menten kinetics for the deamination reaction at high pH, and there is a time lag before the linear steady-state rate is achieved in time-course kinetics for the amination reaction at high pH.[28, 29] From these results it was concluded that AspA is subjected to allosteric activation, in which L-aspartate and Mg^{2+} bind to a separate activator-binding site that is different from the active site. The role of L-aspartate is

therefore two-fold: it acts as substrate and it serves as an activator for AspA. The location of the activator-binding site has not been identified by the crystal structure of unliganded AspA, but Cys430 has been proposed to be located close to the activator-binding site.[28, 31] From the crystal structure of fumarase C, a second binding site was identified and the amino acid residues that form part of this putative activator-binding site include Arg126 and Asn135.[40] A comparison of the crystal structure of AspA with that of fumarase C indicated Gln129 and Asn138, which are found in a short helix segment, as the corresponding residues in AspA.[31]

A general acid-base reaction mechanism was proposed for aspartases as illustrated in Scheme 2A.[2, 11, 31, 41-43] The active site general base abstracts the *pro*-R proton from the C3 position of **1** resulting in a carbanion, which is stabilized as an *aci*-carboxylate intermediate (**8**). This proposed enolate anion intermediate can rearrange to eliminate ammonia and form the product, fumarate (**2**). The rate determining step is the cleavage of the C_{α}-N bond, which may be facilitated by a general acid that donates a proton to the leaving group (NH_3) to form an ammonium ion.[31, 41, 43] Inhibition studies using 3-nitro-2-aminopropionate as inhibitor also supported the formation of an enzyme-stabilized enolate anion (*aci*-carboxylate) as intermediate, since the resonance-stabilized nitronate (*aci*-form) state of this inhibitor binds very tightly to aspartase as a transition state analogue.[44] pH-rate profiles for AspA and the *H. alvei* aspartase differ from each other, thus making it unclear whether the protonation state of the leaving group is that of the ammonia or the ammonium ion.[11, 45] It has been argued that if the amino group is released as ammonia, there might not be the need for a general acid catalyst.[41, 46]

Numerous studies involving site-directed mutagenesis, chemical modification, and mechanism-based inactivation have been done to identify the catalytically important residues of AspA.[2, 47, 48] Until recently, however, several major issues remained unresolved.[39] For example, the identity of the general base catalyst that abstracts the C3 proton, as well as the identity of other catalytic and substrate-binding residues, was still unclear. The question of whether or not substrate binding induces a conformational change that moves other residues into a favorable position in the

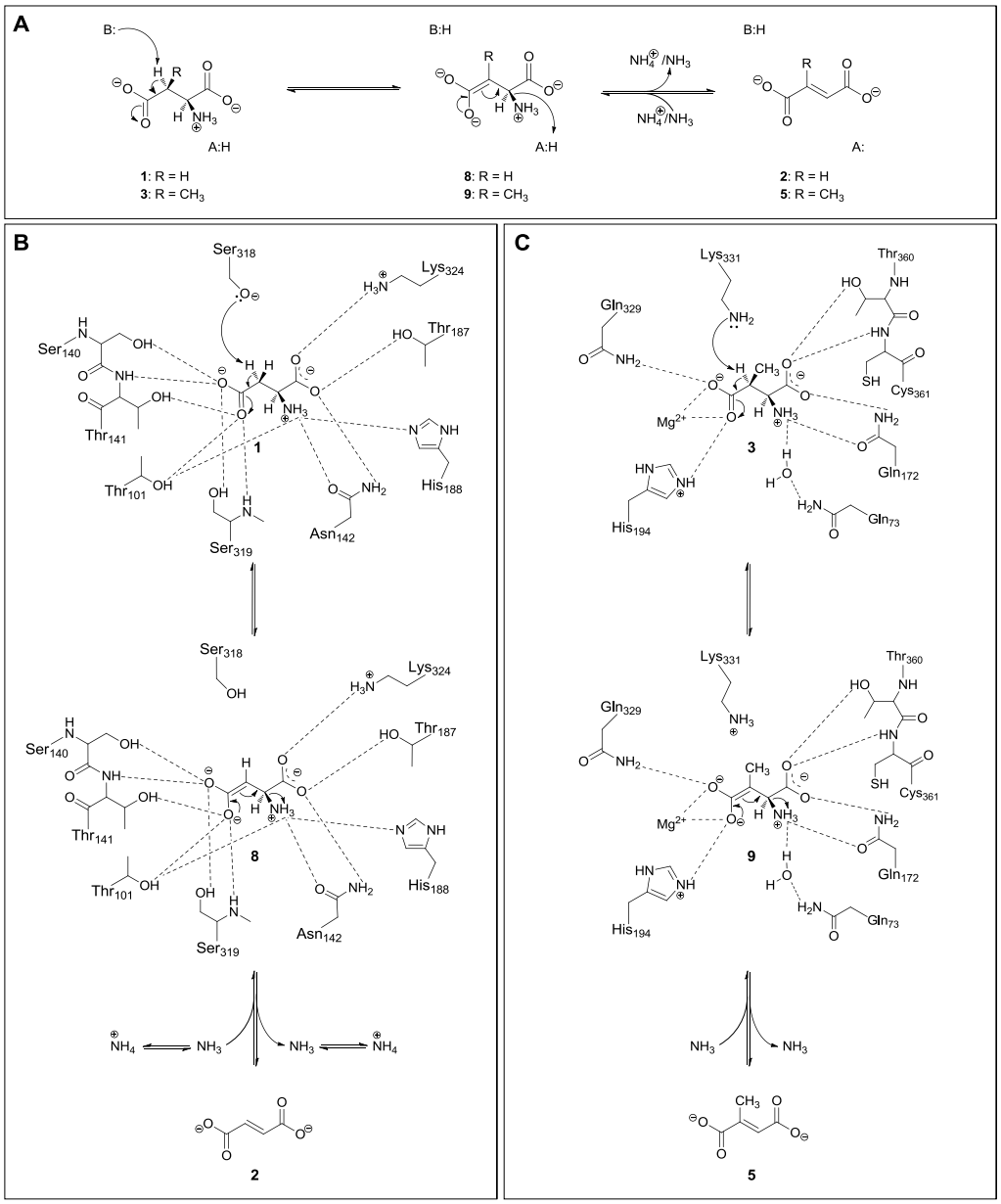

Scheme 2. Schematic representations of the proposed catalytic mechanisms of aspartate and methylaspartate ammonia lyases. (A) Proposed general reaction mechanism for aspartase and metylaspartase. A base in the active site abstracts the proton from the substrate's C3 position. Consequently, a carbanion (enolate anion intermediate) is formed which is stabilized as the aci-acid resonance form. Collapse of the intermediate is followed by C_{α}-N bond cleavage, which results in the elimination of ammonia and may be facilitated by a general acid in some aspartases. (B) Schematic representation of the catalytic mechanism of AspB. Residue Ser318 acts as the catalytic base and abstracts the pro-R proton from the C3 position of 1. The formed enolate anion intermediate (**8**) is stabilized through hydrogen bonding interactions with amino acid residues that line the active site of AspB. The collapse of **8** results in the cleavage of the C_{α}-N bond and the formation of **2** and ammonia. (C) Schematic representation of the catalytic mechanism of MAL. Residue Lys331 acts as the catalytic base and abstracts the C3 proton from **3** to form the enolate anion intermediate **9**. This intermediate is stabilized by interactions with both the Mg^{2+} ion and amino acid residues in the active site. Collapse of the intermediate and C_{α}-N bond cleavage results in **5** and ammonia.

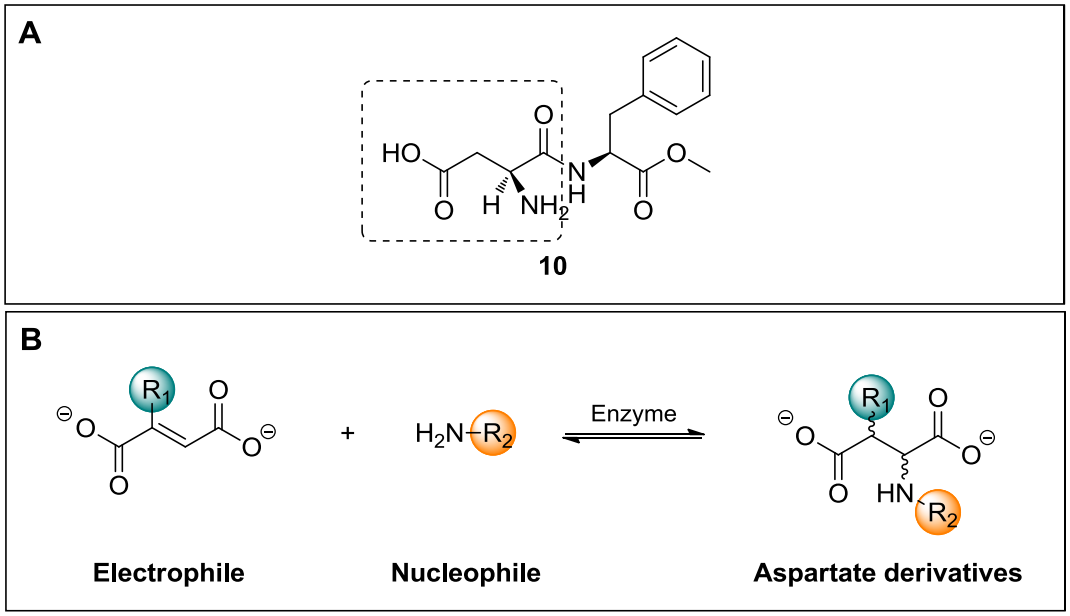

Scheme 3. Biocatalytic preparation of aspartate derivatives. (A) Structure of the artificial sweetener *N*-(L-α-aspartyl)-L-phenylalanine 1-methylester (**10**) with the L-aspartic acid backbone highlighted. (B) Different combinations of electrophiles and nucleophiles are used with aspartase or methylaspartase as biocatalyst to yield various *N*-, 3-, and *N*,3-(di)substituted aspartate derivatives.

active site was also not answered.[39] The structural work on AspA did not address these questions because no crystal structure of AspA in complex with substrate or product was available.[31] In order to resolve these issues recent studies have focused on AspB, since this is a simpler system to work on because of the lack of allosteric activation.[12] In addition, the crystal structure of uncomplexed AspB was already solved at this stage and the location of the putative active site was predicted based on comparisons with AspA and other superfamily members.[49] Manual docking of L-aspartate (**1**) into the putative active site of AspB suggested that the α-carboxylate group of **1** forms hydrogen-bonding interactions with Thr187 and Lys324 (Scheme 2B). On the opposite end of the molecule, the β-carboxylate group forms hydrogen bonds with the hydroxyl groups of Ser140 and Thr141, whereas the amino group of **1** forms hydrogen bonds with the side chains of Thr101, Asn142 and His188.[49] To further verify the role of each residue and to determine the exact mechanism of catalysis, site-directed mutagenesis, pH-rate profile experiments, and inhibition studies were carried out on AspB.[46] Despite all these efforts, the specific residue that acts as

catalytic base in the first step of the proposed mechanism eluded investigators. The SS-loop in the unliganded AspB structure [49] was also highly disordered and therefore its possible role in substrate binding and catalysis was unclear.

Advances in the elucidation of the catalytic mechanism of aspartase were recently achieved by Fibriansah *et al.*[39] They were successful in solving (2.6 Å resolution) the crystal structure of AspB in complex with L-aspartate (**1**) (Figure $1A_{1\text{-}3}$), providing the first detailed view of the substrate-bound active site of an aspartase. This allowed the identification of all active site residues as well as an (improved) understanding of their roles in substrate binding and catalysis (Scheme 2B). Remarkably, AspB forces the bound substrate to adopt a high-energy enolate-like (*aci*-carboxylate-like) conformation that is stabilized by an extensive network of hydrogen bonds between the substrate's β-carboxylate group and residues Thr101, Ser140, Thr141, and Ser319. Furthermore, a large conformational change of the SS-loop takes place from an open conformation in the absence of substrate to one where it closes over the active site in the presence of substrate (Figure $1A_3$). The open conformation of the SS-loop is stabilized by hydrophobic interactions of Ile320 and Met321, which are part of the loop, with a hydrophobic surface patch on the neighboring C-terminal domain. Binding of the substrate is needed in order to close the SS-loop.[39] This conformational change provides additional substrate binding interactions and safeguards the substrate from the solvent during catalysis. As a result the SS-loop, in combination with the C-terminal domain, plays a vital role in the catalytic mechanism of AspB. Most importantly, the closure of the SS-loop positions Ser318 in close proximity to the C3 proton of **1** to enable proton abstraction (Figure $1A_3$ and Scheme 2B). Indeed, mutation of the strictly conserved Ser318 to an alanine resulted in complete loss of AspB activity, suggesting that Ser318 is essential for activity.[39] The exact mechanism by which the intrinsically high pK_a value of Ser318 is lowered to function as a catalytic base is still unclear.

The results of this structural work on AspB[39] thus provide strong support for a catalytic mechanism involving general base-catalyzed formation of the enzyme-stabilized enolate anion intermediate **8** (Scheme 2B). In fact, the highly structured active site environment, the high-energy conformation of the bound substrate, the closed SS-loop conformation, and the extensive hydrogen-bonding network with the β-carboxylate group of the substrate (Scheme 2) show how the active site of aspartase has been optimized for formation and stabilization of the enolate anion (*aci*-carboxylate) intermediate.[39]

Biocatalytic applications

In industry, aspartase is used as biocatalyst for the preparation of enantiopure L-aspartic acid, an important starting compound for the synthesis of artificial sweeteners such as *N*-(L-α-aspartyl)-L-phenylalanine 1-methylester (**10**, Scheme 3A), which is also known as aspartame.[50, 51] Notably, *N*- and 3-substituted derivatives of L-aspartic acid are highly valuable as tools for biological research and as chiral building blocks for a range of pharmaceuticals.[52-54] However, the synthesis of these L-aspartic acid derivatives in enantiopure form remains a major challenge in synthetic chemistry. In principle, the stereo- and regioselective addition of amine nucleophiles to the double bonds of fumarate and its derivatives catalyzed by aspartases appears to be a very attractive strategy for the synthesis of these compounds (Scheme 3B). This strategy, however, is limited by the narrow substrate range of aspartases.[2, 55]

A wide spectrum of compounds (**11-63**, Scheme 4A and 4B) has been tested as potential substrates or inhibitors of AspA.[2, 30, 56] Only L-aspartate-β-semialdehyde (**11**) is deaminated by AspA, but this compound functions as a suicide substrate and its deamination leads to the irreversible inactivation of the enzyme.[2, 56] Compounds **12-31** have been found to act as competitive inhibitors of AspA (Scheme 4A), with all of them containing a carboxylic acid or similarly charged functional group, which seems to be a requirement for enzyme binding.[2, 30] Compounds **32-63** did not act as substrate nor as inhibitor of the enzyme. Some of these compounds

(**57**-**63**; Scheme 4B), as well as additional amino acids (**64**-**76**, Scheme 4C), have also been tested as alternative substrates for AspB in order to determine if this aspartase exhibits a different substrate scope. It was found that AspB displays similar substrate specificity as AspA and does not process these nonnative amino acids.[55]

In 1963 it was reported by Emery that hydroxylamine can be used as an alternative nucleophile in the addition reaction catalyzed by AspA.[57] This observation prompted Weiner and co-workers to test various alternative nucleophiles as potential substrate in the AspB-catalyzed addition reaction.[55] It was found that AspB accepts hydroxylamine, methoxylamine, hydrazine, and methylamine in the addition to fumarate, yielding L-*N*-hydroxyaspartic acid (**77**), L-*N*-methoxyaspartic acid (**78**), L-2-hydrazinosuccinic acid (**79**), and L-*N*-methylaspartic acid (**80**) (Scheme 5). Whereas compounds **78**-**80** could be isolated in excellent yields, compound **77** could not be isolated due to the instability of the compound.[55] Based on the structurally distinct nucleophiles tested, the authors concluded that the nucleophile binding pocket of AspB is designed to bind small amines and excludes any charged or large nucleophiles.[55]

3-METHYLASPARTATE AMMONIA LYASE (MAL)

Properties and catalytic mechanism

The MAL enzyme was purified from cell free extracts of several facultative anaerobic bacteria, and characterized with regard to its biocatalytic properties[14, 16-19] The best studied MALs are those from *C. tetanomorphum* (*Ct*MAL) and *C. amalonaticus* (*Ca*MAL), the corresponding genes of which have been cloned, sequenced, and functionally expressed in *E. coli*.[18, 58] MAL (45 kDa) is a homodimeric protein and depends on divalent (Mg^{2+}) and monovalent (K^{+}) cations for activity.[58-60] The crystal structures of *Ct*MAL[59] and *Ca*MAL[60] revealed that the enzyme is not structurally related to aspartases (Figure $1B_{1\text{-}3}$). Instead, the structures showed that MAL belongs to the enolase superfamily, the members of which share a characteristic TIM barrel fold. The monomer of MAL

has a small N-terminal domain that wraps around the larger C-terminal domain, which is an 8-fold α/β (TIM) barrel (Figure 1B$_1$).[59, 60]

The most recent addition to the library of characterized MALs is MAL from *C. hydrogenoformans* Z-2901 (*Ch*MAL).[21] This organism was isolated from a hot spring in Kunashir Island (Russia) and has an optimal growth temperature of 78°C.[61, 62] The protein (subunit is 46.5 kDa) has a length of 420 amino acids and the sequence is 53% identical and 73% similar to that of *Ct*MAL. The biological function of this protein in *C. hydrogenoformans* is still unknown. Like *Ct*MAL, *Ch*MAL has an optimum pH for activity of 9. However, whereas *Ct*MAL is active from 10-70°C with an optimum temperature for activity of 50°C, *Ch*MAL is active between temperatures of 10-90°C with an optimum temperature for activity of 70°C.[21] The thermostability of the enzymes also varies dramatically. *Ch*MAL has been shown to be stable at 50°C for up to 4 h, retaining >95% of its original activity. In contrast, *Ct*MAL retained only half of its original activity after a 30 minute incubation period at 50°C.[21] This study indicated that *Ch*MAL is the most thermostable MAL purified and characterized to date.

MAL catalyzes the reversible *anti*- and *syn*-addition of ammonia to mesaconate (**5**) to give L-*threo*-(2*S*,3*S*)-3-methylaspartate (**3**) as major product and L-*erythro*-(2*S*,3*R*)-3-methylaspartate (**4**) as minor product, respectively (Scheme 1B). The mechanism of action has been debated over the last ~50 years with various studies aiming to demonstrate the deamination mechanism of MAL.[63-69] Early investigations postulated that MAL catalyzes the deamination reaction through a carbanion mechanism similar to aspartase (Scheme 2A), with cleavage of the C_α-N bond as the rate-limiting step.[63, 64] This hypothesis was supported by the fact that C3 hydrogen-exchange with solvent occurs more rapidly than cleavage of the C_α-N bond. Also, the C3-deuterated substrate **3** used to perform this hydrogen-exchange experiment did not give any primary isotope effect in the deamination reaction.[63, 64]

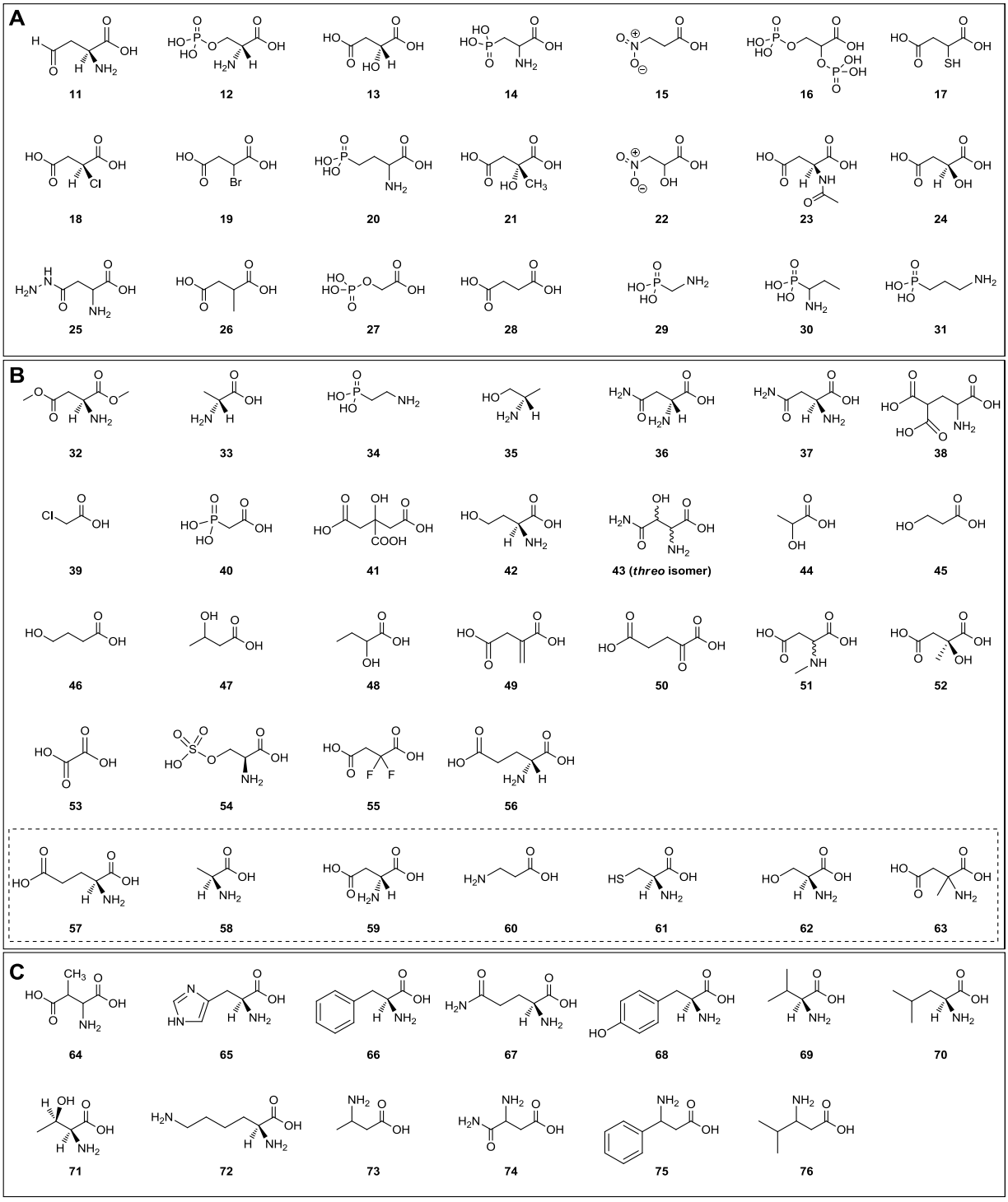

Scheme 4. Compounds investigated as potential inhibitors or substrates for aspartase. (A) L-aspartate-*β*-semialdehyde (**11**) acts as a suicide substrate for AspA.[56] Compounds **12-31** were shown to act as competitive inhibitors of AspA.[2, 30] (B) Compounds **32-63** were shown not to act as competitive inhibitors nor as alternative substrates for AspA.[30] Compounds **57-63** in the dashed box have also been tested on AspB, but were also not accepted as substrates by this enzyme.[55] (C) Compounds **64-76** were shown not to be accepted as alternative substrates by AspB.[55]

Other studies have questioned this carbanion mechanism by suggesting that MAL is mechanistically similar to phenylalanine ammonia lyase (PAL) and histidine ammonia lyase (HAL), and may catalyze the reaction via a covalent enzyme-substrate complex which utilizes an electrophilic dehydroalanine prosthetic group.[58, 69, 70] MAL is irreversible inactivated by *N*-ethylmaleimide and phenylhydrazines, and substrate protects the enzyme from inactivation by these compounds. On the basis of these findings, combined with sequence analysis, it has been suggested that post-translational dehydration of an active site serine (Ser173) may be the origin of this prosthetic group.[58, 69, 70] However, it was later discovered that PAL and HAL do not form a dehydroalanine group through post-translational dehydration, but instead form a MIO-group (4-methylene imidazole-1-one) by cyclization and elimination of water in the active site tripeptide Ala-Ser-Gly.[71, 72] The crystal structures of uncomplexed *Ct*MAL and *Ca*MAL in complex with the natural substrate **3** were reported in 2002 and proved to be essential for the determination of the exact mechanism of the enzyme.[59, 60] It was clear from the structures that MAL is not structurally related to HAL or PAL, and electron density maps did not indicate posttranslational modification of any active site residues. Instead, MAL shows structural homology to the enolase superfamily, the members of which share a common mechanism that involves the general-base catalyzed formation of an enolate anion (*aci*-carboxylate) intermediate. The MAL-substrate complex structure,[60] in combination with structural alignment of MAL with other members of the enolase superfamily,[59] suggested that Lys331 functions as the *S*-specific base catalyst that is responsible for proton abstraction from C3 of substrate **3** (Figure $1B_3$ and Scheme 2C). It was further postulated that His194 may act as the *R*-specific base catalyst and abstracts the C3 proton from substrate **4**. This hypothesis was based on structure comparisons between MAL and other enolase superfamily members where the main chain of His194 superimposes on Lys164 of mandelate racemase (a secondary base), as well as on Lys213 in glucarate dehydratase (primary base).[59]

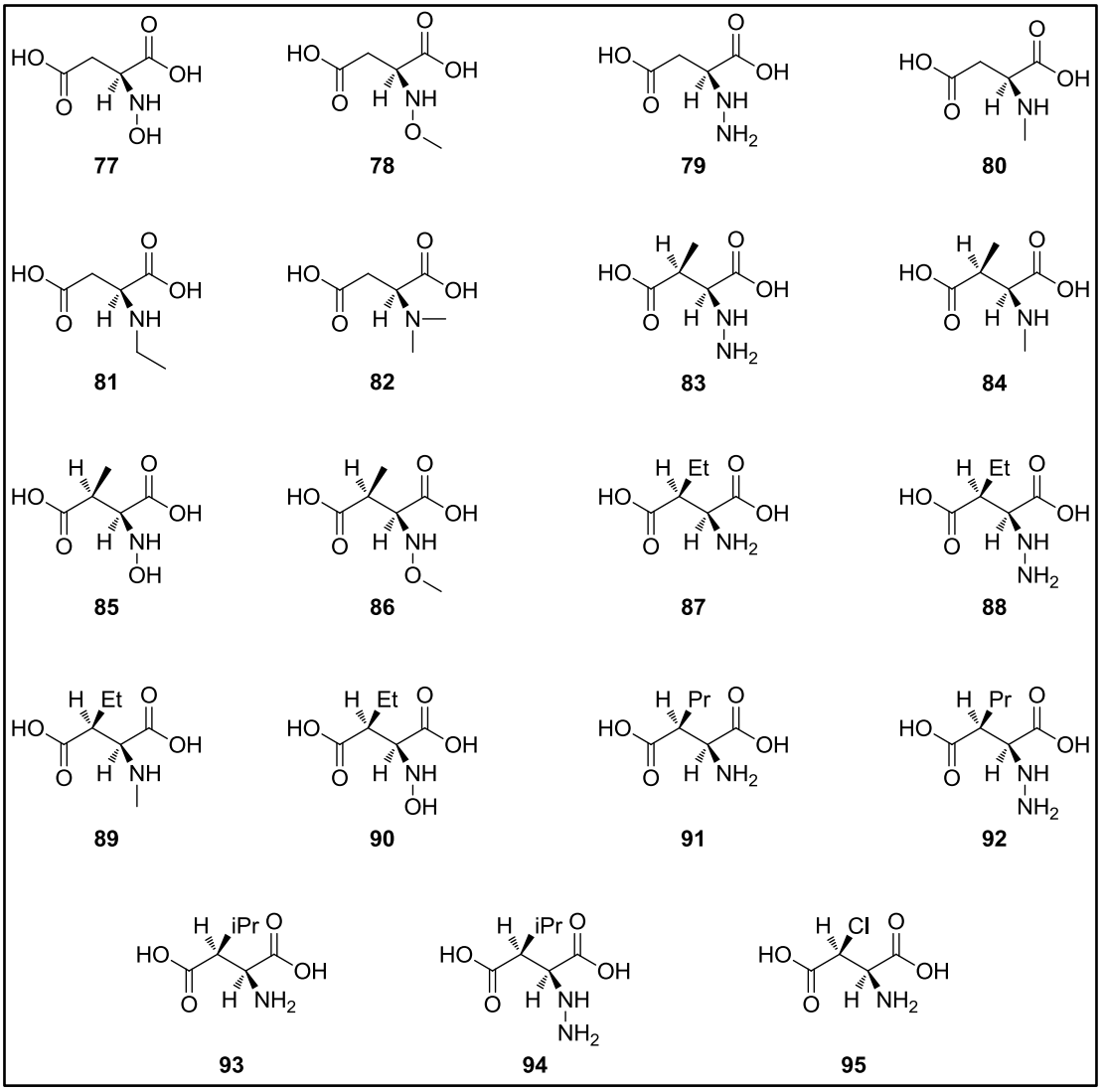

Scheme 5. L-Aspartic acid derivatives obtained from preparative reactions. L-aspartic acid analogs **77-95** were prepared using MAL as biocatalyst.[74-76] Derivatives **77-80** were also prepared with AspB as biocatalyst.[55]

Raj *et al.*[73] investigated the importance of these two proposed catalytic base residues in *Ct*MAL. First, Lys331 was shown to be an essential residue for catalysis, because enzyme activity was lost completely when this amino acid was mutated to a glycine, alanine, histidine, glutamine, or arginine.[73] Second, computer modeling of **4** into the active site of MAL indicated that the C3 proton of **4** is indeed facing towards the imidazole nitrogen atom (Nε2) of His194. Moreover, an alanine mutation at this position disables the protein from accepting **4** as a substrate, but the H194A mutant still has the ability to catalyze the deamination of **3**. It is of synthetic importance that the

H194A mutant is completely diastereoselective, and aminates **5** to give **3** as the sole product.[73] These studies thus showed that MAL catalyzes the reversible deamination reaction by using Lys331 as the *S*-specific general base/acid catalyst and His194 as the *R*-specific base/acid catalyst. It was also shown that MAL does not catalyze the direct epimerization reaction from **3** to **4**, and therefore the two products form exclusively as a result of the *anti*- and *syn*-addition of ammonia to **5**.[73]

The structure of MAL in complex with substrate[60] further showed that specific hydrogen bonds are made between the substrate's β-carboxylate group and the nitrogen atoms (Nε2) of Gln329 and His194 (Figure $1B_3$, Scheme 2C). The importance of these residues for MAL activity was confirmed by site-directed mutagenesis.[73] Importantly, the active site Mg^{2+} ion assists these two residues in binding of the substrate's β-carboxylate group, thereby providing efficient stabilization of the enolate anion intermediate. The Mg^{2+} binding site of MAL is located in the mouth of the TIM barrel and consists of Asp238, Glu273 and Asp307.[59, 60] Each of these amino acids contributes a single oxygen atom as ligand, and in combination with three water molecules (in the unliganded structure) the normal hexagonal coordination of Mg^{2+} is formed.[59] In the substrate bound active site, one of the six ligands to the Mg^{2+} ion is provided by one of the β-carboxyl oxygen atoms of the substrate, replacing a water molecule.[60] The α-carboxylate of the substrate has hydrogen bond interactions with the main chain NH of Cys361, the oxygen atom (Oγ) of Thr360, and the nitrogen atom (Nε2) of Gln172 (Scheme 2C). The C2 amino group fits nicely into a nucleophile binding pocket and has hydrogen bond interactions with the oxygen atom (Oε1) of Gln172 and, via a water molecule, with the nitrogen atom (Nε2) of Gln73. The substrate is further stabilized in the active site by favorable Van der Waals packing interactions between its 3-methyl group and the side chains of Leu384 and Gln172 (*60*). This detailed view of the substrate-bound active site of MAL thus allowed the identification of the active site residues (Figure $1B_3$) as well as an understanding of their roles in catalysis (Scheme 2C). In conclusion, the MAL structures[59, 60] and recent mutagenesis experiments[73] provide strong support for a catalytic mechanism involving general base-catalyzed formation of a highly stabilized enolate anion (carbanion) intermediate (**9**).

Biocatalytic applications

Several studies have focused on the usefulness of *Ct*MAL as a biocatalyst for asymmetric synthesis of aspartic acid derivatives.[74-76] Gani and co-workers showed that *Ct*MAL accepts different fumarate derivatives in the ammonia addition reaction, yielding a range of 3-substituted aspartic acid derivatives (Scheme 5).[74, 75] The same group reported that MAL can also catalyze the addition of a few small amines to fumarate and several 2-alkylfumarates to yield various *N*- and *N*,3-disubstituted aspartic acid derivatives (Scheme 5).[76] Hence, *Ct*MAL has a broader substrate spectrum than the aspartases AspA and AspB, and can be used to synthesize amino acids **77-95** (Scheme 5). Like *Ct*MAL, the thermostable *Ch*MAL also accepts various substituted fumarates and amines, and exhibits high regio- and stereoselectivity.[21] This makes *Ch*-MAL an attractive enzyme for biocatalytic applications, as well as a promising scaffold for protein engineering.

ENGINEERING OF ASPARTATE AND METHYLASPARTATE AMMONIA LYASES

A synthetic strategy in which aspartate and methylaspartate ammonia lyases are used as biocatalysts for the preparation of enantiomerically pure L-aspartic acid derivatives is of high interest (Scheme 3B). However, this strategy is currently limited by the narrow substrate range of these enzymes. It would therefore be very attractive to extend the accessible range of aspartic acid derivatives by the redesign of these lyases to convert new unnatural substrates, which would enlarge their biocatalytic applicability.[77] In fact, aspartase has been subjected to protein engineering by various investigators, but with limited success. Asano *et al*.[78] used directed evolution in an attempt to enlarge the substrate scope of AspA. Interestingly, they found that mutation of Lys327 to an asparagine enables AspA to catalyze the deamination of L-aspartic acid α-amide (β-asparagine), albeit at a very low level.[78] Unfortunately, no other AspA variants with a modified substrate scope have been reported. In our laboratory, we have attempted to broaden the substrate scope of aspartase AspB by rational design and structure-based saturation mutagenesis. However, we were unsuccessful in these engineering attempts, which may have to do with the complex movement of

the SS-loop upon substrate binding, making protein engineering of aspartases a formidable challenge.

In contrast to aspartases, where substrate-dependent closure of the SS-loop positions catalytic and substrate-binding residues in a suitable orientation for catalysis, MAL has an intact catalytic machinery in the uncomplexed enzyme and does not undergo large conformational changes upon substrate binding. This implies that MAL is a more promising template for redesign to convert new unnatural substrates.[79] Raj *et al*.[73] have shown that the diastereoselectivity of the enzyme can be altered by mutation of active-site residues, allowing the preparation of exclusively L-*threo*-3-methylaspartate (**3**, Scheme 1B). The crystal structure of substrate-bound MAL shows that the surface lining of the 3-methyl binding pocket, which is formed in part by Leu384, Phe170 and Tyr356, is composed almost entirely of side chains with little or no interaction between the substrate's 3-methyl group and the main chain atoms.[60] Recently, Poelarends and co-workers have engineered this alkyl binding pocket of MAL and obtained a single active site mutant (L384A) that has a wide electrophile scope including fumarate derivatives with alkyl, aryl, alkoxy, aryloxy, alkylthio and arylthio substituents at the C2 position (Scheme 6).[80] These investigators also engineered the nucleophile (amine) binding pocket of MAL, which is formed in part by Gln73 and Gln172, yielding a single active site mutant (Q73A) that exhibits a broad nucleophile scope including various structurally diverse linear and cyclic alkylamines (Scheme 7).[80] Hence, MAL appears to be the most attractive enzyme to create new biocatalysts for the asymmetric synthesis of enantiomerically pure L-aspartic acid derivatives.

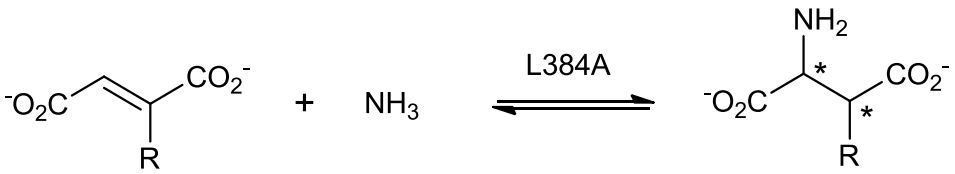

R = H, methyl, ethyl, propyl, butyl, pentyl, hexyl, benzyl, ethoxy, phenoxy, benzyloxy, ethylthio, phenylthio, benzylthio

Scheme 6. Electrophile spectrum of an engineered MAL variant. The MAL-L384A mutant as catalyst in the ammonia addition to fumarate and its 2-substituted derivatives.

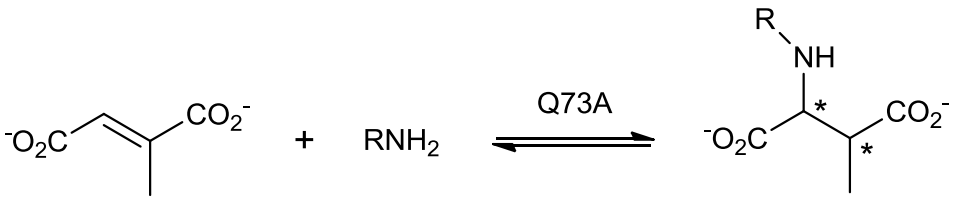

R = H, methyl, ethyl, propyl, butyl, pentyl, hexyl, benzyl, isopropyl, cyclopropyl, cyclobutyl, cyclopentyl, cyclohexyl, (cyclopropyl)methyl, ethoxy, 2-hydroxyethyl, 3-hydroxypropyl, 2-methoxyethyl, *N*-methyl-2-aminoethyl, 2-aminoethyl, 3-aminopropyl

Scheme 7. Nucleophile spectrum of an engineered MAL variant. The MAL-Q73A mutant as catalyst in the amine addition to mesaconate.

CONCLUDING REMARKS

Aspartase and MAL have been under investigation extensively for a number of decades, but the details of their catalytic mechanisms have only been elucidated in recent years. Information on the properties of these enzymes has been extended and the isolation and characterization of enzymes from thermophilic organisms have added more robust enzymes to the arsenal of researchers. There are still limitations around the range of substrates that can be accepted. Hence, there is a need to apply directed evolution techniques to provide biocatalysts with a much broader substrate scope. However, the complex movement of the SS-loop from an open conformation to one that closes over

the active site upon substrate binding makes engineering of the substrate specificity of aspartases a difficult task. We will therefore continue our efforts to further expand the substrate spectrum of MAL, which appears to be a more promising template for protein engineering.

ACKNOWLEDGMENT

Work on AspB and MAL in our laboratory was supported in part by VENI grant 700.54.401 and ECHO grant 700.59.042 from the Division of Chemical Sciences of the Netherlands Organisation of Scientific Research (NWO-CW).

KEYWORDS

Ammonia lyase: an enzyme that catalyzes the formation of an α,β-unsaturated bond by the elimination of ammonia from a substrate molecule.

Deaminase: an enzyme that catalyzes the removal of an amine group from a substrate molecule.

Amino acid: a molecule containing an amine group, a carboxylic acid group, and a side-chain that is specific to each amino acid.

Biocatalysis: the use of natural catalysts, such as enzymes or cells, to perform chemical transformations on organic compounds.

Catalytic mechanism: the mechanism by which a catalyst increases the rate of a chemical transformation.

Crystal structure: a unique arrangement of atoms or molecules within a crystalline liquid or solid

Aspartate: an α-amino acid with the chemical formula $HOOCCH(NH_2)CH_2COOH$.

Methylaspartate: an α-amino acid with the chemical formula $HOOCCH(NH_2)CH(CH_3)COOH$.

REFERENCES

1. Poppe, L., and Retey, J. (2003) Properties and synthetic applications of ammonia-lyases, *Curr. Org. Chem. 7*, 1297-1315.
2. Viola, R. E. (2000) L-aspartase: new tricks from an old enzyme, *Adv. Enzymol. Relat. Areas Mol. Biol. 74*, 295-341.
3. Harden, A. (1901) The chemical action of *Bacillus coli* communis and similar organisms on carbohydrates and allied compounds, *J. Chem. Soc. 79*, 610-628.
4. Quastel, J. H., and Woolf, B. (1926) The equilibrium between L-aspartic acid, fumaric acid and ammonia in presence of resting bacteria, *Biochem. J. 20*, 545-555.
5. Rudolph, F. B., and Fromm, H. J. (1971) The purification and properties of aspartase from *Escherichia coli*, *Arch. Biochem. Biophys. 147*, 92–98.
6. Suzuki, S., Yamaguchi, J., and Tokushige, M. (1973) Studies on aspartase. I. Purification and molecular properties of aspartase from *Escherichia coli*, *Biochim. Biophys. Acta 321*, 369–381.
7. Takagi, J. S., Ida, N., Tokushige, M., Sakamoto, H., and Shimura, Y. (1985) Cloning and nucleotide sequence of the aspartase gene of *Escherichia coli* W, *Nucleic Acids Res. 13*, 2063-2074.
8. Takagi, J. S., Fukunaga, R., Tokushige, M., and Katsuki, H. (1984) Purification, crystallization, and molecular properties of aspartase from *Pseudomonas fluorescens*, *J. Biochem. (Tokyo) 96*, 545–552.
9. Takagi, J. S., Tokushige, M., and Shimura, Y. (1986) Cloning and nucleotide sequence of the aspartase gene of *Pseudomonas fluorescens*, *J. Biochem. (Tokyo) 100*, 697–705.
10. Sun, D., and Setlow, P. (1991) Cloning, nucleotide sequence, and expression of the *Bacillus subtilis ans* operon, which codes for L-asparaginase and L-aspartase, *J. Bacteriol. 173*, 3831–3845.

11. Yoon, M.-Y., Thayer-Cook, K. A., Berdis, A. J., Karsten, W. E., Schnackerz, K. D., and Cook, P. F. (1995) Acid-base chemical mechanism of aspartase from *Hafnia alvei*, *Arch. Biochem. Biophys. 320*, 115–122.

12. Kawata, Y., Tamura, K., Yano, S., Mizobata, T., Nagai, J., Esaki, N., Soda, K., Tokushige, M., and Yumoto, N. (1999) Purification and characterization of thermostable aspartase from *Bacillus* sp. YM55-1, *Arch. Biochem. Biophys. 366*, 40-46.

13. Mizobata, T., and Kawata, Y. (2007) Aspartase: molecular structure, biochemical function and biotechnological applications, In *Industrial Enzymes: "Structure, function and applications"* (Polaina, J., and MacCabe, A. P., Eds.), pp 549-565, Springer, New York.

14. Barker, H. A., Smyth, R. D., Wilson, R. M., and Weissbach, H. (1959) The purification and properties of β-methylaspartase, *J. Biol. Chem. 234*, 320-328.

15. Kato, Y., and Asano, Y. (1997) 3-Methylaspartate ammonia-lyase as a marker enzyme of the mesaconate pathway for (*S*)-glutamate fermentation in *Enterobacteriaceae*, *Arch. Microbiol. 168*, 457–463.

16. Kato, Y., and Asano, Y. (1995) 3-Methylaspartate ammonia-lyase from a facultative anaerobe, strain YG-1002, *Appl. Microbiol. Biotechnol. 43*, 901–907.

17. Kato, Y., and Asano, Y. (1995) Purification and properties of crystalline 3-methylaspartase from two facultative anaerobes, *Citrobacter* sp. strain YG-0504 and *Morganella morganii* strain YG-0601, *Biosci. Biotechnol. Biochem. 59*, 93–99.

18. Kato, Y., and Asano, Y. (1998) Cloning, nucleotide sequencing, and expression of the 3-methylaspartate ammonia-lyase gene from *Citrobacter amalonaticus* strain YG-1002, *Appl. Microbiol. Biotechnol. 50*, 468–474.

19. Asano, Y., and Kato, Y. (1994) Crystalline 3-methylaspartase from a facultative anaerobe, *Escherichia coli* strain YG1002, *FEMS Microbiol. Lett. 118*, 255–258.

20. Khomyakova, M., Bukmez, O., Thomas, L. K., Erb, T. J., and Berg, I. A. (2011) A methylaspartate cycle in haloarchaea, *Science 331*, 334-337.

21. Raj, H., Puthan Veetil, V., Szymanski, W., Dekker, F., Quax, W. J., Feringa, B. L., Janssen, D. B., and Poelarends, G. J. (2012) Characterization of a thermostable methylaspartate ammonia lyase from *Carboxydothermus hydrogenoformans*, *Appl. Microbiol. Biotechnol. 94*, 385-397.

22. Kornberg, H. L., and Morris, J. G. (1963) β-Hydroxyaspartate pathway: a new route for biosyntheses from glyoxylate, *Nature 197*, 456-457.

23. Kornberg, H. L., and Morris, J. G. (1965) The utilization of glycolate by *Micrococcus denitrificans*: the β-hydroxyaspartate pathway, *Biochem. J. 95*, 577-586.

24. Gibbs, R. G., and Morris, J. G. (1965) Purification and properties of *erythro*-β-hydroxyasparate dehydratase from *Micrococcus denitrificans*, *Biochem. J. 97*, 547-554.

25. Wada, M., Matsumoto, T., Nakamori, S., Sakamoto, M., Kataoka, M., Liu, J. Q., Itoh, N., Yamada, H., and Shimizu, S. (1999) Purification and characterization of a novel enzyme, L-*threo*-3-hydroxyaspartate dehydratase, from *Pseudomonas* sp. T62, *FEMS Microbiol. Lett. 179*, 147-151.

26. Wada, M., Nakamori, S., and Takagi, H. (2003) Serine racemase homologue of *Saccharomyces cerevisiae* has L-*threo*-3-hydroxyaspartate dehydratase activity, *FEMS Microbiol. Lett. 225*, 189-193.

27. Maeda, T., Takeda, Y., Murakami, T., Yokota, A., and Wada, M. (2010) Purification, characterization and amino acid sequence of a novel enzyme, D-*threo*-3-hydroxyaspartate dehydratase, from *Delftia* sp. HT23, *J. Biochem. 148*, 705-712.

28. Ida, N., and Tokushige, M. (1985) L-Aspartate-induced activation of aspartase, *J. Biochem. 98*, 35-39.

29. Karsten, W. E., Gates, R. B., and Viola, R. E. (1986) Kinetic studies of L-aspartase from *Escherichia coli*: substrate activation, *Biochemistry 25*, 1299-1303.

30. Falzone, C. J., Karsten, W. E., Conley, J. D., and Viola, R. E. (1988) L-aspartase from *Escherichia coli*: substrate specificity and role of divalent metal ions, *Biochemistry 27*, 9089-9093.

31. Shi, W., Dunbar, J., Jayasekera, M. M., Viola, R. E., and Farber, G. K. (1997) The structure of L-aspartate ammonia-lyase from *Escherichia coli*, *Biochemistry 36*, 9136-9144.

32. Sampaleanu, L. M., Vallee, F., Slingsby, C., and Howell, P. L. (2001) Structural studies of duck δ-1 and δ-2 crystallin suggest conformational changes occur during catalysis, *Biochemistry 40*, 2732-2742.

33. Tsai, M., Koo, J., Yip, P., Colman, R. F., Segall, M. L., and Howell, P. L. (2007) Substrate and product complexes of *Escherichia coli* adenylosuccinate lyase provide new insights into the enzymatic mechanism, *J. Mol. Biol. 370*, 541-554.

34. Turner, M. A., Simpson, A., McInnes, R. R., and Howell, P. L. (1997) Human argininosuccinate lyase: a structural basis for intragenic complementation, *Proc. Natl. Acad. Sci. U S A 94*, 9063-9068.

35. Vallee, F., Turner, M. A., Lindley, P. L., and Howell, P. L. (1999) Crystal structure of an inactive duck δ-II crystallin mutant with bound argininosuccinate, *Biochemistry 38*, 2425-2434.

36. Weaver, T. M., Levitt, D. G., Donnelly, M. I., Stevens, P. P., and Banaszak, L. J. (1995) The multisubunit active site of fumarase C from *Escherichia coli*, *Nat. Struct. Biol. 2*, 654-662.

37. Yang, J., Wang, Y., Woolridge, E. M., Arora, V., Petsko, G. A., Kozarich, J. W., and Ringe, D. (2004) Crystal structure of 3-carboxy-*cis*,*cis*-muconate lactonizing enzyme from *Pseudomonas putida*, a fumarase class II type cycloisomerase: enzyme evolution in parallel pathways, *Biochemistry 43*, 10424-10434.

38. Sampaleanu, L. M., Yu, B., and Howell, P. L. (2002) Mutational analysis of duck δ-2 crystallin and the structure of an inactive mutant with bound substrate provide insight into the enzymatic mechanism of argininosuccinate lyase, *J. Biol. Chem. 277*, 4166-4175.

39. Fibriansah, G., Puthan Veetil, V., Poelarends, G. J., and Thunnissen, A. M. (2011) Structural basis for the catalytic mechanism of aspartate ammonia lyase, *Biochemistry 50*, 6053-6062.

40. Weaver, T., Lees, M., and Banaszak, L. (1997) Mutations of fumarase that distinguish between the active site and a nearby dicarboxylic acid binding site, *Protein Sci. 6*, 834-842.

41. Nuiry, I. I., Hermes, J. D., Weiss, P. M., Chen, C.-Y., and Cook, P. F. (1984) Kinetic mechanism and location of rate-determening steps for aspartase from *Hafnia alvei*, *Biochemistry 23*, 5168–5175.

42. Gawron, O., and Fondy, T. P. (1959) Stereochemistry of the fumarase and aspartase catalyzed reactions and of the Krebs cycle from fumaric acid to *d*-isocitric acid, *J. Am. Chem. Soc. 81*, 6333–6334.

43. Hanson, K. R., and Havir, E. A. (1972) The enzymic elimination of ammonia, In *The Enzymes*, Vol. 3 (Boyer, P. D., Eds.), pp. 75–166, Academic Press, New York, NY.

44. Porter, D. J., and Bright, H. J. (1980) 3-Carbanionic substrate analogues bind very tightly to fumarase and aspartase, *J. Biol. Chem. 255*, 4772-4780.

45. Karsten, W. E., and Viola, R. E. (1991) Kinetic studies of L-aspartase from *Escherichia coli*: pH-dependent activity changes, *Arch. Biochem. Biophys. 287*, 60-67.

46. Puthan Veetil, V., Raj, H., Quax, W. J., Janssen, D. B., and Poelarends, G. J. (2009) Site-directed mutagenesis, kinetic and inhibition studies of aspartate ammonia lyase from *Bacillus* sp. YM55-1, *FEBS J. 276*, 2994-3007.

47. Saribas, A. S., Schindler, J. F., and Viola, R. E. (1994) Mutagenic investigation of conserved functional amino acids in *Escherichia coli* L-aspartase, *J. Biol. Chem. 269*, 6313-6319.

48. Jayasekera, M. M., Shi, W., Farber, G. K., and Viola, R. E. (1997) Evaluation of functionally important amino acids in L-aspartate ammonia-lyase from *Escherichia coli*, *Biochemistry 36*, 9145-9150.

49. Fujii, T., Sakai, H., Kawata, Y., and Hata, Y. (2003) Crystal structure of thermostable aspartase from *Bacillus* sp. YM55-1: structure-based exploration of functional sites in the aspartase family, *J. Mol. Biol. 328*, 635-654.

50. Wubbolts, M. (2002) Addition of amines to C=C bonds, In *Enzyme catalysis in organic synthesis: a comprehensive handbook* (Drauz, K., and Waldmann, H., Eds.) 2nd ed., pp 866-872, Wiley-VCH, Weinheim.

51. Liese, A., Seelbach, K., Bulcholz, A., and Haberland, J. (2006) Processes: Lyases EC 4, In *Industrial biotransformations* (Liese, A., Seelbach, K., and Wandrey, C., Eds.) 2nd ed., pp 494-501, Wiley-VCH, Weinheim.

52. Shimamoto, K. (2008) Glutamate transporter blockers for elucidation of the function of excitatory neurotransmission systems, *Chem. Rec. 8*, 182-199.

53. Mavencamp, T. L., Rhoderick, J. F., Bridges, R. J., and Esslinger, C. S. (2008) Synthesis and preliminary pharmacological evaluation of novel derivatives of L-β-*threo*-benzylaspartate as inhibitors of the neuronal glutamate transporter EAAT3, *Bioorg. Med. Chem. 16*, 7740-7748.

54. Spengler, J., Pelay, M., Tulla-Puche, J., and Albericio, F. (2010) Synthesis of orthogonally protected L-*threo*-β-ethoxyasparagine, *Amino Acids 39*, 161-165.

55. Weiner, B., Poelarends, G. J., Janssen, D. B., and Feringa, B. L. (2008) Biocatalytic enantioselective synthesis of *N*-substituted aspartic acids by aspartate ammonia lyase, *Chem. Eur. J. 14*, 10094-10100.

56. Yumoto, N., Okada, M., and Tokushige, M. (1982) Biospecific inactivation of aspartase by L-aspartic-β-semialdehyde, *Biochem. Biophys. Res. Comm. 104*, 859-866.

57. Emery, T. F. (1963) Aspartase-catalyzed synthesis of *N*-hydroxyaspartic acid, *Biochemistry 2*, 1041-1045.

58. Goda, S. K., Minton, N. P., Botting, N. P., and Gani, D. (1992) Cloning, sequencing, and expression in *Escherichia coli* of the *Clostridium tetanomorphum* gene encoding β-

methylaspartase and characterization of the recombinant protein, *Biochemistry 31*, 10747-10756.

59. Asuncion, M., Blankenfeldt, W., Barlow, J. N., Gani, D., and Naismith, J. H. (2002) The structure of 3-methylaspartase from *Clostridium tetanomorphum* functions via the common enolase chemical step, *J. Biol. Chem. 277*, 8306-8311.

60. Levy, C. W., Buckley, P. A., Sedelnikova, S., Kato, Y., Asano, Y., Rice, D. W., and Baker, P. J. (2002) Insights into enzyme evolution revealed by the structure of methylaspartate ammonia lyase, *Structure 10*, 105-113.

61. Svetlichny, V. A., Sokolova, T. G., Gerhardt, M., Ringpfeil, M., Kostrikina, N. A., and Zavarin, G. A. (1991) *Carboxydothermus hydrogenoformans* gen. nov., sp. nov., a CO-utilizing thermophilic anaerobic bacterium from hydrothermal environments of Kunashir Island, *Syst. Appl. Microbiol. 14*, 254.

62. Wu, M., Ren, Q., Durkin, A. S., Daugherty, S. C., Brinkac, L. M., Dodson, R. J., Madupu, R., Sullivan, S. A., Kolonay, J. F., Haft, D. H., Nelson, W. C., Tallon, L. J., Jones, K. M., Ulrich, L. E., Gonzalez, J. M., Zhulin, I. B., Robb, F. T., and Eisen, J. A. (2005) Life in hot carbon monoxide: the complete genome sequence of *Carboxydothermus hydrogenoformans* Z-2901, *PLoS Genet. 1*, e65.

63. Bright, H. (1964) The mechanism of the β-methylaspartase reaction, *J. Biol. Chem. 239*, 2307-2315.

64. Bright, H. J., Ingraham, L. L., and Lundin, R. E. (1964) The mechanism of the methylaspartate ammonia-lyase reaction: deuterium exchange, *Biochim. Biophys. Acta 81*, 576-584.

65. Botting, N. P., Cohen, M. A., Akhtar, M., and Gani, D. (1988) Primary deuterium isotope effects for the 3-methylaspartase-catalyzed deamination of (2*S*)-aspartic acid, (2*S*,3*S*)-3-methylaspartic acid, and (2*S*,3*S*)-3-ethylaspartic acid, *Biochemistry 27*, 2956-2959.

66. Botting, N. P., and Gani, D. (1992) Mechanism of C-3 hydrogen exchange and the elimination of ammonia in the 3-methylaspartate ammonia-lyase reaction, *Biochemistry 31*, 1509-1520.

67. Archer, C. H., Thomas, N. R., and Gani, D. (1993) Syntheses of (2*S*,3*R*)-3-methylaspartic and (2*S*,3*R*)[3-^{2}H]-3-methylaspartic acids - slow substrates for a *syn*-elimination reaction catalyzed by methylaspartase, *Tetrahedron-Asymmetry 4*, 1141-1152.

68. Archer, C. H., and Gani, D. (1993) Kinetics and mechanism of *syn*-elimination of ammonia from (2*S*,3*R*)-3-methylaspartic acid by methylaspartase, *J. Chem. Soc., Chem. Comm.* 140-142.

69. Gani, D., Archer, C. H., Botting, N. P., and Pollard, J. R. (1999) The 3-methylaspartase reaction probed using ^{2}H- and ^{15}N-isotope effects for three substrates: a flip from a concerted to a carbocationic amino-enzyme elimination mechanism upon changing the C-3 stereochemistry in the substrate from *R* to *S*, *Bioorg. Med. Chem. 7*, 977-990.

70. Pollard, J. R., Richardson, S., Akhtar, M., Lasry, P., Neal, T., Botting, N. P., and Gani, D. (1999) Mechanism of 3-methylaspartase probed using deuterium and solvent isotope effects and active-site directed reagents: identification of an essential cysteine residue, *Bioorg. Med. Chem. 7*, 949-975.

71. Schwede, T. F., Rétey, J., and Schultz, G. E. (1999) Crystal structure of histidine ammonia-lyase revealing a novel polypeptide modification as the catalytic electrophile, *Biochemistry 38*, 5355-5361.

72. Calabrese, J. C., Jordan, D. B., Boodhoo, A., Sariaslani, S., and Vannelli, T. (2004) Crystal structure of phenylalanine ammonia lyase: multiple helix dipoles implicated in catalysis, *Biochemistry 43*, 11403–11416.

73. Raj, H., Weiner, B., Puthan Veetil, V., Reis, C. R., Quax, W. J., Janssen, D. B., Feringa, B. L., Poelarends, G. J. (2009) Alteration of the diastereoselectivity of 3-methylaspartate ammonia lyase by using structure-based mutagenesis, *ChemBioChem. 10*, 2236–2245.

74. Akhtar, M., Botting, N. P., Cohen, M. A., and Gani, D. (1987) Enantiospecific synthesis of 3-substituted aspartic acids via enzymic amination of substituted fumaric acids, *Tetrahedron 43*, 5899-5908.

75. Akhtar, M., Cohen, M. A., and Gani, D. (1987) Stereochemical course of the enzymatic amination of chlorofumaric acid and bromofumaric acid by 3-methylaspartate ammonia-lyase, *Tet. Lett. 28*, 2413-2416.

76. Gulzar, M. S., Akhtar, M., and Gani, D. (1997) Preparation of *N*-substituted aspartic acids via enantiospecific conjugate addition of *N*-nucleophiles to fumaric acids using methylaspartase: Synthetic utility and mechanistic implications, *J. Chem. Soc. Perk. T 1*, 649-655.

77. Turner, N. J. (2011) Ammonia lyases and aminomutases as biocatalysts for the synthesis of α-amino and β-amino acids, *Curr. Opin. Chem. Biol. 15*, 234-240.

78. Asano, Y., Kira, I., and Yokozeki, K. (2005) Alteration of substrate specificity of aspartase by directed evolution, *Biomol. Eng. 22*, 95-101.

79. Glasner, M. E., Gerlt, J. A., and Babbitt, P. C. (2006) Evolution of enzyme superfamilies, *Curr. Opin. Chem. Biol. 10*, 492-497.

80. Raj, H., Szymański, W., de Villiers, J., Rozeboom, H. J., Puthan Veetil, V., Reis, C. R., de Villiers, M., Dekker, F. J., de Wildeman, S., Quax, W. J., Thunnissen, A. -M. W. H., Feringa, B. L., Janssen, D. B., and Poelarends, G. J. (2012) Engineering methylaspartate ammonia lyase for the asymmetric synthesis of unnatural amino acids, *Nat. Chem. 4*, 478-484.

PART ONE

ENGINEERING OF

METHYLASPARTATE AMMONIA LYASE

Chapter 2

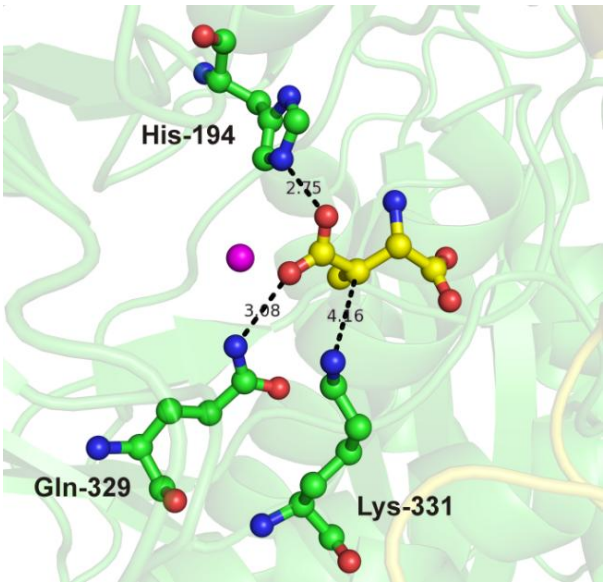

Alteration of the diastereoselectivity of 3-methylaspartate ammonia lyase by using structure-based mutagenesis

Hans Raj,[a] Barbara Weiner,[b] Vinod Puthan Veetil,[a] Carlos R. Reis,[a] Wim J. Quax,[a] Dick B. Janssen,[c] Ben L. Feringa,[b] and Gerrit J. Poelarends[a]

[a] *Department of Pharmaceutical Biology, Groningen Research Institute of Pharmacy, University of Groningen, Antonius Deusinglaan 1, 9713 AV Groningen, The Netherlands.*

[b] *Department of Organic and Molecular Inorganic Chemistry, Stratingh Institute for Chemistry, University of Groningen, Nijenborgh 4, 9747 AG Groningen, The Netherlands.*

[c] *Department of Biochemistry, Groningen Biomolecular Sciences and Biotechnology Institute, University of Groningen, Nijenborgh 4, 9747 AG Groningen, The Netherlands.*

Published in *ChemBioChem* (2009) 10, 2236-2245.

ABSTRACT

3-Methylaspartate ammonia-lyase (MAL) catalyzes the reversible amination of mesaconate to give both (2*S*,3*S*)-3-methylaspartic acid and (2*S*,3*R*)-3-methylaspartic acid as products. The deamination mechanism of MAL is likely to involve general base catalysis, in which a catalytic base abstracts the C-3 proton of the respective stereoisomer to generate an enolate anion intermediate that is stabilized by coordination to the essential active site Mg^{2+} ion. The crystal structure of MAL in complex with (2*S*,3*S*)-3-methylaspartic acid suggests that Lys-331 is the only candidate in the vicinity that can function as a general base catalyst. The structure of the complex further suggests that two other residues, His-194 and Gln-329, are responsible for binding the C-4 carboxylate group of (2*S*,3*S*)-3-methylaspartic acid, and hence are likely candidates to assist the Mg^{2+} ion in stabilizing the enolate anion intermediate. In this study, the importance of Lys-331, His-194 and Gln-329 for the activity and stereoselectivity of MAL was investigated by site-directed mutagenesis. His-194 and Gln-329 were replaced with either an alanine or arginine, whereas Lys-331 was mutated to a glycine, alanine, glutamine, arginine or histidine. The properties of the mutant proteins were investigated by circular dichroism (CD), kinetic analysis, and ^{1}H NMR spectroscopy. The CD spectra of all mutants were comparable to that of wild-type MAL indicating that these mutations did not result in any major conformational changes. Kinetic studies demonstrated that the mutations have a profound effect on the values of k_{cat} and k_{cat}/K_m, implicating Lys-331, His-194 and Gln-329 as mechanistically important. ^{1}H NMR spectra of the amination and deamination reactions catalyzed by the mutant enzymes K331A, H194A, and Q329A showed that these mutants have strongly enhanced diastereoselectivities. In the amination direction, they catalyze the conversion of mesaconate to yield only (2*S*,3*S*)-3-methylaspartic acid, with no detectable formation of (2*S*,3*R*)-3-methylaspartic acid. The results are discussed in terms of a mechanism in which Lys-331, His-194 and Gln-329 are involved in positioning the substrate, and in formation and stabilization of the enolate anion intermediate.

INTRODUCTION

3-Methylaspartate ammonia-lyase (MAL) catalyzes the reversible amination of mesaconate (**1**) to give (2*S*,3*S*)-3-methylaspartic acid (**2**) as a major product and (2*S*,3*R*)-3-methylaspartic acid (**3**) as a minor product (Scheme 1).[1, 2] The enzyme is used by the anaerobic bacterium *Clostridium tetanomorphum* as part of a degradative pathway that converts (*S*)-glutamic acid *via* **2** to finally yield acetyl-CoA.[1, 2] MAL is of considerable biocatalytic interest because it also catalyzes the stereo- and regioselective addition of ammonia to several derivatives of **1** to form a number of 3-alkyl- and 3-halo-substituted aspartic acids.[3] Moreover, the broad nucleophile specificity of MAL enables the use of a range of alternative nucleophiles such as methylamine, ethylamine, hydrazine, and methoxylamine in the conjugate addition reaction.[4] These properties make MAL a promising biocatalyst for the enantiospecific synthesis of both 3- and *N*-substituted aspartic acids, which are interesting building blocks for pharmaceutical synthesis.

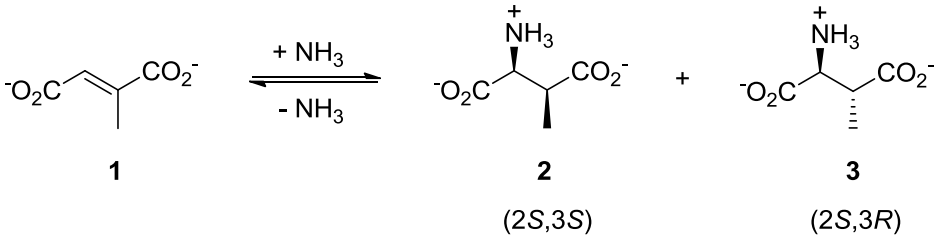

Scheme 1. MAL-catalyzed reversible amination of mesaconate to yield (2*S*,3*S*)- and (2*S*,3*R*)-3-methylaspartic acid.

MAL is a homodimeric enzyme (molecular mass of ~45.5 kDa) that requires both monovalent (i.e., K^+) and divalent (i.e., Mg^{2+}) cations for activity.[1, 2] Several studies have been aimed at demonstrating the deamination mechanism of MAL.[5-11] Some of these have suggested that MAL operates via a carbanion mechanism with rate-limiting C-N bond cleavage.[5, 6] This proposed mechanism is supported by the observation that C-3 hydrogen exchange of the C3-deuterated substrate (**2**, Scheme 1) with solvent occurs more rapidly than C-N bond cleavage. Moreover, no primary isotope effect was observed for the deamination of the C3-deuterated

substrate.[5, 6] Nonetheless, other reports have questioned this carbanion mechanism,[7-11] and up until the structure of MAL was reported, the catalytic mechanism of the enzyme remained unresolved.

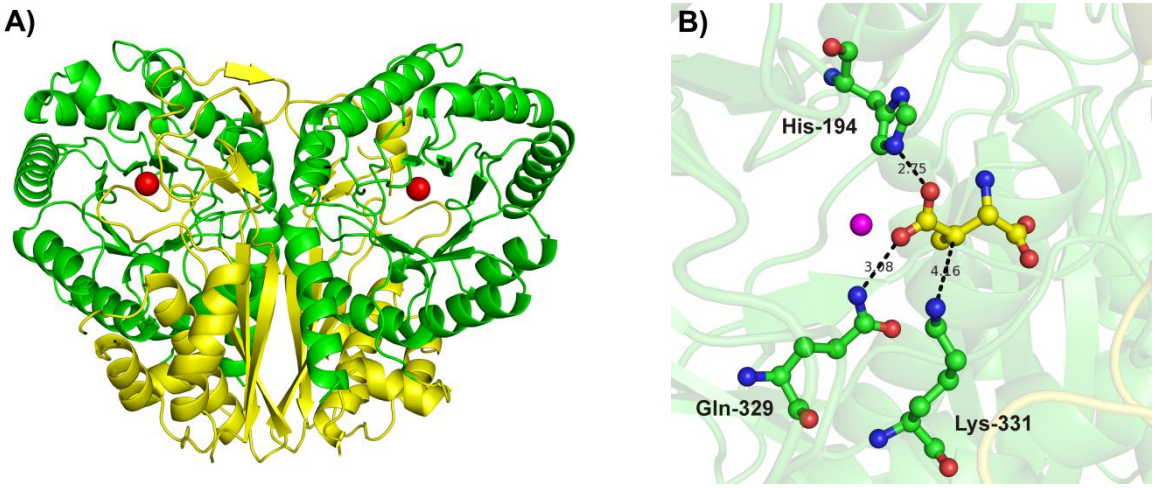

Figure 1. (A) Ribbon diagram of the functional homodimeric structure of *C. amalonaticus* MAL.[13] The location of the active site in each monomer is indicated by the bound Mg^{2+} ion, which is shown as a red sphere. The figure was prepared with PyMOL.[27] (B) A close-up of the active site of *C. amalonaticus* MAL in complex with (2*S*,3*S*)-3-methylaspartic acid.[13] For clarity, only the Mg^{2+} ion (magenta sphere) and the active site residues His-194, Gln-329, and Lys-331 are shown. The roles of these residues and their interactions are discussed in the text. Observed distances (in Å) between active site residues and substrate are indicated. The figure was prepared with PyMOL.[27]

The crystal structure of MAL from *C. tetanomorphum*[12] and that of the isozyme from *Citrobacter amalonaticus*[13] were reported a few years ago. These structures showed that within the functional homodimer, each MAL monomer consists of two domains (Figure 1A). The larger C-terminal domain is an 8-fold α/β-barrel, and the smaller N-terminal domain mainly consists of β-strands. The active site carrying the essential Mg^{2+} ion is located in a large cleft between the two domains. Structure comparisons identified MAL as a member of the enolase superfamily.[12, 13] Despite little sequence identity, the overall α/β-barrel topology and the active site architecture of MAL are strikingly similar to those of enolase, the title enzyme of this superfamily. Interestingly, the members of the enolase superfamily catalyze different reactions but share a common catalytic

step: the metal ion assisted, general-base catalyzed abstraction of the α-proton of a carboxylic acid substrate to generate an enzyme-stabilized enolate anion intermediate.[14] On the basis of the structural homology to the enolase superfamily, coupled with the earlier results of kinetic isotope studies, it was proposed that MAL functions via the common enolase catalytic step, and thus generates and stabilizes an enolate anion intermediate (**4**, Scheme 2).[12, 13]

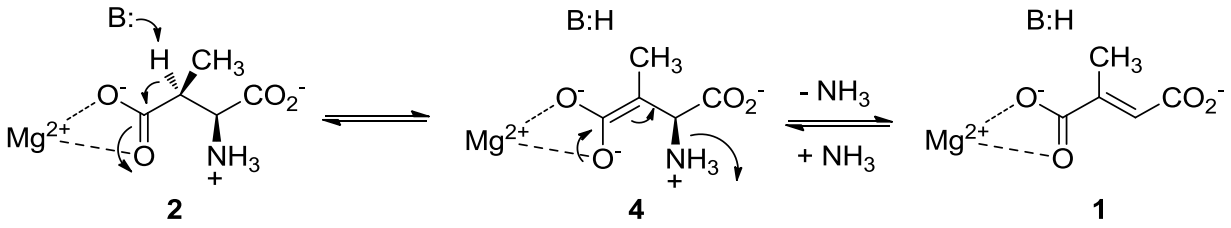

Scheme 2. Proposed enolate anion intermediate along the reaction pathway of MAL.

Although a general base catalyst for the deamination activity of MAL has not been determined, Lys-331 appears to be a likely candidate because it occupies a similar position to the general base Lys-345 in enolase.[12, 13] Moreover, the crystal structure of *C. amalonaticus* MAL in complex with **2** shows that Lys-331 is the only candidate in the vicinity of C-3 that can function as a general base catalyst (Figure 1B).[13] Two other residues, His-194 and Gln-329, are implicated in binding the C-4 carboxylate group of **2** (Figure 1B),[13] and thus are likely candidates for assisting the Mg^{2+} ion in stabilizing the enolate anion intermediate. It was further postulated that His-194 may also function as the second base (in addition to Lys-331) that abstracts the C-3 proton of the stereoisomer **3** (Scheme 1).[12]

The objective of the present work is two-fold. First, we demonstrate the importance of His-194, Gln-329, and Lys-331 for the MAL-catalyzed reactions. Second, we show that mutations of these active-site residues alter the diastereoselectivity of MAL. This led to a single amino acid MAL variant (H194A) that has useful properties for the stereoselective synthesis of isomerically pure (2*S*,3*S*)-3-methylaspartic acid. The results are discussed in terms of a mechanism in which

His-194, Gln-329, and Lys-331 are involved in binding and positioning of the substrate, and in formation and stabilization of the enolate anion intermediate.

RESULTS

Expression and purification of MAL

The gene coding for MAL was amplified from genomic DNA of *C. tetanomorphum* and fused into the start codon of the expression vector pBAD/*Myc*-His A, resulting in the construct pBAD(MAL-His). Sequencing of the cloned MAL gene verified that no mutations had been introduced during the amplification and cloning procedures. The MAL gene in pBAD(MAL-His) is under transcriptional control of the *araBAD* promoter and the recombinant enzyme was produced upon induction with arabinose in *E. coli* TOP10 as a C-terminal hexahistidine fusion protein. Production of soluble and active MAL was most efficient when cells were cultivated at 17°C and when 0.004% (w/v) arabinose was used. The recombinant enzyme was purified by a one-step Ni-based immobilized metal affinity chromatography protocol, which typically provides 10-15 mg of homogeneous enzyme per liter of culture.

Kinetic and ^{1}H NMR analysis of the MAL-catalyzed amination of 1

A mixture containing MAL, mesaconate (**1**), and ammonium chloride was monitored by ^{1}H NMR spectroscopy to verify that the products of the reaction are (2*S*,3*S*)-3-methylaspartic acid (**2**) and (2*S*,3*R*)-3-methylaspartic acid (**3**), as has been previously reported.[2] Indeed, the enzymatic amination of **1** yields **2** and **3**, as indicated by signals in the NMR spectra consistent with the structures of these amino acid products (Figure 2A).[15] Although the ^{1}H NMR spectra showed signals for both **2** and **3**, those corresponding to **2** predominated in the initial spectra whereas signals for **3** appeared only in the later spectra. These observations confirm that MAL catalyzes the

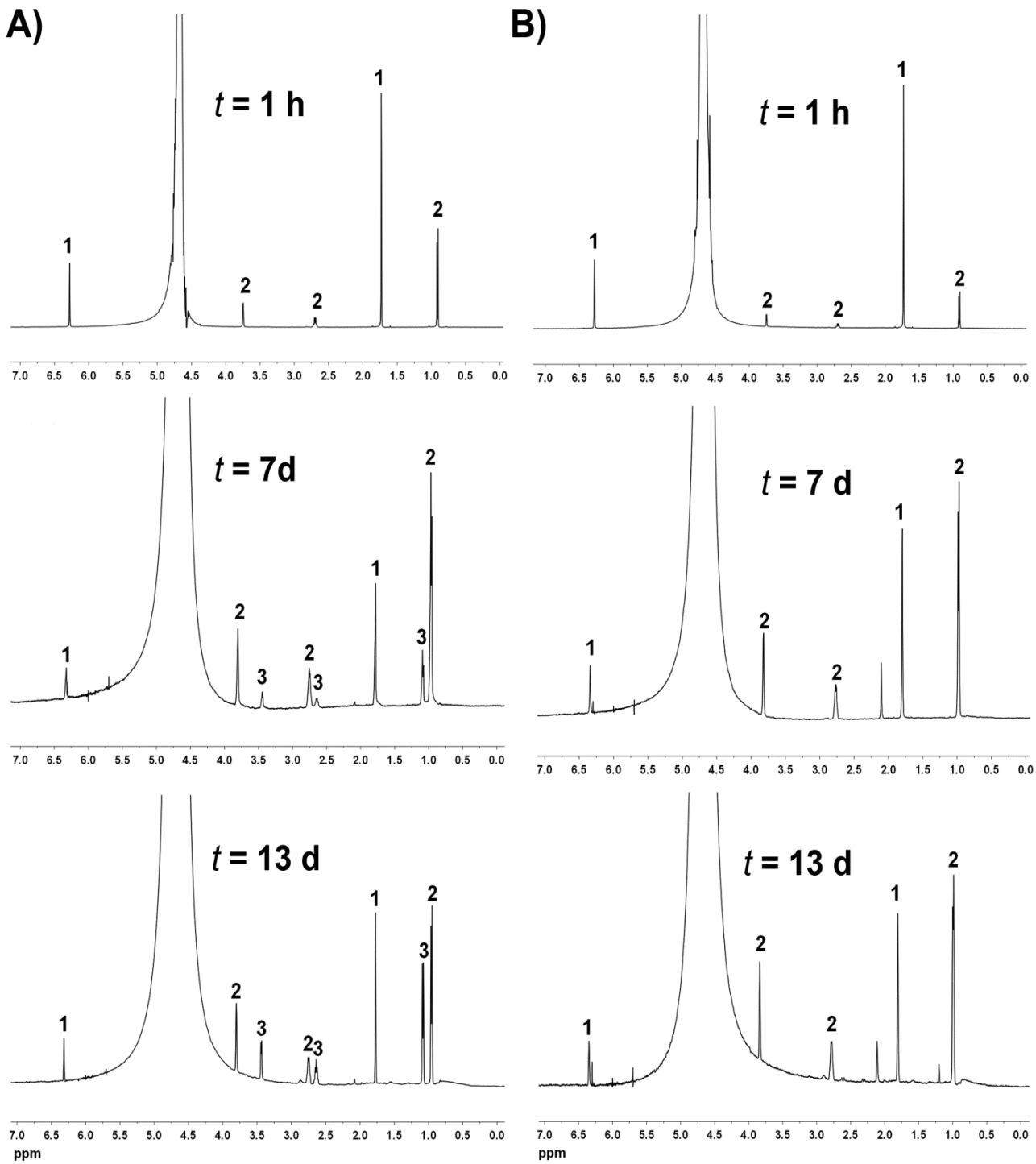

Figure 2. ^{1}H NMR spectra monitoring the amination of **1** by MAL (A) and the H194A mutant (B). The ^{1}H NMR signals for compounds **1**, **2**, and **3** are indicated (see Supporting Information for assignment of the signals). Spectra were recorded after 1 h, 7 days, and 13 days, respectively. The ^{1}H NMR spectra of the K331A and Q329A mutants (not shown) were comparable to those of the H194A mutant; that is, there was no detectable formation of **3** in the incubation mixtures. The less prominent singlets at 1.20 and 2.11 ppm correspond to impurities resulting from multiple additions of protein.

rapid conversion of **1** to the natural substrate **2**, as well as the slow conversion of **1** to **3**. After a 13 day-incubation period, the MAL-catalyzed reaction was complete, resulting in 45% **2** and 35% **3**.

A previously described assay[3] was used to measure the kinetic parameters for MAL in the amination direction. Accordingly, the rate of amination of **1** was monitored by following the depletion of **1** at 270 nm in 500 mM Tris-HCl buffer (pH 9.0) containing 20 mM $MgCl_2$ and 400 mM NH_4Cl at 30°C. A k_{cat} of 61 (± 1) s^{-1} and a K_m of 0.7 (± 0.02) mM were found, which results in a k_{cat}/K_m of ~8.7 x 10^4 M^{-1} s^{-1} (Table 1).

Table 1. Apparent kinetic parameters for the MAL-, K331A-, H194A-, and Q329A-catalyzed amination of mesaconic acid (**1**)[a].

Enzyme	k_{cat} (s^{-1})	K_m (for 1) (mM)	k_{cat}/K_m (M^{-1} s^{-1})
MAL	61 ± 1	0.7 ± 0.02	8.7×10^4
K331A	ND	ND	<0.001
H194A	8.4 ± 0.3	14 ± 1	6.0×10^2
Q329A	0.25 ± 0.02	1.7 ± 0.2	1.5×10^2

[a]The steady state kinetic parameters were determined in 500 mM Tris-HCl buffer (pH 9.0) containing 20 mM $MgCl_2$ and 400 mM NH_4Cl at 30°C. Errors are standard deviations. ND, not determined.

Kinetic and ^{1}H NMR analysis of the MAL-catalyzed deamination of 2

The rate of deamination of **2** by MAL was monitored by following the formation of **1** at 240 nm in 500 mM Tris-HCl buffer (pH 9.0) containing 20 mM $MgCl_2$ and 1 mM KCl at 30°C.[3] For the deamination of **2**, a k_{cat} of 89 (± 4) s^{-1} and a K_m of 1.0 (± 0.1) mM were found, which results in a k_{cat}/K_m of 8.9 x 10^4 M^{-1} s^{-1} (Table 2).

A mixture containing MAL and **2** was also monitored by ^{1}H NMR spectroscopy to verify that the product of the reaction is **1**. The enzymatic conversion of **2** yields **1**, as indicated by a

singlet at 1.74 ppm and a singlet at 6.28 ppm (Figure S4, Supporting Information), which correspond to the protons at the C-3 methyl group and C-2, respectively. In addition, signals corresponding to **3** are also present. After a 13 day-incubation period, the MAL-catalyzed reaction results in 41% **1** and 2% **3**.[16] Hence, **1** is the major product of the MAL-catalyzed conversion of **2**.

^{1}H NMR analysis of the MAL-catalyzed deamination of 3

^{1}H NMR analysis of the diastereoisomer **3** revealed that the provided material contains 94-95% of the required diastereoisomer **3** and 5-6% of the unwanted diastereoisomer **2**. This finding precluded the use of the material in kinetic experiments. Nevertheless, it was possible to monitor the deamination of **3** by ^{1}H NMR spectroscopy and identify the products of the reaction. The ^{1}H NMR spectra showed the disappearance of signals corresponding to **3** and the appearance of new signals corresponding to **1** and **2**. Signals corresponding to **1** predominated in the initial spectra whereas signals for **2** increased in the later spectra. After a lengthy incubation period (~2 weeks), the MAL-catalyzed reaction was complete, resulting in 79% **1** and 12% **2** (Figure S5, Supporting Information).

Mutagenesis of His-194, Lys-331, and Gln-329

In order to investigate the importance of His-194, Lys-331, and Gln-329 for the activity and stereoselectivity of MAL, single site-directed mutants were constructed in which His-194 and Gln-329 were replaced with either an alanine or arginine (H194A, H194R, Q329A, and Q329R) and Lys-331 with a glycine, alanine, glutamine, histidine, or arginine (K331G, K331A, K331Q, K331H, and K331R). DNA sequencing verified that only the intended mutations had been introduced into each mutant gene. The mutants were overexpressed in *E. coli* strain TOP10 and purified to >95% homogeneity (as assessed by SDS-PAGE) using the Ni-based immobilized metal affinity chromatography protocol described for wild-type MAL. The yields (in milligrams of homogeneous protein per liter of cell culture) of the mutants varied from 10 mg to 20 mg.

It was shown by non-denaturing PAGE (data not shown) that the native molecular mass for each mutant is comparable to that of wild-type, indicating that the oligomeric association of the mutants was still intact. The structural integrity of the mutants was also assessed by circular dichroism (CD). The CD spectra of the mutants were comparable to that of the wild-type indicating that these mutations did not result in any major conformational changes (Figure S6, Supporting Information).

Kinetic and ^{1}H NMR analysis of the deamination of 2 by the MAL mutants

The activities of the MAL mutants were initially assayed using the natural substrate **2**. It was found that substitution of Lys-331 by a glycine, alanine, histidine, glutamine, or arginine essentially abolished enzymatic activity, underscoring the importance of this residue for the MAL-catalyzed deamination of **2**. Under the conditions of the kinetic assays, no activity could be detected for these mutants. Substitution of either His-194 or Gln-329 by an arginine also resulted in mutant enzymes that were inactive. The H194A and Q329A mutants, however, deaminate **2** although at a reduced catalytic efficiency (Table 2). For the H194A mutant, there is a slight (1.8-fold) increase in K_m and a ~160-fold decrease in k_{cat}, which results in a ~290-fold reduction in k_{cat}/K_m. For the Q329A mutant, there is a ~8900-fold decrease in k_{cat}, whereas the K_m is not affected. Hence, this results in a ~8900-fold reduction in k_{cat}/K_m.

The deamination activities of the three alanine mutants (H194A, K331A, and Q329A) were also assessed by ^{1}H NMR spectroscopy after a lengthy (~2 weeks) incubation period. Using **2**, the H194A- and Q329A-catalyzed reactions resulted in 40% **1** and 3% **3**, whereas the K331A-catalyzed reaction showed only a trace amount of product (2% **1** and 2% **3**).[16] These observations parallel those of the kinetic assays and suggest that Lys-331 is more critical for the deamination activity of MAL than His-194 and Gln-329.

Table 2. Kinetic parameters for the MAL-, K331A-, H194A-, and Q329A-catalyzed deamination of (2*S*,3*S*)-3-methylaspartic acid (**2**)[a].

Enzyme	k_{cat} (s^{-1})	K_m (mM)	k_{cat}/K_m (M^{-1} s^{-1})
MAL	89 ± 4	1.0 ± 0.1	8.9×10^4
K331A	ND	ND	<0.001
H194A	0.55 ± 0.01	1.8 ± 0.2	3.1×10^2
Q329A	0.01 ± 0.001	1.0 ± 0.1	1.0×10^1

[a]The steady state kinetic parameters were determined in 500 mM Tris-HCl buffer (pH 9.0) containing 20 mM $MgCl_2$ and 1 mM KCl at 30°C. Errors are standard deviations. ND, not determined.

pH dependence of the kinetic parameters of MAL and the H194A mutant using 2

In order to determine the pK_a of the basic group on the enzyme important for catalysis (the presumed general base catalyst) and to evaluate the effect of the alanine mutation on this pK_a, the pH dependence of the k_{cat}/K_m for the MAL- and H194A-catalyzed deamination of **2** was determined over the pH range 6.0-9.5. The other two alanine mutants, K331A and Q329A, were not active enough with **2** and thus could not be measured. The log (k_{cat}/K_m) vs pH profiles of MAL and H194A both show a single ascending limb with a slope of 1 (Figure 3).[17] For wild-type MAL, a pK_a value of 7.8 ± 0.1 was found. For the H194A mutant, a pK_a value of 8.2 ± 0.1 was found. Hence, within the estimated errors, there is no significant effect of the H194A substitution on the pK_a for the ascending limb.

^{1}H NMR analysis of the K331A-, H194A-, and Q329A-catalyzed deamination of 3

The deamination of the non-natural substrate **3** by the alanine mutants was monitored by ^{1}H NMR spectroscopy. After a 13 day-incubation period, the Q329A-catalyzed reaction resulted in 10% **1**. The contaminant **2**, which is the natural substrate for the enzyme, was selectively processed by Q329A at a rate much faster than for **3**. The H194A mutant also processed the contaminant **2**,

resulting in 6% **1**, but showed no detectable activity towards **3**. The mixture containing the K331A mutant showed no product.

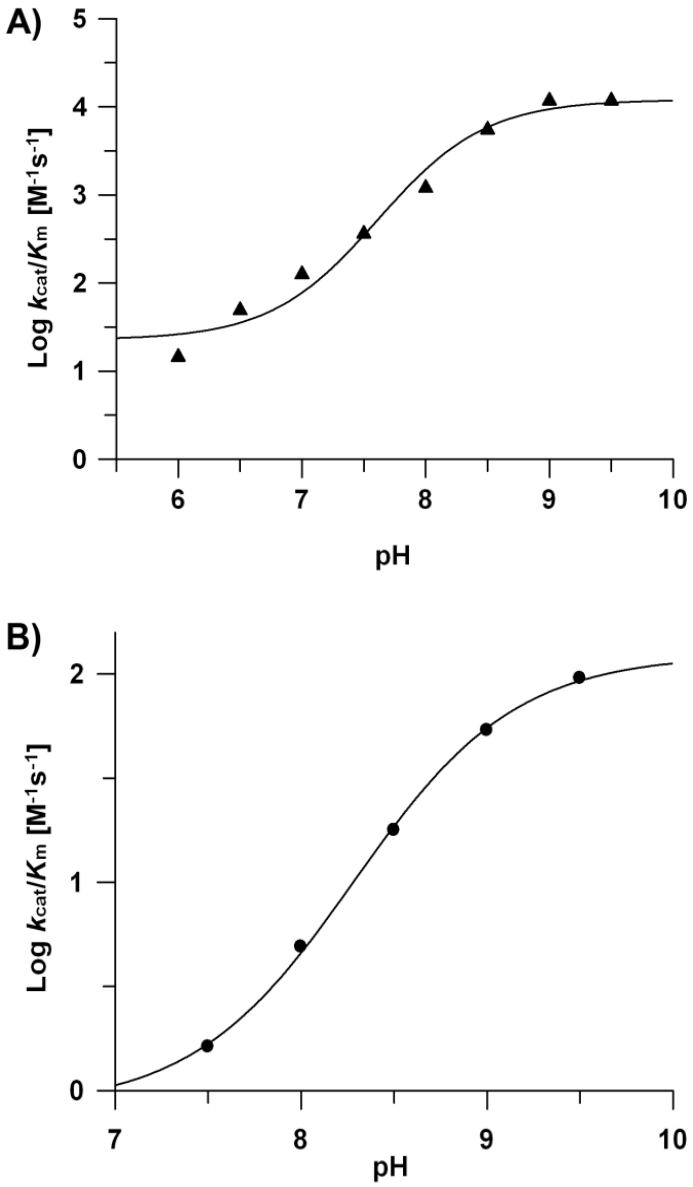

Figure 3. pH-dependence of log (k_{cat}/K_m) for the deamination of **2** by wild-type MAL (A) and the H194A mutant (B). The pK_a values are discussed in the text.

Kinetic and ^{1}H NMR analysis of the amination of 1 by the MAL mutants

The kinetic parameters for the amination reactions catalyzed by the MAL mutants were determined and compared to those measured for the wild-type MAL-catalyzed amination of **1** (Table 1). For the Q329A mutant, there is a slight increase in K_m (~2.4-fold) and a ~240-fold decrease in k_{cat}, which

results in a ~600-fold reduction in k_{cat}/K_m. For the H194A mutant, there is a 20-fold increase in K_m and only a ~7-fold decrease in k_{cat}, which results in a ~140-fold reduction in k_{cat}/K_m. Under the conditions of the kinetic assay, no activity could be detected for the other mutants (H194R, Q329R, K331G, K331A, K331Q, K331H, and K331R).

The amination of **1** by the three alanine mutants (H194A, Q329A, and K331A) was also monitored by ^{1}H NMR spectroscopy to identify the diastereoisomeric products of the reaction. After a 13 day-incubation period, the K331A-, Q329A-, and H194A-catalyzed reactions resulted in 30%, 58%, and 85% diastereoisomer **2**, respectively (Figure 2B; data not shown). Interestingly, and in contrast to the wild-type MAL-catalyzed amination of **1** (Figure 2A), there was no detectable formation of diastereoisomer **3** in the incubation mixtures. [For comparison, conversion of 35% of **1** by wild-type MAL results in 19% **2** and 16% **3**.] These observations indicate that the H194A, Q329A, and K331A mutants have enhanced diastereoselectivities and catalyze the highly stereoselective conversion of **1** to **2**, with no detectable conversion of **1** to **3**.

DISCUSSION

Previous studies of the stereoselectivity of *C. tetanomorphum* MAL indicated that the wild-type enzyme catalyzes the reversible *anti*- and *syn*-addition of ammonia to mesaconate (**1**) to yield (2*S*,3*S*)-3-methylaspartic acid (**2**) and (2*S*,3*R*)-3-methylaspartic acid (**3**), respectively.[2, 9] The determination of the X-ray structure of *C. amanolaticus* MAL in complex with the natural substrate **2** has provided the essential structural information for the identification of the substrate interactions within the enzyme-substrate complex.[13] Guided by the structure of this complex, we have selected three active site residues in *C. tetanomorphum* MAL[12] for mutagenesis to provide insight into the structural determinants of the reactivity and stereoselectivity of MAL.[18] The results of these studies are interpreted here and discussed in terms of a two-base mechanism, in which the proton abstraction/addition steps are effected by (*S*)- and (*R*)-specific general base/acid catalysts juxtaposed on either side of the (chiral) C-3 carbon of the substrate.

We first verified that both **2** and **3** are formed as products of the MAL-catalyzed amination of **1** by ^{1}H NMR spectroscopy. It was found that stereoisomer **2** is formed at a rate much faster than stereoisomer **3**. [At equilibrium, the ratio of **2**:**3** is ~1.3.] Second, we confirmed that MAL does not catalyze the direct epimerization of the two stereoisomers. This was evident from a prolonged incubation of MAL with **2**, which yielded **1** as the major product and gave only a trace amount of **3**. Another notable observation is that the incubation of MAL with **3** finally gives **2** (in 12% yield), but only after a significant amount of **1** had accumulated in the reaction mixture. This suggests that MAL first catalyzes the *syn*-elimination of ammonia from **3** to yield **1**, followed by the *anti*-addition of ammonia to **1** to give **2**. These observations indicate that the formation of **2** and **3** as products of the MAL-catalyzed amination of **1** is not the result of the MAL-catalyzed amination of **1** to **2** followed by the slow direct epimerization of **2** to **3**. Hence, MAL indeed catalyzes the rapid *anti*-addition and the much slower *syn*-addition of ammonia to **1** to give **2** and **3**, respectively.

The crystal structure of *C. amalonaticus* MAL in complex with **2** shows that Lys-331 is the only candidate in the vicinity of C-3 that can function as the (*S*)-specific base/acid catalyst (Figure 1B).[13] This lysine residue is conserved in all characterized 3-methylaspartate ammonia lyases. Moreover, a comparison of the active site structures of MAL and enolase shows that Lys-331 in MAL superimposes to within 1 Å of the previously identified general base Lys-345 in enolase.[13] To assess its role in catalysis, we have mutated Lys-331 to a glycine, alanine, histidine, glutamine, or arginine. Examination of the kinetic properties for these mutants clearly shows that Lys-331 is an essential residue in the MAL-catalyzed reactions because all five mutations at this position result in a dramatic loss of activity (there is a $>10^7$-fold drop in the value of k_{cat}/K_m using **2**). The mutant enzymes appear to retain an intact overall structural integrity as shown by CD spectroscopy. It is therefore reasonable to conclude that Lys-331 is crucial for catalysis because it functions as the (*S*)-specific base catalyst in the deamination of **2** and, hence, as the acid catalyst (the conjugate acid of Lys-331) in the corresponding reverse *anti*-addition reaction (Scheme 3).

From the ascending limb of the log (k_{cat}/K_m) vs pH profile of MAL, a residue with a pK_a of ~7.8, which must be deprotonated for optimal activity, may be the general base catalyst involved in abstraction of the C-3 proton of **2**. While the pK_a value of Lys-331 in MAL has not been directly measured by NMR spectroscopy, it can be inferred from these results that the kinetic pK_a value of 7.8 is likely due to Lys-331.

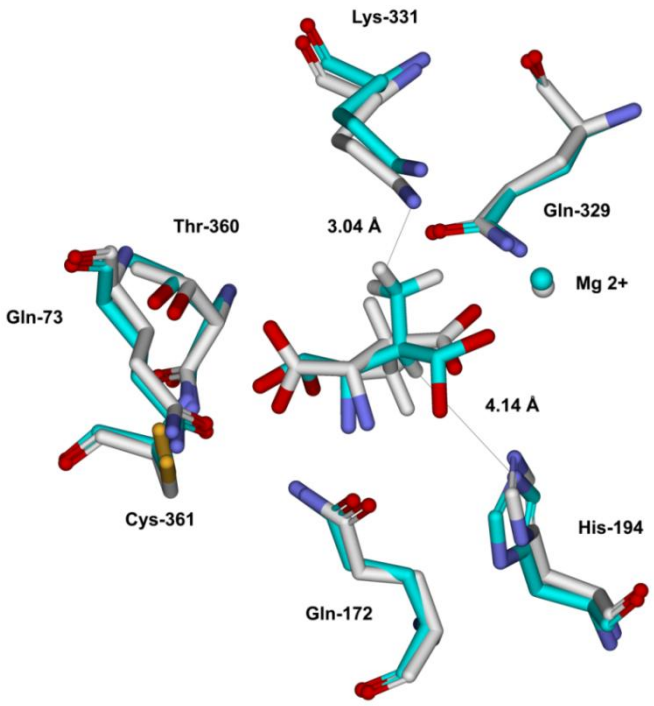

Figure 4. Close-up view of two superimposed active sites of *C. amalonaticus* MAL, one in complex with the natural substrate (2*S*,3*S*)-3-methylaspartic acid (**2**)[13] (shown in grey) and the other with the most favored conformation of the modeled non-natural substrate (2*S*,3*R*)-3-methylaspartic acid (**3**) (shown in cyan). The orientation of **2** suggests that its C-3 proton is abstracted by Lys-331, whereas the orientation of **3** suggests that its C-3 proton is abstracted by His-194. The Figure was prepared with Discovery Studio 1.7.

In the structure of the MAL-substrate complex, His-194 and Gln-329 are hydrogen bonded to the C-4 carboxylate group of **2** (Figure 1B).[13] This suggests roles for these residues in binding the substrate, and possible intermediates, in the reaction mechanism of MAL. In this study, His-194 and Gln-329 were mutated to assess their role in catalysis. The best characterized mutants are the H194A and Q329A mutants, which have measurable activity and show no significant differences in their CD spectra compared to that of wild-type MAL. Examination of the kinetic properties for the

two mutants in the deamination direction (using **2**) shows that there is a small effect on K_m and a much larger effect on k_{cat}. This suggests important roles for His-194 and Gln-329 in catalysis. The somewhat larger effect of these mutations on the value of K_m in the amination direction may suggest a more important role for His-194 and Gln-329 in binding **1** than **2**.

A major part of the loss in activity of the H194A and Q329A mutants is likely due to the removal of optimal hydrogen-bonding interactions with the proposed enolate anion intermediate formed at the C-4 carbonyl position of **2** (or **1** in the corresponding reverse reaction), making the abstraction of a proton from the C-3 position less favorable. Presumably, His-194 and Gln-329, together with the essential Mg^{2+} ion, polarize the C-4 carboxylate group and stabilize the enolate anion intermediate (**4**) formed upon abstraction of the C-3 proton (Scheme 3). An electrophilic residue whose role is to assist the Mg^{2+} ion in providing the charge neutralization that is essential for the activation of the α-proton and for stabilization of the enolate anion intermediate has also been identified in mandelate racemase (Lys-164) and some other enolase superfamily members.[14, 19]

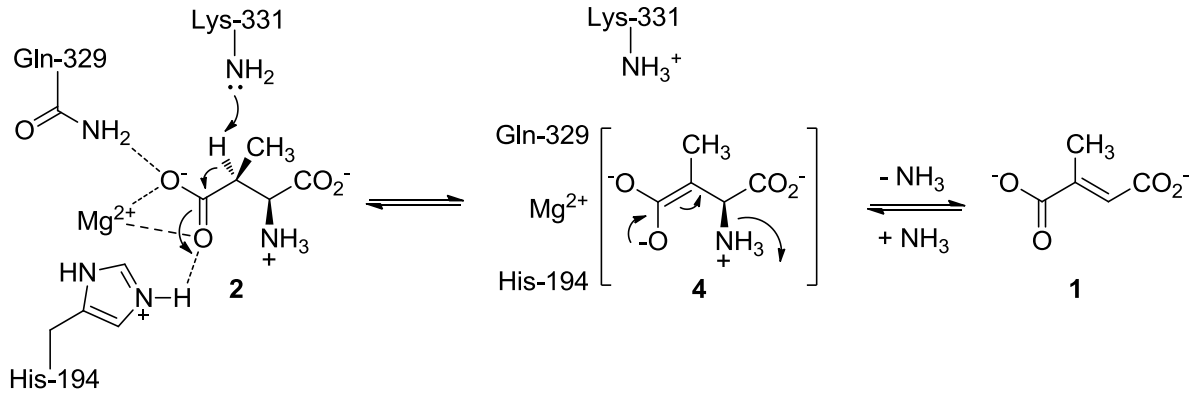

Scheme 3. A schematic representation of the proposed catalytic mechanism of MAL, showing the key participants in the deamination of (2*S*,3*S*)-3-methylaspartic acid.

In addition to its presumed role as electrophilic residue, His-194 may also function as the (*R*)-specific base/acid catalyst. Naismith and co-workers first proposed this role for His-194 based on structure comparisons of enolase superfamily members.[12] The side chain of His-194

superimposes on that of the second base Lys-166 in mandelate racemase and the principal base Lys-213 in glucarate dehydratase.[12] Moreover, if the three-dimensional structure of **3** is modeled into the active site of MAL, using the X-ray structure of MAL in complex with **2** as a guide, then the C-3 proton of **3** is faced towards the imidazole nitrogen (Nε2) of His-194 (Figure 4). Our experiments clearly show that His-194 is an important determinant of the stereoselectivity of MAL because an alanine mutation at this position results in a mutant enzyme that appears to have lost its ability to catalyze proton abstraction/addition from the (*R*) face (the His-194 side) of the substrate. Indeed, the H194A mutant has no detectable deamination activity with **3** and catalyzes the highly stereoselective conversion of **1** to **2**, with no detectable formation of **3**. Taken together, these observations are consistent with a role of His-194 as the (*R*)-specific general base catalyst for the deamination of **3** and, hence, as the acid catalyst (the conjugate acid of His-194) in the corresponding reverse *syn*-addition reaction.

In view of the presumed role of His-194 as the (*R*)-specific general base/acid catalyst, mutation of Lys-331 or Gln-329 to an alanine gave results that were somewhat unexpected. Initially, it was thought that mutation of Lys-331 would only effect proton abstraction/addition from the (*S*) face (the Lys-331 side) of the substrate. Surprisingly, however, the K331A mutant lost its ability to catalyze proton abstraction/addition from the (*R*) face of the substrate, while retaining a very low-level proton abstraction/addition activity from the (*S*) face of the substrate. Like K331A, the Q329A mutant also catalyzes the highly stereoselective conversion of **1** to **2** with no detectable formation of **3**. But, in contrast to K331A, the Q329A mutant still has a detectable low-level deamination activity with **3**.

One potential explanation for the alteration in diastereoselectivity of the K331A and Q329A mutants is that mutation of Lys-331 or Gln-329 to an alanine causes different interactions between substrate and enzyme and may influence the geometry of a Michaelis complex that undergoes proton abstraction/addition from the (*R*) face of the substrate. In this scenario, the removal of the

native interactions with the substrate locate the substrate in an unfavorable position to undergo proton abstraction/addition by His-194, the presumed (*R*)-specific base/acid catalyst. Another explanation for the loss in proton abstraction/addition activity from the (*R*) face of the substrate is that mutation of Lys-331 or Gln-329 by an alanine directly influences the orientation of the His-194 side chain. Crystallographic studies of the H194A, K331A and Q329A mutants, and of wild-type MAL in complex with **3**, would be an important step toward understanding how these mutations affect the stereochemical properties of MAL.

The current investigation has clearly demonstrated that the stereoselectivity of MAL can be enhanced by mutation of the active site residues His-194, Lys-331 and Gln-329. Interestingly, the mutation of Gln-73 or Gln-172, two residues implicated in binding the C-2 amino group of **2** (Figure 4), to an alanine has a profound effect on the values of k_{cat} and k_{cat}/K_m (using **2**) but no significant effect on the stereoselectivity of MAL. Like wild-type MAL, the Q73A and Q172A mutants catalyze the amination of **1** to give both **2** and **3** as products [H. Raj and G.J. Poelarends (2009), unpublished results]. Hence, His-194, Gln-329, and Lys-331 appear to be the major determinants of the stereoselectivity of MAL. The enhancement of the stereoselectivity should make it possible to utilize single amino acid variants of MAL (e.g., H194A) in stereo- and regioselective amination reactions to produce 3-substituted aspartic acid isomers with a very high diastereomeric excess. Such efforts are being pursued in our laboratories.

EXPERIMENTAL SECTION

Materials

DL-*threo*-3-methylaspartic acid, mesaconic acid, and L-arabinose were purchased from Sigma-Aldrich Chemical Co. (St. Louis, MO). (2*S*,3*R*)-3-Methylaspartic acid (95% purity) was purchased from Syncom (Groningen, The Netherlands). Ingredients for buffers and media were obtained from Duchefa Biochemie (Haarlem, The Netherlands) or Merck (Darmstadt, Germany). Molecular biology reagents, including restriction enzymes, PCR reagents, T4 DNA ligase, DNA ladders, agarose, and protein molecular weight standards were obtained from F. Hoffmann-LaRoche, Ltd. (Basel, Switzerland), Promega Corp. (Madison, WI), Invitrogen Corp. (Carlsbad, CA), Finnzymes (Espoo, Finland) or New England Biolabs (Ipswich, MA). PCR purification, gel extraction, and Miniprep kits were provided by Macherey-Nagel (Düren, Germany). Pre-packed PD-10 Sephadex G-25 columns were purchased from GE Healthcare Bio-Sciences AB (Uppsala, Sweden). Oligonucleotides for DNA amplification were synthesized by Operon Biotechnologies (Cologne, Germany).

Bacterial strains, plasmids, and growth conditions

E. coli strain XL1-Blue (Stratagene, La Jolla, CA) was used for cloning and isolation of plasmids. *E. coli* strain TOP10 (Invitrogen) was used in combination with the pBAD/*Myc*-His A vector (Invitrogen) for recombinant protein production. *C. tetanomorphum* ATCC 15920, the genomic DNA source for the MAL gene, was purchased from DSMZ GmbH (Braunschweig, Germany). *E. coli* cells were grown in Luria-Bertani (LB) media. When required, Difco agar (15 g/L), ampicillin (Ap, 100 μg/mL), and/or arabinose (0.004% *w/v*) were added to the medium.

General methods

Techniques for restriction enzyme digestions, ligation, transformation, and other standard molecular biology manipulations were based on methods described elsewhere[20] or as suggested by the manufacturer. The PCR was carried out in a DNA thermal cycler (model GS-1) obtained from

Biolegio (Nijmegen, The Netherlands). DNA sequencing was performed by ServiceXS (Leiden, The Netherlands) or Macrogen (Seoul, Korea). Protein was analyzed by polyacrylamide gel electrophoresis (PAGE) under either denaturing conditions using sodium dodecyl sulfate (SDS) or native conditions on gels containing polyacrylamide (7.5-10%). The gels were stained with Coomassie brilliant blue. Protein concentrations were determined by the Waddell method.[21] Kinetic data were obtained on a V-650 spectrophotometer from Jasco (IJsselstein, The Netherlands). The cuvettes were mixed using a stirr/add cuvette mixer (Bel-Art Products, Pequannock, NJ). The kinetic data were fitted by nonlinear regression data analysis using the Grafit program (Erithacus, Software Ltd., Horley, U.K.) obtained from Sigma Chemical Co. The CD spectra were recorded on a model 62A-DS spectropolarimeter from AVIV Biomedical Inc. (Lakewood, NJ). ^{1}H NMR spectra were recorded on a Varian Inova 500 (500 MHz) spectrometer using a pulse sequence for selective presaturation of the water signal. Chemical shifts for protons are reported in parts per million scale (δ scale) downfield from tetramethylsilane and are referenced to protium in the NMR solvents (H_2O: $\delta = 4.67$).

Construction of the expression vector for the production of MAL

The MAL gene was amplified by the PCR using two synthetic primers, a small amount of biomass from *C. tetanomorphum* as the genomic DNA source, and the PCR reagents supplied in the Expand High Fidelity PCR system following the protocol supplied with the system (F. Hoffmann-La Roche, Ltd.). The forward primer (5'-ATA**CATATG**AAAATTGTTGACGTACTTTG-3') contains a *Nde*I restriction site (in bold) followed by 20 bases corresponding to the coding sequence of the MAL gene. The reverse primer (5'-CAT**AAGCTT**TTTTCTTCTTCCTACAAG-3') contains a *Hin*dIII restriction site (in bold) followed by 18 bases corresponding to the complementary sequence of the MAL gene. The resulting PCR product and the pBAD*N*/*Myc*-His A vector were digested with *Nde*I and *Hin*dIII restriction enzymes, purified, and ligated using T4 DNA ligase. The pBAD*N*/*Myc*-His A vector is a variant of the commercially available pBAD/*Myc*-His A vector in which the unique

*Nco*I site is replaced with *Nde*I.[22] Aliquots of the ligation mixture were transformed into competent *E. coli* TOP10 cells. Transformants were selected at 37°C on LB/Ap plates. Plasmid DNA was isolated from several colonies and analyzed by restriction analysis for the presence of the insert. The cloned MAL gene was sequenced to verify that no mutations had been introduced during the amplification of the gene. The newly constructed expression vector was named pBAD(MAL-His).

Construction of MAL mutants

Mutants of MAL were generated by the overlap extension PCR method[23] using plasmid pBAD(MAL-His) as the template. The final PCR products were gel purified, digested with *Nde*I and *Hin*dIII restriction enzymes, and ligated in frame with both the initiation ATG start codon and the sequence that codes for the polyhistidine region of the expression vector pBAD*N*/*Myc*-His A. All mutant genes were completely sequenced (with overlapping reads) to verify that only the intended mutation had been introduced.

Expression and purification of MAL wild-type and mutants

The MAL enzyme, either wild-type or mutant, was produced in *E. coli* TOP10 using the pBAD expression system. Fresh TOP10 cells containing the appropriate expression plasmid were collected from a LB/Ap plate using a sterile loop and used to inoculate LB/Ap medium (15 mL). After growth for 8 h at 37°C, a sufficient quantity of the culture was used to inoculate fresh LB/Ap medium (300 mL), containing arabinose (0.004%, w/v), in a 1 L Erlenmeyer flask to an initial A_{600} of ~0.1. Cultures were grown for 4 days at 17°C with vigorous shaking. Cells were harvested by centrifugation (6000*g*, 15 min) and stored at -20°C until further use.

In a typical purification experiment, cells of three 300-mL cultures were thawed, combined, and suspended in lysis buffer (10 mL, 50 mM NaH_2PO_4, 300 mM NaCl, 10 mM imidazole, pH 8.0). Cells were disrupted by sonication for 4 x 1 min (with 4-6 min rest in between each cycle) at a 60

W output, after which unbroken cells and debris were removed by centrifugation (10,000*g*, 45 min). The supernatant was filtered through a 0.45 μM-pore diameter filter and incubated with Ni-NTA (1 mL slurry in a small column at 4°C for ≥18 h), which had previously been equilibrated with lysis buffer. The non-bound proteins were eluted from the column by gravity flow. The column was first washed with lysis buffer (10 mL) and then with buffer A (50 mM NaH_2PO_4, 300 mM NaCl, 20 mM imidazole, pH 8.0; 10 mL). Retained proteins were eluted with buffer B (50 mM NaH_2PO_4, 300 mM NaCl, 250 mM imidazole, pH 8.0; 2.0 mL). Fractions (~0.5 mL) were analyzed by SDS-PAGE on gels containing acrylamide (10%), and those that contained purified MAL were combined and the buffer was exchanged against Tris buffer (50 mM, pH 8.0), containing $MgCl_2$ (2 mM) and KCl (0.1 mM), using a pre-packed PD-10 Sephadex G-25 gel filtration column. The purified enzyme was stored at +4°C or −80°C until further use.

Circular dichroism spectroscopy

Circular dichroism spectra of the wild-type protein and the purified mutants were measured in Tris-HCl buffer (10 mM, pH 8.0), containing $MgCl_2$ (2 mM) and KCl (0.1 mM), at a concentration of approximately 3.2 μM in a CD cell with a 1.0-mm optical path length.

Kinetic assays

The assays used for the spectrophotometric determination of the deamination of **2** and to follow the amination of **1** are based on protocols reported elsewhere.[3] Accordingly, the deamination of **2** by MAL was monitored by following the formation of **1** at 240 nm (ε = 3850 M^{-1} cm^{-1}) in Tris-HCl buffer (500 mM, pH 9.0) containing $MgCl_2$ (20 mM) and KCl (1 mM) at 30°C. An aliquot of MAL, either wild-type or mutant, was diluted into buffer (20 mL) and incubated for 30 min at 30°C. The 30 min equilibration period results in more reproducible kinetic data. Subsequently, a 1-mL portion was transferred to a 10 mm quartz cuvette and the enzyme activity was assayed by the addition of a small quantity (1-10 μL) of **2** from a stock solution. The stock solutions were made up by

dissolving the appropriate amount of DL-*threo*-3-methylaspartic acid, a 1:1 mixture of the enantiomers (2*S*,3*S*)-3-methylaspartic acid and (2*R*,3*R*)-3-methylaspartic acid, in Tris-HCl buffer (500 mM, pH 9.0) to obtain the desired concentration of **2**. The (2*R*,3*R*)-enantiomer is not a substrate nor an inhibitor of MAL. The concentrations of **2** used in the assay ranged from 0.5 to 20 mM.

The rate of amination of **1** was monitored by following the depletion of **1** at 270 nm ($\varepsilon = 482$ M^{-1} cm^{-1}) in Tris-HCl buffer (500 mM, pH 9.0) containing $MgCl_2$ (20 mM) and NH_4Cl (400 mM) at 30°C.[3] An aliquot of MAL, either wild-type or mutant, was diluted into buffer (20 mL) and incubated for 30 min at 30°C. Subsequently, a 1-mL portion was transferred to a 1 or 10 mm quartz cuvette and the enzyme activity was assayed by the addition of a small quantity (1-10 μL) of **1** from a stock solution. The stock solutions were made up in Tris-HCl buffer (500 mM, pH 9.0). The concentrations of **1** used in the assay ranged from 0.1 to 50 mM.

pH dependence of the kinetic parameters of MAL and H194A

The pH dependence of the steady-state kinetic parameters was determined in Tris buffer (500 mM) containing $MgCl_2$ (20 mM) and KCl (1 mM) with pH values ranging from 6.0 to 9.5. For each pH value, a sufficient quantity of enzyme (from a stock solution in Tris buffer (50 mM, pH 8.0) containing 2 mM $MgCl_2$ and 0.1 mM KCl) was equilibrated in buffer (20 mL) for 30 min at 30°C. The addition of enzyme did not significantly change the pH. Subsequently, aliquots (1 mL) were removed and assayed for activity using concentrations of **2** ranging from 0.5 to 50 mM. Stock solutions of **2** were made in Tris buffer (500 mM). The pH of the stock solutions was adjusted to each desired pH value (6.0-9.5). The volume of substrate added was 20 μL or less in all experiments.

^{1}H NMR spectroscopic product analysis of the amination of 1 by MAL wild-type and mutants

The products of the amination of **1** by wild-type MAL and the MAL mutants were identified by ^{1}H NMR spectroscopy using a procedure described elsewhere[2] with the following modifications. In separate experiments, MAL, K331A, H194A or Q329A was incubated with **1**, and the reactions were followed by ^{1}H NMR spectroscopy. Reaction mixtures consisted of 350 μL of Na_2HPO_4 buffer (100 mM, containing 20 mM $MgCl_2$ and 1 mM KCl, pH 9.0), D_2O (50 μL), NH_4Cl (100 μL, 5 M), and an aliquot of **1** (100 μL) from a 500 mM stock solution. The stock solution of **1** was made in Na_2HPO_4 buffer (100 mM), and the pH of the solution was adjusted to 9.0 with aliquots of an aqueous NaOH solution (1 M). A quantity of enzyme (50 μL) was added from a stock solution and the reaction mixtures were incubated at 22°C. The concentrations of the protein stock solutions were 12.3 mg/mL for MAL, 13.4 mg/mL for K331A, 10.7 mg/mL for H194A, and 14.4 mg/mL for Q329A. Additional aliquots of enzyme (50 μL) were added to the individual mixtures after 3, 6, 9, and 12 days. ^{1}H NMR spectra were recorded 1 h, 3 days, 7 days, and 13 days after the first addition of enzyme. Product amounts were estimated by integration of the signals corresponding to **2** and **3**, if present. The ^{1}H NMR signals for **1**, **2**, and **3** are given in the Supporting Information (Figures S1, S2 and S3).

^{1}H NMR spectroscopic product analysis of the reaction of wild-type and mutant MAL with 2 or 3

The products of the deamination of **2** or **3** by wild-type MAL and the MAL mutants were identified by ^{1}H NMR spectroscopy. In separate experiments, MAL, K331A, H194A or Q329A was incubated with **2** or **3**. Reaction mixtures consisted of 400 μL of Na_2HPO_4 buffer (100 mM, containing 20 mM $MgCl_2$ and 1 mM KCl, pH 9.0), D_2O (40 μL), and an aliquot of **2** or **3** (150 μL) from a 500 mM stock solution. The stock solutions of **2** and **3** were made in Na_2HPO_4 buffer (100 mM), and the pH of the solutions was adjusted to 9.0 with aliquots of an aqueous NaOH solution (1 M). A quantity of enzyme (50 μL) was added from a stock solution and the reaction mixtures were

incubated at 22°C. The concentrations of the protein stock solutions were 15.7 mg/mL for MAL, 12.8 mg/mL for K331A, 7.4 mg/mL for H194A, and 8.8 mg/mL for Q329A. Additional aliquots of enzyme (50 μL) were added to the individual mixtures after 3, 6, 9, and 12 days. The eight reaction mixtures were examined by ^{1}H NMR spectroscopy after a 13 day-incubation period, and the product amounts were estimated by integration of the signals corresponding to **1**, **2** and **3**, if present.

Molecular docking

Comparative docking simulations were performed using Discovery Studio 1.7 (Accelrys, San Diego, CA, USA). Models for the enzymes were based on the structures of *C. amanolaticus* MAL in complex with **2**[13] and *C. tetanomorphum* MAL in the absence of a bound ligand[12] (Protein Data Bank ID 1KKR and 1KCZ, respectively). Hydrogens were added automatically. Models of the substrates were constructed and energy minimized using the CHARMm (Momany and Rone) forcefield.[24] Minimization was done using a dielectric constant of 1 and a non-bonded cutoff distance of 12 Å. The substrates were docked using the grid-based approach CDOCKER, a molecular dynamics (MD) simulated-annealing-based algorithm,[25, 26] using as coordinates the experimentally determined binding site for **2** in *C. amanolaticus* MAL. Initially, the enzyme active site was fixed and the atoms of the substrate, either **2** or **3**, were allowed to move. For subsequent rounds of minimization, the constraints on the amino acids forming the active site were removed and replaced by distance constraints based on the reported distances observed in X-ray structure of MAL complexed with **2**. A final minimization step was applied to each ligand docked pose, consisting of 300 steps of steepest descent followed by 2500 iterations of the adopted basis-set Newton–Raphson algorithm using an energy tolerance of 0.001 Kcal mol^{-1}.

ACKNOWLEDGEMENTS

We gratefully acknowledge Gea K. Schuurman-Wolters (Department of Biochemistry, University of Groningen) for her assistance in acquiring the CD spectra. We are also grateful to Pieter van der Meulen (Molecular Dynamics group, University of Groningen) for his assistance in acquiring the NMR spectra. We thank Dr. Stefaan de Wildeman, Dr. Oliver May, Dr. Friso van Assema, and Dr. Bernard Kaptein (DSM Geleen, The Netherlands) for insightful discussions. This research was financially supported by the Netherlands Ministry of Economic Affairs and the B-Basic partner organizations (www.b-basic.nl) through B-Basic, a public-private NWO-ACTS programme. G.J.P. was supported by VENI and VIDI grants from the Division of Chemical Sciences of the Netherlands Organisation of Scientific Research (NWO-CW).

Abbreviations; Ap, ampicillin; CD, circular dichroism; LB, Luria-Bertani; MAL, 3-methylaspartate ammonia-lyase; NMR, nuclear magnetic resonance; SDS-PAGE, sodium dodecyl sulfate-polyacrylamide gel electrophoresis.

REFERENCES

1. H. A. Barker, R. D. Smyth, R. M. Wilson, H. Weissbach, *J. Biol. Chem.* **1959**, *234*, 320-328.
2. S. K. Goda, N. P. Minton, N. P. Botting, D. Gani, *Biochemistry* **1992**, *31*, 10747-10756.
3. N. P. Botting, M. Akhtar, M. A. Cohen, D. Gani, *Biochemistry* **1988**, *27*, 2953-2955.
4. M. S. Gulzar, M. Akhtar, D. Gani, *J. Chem. Soc., Perkin Trans. 1* **1997**, 649-655.
5. H. J. Bright, *J. Biol. Chem.* **1964**, *239*, 2307-2315.
6. H. J. Bright, L. L. Ingraham, R. E. Lundin, *Biochim. Biophys. Acta* **1964**, *81*, 576.
7. N. P. Botting, M. A. Cohen, M. Akhtar, D. Gani, *Biochemistry* **1988**, *27*, 2956-2959.
8. N. P. Botting, D. Gani, *Biochemistry* **1992**, *31*, 1509-1520.
9. C. H. Archer, N. R. Thomas, D. Gani, *Tetrahedron Asym.* **1993**, *4*, 1141-1152.
10. C. H. Archer, D. Gani, *J. Chem. Soc., Chem. Commun.* **1993**, 140-142.

11. D. Gani, C. H. Archer, N. P. Botting, J. R. Pollard, *Bioorg. Med. Chem.* **1999**, *7*, 977-990.

12. M. Asuncion, W. Blankenfeldt, J. N. Barlow, D. Gani, J. H. Naismith, *J. Biol. Chem.* **2002**, *277*, 8306-8311.

13. C. W. Levy, P. A. Buckley, S. Sedelnikova, Y. Kato, Y. Asano, D. W. Rice, P. J. Baker, *Structure* **2002**, *10*, 105-113.

14. P. C. Babbitt, M. S. Hasson, J. E. Wedekind, D. R. J. Palmer, W. C. Barrett, G. H. Reed, I. Rayment, D. Ringe, G. L. Kenyon, J. A. Gerlt, *Biochemistry* **1996**, *35*, 16489-16501.

15. The diastereoisomer **2** can be easily distinguished from the diastereoisomer **3** in ^{1}H NMR spectra by examining the chemical shifts for the signals due to the protons of the methyl groups, which occur at ~0.95 and ~1.08 ppm, respectively.

16. The purchased material used as substrate **2** is actually a 1:1 mixture of the enantiomers (2*S*,3*S*)- and (2*R*,3*R*)-3-methylaspartic acid. The (2*R*,3*R*)-enantiomer is not a substrate nor an inhibitor of MAL. Hence, the maximal yield of **1** in these experiments is 50%.

17. A pK_a reflecting the α-amino group of **2** is not observed in the log (k_{cat}/K_m) vs pH profile since data were not collected to high enough pH to define such a pK_a. It is important to note that the proposed protonation state of the α-amino group (Schemes 1-3) is consistent with the observation that this group occupies a region of the active site pocket that is solvent exposed.[13]

18. A comparison of the crystal structures of *C. amanolaticus* MAL (in complex with **2**)[13] and *C. tetanomorphum* MAL (in the absence of a bound ligand)[12] shows that all active site residues are positionally conserved, although the side-chain orientation of Lys-331 is somewhat different. Moreover, modeling of the three-dimensional structure of **2** into the active site of *C. tetanomorphum* MAL, using the X-ray structure of the *C. amanolaticus* MAL in complex with **2** as a guide, gives similar substrate interactions within the two enzyme active sites (data not shown). These observations suggest that both MAL enzymes have a highly similar substrate binding mode and catalytic mechanism.

19. B. Mitra, A. T. Kallarakal, J. W. Kozarich, J. A. Gerlt, J. G. Clifton, G. A. Petsko, G. L. Kenyon, *Biochemistry* **1995**, *34*, 2777-2787.

20. J. Sambrook, E. F. Fritsch, T. Maniatis, *Molecular Cloning: A Laboratory Manual*, 2nd ed., Cold Spring Harbor Laboratory Press, Cold Spring Harbor, NY, **1989**.

21. W. J. Waddell, *J. Lab. Clin. Med.* **1956**, *48*, 311-314.

22. N. M. Kamerbeek, M. W. Fraaije, D. B. Janssen, *Eur. J. Biochem.* **2004**, *271*, 2107-2116.

23. S. N. Ho, H. D. Hunt, R. M. Horton, J. K. Pullen, L. R. Pease, *Gene* **1989**, *77*, 51-59.

24. A. D. J. MacKerell, B. R. Brooks, C. L. I. Brooks, L. Nilsson, B. Roux, Y. Won, M. Karplus in *Encyclopedia of Computational Chemistry* (Ed.: P. V. Schleyer), John Wiley, Chichester, **1998**, pp. 271–277.

25. J. A. Erickson, M. Jalaie, D. H. Robertson, R. A. Lewis, M. Vieth, *J. Med. Chem.* **2004**, *47*, 45–55.

26. G. Wu, D. H. Robertson, C. L. Brooks, III, M. Vieth, *J. Comput. Chem.* **2003**, *24*, 1549–1562.

27. W. L. DeLano, *The PyMOL molecular graphics system*, DeLano Scientific, San Carlos, CA, USA, **2002**. (http://www.pymol.org).

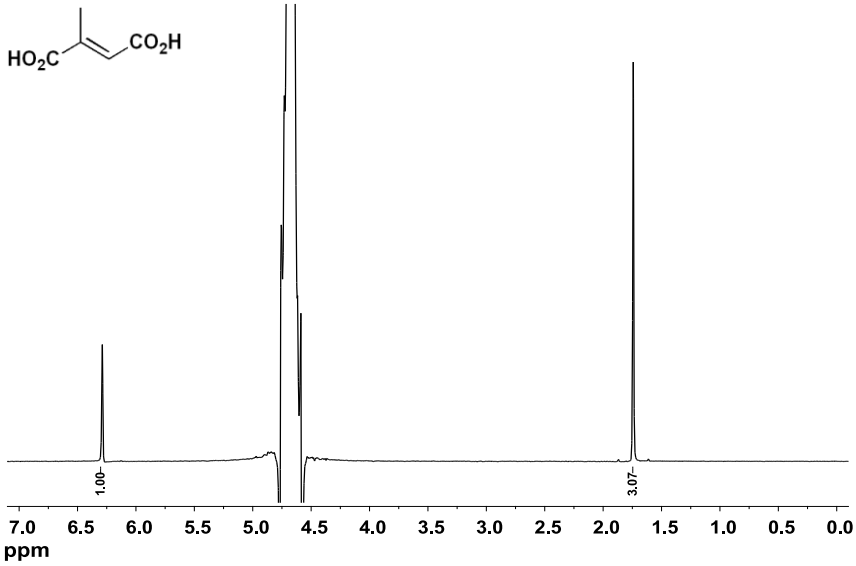

Figure S1. ^{1}H NMR spectrum of mesaconate (**1**). δ = 1.73 (s, 3H; CH_3), 6.28 (s, 1H; CH).

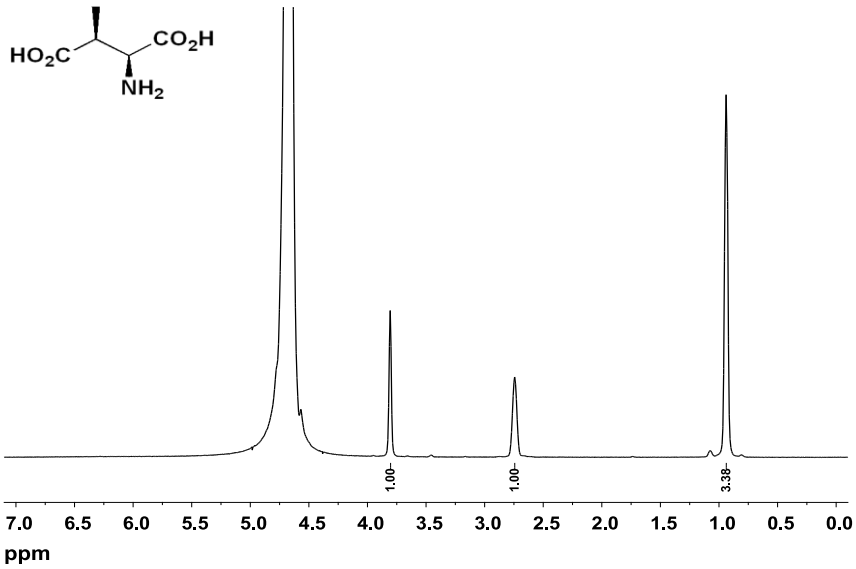

Figure S2. ^{1}H NMR spectrum of the material used as substrate **2**, which is a 1:1 mixture of the enantiomers (2*S*,3*S*)- and (2*R*,3*R*)-3-methylaspartic acid. The (2*R*,3*R*)-enantiomer is not a substrate nor an inhibitor of MAL. δ = 0.94 (s, 3H; CH_3), 2.74 (s, 1H; CH), 3.81 (s, 1H; CH).

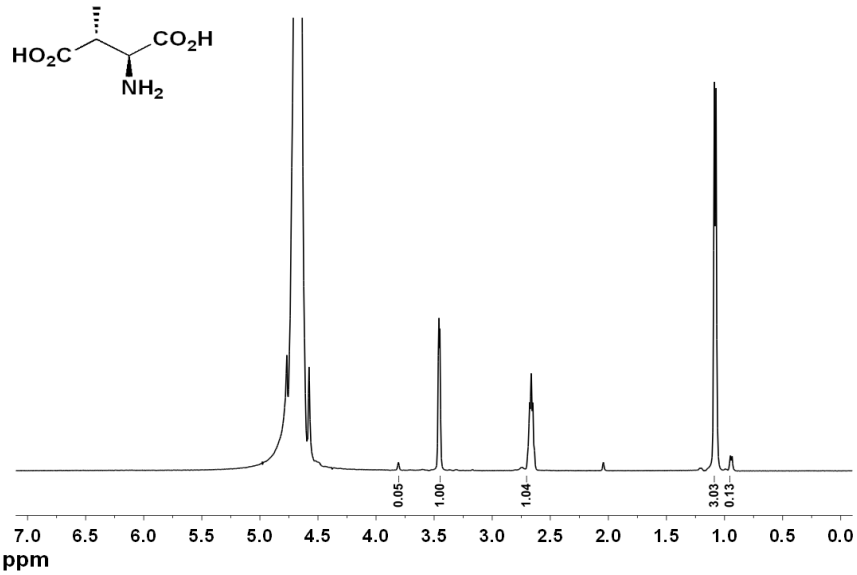

Figure S3. ^{1}H NMR spectrum of (2*S*,3*R*)-3-methylaspartic acid (**3**). δ = 1.08 (d, ^{3}J = 7.0 Hz, 3H; CH_3), 2.63-2.70 (m, 1H; CH), 3.46 (d, ^{3}J = 4.0 Hz, 1H; CH). Contaminant **2** (5-6%): δ = 0.94 (d), 2.04 (s), 2.74 (m), 3.81 (s).

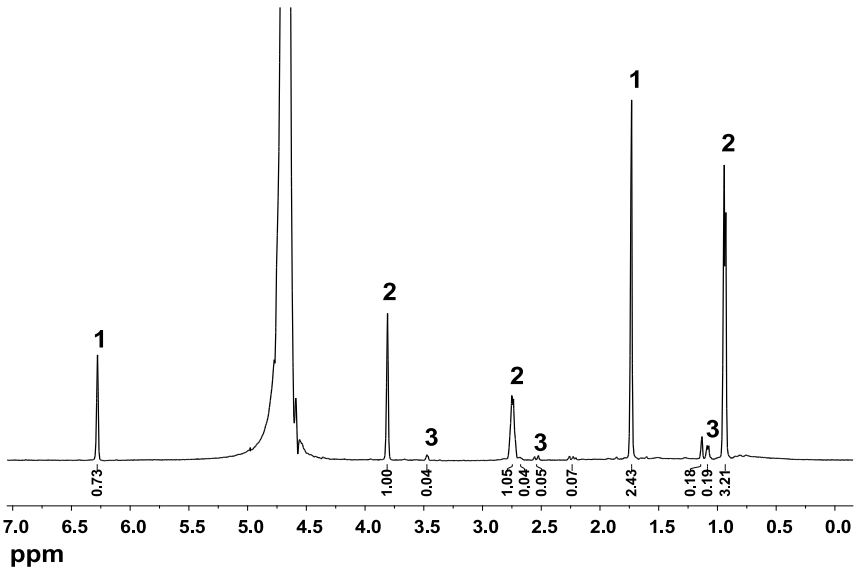

Figure S4. ^{1}H NMR spectrum identifying the products of the MAL-catalyzed deamination of **2**. The spectrum was taken after a 13 day-incubation period. Ratio **1** : **2** : **3** = 41 : 57 : 2. δ = 0.93 (d, ^{3}J = 6.5 Hz, 3H; CH_3), 1.08 (d, ^{3}J = 7.5 Hz, 3H; CH_3), 1.74 (s, 3H; CH_3), 2.71-2.78 (m, 2H; CH), 3.46-3.48 (m, 1H; CH), 3.81 (s, 1H; CH), 6.28 (s, 1H; CH_3). Impurity δ = 1.13 (s), 2.24 (d), 2.54 (d).

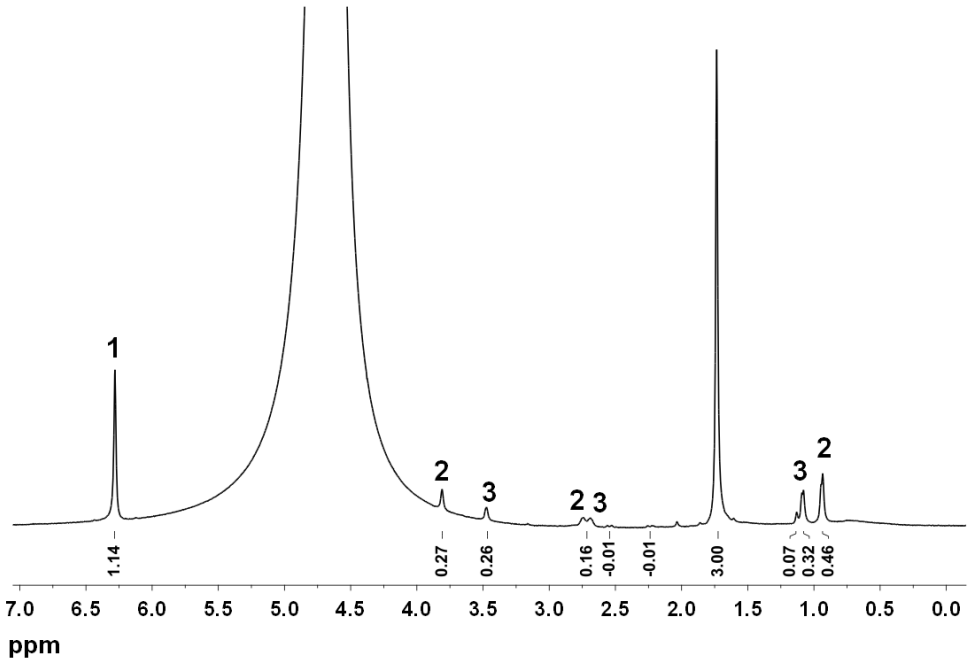

Figure S5. ^{1}H NMR spectrum identifying the products of the MAL-catalyzed deamination of **3**. The spectrum was taken after a 13 day-incubation period. Ratio **1** : **2** : **3** = 79 : 12 : 9. δ = 0.93 (d, ^{3}J = 6.5 Hz, 3H; CH_3), 1.08 (d, ^{3}J = 7.5 Hz, 3H; CH_3), 1.74 (s, 3H; CH_3), 2.65-2.78 (m, 2H, CH), 3.47 (s, 1H; CH), 3.81 (s, 1H; CH), 6.28 (s, 1H; CH_3). Impurity δ=1.13 (s), 2.24 (d), 2.54 (d).

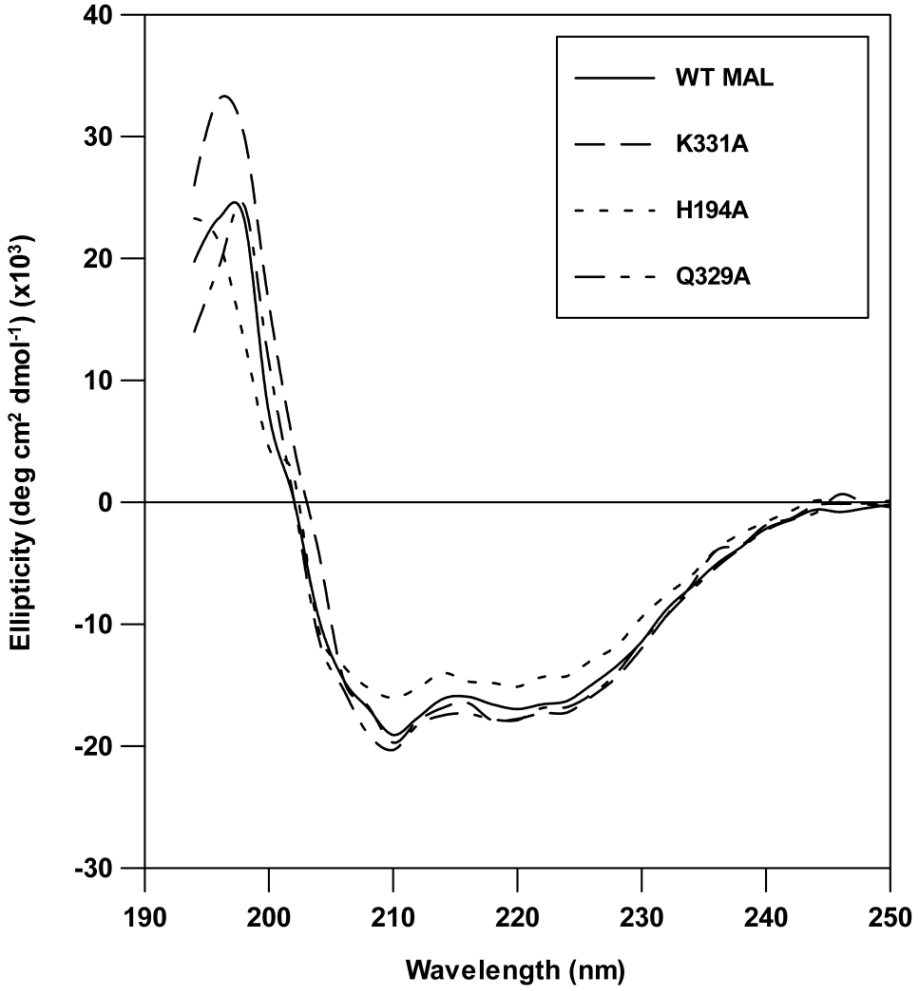

Figure S6. Superimposed far-UV CD spectra of wild-type and mutant enzymes. The CD spectra of all the mutants were comparable to that of wild-type MAL, but for clarity only the CD spectra of the K331A, H194A, and Q329A mutants are shown. Spectra were measured in 10 mM Tris buffer (pH 8.0), containing 2 mM $MgCl_2$ and 0.1 mM KCl, at a protein concentration of approximately 3.2 µM.

Chapter 3

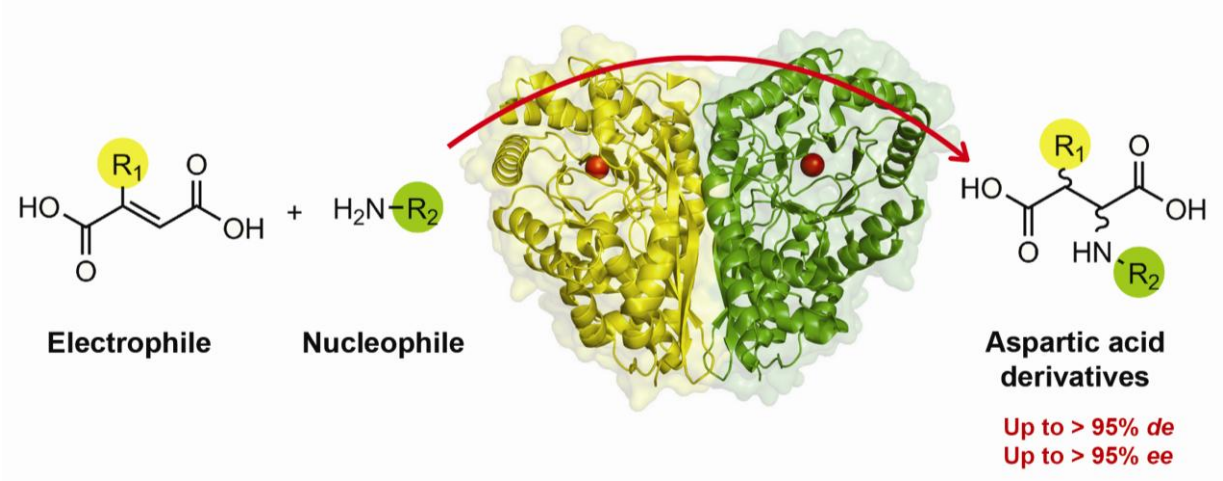

Engineering methylaspartate ammonia lyase for the asymmetric synthesis of unnatural amino acids

Hans Raj,[a] Wiktor Szymański,[b,c] Jandré de Villiers,[a] Henriëtte J. Rozeboom,[d] Vinod Puthan Veetil,[a] Carlos R. Reis,[a] Marianne de Villiers,[a] Frank J. Dekker,[e] Stefaan de Wildeman,[f] Wim J. Quax,[a] Andy-Mark W.H. Thunnissen,[d] Ben L. Feringa,[c] Dick B. Janssen,[b] and Gerrit J. Poelarends[a]

Departments of [a]Pharmaceutical Biology and [e]Pharmaceutical Gene Modulation, Groningen Research Institute of Pharmacy, University of Groningen, Antonius Deusinglaan 1, 9713 AV Groningen, The Netherlands.

[b]Department of Biochemistry and [d]Laboratory of Biophysical Chemistry, Groningen Biomolecular Sciences and Biotechnology Institute, University of Groningen, Nijenborgh 4, 9747 AG Groningen, The Netherlands.

[c]Center for Systems Chemistry, Stratingh Institute for Chemistry, University of Groningen, Nijenborgh 4, 9747 AG Groningen, The Netherlands.

[f]DSM Pharmaceutical Products, P.O. Box 18, 6160 MD, Geleen, The Netherlands.

Published in *Nature Chemistry* (2012) 4, 478-484.

ABSTRACT

The redesign of enzymes to produce catalysts for a pre-defined transformation remains a major challenge in protein engineering. Here, we describe the structure-based engineering of methylaspartate ammonia lyase - which, in nature, catalyses the conversion of 3-methylaspartate to ammonia and 2-methylfumarate - to accept a variety of substituted amines and fumarates and catalyse the asymmetric synthesis of aspartic acid derivatives. We obtained two single active site mutants, one exhibiting wide nucleophile scope including structurally diverse linear and cyclic alkylamines and one with broad electrophile scope including fumarate derivatives with alkyl, aryl, alkoxy, aryloxy, alkylthio and arylthio substituents at the C2 position. Both mutants have an enlarged active site that accommodates the new substrates while retaining the high stereo- and regioselectivity of the wild-type enzyme. As an example we demonstrate a highly enantio- and diastereoselective synthesis of *threo*-3-benzyloxyaspartate - an important inhibitor of neuronal excitatory glutamate transporters in the brain.

INTRODUCTION

Optically pure α-amino acids are highly valuable as tools for biological research and as chiral building blocks for pharmaceuticals and (agro)chemicals.[1] The industrial and academic interest in these compounds, combined with the potential advantages of replacing conventional chemical processes by biocatalysis, has fueled the development of enzymatic synthesis routes for enantiomerically pure α-amino acids. Various enzymatic synthesis routes have been developed using e.g. hydantoinases, dehydrogenases, acylases, aminotransferases, ammonia lyases and amidases,[1-5] with the most attractive ones being those that are based on asymmetric synthesis in which a prostereogenic substrate is converted to an optically pure α-amino acid with 100% theoretical yield. For example, the asymmetric addition of ammonia to the double bonds of unsaturated acids catalyzed by ammonia lyases is a very attractive strategy for the synthesis of chiral α-amino acids.[5] This strategy makes use of readily available starting substrates without the need for cofactor recycling, the implementation of dynamic kinetic resolution strategies, or additional catalysts. However, it is limited by the narrow substrate range of ammonia lyases.

3-Methylaspartate ammonia lyase (MAL) catalyzes the reversible addition of ammonia (**2a**) to mesaconate (**1b**) to yield *threo*-(2*S*,3*S*)-3-methylaspartate (*threo*-**3a**) and *erythro*-(2*S*,3*R*)-3-methylaspartate (*erythro*-**3a**) as products (Table 1).[6-10] MAL is used by the bacterium *Clostridium tetanomorphum* as part of a degradative pathway that converts (*S*)-glutamic acid via *threo*-**3a** to yield acetyl-CoA.[6, 11] The crystal structure of MAL and that of the isozyme from *Citrobacter amalonaticus* have been solved by X-ray crystallography.[12, 13] Based on kinetic isotope measurements,[14, 15] the structural studies[12, 13, 16] and mutagenesis experiments,[8] a mechanism has emerged for the MAL-catalyzed reaction. In this proposed mechanism, an (*S*)- or (*R*)-specific catalytic base abstracts the C-3 proton of the respective stereoisomer of **3a** to generate an enolate intermediate that is stabilized by coordination to the essential active site Mg^{2+} ion. Collapse of this intermediate results in the elimination of ammonia and yields mesaconate.

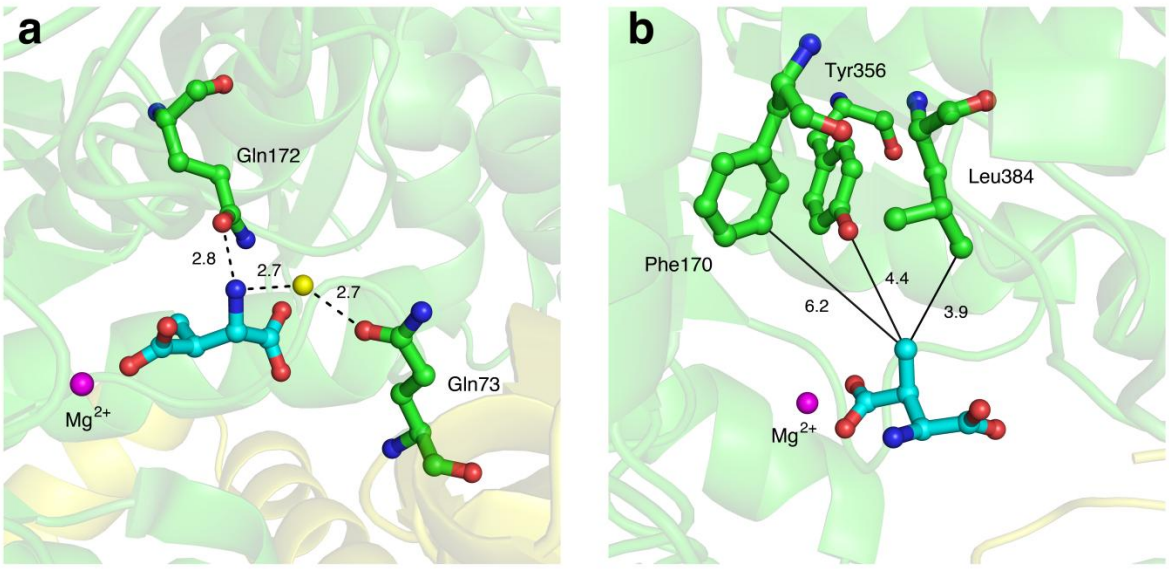

Figure 1. Crystal structure of wild-type MAL in complex with the natural substrate *threo*-(2*S*,3*S*)-3-methylaspartate. (**a**), A close up of the active site showing the hydrogen bond interactions between the substrate's amino group and the side chains of Gln73 (via a water molecule) and Gln172. The carbon atoms of the active site residues are shown in green, whereas those of the substrate are shown in cyan. Hydrogen bonds are represented as dashed lines. The magnesium ion and water molecule are shown as magenta and yellow spheres, respectively. (**b**) A close up of the active site showing the observed distances (in Å, atoms connected by solid lines) between the substrate's methyl group and the side chains of the three residues (Phe170, Tyr356 and Leu384) that are involved in formation of the alkyl binding pocket. The coloring scheme is the same as in Fig. 1a. The figures were prepared with PyMOL (http://www.pymol.org).

Unfortunately, the substrate scope of MAL is very narrow, reasonable activity being observed only with a few small substituted amines and fumarates, yielding a limited number of substituted aspartic acids.[17-19] Hence, it would be very attractive to extend the accessible range of aspartic acid derivatives by the redesign of MAL to convert various unnatural substrates, which would enlarge its biocatalytic applicability. In this report, we describe the use of an efficient engineering strategy, which is based on saturation mutagenesis at carefully chosen sites lining the substrate binding pocket,[20-24] to expand both the nucleophile and electrophile spectrum of MAL. We have obtained two single active site mutants, one that accepts a large set of non-native amines and one that accepts various non-native fumarate derivatives. These engineered MALs have potential as catalysts for

asymmetric synthesis of a large variety of substituted aspartic acids, which are valuable as tools for biological research and as building blocks for chemical and pharmaceutical synthesis.[25-31] This potential is illustrated by the mutant MAL-catalyzed synthesis of *threo*-3-benzyloxyaspartate, a widely used non-transportable blocker for all subtypes of neuronal excitatory amino acid transporters.[25, 26]

RESULTS

Expansion of the nucleophile spectrum of MAL

The crystal structure of MAL complexed with the natural substrate *threo*-(2*S*,3*S*)-3-methylaspartate (*threo*-**3a**)[13] suggests that the side chains of Q73 and Q172 are involved in formation of the binding pocket for the substrate's amino group (Fig. 1a). To engineer this putative amine binding pocket, three focused libraries were generated by saturation mutagenesis at positions 73, 172 and 73/172, using NNS degeneracy.[32] As the model reaction for activity screening, the addition of methylamine (**2b**) to mesaconate (**1b**) was chosen (Table 1). This small alkylamine is a poor substrate for wild-type MAL. We reasoned that if mutants displaying substantial activity were to be found in any of the libraries, then they could be tested for their ability to process larger and more challenging amines as well (e.g., amines **2c**-**2u**).

The three libraries were used to transform *Escherichia coli* cells. The double-site library was screened by evaluating ~1200 transformants, whereas ~400 transformants were evaluated for each single-site library. While the library at position 172 failed to contain any active mutants, screening of the libraries corresponding to positions 73 and 73/172 resulted in the identification of six mutants with pronounced activity towards methylamine addition. DNA sequencing revealed that all positive hits carry mutations at position 73, namely Q73A, Q73G, Q73N, Q73P, Q73S, and Q73T. These mutants and the wild-type enzyme were overexpressed, purified to homogeneity, and assayed for their ability to catalyze ammonia or methylamine addition to mesaconate. When compared to wild-type MAL, all mutants display a significant decrease in ammonia addition activity and a large

Table 1. Q73A-catalyzed amine (**2a-2u**) addition to mesaconate (**1b**).

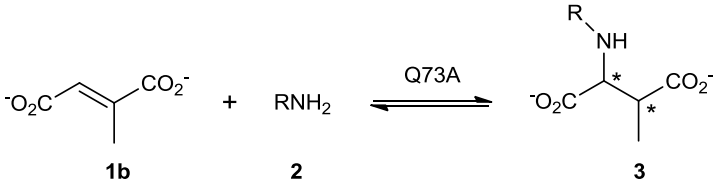

1b **2** **3**

Entry	nucleophile	R-group	product	conv. (%)[a]	*de* (%)	*ee* (%)
1	**2a**	H	**3a**	79[b]	5 (*threo*)[c]	ND[e]
2	**2b**	methyl	**3b**	74	>95 (*threo*)[c]	ND
3	**2c**	ethyl	**3c**	51	>95 (*threo*)[c]	>99[f]
4	**2d**	propyl	**3d**	53	>95 (*threo*)[c]	>99[f]
5	**2e**	butyl	**3e**	60	>95 (*threo*)[c]	>99[f]
6	**2f**	pentyl	**3f**	29	>95 (*threo*)[c]	ND
7	**2g**	hexyl	**3g**	17	>95 (*threo*)[c]	ND
8	**2h**	isopropyl	**3h**	8	>95 (*threo*)[c]	>99[f]
9	**2i**	cyclobutyl	**3i**	65	>95 (*threo*)[c]	>99[f]
10	**2j**	cyclopentyl	**3j**	36	>95 (*threo*)[c]	ND
11	**2k**	cyclohexyl	**3k**	21	>95 (*threo*)[c]	ND
12	**2l**	(cyclopropyl)methyl	**3l**	61	>95 (*threo*)[c]	>99[f]
13	**2m**	benzyl	**3m**	6	>95 (*threo*)[c]	ND
14	**2n**	cyclopropyl	**3n**	75	>95 (*threo*)[d]	ND
15	**2o**	ethoxy	**3o**	99	>95 (*threo*)[d]	ND
16	**2p**	2-hydroxyethyl	**3p**	37[b]	>95 (*threo*)[d]	ND
17	**2q**	3-hydroxypropyl	**3q**	56	80 (*threo*)[d]	ND
18	**2r**	2-methoxyethyl	**3r**	60	>95 (*threo*)[d]	ND
19	**2s**	*N*-methyl-2-aminoethyl	**3s**	80	>95 (*threo*)[d]	ND
20	**2t**	2-aminoethyl	**3t**	90	>95 (*threo*)[d]	ND
21	**2u**	3-aminopropyl	**3u**	78	>95 (*threo*)[d]	ND

[a]Reactions were allowed to proceed for 7 days in order to detect formation of low amounts of *erythro* product isomers, if present. [b]Reaction was allowed to proceed for 14 days. [c]The diastereomeric excess (defined as excess of *threo* isomer over *erythro* isomer) of the amino acid product was determined by comparison of its ^{1}H NMR signals in the crude reaction mixture to those of synthesized authentic standards with known *threo* or *erythro* configuration. [d]The purified amino acid product could be tentatively assigned the *threo* configuration on the basis of analogy. [e]ND, not determined. [f]The enantiomeric excess of the isolated product was determined by chiral HPLC using a synthesized authentic standard with *threo*-(DL) configuration

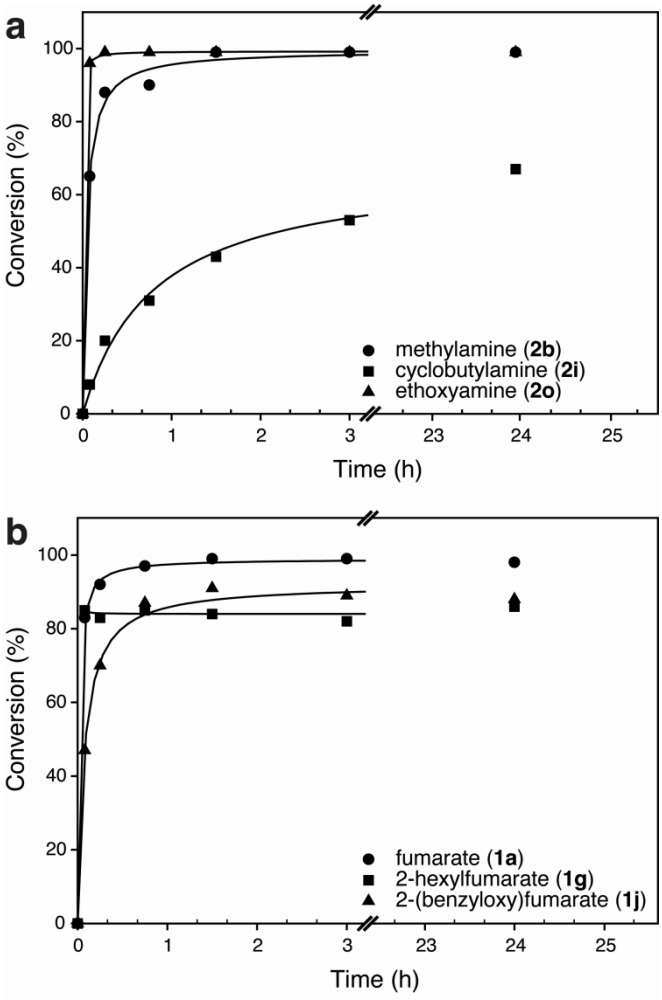

Figure 2. Enzyme-catalyzed transformations under optimized reaction conditions. (**a**) Progress curves of the Q73A-catalyzed (0.05 mol%) addition of methylamine (**2b**, 3 M), cyclobutylamine (**2i**, 2 M) or ethoxyamine (**2o**, 3 M) to mesaconate (26 mM) as monitored by ^{1}H NMR spectroscopy. (**b**) Progress curves of the L384A-catalyzed (0.05 mol%) addition of ammonia (5 M) to fumarate (**1a**), 2-hexylfumarate (**1g**) or 2-(benzyloxy)fumarate (**1j**) (each at 30 mM) as monitored by ^{1}H NMR spectroscopy.

increase in methylamine addition activity (Supplementary Fig. 1). The Q73A mutant showed the highest catalytic rate for methylamine addition to mesaconate and was therefore selected for further study.

A comparison of the k_{cat}/K_m values shows that the Q73A mutant is at least 140-fold more efficient in the addition of methylamine than wild-type MAL (Supplementary Table 1). Wild-type MAL, however, is ~500-fold more efficient in the ammonia addition reaction. Hence, the Q73A mutation moved the specificity of MAL away from ammonia and towards methylamine (>70,000-

fold shift in nucleophile specificity as defined by k_{cat}/K_m values). ^{1}H NMR spectroscopic analysis showed that the Q73A-catalyzed ammonia and methylamine additions to mesaconate lead to the same amino acid products as the corresponding wild-type MAL-catalyzed reactions (Supplementary Fig. 2). This demonstrates that the Q73A mutation does not affect the regio- or diastereoselectivity of the enzyme. Whereas the enzyme-catalyzed ammonia addition reaction yields an ~1:1 mixture of *threo* and *erythro* isomers of 3-methylaspartate (Table 1, **3a**),[8] the enzyme-catalyzed methylamine addition reaction is highly diastereoselective and gives exclusively the *threo* isomer of *N*,3-dimethylaspartate (**3b**) (Table 1, Supplementary Fig. 2).[19]

To investigate its nucleophile scope, we used ^{1}H NMR spectroscopy to determine the ability of the Q73A mutant to add a variety of structurally different amines (**2c**-**2u**, Table 1) to mesaconate (10-fold molar excess of amine over mesaconate, 0.01 mol% of biocatalyst, room temperature). These amines are not accepted as substrates by wild-type MAL, with the exception of **2c**, **2n**, **2p** and **2t** which show minimal conversion (<3%) upon prolonged (2 weeks) incubation. Given that MAL catalyzes the fast *anti*-addition and much slower *syn*-addition of ammonia to mesaconate,[8] leading to *threo* and *erythro* isomers of the corresponding product, respectively, we allowed the unnatural amine addition reactions to run for 7 days in order to detect formation of low amounts of *erythro* product isomers, if present. Remarkably, the Q73A mutant processed all amines tested (Table 1), including those having bulky substituents such as hexyl, cyclohexyl and benzyl, which demonstrates its surprisingly broad nucleophile scope. Control experiments showed that the amines do not react with mesaconate in the absence of enzyme.

For amines **2c**-**2m** (Table 1, entries 3-13), the single products of the Q73A-catalyzed additions to mesaconate were identified as the *threo* isomers of the corresponding *N*-substituted 3-methylaspartic acids (**3c**-**3m**) by comparison of their ^{1}H NMR signals in the crude reaction mixtures to those of chemically synthesized authentic standards with known relative configuration (Supplementary Fig. 3). No other regio- or diastereoisomers were observed. For a few selected

amines (**2c**-**2e**, **2h**, **2i** and **2l**), preparative scale reactions were performed (1.2 mmol **1b**). Purification of the amino acid products and analysis by HPLC on a chiral stationary phase (Supplementary Fig. 4) revealed that the Q73A mutant is also highly enantioselective, producing **3c**-**3e**, **3h**, **3i** and **3l** with >99% *ee* (Table 1). In the case of the other amines (Table 1, entries 14-21), the Q73A-catalyzed addition reactions were performed on a 3.1 mmol scale (**1b**). The products were isolated and identified as the corresponding *N*-substituted 3-methylaspartic acids (**3n-3u**). While the relative configuration of products **3n-3u** has not been determined by comparison to authentic standards, we assume the relative configuration to be *threo* for all products **3b-3u**.

To further demonstrate the preparative usefulness of the Q73A mutant, we optimized the reaction conditions for a few structurally distinct amines (**2b**, **2i** and **2o**). With 0.05 mol% biocatalyst and a 115-fold molar excess of **2b** or **2o** (3 M each) over mesaconate (26 mM), the reactions are complete within 20 to 60 min at 25°C, achieving final conversions of almost 100% (Fig. 2a). For amine **2i**, a lower concentration (2 M) had to be used to avoid protein precipitation. Nevertheless, the reaction reaches equilibrium (~65% conversion) in just a few hours. These results clearly demonstrate the potential of the Q73A mutant for application in selective synthesis of various *N*-substituted 3-methylaspartic acids.

Expansion of the electrophile spectrum of MAL

The structure of MAL in complex with *threo*-(2*S*,3*S*)-3-methylaspartate[13] suggests that the side chains of F170, Y356 and L384 are involved in formation of the binding pocket for the substrate's methyl group (Fig. 1b). To engineer this putative alkyl binding pocket, three focused libraries were generated by saturation mutagenesis at positions 170, 356 and 384, using NNS degeneracy. As the model reaction for activity screening, the addition of ammonia to 2-hexylfumarate (Table 2, **1g**) was chosen. Compound **1g** is not at all converted by wild-type MAL, even after an incubation period of several weeks. The hope was that active mutants with the ability to aminate electrophiles with large substituents at the C-2 position (e.g., **1e-1g**, **1i**, **1j**, **1l-1n**) can be identified in this way.

Table 2. MAL- and L384A-catalyzed ammonia addition to fumarates **1a-1n**.

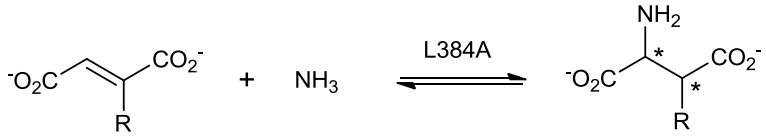

1 **2a** **4**

entry	electrophile	R-group	product	conv. (%)[a] wild-type	conv. (%)[a] L384A	conv. (%)[a,b] L384A	*d.e.* (%)[d]	*e.e.* (%)
1	**1a**	H	**4a**	100	99	99 (80)[c]	-	>99 (*S*)[j]
2	**1b**	methyl	**4b**	80	75	73 (60)[c]	56 (*threo*)[e]	ND[k]
3	**1c**	ethyl	**4c**	74	76	73 (45)[c]	>95 (*threo*)[e]	ND
4	**1d**	propyl	**4d**	57	67	66 (46)[c]	>95 (*threo*)[e]	ND
5	**1e**	butyl	**4e**	0	59	57 (36)[c]	2[f]	ND
6	**1f**	pentyl	**4f**	0	52	52 (23)[c]	>95[f]	ND
7	**1g**	hexyl	**4g**	0	53	53 (48)[c]	>95[f]	ND
8	**1h**	ethoxy	**4h**	46	43	45 (24)[c]	70 (*threo*)[g]	ND
9	**1i**	phenoxy	**4i**	0	44	46 (20)[c]	>95[f]	ND
10	**1j**	benzyloxy	**4j**	0	60	65 (50)[c]	>95 (*threo*)[h]	>99[l]
11	**1k**	ethylthio	**4k**	36	50	81 (22)[c]	36 (*threo*)[i]	ND
12	**1l**	phenylthio	**4l**	0	34	45 (13)[c]	30 (*threo*)[i]	ND
13	**1m**	benzylthio	**4m**	0	42	55 (30)[c]	20 (*threo*)[i]	ND
14	**1n**	benzyl	**4n**	0	90	90 (55)[c]	>95 (*threo*)[g]	ND

[a]Reactions were allowed to proceed for 7 days. [b]Preparative scale. [c]Yield (%) of isolated product after ion exchange chromatography. [d]The diastereomeric excess (*de*) is defined as excess of *threo*-isomer over *erytho*-isomer. [e]The relative configuration of the isolated product(s) was assigned by ^{1}H NMR using the product(s) of the corresponding wild-type MAL catalyzed reaction as reference sample and by referring to the literature.[17] [f]The relative configurations have not been determined. [g]The relative configuration of the isolated product(s) was assigned by referring to the literature.[29, 31] [h]The relative configuration of isolated product was assigned by ^{1}H NMR spectroscopy using an authentic standard with known *threo* configuration and by referring to the literature.[30] [i]The isolated amino acid products were first esterified and acetylated, after which the relative configuration of the products could be tentatively assigned by ^{1}H NMR spectroscopy on the basis of comparison to chemically synthesized reference molecules (see Supplementary Methods). [j]The *ee* value of isolated product was determined by chiral HPLC using authentic standards with known *R* or *S* configuration. [k]ND, not determined. [l]The *ee* value of isolated product was determined by chiral HPLC using authentic *threo*-(DL)-**4j** as standard.

The three libraries were introduced into *E. coli* cells, after which the library corresponding to position 384 was screened by evaluating ~400 transformants and ~200 transformants were evaluated for each of the other two libraries. Whereas the libraries corresponding to positions 170 and 356 failed to give any active mutants, screening of the library corresponding to position 384 resulted in several positive hits. Analysis by DNA sequencing revealed that all positive hits carry either an alanine or glycine mutation at position 384. These two mutants and the wild-type enzyme were overexpressed, purified to homogeneity, and tested for their ability to catalyze the addition of ammonia to either mesaconate or 2-hexylfumarate. Gratifyingly, the L384G and L384A mutants exhibit pronounced amination activity towards 2-hexylfumarate (Supplementary Fig. 5). Both mutants display a significant decrease in amination activity towards mesaconate when compared to wild-type MAL. Hence, the mutations moved the electrophile specificity of MAL away from the natural substrate mesaconate and towards the unnatural substrate 2-hexylfumarate. Because the L384A mutant showed higher activity towards a range of fumarate derivatives, it was selected for further study.

Kinetic parameters were determined for the L384A mutant using substrates **1a-1g**, which have varying 2-alkyl chain length (Table 2), and compared to those measured for the wild-type enzyme (Supplementary Table 2). As previously reported,[17, 18] wild-type MAL only displays activity towards fumarates with a short alkyl substituent (**1a-1d**). Mutant L384A, however, shows activity for all tested substrates. It displays both higher affinity (lower K_m values) and higher activity (larger k_{cat} values) for substrates with a long alkyl chain (**1d-1g**) than for those with a short alkyl chain (**1a-1c**). While wild-type MAL is at least 100-fold more efficient in the amination of **1a-1c**, the L384A mutant is ~13-fold more efficient in the amination of **1d**. In the case of the large substrates **1e-1g**, which are not at all converted by wild-type MAL, it was not possible to determine the rate enhancement, but it must be much higher than that observed for **1d**.

To further explore the electrophile scope of the L384A mutant, its ability to catalyze the amination of substrates with aryl, alkoxy, aryloxy, alkylthio, and arylthio substituents at the C-2 position (**1h-1n**) was tested by using ^{1}H NMR spectroscopy (Table 2). The wild-type enzyme only displays amination activity for compounds **1h** and **1k**, which, like substrates **1a-1d**, have small R-groups at the C-2 position (Table 2, entries 1-4, 8, 11). Strikingly, the L384A mutant exhibits activity towards all substrates tested (Table 2), demonstrating its broad electrophile scope. Control experiments showed that the fumarate derivatives do not undergo amination in the absence of enzyme.

The L384A-catalyzed aminations of **1a-1n** were also performed on a preparative (3.1 mmol) scale (Table 2). Reactions (10-fold molar excess of ammonia over unsaturated acid, 0.01 mol% of biocatalyst, room temperature) were allowed to run for 7 days in order to detect formation of low amounts of *erythro* product isomers, if present. The products were isolated and identified as aspartate (**4a**) and its 3-substituted derivatives **4b-4n**, respectively. While these L384A-catalyzed amination reactions provided high regioselectivities, varying degrees of diastereoselectivity were obtained with the single or predominant diastereoisomer having the *threo* configuration (Table 2). Analysis of products **4a** and **4j** by chiral HPLC revealed that the L384A-catalyzed amination reactions are highly enantioselective, producing these amino acids with >99% *ee* (Table 2).

The preparative usefulness of the L384A mutant was further demonstrated by transformations using 0.05 mol% biocatalyst, 5 M ammonia, and 30 mM of the structurally distinct unsaturated acids **1a**, **1g** or **1j** (167-fold molar excess of ammonia over unsaturated acid). Under these optimized conditions, the reactions are complete within 10 to 60 min at 25°C, achieving final conversions of ~85 to 100% (Fig. 2b). These results clearly demonstrate the potential of the L384A mutant for application in selective synthesis of valuable α-amino acids.

Structural basis for the expanded substrate spectrum

To obtain insight into how the active sites of the Q73A and L384A mutants are remodelled to accommodate the new substrates, we determined their X-ray crystal structures at 2.0 Å and 1.9 Å resolution, respectively (Supplementary Table 3). A comparison of the Q73A and L384A structures with that of wild-type MAL revealed no significant changes in overall structure nor in main chain and side chain conformations of the active site residues (Fig. 3). These results demonstrate that the expanded substrate spectrum of the Q73A and L384A mutants is not due to major structural changes but is related to the replacement of a large active site residue by a smaller one, resulting in an enlarged active site that can accommodate the new substrates (Fig. 3).

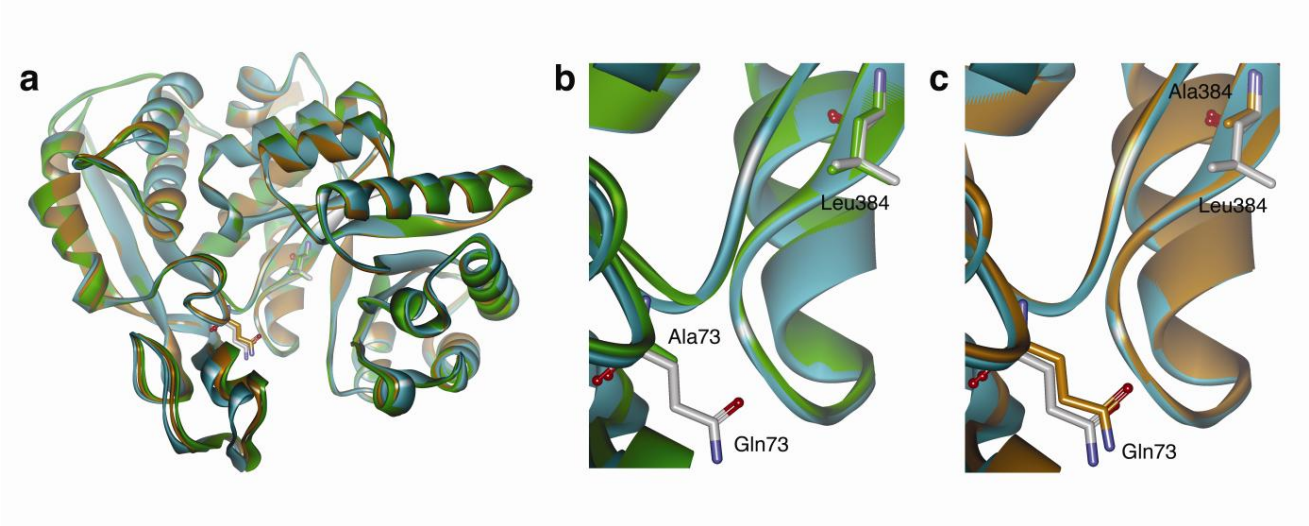

Figure 3. Structural comparison of wild-type MAL and the Gln73Ala and Leu384Ala mutants. (**a**) Overlay of the structures of wild-type MAL (cyan ribbons) and the Gln73Ala (green ribbons) and Leu384Ala (orange ribbons) mutants. The structures of the Gln73Ala (PDB code 3ZVH) and Leu384Ala (PDB code 3ZVI) mutants can be superimposed to the wild-type MAL structure[12] (PDB code 1KCZ) with a root-mean-square-deviation (RMSD) of 0.53-0.74 Å, considering all atoms in the two subunits that occupy the different crystallographic asymmetric units. When considering only the atoms of residues that are within 5 Å of the residues at positions 73 and 384, the RMSD is 0.19-0.50 Å. (**b**) Overlay of the active sites of wild-type MAL and the Gln73Ala mutant. The coloring scheme is the same as in Fig. 3a. (**c**) Overlay of the active sites of wild-type MAL and the Leu384Ala mutant. The coloring scheme is the same as in Fig. 3a. In all three figures, the residues at positions 73 and 384 are shown as sticks. For clarity, these sticks are shown in grey for wild-type MAL. The figures were prepared with Discovery Studio 2.5.

To further demonstrate that the active sites of the Q73A and L384A mutants can accommodate larger substrates than the active site of wild-type MAL, we performed comparative docking simulations. Figure 4a shows an overlay of the docking model of wild-type MAL in complex with the natural substrate *threo*-(2*S*,3*S*)-3-methylaspartic acid (*threo*-**3a**) and the docking model of mutant Q73A complexed with the unnatural substrate *threo*-(2*S*,3*S*)-2-(cyclohexylamino)-3-methylbutanedioic acid (**3k**), respectively. This comparison clearly shows that compound **3k** does not fit into the active site of wild-type MAL because residue Q73, instead of the shorter A73, partially fills the volume that is occupied by the cyclohexylamino moiety of substrate **3k** in the Q73A-substrate complex. The observation that residue Q73 occludes the amine binding pocket thus explains why cyclohexylamine **2k** and other large amines are not accepted as substrates by wild-type MAL. An overlay of the docking model of wild-type MAL complexed with *threo*-**3a** and that of mutant L384A in complex with the unnatural substrate *threo*-(2*S*,3*S*)-3-pentylaspartic acid (**4f**) is shown in Fig. 4b. This comparison shows that the mutation of residue L384 to the shorter A384 prevents a clash between the substrate's pentyl group and the large leucine residue found at position 384 in wild-type MAL, thus rationalizing the ability of the L384A mutant to convert large electrophiles.

DISCUSSION

Wild-type MAL accepts only a few amines as alternative nucleophiles for ammonia and a few fumarate derivatives as alternative electrophiles for mesaconate.[17-19] Therefore, the goal of this study was to expand both the nucleophile and electrophile scope of MAL. This goal was achieved by using an engineering strategy that involves randomization at carefully chosen sites lining the substrate binding pocket of the enzyme. The major benefit of this structure-guided engineering strategy lies in the reduction of the sequence space that has to be covered in order to identify valuable mutants.[20-24]

Engineering of the amine binding pocket (Fig. 1a) yielded a mutant (Q73A) that has a very broad nucleophile scope and excellent regio- and stereoselectivity, producing the *threo* isomers of the *N*-substituted 3-methylaspartic acids **3b-3u** with very high diasteromeric and enantiomeric excess (Table 1). These results demonstrate that the high regio- and stereoselectivity of the Q73A-catalyzed addition reactions is not influenced by the different substituents on the amine substrate. This is of high synthetic significance, especially when compared to the Q73A-catalyzed ammonia addition to mesaconate (the natural reaction), which shows low diastereoselectivity (Table 1, entry 1). Recently, a mechanism was proposed for MAL,[8, 12, 13] in which the proton abstraction/addition steps are effected by K331 and H194 as the (*S*)- and (*R*)-specific general base/acid catalysts, respectively, which are juxtaposed on either side of the chiral C-3 carbon of the amino acid substrate. In view of this mechanism, the high diastereoselectivity of the Q73A-catalyzed amine addition reactions could be explained by assuming that the substituents on the amine substrate sterically hinder protonation of the C-3 carbon (numbering according to the amino acid product) of mesaconate by H194, thereby preventing the formation of *erythro* isomers. Structural analysis of the Q73A mutant showed that this mutant enzyme has an enlarged amine binding pocket, without changes in the orientation of active site residues, thus rationalizing its ability to convert the new amine substrates.

Engineering of the alkyl binding pocket (Fig. 1b) yielded a mutant (L384A) that has a very broad electrophile scope and excellent regio- and enantioselectivity in the amination reaction, producing (*S*)-aspartic acid (**4a**) and its 3-substituted derivatives **4b-4n** (Table 2). The structure of L384A showed that this mutant enzyme has an enlarged alkyl binding pocket, with an otherwise unchanged active site geometry, thus rationalizing its ability to convert fumarate derivatives with large substituents. In contrast to the Q73A-catalyzed amine additions, the L384A-catalyzed amination of the fumarate derivatives gives varying degrees of diastereoselectivity. This irregular pattern of diastereoselectivities is an interesting phenomenon and suggests that some of the

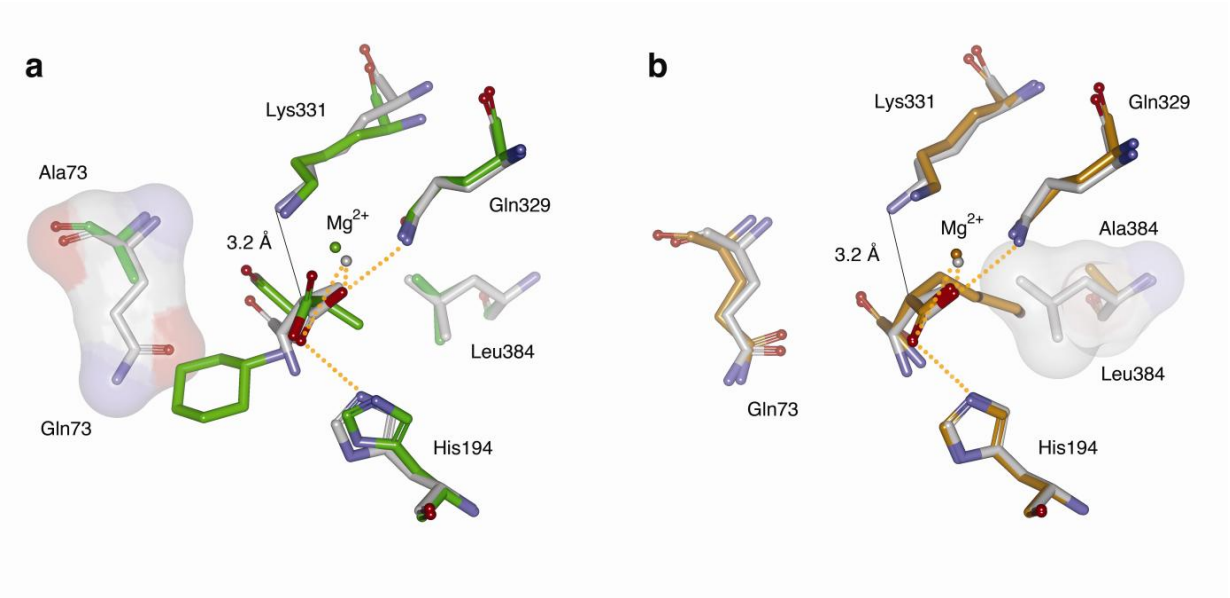

Figure 4. Molecular docking of substrates in the active sites of wild-type MAL and the two MAL mutants. (**a**) Overlay of the most favorable docked conformations of *threo*-(2*S*,3*S*)-3-methylaspartic acid (*threo*-**3a**) and *threo*-(2*S*,3*S*)-2-(cyclohexylamino)-3-methylbutanedioic acid (**3k**) in the active sites of wild-type MAL (grey) and the Gln73Ala mutant (green), respectively. Residue Gln73 in wild-type MAL is represented by a solvent accessible surface calculated with a probe radius of 1.4 Å. (**b**) Overlay of the most favorable docked conformations of *threo*-**3a** and *threo*-(2*S*,3*S*)-3-pentylaspartic acid (**4f**) in the active sites of wild-type MAL (grey) and the Leu384Ala mutant (orange), respectively. Residue Leu384 in wild-type MAL is represented by a solvent accessible surface calculated with a probe radius of 1.4 Å. In both figures, interactions between active site residues or the Mg^{2+} ion and substrate *threo*-**3a** in wild-type MAL are displayed as orange dashed lines. The distance between the substrate's C-3 atom and the side chain of Lys331 is shown in Å (atoms connected by a solid line). The figures were prepared with Discovery Studio 2.5.

fumarate derivatives, like the natural substrate mesaconate, are optimally positioned to undergo protonation by both K331 and H194 from either face of the substrate, producing the undesired mixture of *threo* and *erythro* isomers, whereas others are bound in a position which does not favor protonation by H194, yielding only the desired *threo*-isomers. Nonetheless, the synthetic potential of the L384A mutant is convincingly demonstrated by its use as catalyst in the stereoselective synthesis (*de* values are >95%) of *threo*-3-benzyloxyaspartate (**4j**) and *threo*-3-benzylaspartate (**4n**), which are important compounds to study the role of glutamate transporters in the brain.[26-28]

In summary, we provide evidence that a single amino acid substitution is sufficient to dramatically expand the nucleophile or electrophile spectrum of MAL. The results provide support for the notion that structure-guided saturation mutagenesis of sites lining the substrate binding pocket is a powerful strategy to create enzymes that can accommodate nonnative substrates and perform reactions not observed in Nature.[22] The new designer enzymes catalyze attractive and straightforward asymmetric transformations in water, making use of readily available starting substrates, without the need for organic (co)solvents or the implementation of dynamic kinetic resolution strategies. These represent very desirable features in view of the quest for environmentally benign and atom efficient processes. The potential of the two engineered MALs for application in selective synthesis of new and valuable aspartic acid derivatives has been demonstrated, given that the product yields may be further improved by optimizing the reaction conditions and purification protocols. The Q73 and L384 residues represent good targets for future combinatorial mutagenesis experiments (see Supplementary Results & Discussion), potentially yielding new biocatalysts with an even larger substrate scope.

METHODS

Mutant library preparation and screening

Site-saturation mutagenesis libraries were generated by overlap extension PCR[33] using plasmid pBAD(MAL-His)[8] as template and the primers listed in Supplementary Table 4. Detailed procedures for library preparation and screening are provided in the Supplementary Methods.

Enzyme expression, purification and kinetic characterization

Wild-type MAL and MAL mutants were overproduced in *E. coli* TOP10 cells and purified to homogeneity as described before.[8] Procedures for the kinetic characterization of MAL (wild-type or mutants) are provided in the Supplementary Methods.

General procedure for monitoring the addition of various amines to mesaconate

The ability of wild-type MAL and the Q73A mutant to add different amines (**2a-2u**) to mesaconate (**1b**) was examined by using ^{1}H NMR spectroscopy. Reaction mixtures consisted of 500 µl of a 1 M stock solution of amine in water (pH 9.0, containing 20 mM $MgCl_2$), 100 µl of 500 mM **1b** in water (pH 9.0, containing 20 mM $MgCl_2$), and 50 µl of D_2O. In the case of amines **2f**, **2g** and **2m** 500 µl of a 250 (**2f**) or 125 mM (**2g** and **2m**) stock solution was added to the reaction mixtures to avoid protein precipitation. Reactions were started by the addition of 200 µg of freshly purified enzyme, and reaction mixtures were incubated at 22°C. ^{1}H NMR spectra were recorded 3 h, 3 d, and 7 d after the addition of enzyme. Product amounts were estimated by integration of the respective product signals, if present.

General procedure for monitoring the amination of various electrophiles

The ability of wild-type MAL and the L384A mutant to add ammonia to different electrophiles (**1a-1n**) was examined by using ^{1}H NMR spectroscopy. Reaction mixtures consisted of 500 µl of a 1 M stock solution of NH_4Cl in water (pH 9.0, containing 20 mM $MgCl_2$), 50 µl D_2O, and 200 µl of a 250 mM stock solution (or 100 µl of a 500 mM stock solution) of electrophile in water (pH 9.0, containing 20 mM $MgCl_2$). Reactions were started by the addition of 200 µg of freshly purified enzyme, and reaction mixtures were incubated at 22°C. ^{1}H NMR spectra were recorded 3 h, 3 d, and 7 d after the addition of enzyme. Product amounts were estimated by integration of the respective product signals, if present.

Starting substrates

Amines **2a-2u** and unsaturated acids **1a** and **1b** were purchased from Sigma-Aldrich Chemical Co (St. Louis, MO) or Merck (Darmstadt, Germany). Unsaturated acids **1c-1n** were prepared according to experimental procedures described in the Supplementary Methods.

Identification of the amino acid products

Procedures for the enzymatic synthesis and purification of amino acids **3n-3u** and **4a-4n** are described in the Supplementary Methods. The relative configuration of products **4b-4d**, **4h**, **4j**, and **4n** was determined by comparison of their ^{1}H NMR signals to those of commercially available or wild-type MAL-synthesized[17] authentic standards with known configuration, and/or by referring to the literature.[29-31] Compound *threo*-DL-**4j** was purchased from Tocris Bioscience (Missouri, USA). The procedures to establish the relative configuration of products **4k-4m** are provided in the Supplementary Methods. The enantiomeric excess of products **4a** and **4j** was determined by chiral HPLC using a Chirex 3126-(D)-penicillamine column (250 mm x 4.6 mm, Phenomenex, USA) or a Nucleosil chiral-1 column (250 mm x 4 mm, Macherey-Nagel, Germany), respectively. Authentic standards L-**4a** and D-**4a** were purchased from Sigma-Aldrich Chemical Co. HPLC conditions and observed retention times are given in the Supplementary Methods.

Identity and configuration of amino acid products 3a-3m

The identity and relative configuration of products **3a-3m** were determined by comparative ^{1}H NMR analysis of the crude reaction mixtures and authentic compounds with known relative configuration. The experimental procedures for the synthesis of these authentic standards are provided in the Supplementary Methods. Products **3c-3e**, **3h**, **3i**, and **3l** were also purified from preparative scale (0.15 g **1b**) reactions and their enantiomeric excess was determined by chiral HPLC. The HPLC conditions, procedures for the synthesis of the *threo*-DL standards, and the observed retention times are provided in the Supplementary Methods.

Optimization of reaction conditions for amino acid synthesis

By increasing both the amount of biocatalyst and the molar excess of amine over mesaconate, excellent conversions were achieved for several Q73A-catalyzed amine additions within short reaction times. The optimized reaction conditions were as follows. Reaction mixtures (30 ml)

consisted of 3 M amine (either **2b** or **2o**) and 26 mM **1b** in 20 mM $MgCl_2$ (final pH = 9). In the case of amine **2i**, a lower concentration (2 M) was used to avoid protein precipitation. The reactions were started by the addition of freshly purified enzyme (0.05 mol%), and reaction mixtures were incubated at 25°C. Aliquots of each reaction mixture (5 ml) were withdrawn 5 min, 15 min, 45 min, 90 min, 180 min, and 24 h after the addition of enzyme. For each sample, the reaction was stopped by incubating the reaction mixture at 100°C for 5 min.

Optimized conditions for several L348A-catalyzed amination reactions were as follows. Reaction mixtures (6-12 ml) consisted of 5 M NH_4Cl and 30 mM **1a**, **1g** or **1j** in 20 mM $MgCl_2$ (final pH = 9). The reactions were started by the addition of freshly purified enzyme (0.05 mol%), and reaction mixtures were incubated at 25°C. Aliquots (1-2 ml) of the reaction mixtures were withdrawn 5 min, 15 min, 45 min, 90 min, 180 min, and 24 h after the addition of enzyme. For each sample, the reaction was stopped by incubating the reaction mixture at 100°C for 5 min.

Each sample was dried *in vacuo*, followed by resuspending the resulting residue in ~10 ml of water for lyophilization. This process was repeated 5 to 10 times in order to remove the excess of amine/ammonia to enable analysis by ^{1}H NMR spectroscopy. The final residue was dissolved in 800 µl D_2O. The conversion of substrate to product was estimated by integration of the respective substrate and product signals.

Crystallization, structure determination and molecular docking

The procedures used for crystallization, structure determination, and comparative docking simulations are described in the Supplementary Methods.

ACKNOWLEDGMENTS

We thank Bian Wu, Bernard Kaptein and Oliver May for helpful discussions. This research was financially supported by VENI grant 700.54.401 and ECHO grant 700.59.042 (both to G.J.P.) from the Division of Chemical Sciences of the Netherlands Organisation of Scientific Research (NWO-CW), and by the Netherlands Ministry of Economic Affairs and the B-Basic partner organizations (www.b-basic.nl) through B-Basic, a public-private NWO-ACTS programme (ACTS = Advanced Chemical Technologies for Sustainability).

REFERENCES

1. Sonke, T., Kaptein, B. & Schoemaker, H.E. Use of enzymes in the synthesis of amino acids. In *Amino acids, Peptides and Proteins in Organic Chemistry* (ed. Hughes, A.B.) **1**, 77-117 (Wiley-VCH, Weinheim, 2009).
2. Wohlgemuth, R. Biocatalysis - key to sustainable industrial chemistry. *Curr. Opin. Biotechnol.* **21**, 713-724 (2010).
3. Panke, S. & Wubbolts, M. Advances in biocatalytic synthesis of pharmaceutical intermediates. *Curr. Opin. Chem. Biol.* **9**, 188-194 (2005).
4. Panke, S., Held, M. & Wubbolts, M. Trends and innovations in industrial biocatalysis for the production of fine chemicals. *Curr. Opin. Biotechnol.* **15**, 272-279 (2004).
5. Turner, N.J. Ammonia lyases and aminomutases as biocatalysts for the synthesis of α-amino and β-amino acids. *Curr. Opin. Chem. Biol.* **15**, 234-240 (2011).
6. Barker, H.A., Smyth, R.D., Wilson, R.M. & Weissbach, H. The purification and properties of β-methylaspartase. *J. Biol. Chem.* **234**, 320-328 (1959).
7. Goda, S.K., Minton, N.P., Botting, N.P. & Gani, D. Cloning, sequencing, and expression in *Escherichia coli* of the *Clostridium tetanomorphum* gene encoding β-methylaspartase and characterization of the recombinant protein. *Biochemistry* **31**, 10747-10756 (1992).

8. Raj, H. *et al*. Alteration of the diastereoselectivity of 3-methylaspartate ammonia lyase by using structure-based mutagenesis. *Chembiochem* **10**, 2236-2245 (2009).
9. Bright, H.J. Divalent metal activation of β-methylaspartase. The importance of ionic radius. *Biochemistry* **6**, 1191-1203 (1967).
10. Bright, H.J. On the mechanism of divalent metal activation of β-methylaspartase. *J. Biol. Chem.* **240**, 1198-1210 (1965).
11. Kato, Y. & Asano, Y. 3-Methylaspartate ammonia-lyase as a marker enzyme of the mesaconate pathway for (*S*)-glutamate fermentation in Enterobacteriaceae. *Arch. Microbiol.* **168**, 457-463 (1997).
12. Asuncion, M., Blankenfeldt, W., Barlow, J.N., Gani, D. & Naismith, J.H. The structure of 3-methylaspartase from *Clostridium tetanomorphum* functions via the common enolase chemical step. *J. Biol. Chem.* **277**, 8306-8311 (2002).
13. Levy, C.W. *et al*. Insights into enzyme evolution revealed by the structure of methylaspartate ammonia lyase. *Structure* **10**, 105-113 (2002).
14. Bright, H.J., Ingraham, L.L. & Lundin, R.E. The mechanism of the methylaspartate ammonia-lyase reaction: deuterium exchange. *Biochim. Biophys. Acta* **81**, 576-584 (1964).
15. Bright, H. The mechanism of the β-methylaspartase reaction. *J. Biol. Chem.* **239**, 2307-2315 (1964).
16. Babbitt, P.C. *et al*. The enolase superfamily: a general strategy for enzyme-catalyzed abstraction of the α-protons of carboxylic acids. *Biochemistry* **35**, 16489-16501 (1996).
17. Akhtar, M., Botting, N.P., Cohen, M.A. & Gani, D. Enantiospecific synthesis of 3-substituted aspartic acids via enzymic amination of substituted fumaric acids. *Tetrahedron* **43**, 5899-5908 (1987).
18. Botting, N.P., Akhtar, M., Cohen, M.A. & Gani, D. Substrate specificity of the 3-methylaspartate ammonia-lyase reaction: observation of differential relative reaction rates for substrate-product pairs. *Biochemistry* **27**, 2953-2955 (1988).

19. Gulzar, M.S., Akhtar, M. & Gani, D. Preparation of *N*-substituted aspartic acids via enantiospecific conjugate addition of *N*-nucleophiles to fumaric acids using methylaspartase: synthetic utility and mechanistic implications. *J. Chem. Soc. Perkin Trans.* **I**, 649-656 (1997).
20. Lutz, S. & Bornscheuer, U.T. *Protein Engineering Handbook*. Vol. **1-2** (Wiley-VCH, Wienheim, 2009).
21. Reetz, M.T., Bocola, M., Carballeira, J.D., Zha, D. & Vogel, A. Expanding the range of substrate acceptance of enzymes: combinatorial active-site saturation test. *Angew. Chem. Int. Ed Engl.* **44**, 4192-4196 (2005).
22. Morley, K.L. & Kazlauskas, R.J. Improving enzyme properties: when are closer mutations better? *Trends Biotechnol.* **23**, 231-237 (2005).
23. Arnold, F.H. & Georgiou, G. *Methods in Molecular Biology* (Directed Enzyme Evolution). Vol. **230** (Humana Press, Totowa, 2003).
24. Turner, N.J. Directed evolution drives the next generation of biocatalysts. *Nat. Chem. Biol.* **5**, 567-573 (2009).
25. Shimamoto, K. *et al*. Characterization of novel L-*threo*-β-benzyloxyaspartate derivatives, potent blockers of the glutamate transporters. *Mol. Pharmacol.* **65**, 1008-1015 (2004).
26. Shimamoto, K. Glutamate transporter blockers for elucidation of the function of excitatory neurotransmission systems. *Chem. Rec.* **8**, 182-199 (2008).
27. Esslinger, C.S. *et al*. The substituted aspartate analogue L-β-*threo*-benzyl-aspartate preferentially inhibits the neuronal excitatory amino acid transporter EAAT3. *Neuropharmacology* **49**, 850-861 (2005).
28. Bridges, R.J. & Esslinger, C.S. The excitatory amino acid transporters: pharmacological insights on substrate and inhibitor specificity of the EAAT subtypes. *Pharmacol. Ther.* **107**, 271-285 (2005).

29. Mavencamp, T.L., Rhoderick, J.F., Bridges, R.J. & Esslinger, C.S. Synthesis and preliminary pharmacological evaluation of novel derivatives of L-β-*threo*-benzylaspartate as inhibitors of the neuronal glutamate transporter EAAT3. *Bioorg. Med. Chem.* **16**, 7740-7748 (2008).
30. Shimamoto, K. *et al*. Syntheses of optically pure β-hydroxyaspartate derivatives as glutamate transporter blockers. *Bioorg. Med. Chem. Lett.* **10**, 2407-2410 (2000).
31. Spengler, J., Pelay, M., Tulla-Puche, J. & Albericio, F. Synthesis of orthogonally protected L-*threo*-β-ethoxyasparagine. *Amino Acids* **39**, 161-165 (2010).
32. LaBean, T.H. & Kauffman, S.A. Design of synthetic gene libraries encoding random sequence proteins with desired ensemble characteristics. *Protein Sci.* **2**, 1249-1254 (1993).
33. Ho, S.N., Hunt, H.D., Horton, R.M., Pullen, J.K. & Pease, L.R. Site-directed mutagenesis by overlap extension using the polymerase chain reaction. *Gene* **77**, 51-59 (1989).

Supporting Information

CONTENTS

SUPPLEMENTARY METHODS

Mutant library preparation

The plasmid pBAD(MAL-His)[1] contains the wild-type MAL gene under the transcriptional control of the *araBAD* promoter. The libraries Q73NNS, Q172NNS, Q73NNS/Q172NNS, F170NNS, Y356NNS and L384NNS were generated by the overlap extension PCR method[2] using plasmid pBAD(MAL-His) as the template and the primers listed in Supplementary Table 4. The final PCR products were gel purified, digested with *Nde*I and *Hin*dIII restriction enzymes, and ligated in frame with both the initiation ATG start codon and the sequence that codes for the polyhistidine region of the expression vector pBAD*N*/*Myc*-His A.[3] An aliquot of each ligation mixture was transformed into competent *E. coli* TOP10 cells. Transformants were selected at 37^{o}C on Luria-Bertani (LB) agar plates containing 100 μg/ml ampicillin (Ap). For each library, plasmid DNA was isolated from several colonies chosen at random, and analyzed by restriction analysis for the presence of the insert. Plasmids containing the insert were sequenced to verify that the correct mutations had been introduced during the amplification of the MAL gene. Libraries were stored at -80°C as plasmid DNA isolated from at least 1000 (in the case of the single-site libraries) or 3000 (in the case of the double-site library) transformants.

Mutant library screening

Individual colonies from freshly transformed *E. coli* TOP 10 cells were placed into 2.2-ml 96-deep-well plates containing (in each well) 1.5 ml of LB medium with 100 μg/ml Ap and 0.004% (w/v) arabinose as inducer. After cell growth at 22°C for 96 h with shaking at 800 rpm, a duplicate plate was made on solid LB-Ap medium. After cell growth overnight at 37°C, this duplicate plate was stored at 4°C. The remaining cells from the original plate were harvested by centrifugation at 4000 rpm and 4°C for 20 min and the supernatants were discarded. Each cell pellet was resuspended in 400 μl of Bug-Buster (Novagen) and incubated at 800 rpm and 30°C for 45 min. Cell debris was removed by centrifugation at 4000 rpm and 4°C for 50 min. The supernatants from each well were

transferred into a new plate and stored at 4°C (<24 h) until further use. For each library, small aliquots of several randomly chosen supernatants were analyzed by SDS-PAGE (on gels containing 10% acrylamide) to confirm expression of the MAL protein.

For libraries Q73NNS, Q172NNS and Q73NNS/Q172NNS, 50 µl of each cleared supernatant was transferred to a 0.3-ml 96-well plate. Then in each well, 150 µl of substrate solution (400 mM methylamine and 5 mM mesaconate in 0.5 M Tris-HCl buffer, pH 9.0, containing 20 mM $MgCl_2$) was added. The reactions were monitored by following mesaconate depletion at 270 nm ($\varepsilon = 483\ M^{-1}\ cm^{-1}$) and 30°C for 120 min using a SpectroStar Omega UV-plate reader from Isogen Life Science (De Meern, The Netherlands). For libraries F170NNS, Y356NNS, and L384NNS, 50 µl of each cleared supernatant was mixed with 150 µl of a different substrate solution (5 mM 2-*n*-hexylfumarate and 400 mM NH_4Cl in 0.5 M Tris-HCl buffer, pH 9.0, containing 20 mM $MgCl_2$) in a 0.3-ml 96-well plate. The reactions were monitored by following the depletion of 2-*n*-hexylfumarate at 270 nm ($\varepsilon = 742\ M^{-1}\ cm^{-1}$) and 30°C for 120 min using the UV-plate reader. Active clones were collected from the corresponding duplicate plate. From each positive hit, plasmid DNA was extracted and the entire MAL gene sequenced to identify the mutation(s).

Ammonia addition to mesaconate and product identification

The products of the ammonia addition to mesaconate (**1b**) by wild-type MAL and the MAL mutants Q73A and L384A were identified by ^1H NMR spectroscopy using a previously described procedure[1] with the following modifications. In separate experiments, wild-type MAL, mutant Q73A, or mutant L384A was incubated with ammonium chloride and **1b**, and the reactions were followed by ^1H NMR spectroscopy. Reaction mixtures consisted of 500 µl of 1 M NH_4Cl (containing 20 mM $MgCl_2$, pH 9.0), 50 µl of D_2O, and 100 µl of 500 mM **1b** (pH 9.0, containing 20 mM $MgCl_2$). The reactions were started by the addition of 200 µg of freshly purified enzyme and reaction mixtures were incubated at 22°C. An additional amount (200 µg) of enzyme was added to the individual mixtures after 7 d. ^1H NMR spectra were recorded 3 h, 7 d and 14 d after the first

addition of enzyme. Product amounts were estimated by integration of the signals corresponding to *threo*-(2*S*,3*S*)-3-methylaspartate (*threo*-**3a**) and *erythro*-(2*S*,3*R*)-3-methylasparate (*erythro*-**3a**).

Kinetic characterization

The wild-type MAL and the Q73A mutant catalyzed ammonia or methylamine addition to mesaconate was monitored by following the depletion of mesaconate at 270 nm in 500 mM Tris-HCl buffer (pH 9.0) containing 20 mM $MgCl_2$ and 5 mM mesaconate at 30°C. The concentrations of ammonia and methylamine used in the assay ranged from 10 to 500 mM and 0.1 to 2 M, respectively. The wild-type MAL and the L384A mutant catalyzed amination of substrates **1a-1g** was monitored by following the depletion of substrate at 240 or 270 nm in 500 mM Tris-HCl buffer (pH 9.0) containing 20 mM $MgCl_2$ and 400 mM NH_4Cl at 30°C. The concentrations of substrate **1a-1g** used in the assay ranged from 0.1 to 60 mM. All substrate stock solutions were prepared in 500 mM Tris-HCl buffer, and the pH was adjusted to 9.0. Molar absorption coefficients were determined in the same buffer (Supplementary Table 5).

Crystallization and structure determination

Prior to setting up crystallization screens, the isolated MAL mutants Q73A and L384A were further purified by gel filtration chromatography on a Superdex 200 column (GE Healthcare) using 50 mM Tris-HCl (pH 8.0), containing 2 mM $MgCl_2$ and 0.1 mM KCl, as a running buffer. The proteins eluted as dimers with an apparent molecular weight of ~110 kDa. The purified proteins were concentrated to 10 mg/ml using an Amicon centrifugal filtration device with a 10 kDa molecular mass cut-off. A nanodrop crystallization robot (Mosquito, TTP Labtech) was employed for the initial screening of crystallization conditions using the sitting-drop vapour-diffusion method at 295 K. Screens included PACT premier (Molecular Dimensions) and Cryo Screens I and II (Emerald Biosystems). Lead optimization was performed manually in a hanging drop setup using custom-made plates, and resulted in the growth of well-diffracting crystals with an average size of 0.3 x 0.1

x 0.1 mm^3. The optimized crystallization solution contained 14-16% (w/v) PEG6000, 100 mM MES (pH 6.0), and 100 mM $MgCl_2$.

Diffraction data were measured from shock-cooled crystals that were cryo-protected by briefly soaking in 18% (w/v) PEG6000, 100 mM MES, pH 6.0, 100 mM $MgCl_2$, containing 20% (v/v) glycerol. Data collection was performed using an in-house Bruker AXS rotating anode generator equipped with a DIP2030 image plate detector. Data were integrated and scaled with XDS[4] and merged with SCALA.[5] The crystals of mutants Q73A and L384A diffracted to 2.0 Å and 1.9 Å resolution, respectively, and had the same symmetry and unit cell dimensions as those reported previously for native *C. tetanomorphum* MAL.[6] The structures of the MAL mutants were determined by the maximum-likelihood molecular replacement method, as implemented in the program PHASER,[7] using the native *C. tetanomorphum* MAL structure (PDB code 1KCZ) as a search model. Inspection of $2F_o$-F_c and F_o-F_c Fourier maps confirmed the single amino acid replacement in each mutant structure. In addition, residue C361 in monomers A and B of Q73A was oxidized and identified as an *S*-hydroxycysteine and cysteine sulfonic acid, respectively, like reported previously for native *C. tetanomorphum* MAL.[6] In the asymmetric unit of the L384A crystal, however, residue C361 of monomers A and B had a different covalently attached adduct, most likely an amidopropyl (i.e., 3-amino-3-oxopropyl) moiety. Since the amidopropyl adduct was not present in the purified protein (as revealed by mass spectrometry), it must have been acquired during crystallization. Nonetheless, the modification leaves the overall active site architecture otherwise unchanged. Model rebuilding and refinement were performed with the programs COOT[8] and REFMAC5.[9] The program MolProbity[10] was used for structure validation. The crystallographic R-factors of the refined models are 0.198 (R_{free} = 0.249) at 2.0 Å resolution and 0.162 (R_{free} = 0.210) at 1.9 Å resolution for Q73A and L384A, respectively (Supplementary Table 3).

Molecular docking

Comparative docking simulations were performed using Discovery Studio 2.5 (Accelrys, San Diego, CA, USA). Models for the enzymes were based on the newly determined structures of the Q73A (PDB code 3ZVH) and L384A (PDB code 3ZVI) mutants and that of the corresponding wild-type *C. tetanomorphum* MAL (PDB code 1KCZ).[6] A comparison of the unliganded structure of *C. tetanomorphum* MAL[6] with that of *C. amalonaticus* MAL in complex with the natural substrate *threo*-(2*S*,3*S*)-3-methylaspartic acid[11] (PDB code 1KKR) revealed that the side chain of the catalytic active site residue K331 adopts a different conformation in the unliganded versus substrate-bound MAL structure. Consequently, we introduced distance restraints on K331 (based on the coordinates of the K331 in the substrate-bound *C. amalonaticus* MAL structure) in both wild-type *C. tetanomorphum* MAL and the mutants Q73A and L384A. The three structures were then energy minimized using the CHARMm (Momany and Rone) forcefield.[12, 13] Models of the substrates, *threo*-(2*S*,3*S*)-3-methylaspartate (**3a**), *threo*-(2*S*,3*S*)-2-(cyclohexylamino)-3-methylbutanedioate (**3k**) and *threo*-(2*S*,3*S*)-3-pentylaspartate (**4f**), were constructed and the energy minimized using the CHARMm forcefield. Minimization was done by using a dielectric constant of 1 and a nonbonded cutoff distance of 12 Å. The substrates were docked in the respective structure by using the grid-based approach CDOCKER,[14, 15] a molecular dynamics simulated-annealing-based algorithm. The enzyme active site was fixed, and the atoms of the substrate were allowed to move. Subsequently, the constraints on the amino acids forming the active site were removed and the ligand-docked structures were refined by energy minimization using CHARMm. A final minimization step was applied that consisted of 100 steps of steepest descent followed by 500 iterations of the adopted basis-set Newton–Raphson algorithm using an energy tolerance of 0.001 Kcal $mol^{-1}Å^{-1}$.

Preparative scale enzymatic synthesis of a mixture of *threo*-(2*S*,3*S*)- and *erythro*-(2*S*,3*R*)-3-methylaspartic acid

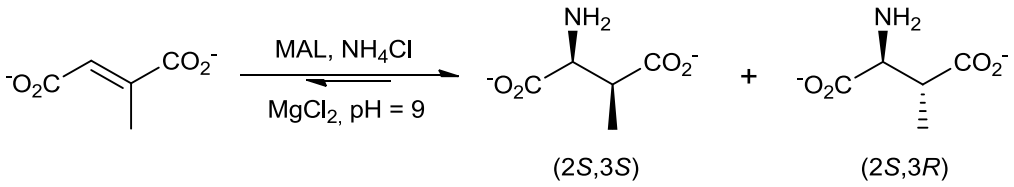

Mesaconic acid (1.0 g, 7.69 mmol) was suspended in water (8.7 ml) and added to a solution of ammonium chloride (5.0 M, 15.4 ml) containing $MgCl_2$ (20 mM). The pH of the mixture was adjusted to 9.0 by the addition of small aliquots of either an aqueous NaOH or HCl solution. Wild-type MAL (7.5 mg in 0.5 ml of water) was added and the reaction mixture was incubated at 22°C. After 45 h, another portion of the enzyme (7.5 mg in 0.5 ml of water) was added. After a total incubation time of 116 h, the solvent was evaporated and the residue was redissolved in aqueous HCl (1 N, 10 ml). The mixture was loaded onto a column packed with ion-exchange resin (10.0 g of Dowex 50W X8, 50-100 mesh), which was pre-treated with 2 M aqueous ammonia (4 column volumes), 1 N HCl (2 column volumes) and distilled water (4 column volumes). The column was washed with distilled water (1 column volume) and the product was eluted with 2 M aqueous ammonia (2 column volumes). The ninhydrin-positive fractions were collected and lyophilized to yield 800 mg (71% isolated yield) of an ~1:1 mixture of *threo*-(2*S*,3*S*)- and *erythro*-(2*S*,3*R*)-3-methylaspartic acid. This mixture of 3-methylaspartic acid isomers, with known absolute configuration,[1] was used as starting material in the synthesis of isomeric mixtures of amino acids **3c-3m** (see below).

***threo*-(2*S*,3*S*)-3-methylaspartic acid:** ^{1}H NMR (400 MHz, D_2O): δ 0.98 (d, 3H, ^3J = 7.6 Hz, C**H**$_3$CH), 2.79 (dq, 1H, ^3J = 7.6 Hz, ^3J = 3.2 Hz, CH_3C**H**), 3.96 (d, 1H, ^3J = 3.2 Hz, C**H**NH_2).

***erythro*-(2*S*,3*R*)-3-methylaspartic acid:** ^{1}H NMR (400 MHz, D_2O): δ 1.12 (d, 3H, ^{3}J = 7.6 Hz, C**H**$_3$CH), 2.73 (dq, 1H, ^{3}J = 7.6 Hz, ^{3}J = 6.0 Hz, CH_3C**H**), 3.50 (d, 1H, ^{3}J = 6.0 Hz, C**H**NH_2).

Chemical synthesis of *N*-substituted 3-methylaspartic acid derivatives 3c-3m

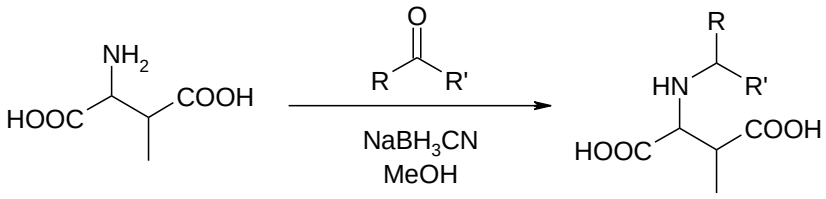

In order to establish the identity and relative configuration of the amino acid products of the Q73A-catalyzed amine (**2c-2m**) additions to mesaconate, we have synthesized the expected amino acid products **3c-3m** both as *threo*-isomers and as a mixture of *threo*- and *erythro*-isomers via reductive amination. The general procedure is as follows. 3-Methylaspartic acid (1.00 mmol, 147 mg) was suspended in methanol (3 ml) at room temperature. Carbonyl compound (1.20 mmol) was added, followed by sodium cyanoborohydride (1.50 mmol, 95 mg), and the incubation mixture was stirred at room temperature. After 20 h, the undissolved substrate was filtered off and the solvent was evaporated. The residue was triturated with ethyl acetate (3 x 10 ml) and dried under vacuum. This reductive amination reaction was carried out both on commercially available *threo*-DL-3-methylaspartic acid as well as on the mixture of *threo*-(2*S*,3*S*)- and *erythro*-(2*S*,3*R*)-3-methylaspartic acid, which was synthesized by using wild-type MAL as described above. A comparison of the ^{1}H NMR signals of these synthesized reference molecules to those obtained with the (lyophilized) crude enzyme reaction mixtures established the identity and relative configuration of the enzymatic products **3c-3m**.

***threo*-DL-2-(ethylamino)-3-methylbutanedioic acid (3c)**

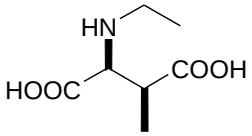

^{1}H NMR (400 MHz, D_2O): δ 0.99 (d, 3H, ^3J = 7.6 Hz, C**H$_3$**CH), 1.16 (t, 3H, ^3J = 7.2 Hz, C**H$_3$**CH$_2$), 2.75 (dq, 1H, ^3J = 7.2 Hz, ^3J = 3.2 Hz, CH$_3$C**H**), 2.85-3.10 (m, 2H, C**H$_2$**NH), 3.71 (d, 1H, ^3J = 3.2 Hz, C**H**NH); ^{13}C NMR (125 MHz, D_2O): δ 10.9, 12.0, 41.0, 43.4, 63.6, 172.7, 181.6; HRMS (ESI+): calcd. for $C_7H_{13}NO_4Na$, 198.0737; found, 198.0720; HPLC (Chirex 3126-D-penicillamine, 2 mM aq. $CuSO_4$:isopropanol 90:10, flow 0.9 ml/min): $R_{t\text{-}1}$ = 11.0 min, $R_{t\text{-}2}$ = 18.4 min. The diastereomeric ratio (d.r.) can be determined by integration of the ^{1}H NMR signals at 3.71 ppm (*threo* isomer) and 3.84 ppm (*erythro* isomer) corresponding to the C**H**NH proton.

***threo*-DL-2-(propylamino)-3-methylbutanedioic acid (3d)**

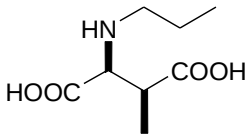

^{1}H NMR (400 MHz, D_2O): δ 0.84 (t, 3H, ^3J = 7.2 Hz, C**H$_3$**CH$_2$), 0.98 (d, 3H, ^3J = 7.2 Hz, C**H$_3$**CH), 1.52-1.65 (m, 2H, CH$_3$C**H$_2$**), 2.73 (dq, 1H, ^3J = 7.6 Hz, ^3J = 3.2 Hz, CH$_3$C**H**), 2.74-2.81 (m, 1H, C**H**$_2$NH), 2.98-3.02 (m, 1H, C**H**$_2$NH), 3.69 (d, 1H, ^3J = 3.2 Hz, C**H**NH); ^{13}C NMR (125 MHz, D_2O): δ 10.4, 12.1, 19.4, 40.8, 49.9, 64.0, 172.5, 181.8; HRMS (ESI+): calcd. for $C_8H_{16}NO_4$, 190.1074; found, 190.1071; HPLC (Chirex 3126-D-penicillamine, 2 mM aq. $CuSO_4$:isopropanol 90:10, flow 0.9 ml/min): $R_{t\text{-}1}$ = 15.9 min, $R_{t\text{-}2}$ = 27.7 min. The d.r. can be determined by integration of the ^{1}H NMR signals at 0.98 ppm (*threo* isomer) and 1.08 ppm (*erythro* isomer) corresponding to the CHC**H$_3$** protons.

***threo*-DL-2-(butylamino)-3-methylbutanedioic acid (3e)**

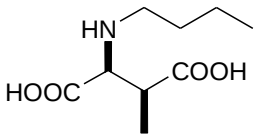

^{1}H NMR (400 MHz, D_2O): δ 0.78 (t, 3H, ^3J = 7.2 Hz, C**H$_3$**CH$_2$), 0.98 (d, 3H, ^3J = 7.6 Hz, C**H$_3$**CH), 1.15-1.32 (m, 2H, CH$_3$C**H$_2$**), 1.47-1.62 (m, 2H, CH$_3$CH$_2$C**H$_2$**), 2.73 (dq, 1H, ^3J = 7.6 Hz, ^3J = 3.2 Hz, CH$_3$C**H**), 2.78-2.90 (m, 1H, C**H**$_2$NH), 2.98-3.05 (m, 1H, C**H**$_2$NH), 3.69 (d, 1H, ^3J = 3.2 Hz, C**H**NH); ^{13}C NMR (125 MHz, D_2O): δ 12.1, 12.9, 19.3, 27.8, 40.8, 48.0, 64.0, 172.6, 181.8; HRMS (ESI+): calcd. for $C_9H_{18}NO_4$,

204.1230; found, 204.1229; HPLC (Chirex 3126-D-penicillamine, 2 mM aq. $CuSO_4$:isopropanol 90:10, flow 0.9 ml/min): R_{t-1} = 49.7 min, R_{t-2} = 84.6 min. The d.r. can be determined by integration of the ^{1}H NMR signals at 0.98 ppm (*threo* isomer) and 1.06 ppm (*erythro* isomer) corresponding to the CHC**H$_3$** protons.

threo-DL-2-(pentylamino)-3-methylbutanedioic acid (3f)

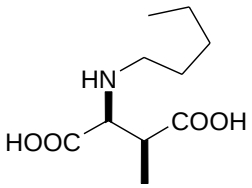

^{1}H NMR (400 MHz, D_2O): δ 0.74 (t, 3H, ^3J = 7.2 Hz, C**H$_3$**CH$_2$), 0.98 (d, 3H, ^3J = 7.6 Hz, C**H$_3$**CH), 1.15-1.26 (m, 4H, CH$_3$C**H$_2$**C**H$_2$**), 1.50-1.62 (m, 2H, NHCH$_2$C**H$_2$**), 2.72 (dq, 1H, ^3J = 7.6 Hz, ^3J = 3.2 Hz, CH$_3$C**H**), 2.77-2.89 (m, 1H, C**H**$_2$NH), 2.96-3.07 (m, 1H, C**H**$_2$NH), 3.68 (d, 1H, ^3J = 3.2 Hz, C**H**NH); ^{13}C NMR (125 MHz, D_2O): δ 12.2, 13.3, 21.6, 25.4, 28.0, 40.8, 48.2, 64.0, 172.6, 181.8; HRMS (ESI+): calcd. for $C_{10}H_{20}NO_4$, 218.1395; found, 218.1393. The d.r. can be determined by integration of the ^{1}H NMR signals at 3.68 ppm (*threo* isomer) and 3.71 ppm (*erythro* isomer) corresponding to the C**H**NH proton.

threo-DL-2-(hexylamino)-3-methylbutanedioic acid (3g)

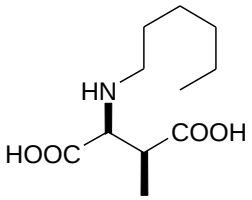

^{1}H NMR (300 MHz, D_2O): δ 0.75 (t, 3H, ^3J = 6.6 Hz, C**H$_3$**CH$_2$), 0.96 (d, 3H, ^3J = 7.5 Hz, C**H$_3$**CH), 1.09-1.30 (m, 6H, CH$_3$(C**H$_2$**)**$_3$**), 1.46-1.56 (m, 2H, NHCH$_2$C**H$_2$**), 2.52-2.82 (m, 3H, CH$_3$C**H**, C**H$_2$**NH), 3.54 (d, 1H, ^3J = 3.3 Hz, C**H**NH); ^{13}C NMR (125 MHz, D_2O): δ 12.2, 13.4, 22.0, 25.8, 26.8, 30.8, 42.3, 48.2, 64.7, 175.8, 182.4; HRMS (ESI+): calcd. for $C_{11}H_{22}NO_4$, 232.1553; found, 232.1551. The d.r. can be determined by integration of the ^{1}H NMR signals at 3.53 ppm (*threo* isomer) and 3.67 ppm (*erythro* isomer) corresponding to the C**H**NH proton.

***threo*-DL-2-(*iso*-propylamino)-3-methylbutanedioic acid (3h)**

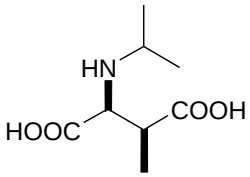

^{1}H NMR (400 MHz, D_2O): δ 0.91 (d, 3H, ^3J = 7.2 Hz, C**H**$_3$CHCOOH), 1.02 (d, 3H, ^3J = 6.8 Hz, C**H**$_3$CH), 1.06 (d, 3H, ^3J = 6.8 Hz, C**H**$_3$CH), 2.61 (dq, 1H, ^3J = 7.2 Hz, ^3J = 4.0 Hz, CH_3C**H**), 2.93 (app hept, 1H, ^3J = 6.8 Hz, C**H**$(CH_3)_2$), 3.62 (d, 1H, ^3J = 4.0 Hz, C**H**NH); ^{13}C NMR (125 MHz, D_2O): δ 12.2, 19.2, 20.6, 42.5, 50.2, 62.6, 176.3, 182.1; HRMS (ESI+): calcd. for $C_8H_{16}NO_4$, 190.1074; found, 190.1071; HPLC (Chirex 3126-D-penicillamine, 2 mM aq. $CuSO_4$:isopropanol 90:10, flow 0.9 ml/min): $R_{t\text{-}1}$ = 9.2 min, $R_{t\text{-}2}$ = 19.7 min. The d.r. can be determined by integration of the ^{1}H NMR signals at 2.61 ppm (*threo* isomer) and 2.37 ppm (*erythro* isomer) corresponding to the C**H**CH_3 protons.

***threo*-DL-2-(*cyclo*-butylamino)-3-methylbutanedioic acid (3i)**

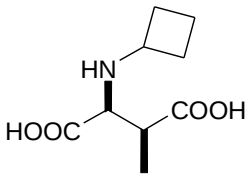

^{1}H NMR (400 MHz, D_2O): δ 0.91 (d, 3H, ^3J = 7.2 Hz, C**H**$_3$CH), 1.45-2.10 (m, 6H, *c*-butyl), 2.61 (dq, 1H, ^3J = 7.2 Hz, ^3J = 3.6 Hz, CH_3C**H**), 3.30-3.42 (m, 1H, *c*-butyl), 3.44 (d, 1H, ^3J = 3.6 Hz, C**H**NH); ^{13}C NMR (125 MHz, D_2O): δ 12.1, 14.4, 27.8, 28.2, 42.9, 52.2, 62.4, 177.0, 182.4; HRMS (ESI+): calcd. for $C_9H_{16}NO_4$, 202.1074; found, 202.1071; HPLC (Chirex 3126-D-penicillamine, 2 mM aq. $CuSO_4$:isopropanol 90:10, flow 0.9 ml/min): $R_{t\text{-}1}$ = 34.7 min, $R_{t\text{-}2}$ = 57.9 min. The d.r. can be determined by integration of the ^{1}H NMR signals at 2.61 ppm (*threo* isomer) and 2.70 ppm (*erythro* isomer) corresponding to the C**H**CH_3 protons.

***threo*-DL-2-(*cyclo*-pentylamino)-3-methylbutanedioic acid (3j)**

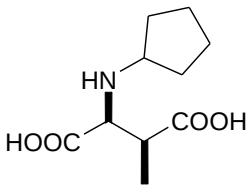

^{1}H NMR (400 MHz, D_2O): δ 0.95 (d, 3H, ^3J = 7.6 Hz, C**H**$_3$CH), 1.42-1.63 (m, 6H, *c*-pent), 1.74-1.91 (m, 2H, *c*-pent), 2.70 (dq, 1H, ^3J = 7.6 Hz, ^3J = 3.2 Hz, CH_3C**H**), 3.32-3.40 (m, 1H, C**H**NH, *c*-pentyl), 3.70 (d, 1H, ^3J = 3.2 Hz, CHC**H**NH); ^{13}C NMR (125 MHz, D_2O): δ 12.2, 23.3, 23.4, 29.0, 30.5, 41.4, 60.0, 63.0, 173.8, 181.9; HRMS (ESI+): calcd. for $C_{10}H_{17}NO_4Na$, 238.1050; found, 238.1031. The d.r. can be

determined by integration of the ^{1}H NMR signals at 3.70 ppm (*threo* isomer) and 3.73 ppm (*erythro* isomer) corresponding to the C**H**NH proton.

threo-DL-2-(*cyclo*-hexylamino)-3-methylbutanedioic acid (3k)

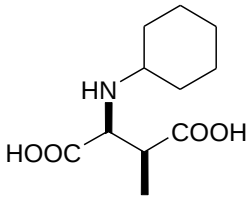

^{1}H NMR (400 MHz, D_2O): δ 0.98 (d, 3H, ^{3}J = 7.6 Hz, C**H$_3$**CH), 1.03-1.55 (m, 6H, (C**H$_2$**)$_3$), 1.59-1.71 (m, 2H, (C**H$_2$**)CHNH), 1.86-1.97 (m, 2H, (C**H$_2$**)CHNH), 2.74 (dq, 1H, ^{3}J = 7.6 Hz, ^{3}J = 3.2 Hz, CH_3C**H**), 2.88-2.97 (m, 1H, C**H**NH, *c*-hexyl), 3.77 (d, 1H, ^{3}J = 3.2 Hz, C**H**NH); ^{13}C NMR (125 MHz, D_2O): δ 12.3, 24.0, 24.1, 24.7, 29.0, 30.1, 40.9, 58.5, 61.6 172.9, 181.7; HRMS (ESI+): calcd. for $C_{11}H_{19}NO_4$, 230.1387; found, 230.1385. The d.r. can be determined by integration of the ^{1}H NMR signals at 3.77 ppm (*threo* isomer) and 3.80 ppm (*erythro* isomer) corresponding to the C**H**NH proton.

threo-DL-2-(*cyclo*-propyl-methylamino)-3-methylbutanedioic acid (3l)

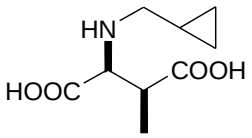

^{1}H NMR (400 MHz, D_2O): δ 0.21-0.28 (m, 2H, *c*-propyl), 0.50-0.65 (m, 2H, *c*-propyl), 0.91-1.09 (m, 1H, *c*-propyl), 1.01 (d, 3H, ^{3}J = 7.6 Hz, C**H$_3$**CH), 2.71 (dd, 1H, ^{2}J = 12.8 Hz, ^{3}J = 4.8 Hz, C**H$_2$**NH), 2.75 (dq, 1H, ^{3}J = 7.2 Hz, ^{3}J = 2.8 Hz, CH_3C**H**), 2.97 (dd, 1H, ^{2}J = 12.8 Hz, ^{3}J = 7.2 Hz, C**H$_2$**NH), 3.78 (d, 1H, ^{3}J = 2.8 Hz, C**H**NH); ^{13}C NMR (125 MHz, D_2O): δ 3.7, 3.8, 7.1, 12.1, 40.8, 53.0, 63.4, 172.6, 181.8; HRMS (ESI+): calcd. for $C_9H_{16}NO_4$, 202.1074; found, 202.1071; HPLC (Chirex 3126-D-penicillamine, 2 mM aq. $CuSO_4$:isopropanol 90:10, flow 0.9 ml/min): $R_{t\text{-}1}$ = 16.3 min, $R_{t\text{-}2}$ = 23.2 min. In this case, only the *threo*-isomer has been synthesized, the ^{1}H NMR spectrum of which is consistent with that of enzymatically prepared **3l**.

***threo*-DL-2-(benzylamino)-3-methylbutanedioic acid (3m)**

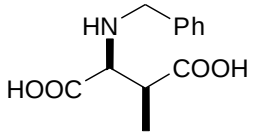

^{1}H NMR (400 MHz, D_2O): δ 0.98 (d, 3H, ^3J = 7.6 Hz, C**H**$_3$CH), 2.72 (dq, 1H, ^3J = 7.6 Hz, ^3J = 3.2 Hz, CH$_3$C**H**), 3.70 (d, 1H, ^3J = 3.2 Hz, C**H**NH), 4.04 (d, 1H, ^2J = 12.8 Hz, PhC**H**$_2$), 4.24 (d, 1H, ^2J = 12.8 Hz, PhC**H**$_2$), 7.20-7.40 (m, 5H, Ar**H**); ^{13}C NMR (125 MHz, D_2O): δ 12.2, 40.7, 51.3, 62.9, 129.4, 129.8, 130.2, 131.0, 172.3, 181.7; HRMS (ESI+): calcd. for $C_{12}H_{16}NO_4$, 238.1074; found, 238.1071. The d.r. can be determined by integration of the ^{1}H NMR signals at 3.70 ppm (*threo* isomer) and 3.85 ppm (*erythro* isomer) corresponding to the C**H**NH proton.

Preparative scale enzymatic synthesis of *N*-substituted 3-methylaspartic acids 3n-3u

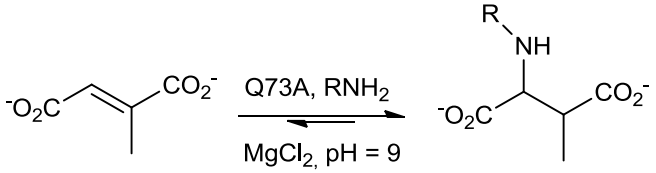

3

3n R = cyclopropyl
3o R = ethoxy
3p R = 2-hydroxyethyl
3q R = 3-hydroxypropyl
3r R = 2-methoxyethyl
3s R = *N-m*ethyl-2-aminoethyl
3t R = 2-aminoethyl
3u R = 3-aminopropyl

The *N*-substituted 3-methylaspartic acid derivatives **3n-3u** were synthesized by using mutant Q73A as catalyst in the amine (**2n-2u**) additions to mesaconate (**1b**). A solution of mesaconic acid (0.40 g, 3.1 mmol), amine (31 mmol) and $MgCl_2$ (20 mM) was prepared in water (25 ml), and the pH was adjusted to 9.0 by the addition of small aliquots of either an aqueous NaOH or HCl solution. The reactions were started by the addition of 5 mg of freshly purified enzyme (i.e., the Q73A mutant), and the reaction mixtures were incubated at 22°C. An additional amount (5 mg) of enzyme was added to the individual mixtures after 4 d, because the enzyme loses about 50% of its original activity after 4 days of incubation. The progress of each reaction was monitored by using ^{1}H NMR spectroscopy and spectra were recorded 1 d and 7 d after the first addition of enzyme. All reactions were terminated after 7 d, except for the reaction with ethanolamine (**2p**), which was terminated

after 14 d. The individual reaction mixtures were lyophilized, after which the amino acid product was purified using cation exchange chromatography (Dowex, 50W X8, 100-200 mesh size, Merck). A Dowex column (10.0 g resin per 1 g of mesaconic acid) was prepared by pre-treatment with a solution of aqueous NH_3 (2 M, 4 column volumes), aqueous HCl (1 N, 2 column volumes) and distilled water (4 column volumes). The lyophilized reaction mixture was suspended in aqueous HCl (1 N, 20 ml) and loaded onto the column. The column was washed with distilled water (1 column volume) and the product was eluted with aqueous NH_3 (2 M, 2 column volumes). The ninhydrin-positive fractions were collected and concentrated under reduced pressure, followed by lyophilization to give the purified amino acid product.

2-(cyclopropylamino)-3-methylbutanedioic acid (3n)

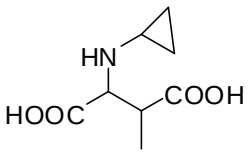

Conversion 80% (^{1}H NMR after 7 d). Yield 42%. Pale brown solid. ^{1}H NMR (200 MHz, CD_3OD): δ 0.60-0.95 (m, 4H, *c*-propyl), 1.04 (d, 3H, ^3J = 7.6 Hz, C**H$_3$**CH), 2.60-2.86 (m, 2H, CH_3C**H**, C**H**CH_2, *c*-propyl), 3.72 (d, 1H, ^3J = 3.7 Hz, C**H**NH); ^{13}C NMR (50 MHz, CD_3OD): δ 3.6, 5.2, 13.2, 31.3, 41.5, 66.5, 172.4, 181.6; HRMS (ESI+): calcd. for $C_8H_{14}NO_4$, 188.0923; found, 188.0917.

2-(ethoxyamino)-3-methylbutanedioic acid (3o)

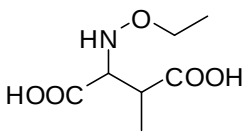

Conversion 100% (^{1}H NMR after 7 d). Yield 38%. White solid. ^{1}H NMR (500 MHz, D_2O): δ 0.87 (d, 3H, ^3J = 7.3 Hz, CHC**H$_3$**), 0.98 (t, 3H, ^3J = 7.0 Hz, C**H$_3$**CH_2O), 2.56 (dq, 1H, ^3J = 7.1 Hz, ^3J = 4.8 Hz, CH_3C**H**), 3.63 (q, 2H, ^3J = 7.1 Hz, CH_3C**H$_2$**O), 3.72 (d, 1H, ^3J = 4.6 Hz, C**H**NH); ^{13}C NMR (125 MHz, D_2O): δ 12.2, 13.1, 42.1, 61.5, 67.1, 178.4, 181.9; HRMS (ESI+): calcd. for $C_7H_{14}NO_5$, 192.0872; found, 192.0866.

2-(2-hydroxyethyl-amino)-3-methylbutanedioic acid (3p)

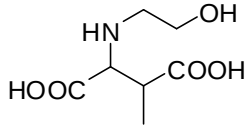

Conversion 32% (^{1}H NMR after 14 d). Yield 9%. White solid. ^{1}H NMR (500 MHz, D_2O): δ 1.26 (d, 3H, ^3J = 7.5 Hz, CHC**H$_3$**), 3.16-3.27 (m, 2H, NHC**H$_2$**CH$_2$), 3.32-3.36 (m, 1H, CH$_3$C**H**), 3.89 (t, 2H, ^3J = 5.1 Hz, CH$_2$C**H$_2$**OH), 4.06 (d, 1H, ^3J = 3.0 Hz, NHC**H**); ^{13}C NMR (125 MHz, D_2O): δ 14.1, 42.2, 52.4, 59.2, 65.8, 173.9, 180.4. HRMS (ESI+): calcd. for $C_7H_{14}NO_5$, 192.0872; found, 192.0866.

2-(3-hydroxypropyl-amino)-3-methylbutanedioic acid (3q)

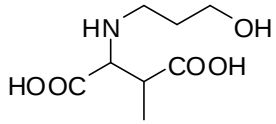

Conversion 57% (^{1}H NMR after 7 d). Yield 45%. White solid. Signals corresponding to two diastereoisomers (d.r. = 90:10) were observed in the ^{1}H NMR spectra. Major diastereoisomer: ^{1}H NMR (200 MHz, D_2O): δ 0.99 (d, 3H, ^3J = 7.5 Hz, CHC**H$_3$**), 1.75-1.90 (m, 2H, CH$_2$C**H$_2$**CH$_2$), 2.75 (dq, 1H, ^3J = 7.6 Hz, ^3J = 3.1 Hz, CH$_3$C**H**), 2.80-3.25 (m, 2H, NHC**H$_2$**CH$_2$), 3.57 (t, 2H, ^3J = 6.1 Hz, CH$_2$C**H$_2$**OH), 3.70 (d, 1H, J = 3.1 Hz, NHC**H**); ^{13}C NMR (50 MHz, D_2O): δ 11.9, 27.9, 38.8, 45.9, 59.0, 63.9, 172.1, 181.1; HRMS (ESI+): calcd. for $C_8H_{16}NO_5$, 206.1029; found, 206.1023.

2-(2-methoxyethyl-amino)-3-methylbutanedioic acid (3r)

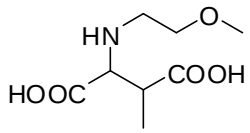

Conversion 57% (^{1}H NMR after 7 d). The product was purified using two column chromatography steps, but still contained trace amounts of the starting substrate 2-methoxyethylamine (**2r**). Yield 45%. White solid. ^{1}H NMR (200 MHz, D_2O): δ 1.01 (d, 3H, ^3J = 7.5 Hz, CHC**H$_3$**) 2.74 (dq, 1H, ^3J = 7.6 Hz, ^3J = 3.2 Hz, CH$_3$C**H**), 3.00-3.10 (m, 2H, CH$_2$C**H$_2$**NH), 3.26 (s, 3H, OC**H$_3$**), 3.52-3.64 (m, 2H, CH$_2$C**H$_2$**O), 3.75 (d, 1H, ^3J = 3.2 Hz, C**H**NH); ^{13}C NMR (50 MHz, D_2O): δ 11.9, 38.8, 40.4, 47.0, 58.1, 63.9, 172.0, 181.6; HRMS (ESI+): calcd. for $C_8H_{15}NO_5Na$, 228.0848; found, 228.0842.

2-(*N*-(2-methylamino-ethyl)amino)-3-methylbutanedioic acid (3s)

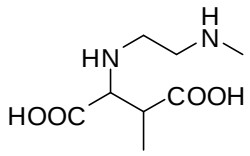

Conversion 94% (^{1}H NMR after 7 d). Yield 66%. Pale brown solid. ^{1}H NMR (200 MHz, D_2O): δ 0.95 (d, 3H, ^3J = 7.6 Hz, C**H$_3$**CH), 2.64 (s, 3H, C**H$_3$**NH), 2.75 (dq, 1H, ^3J = 7.5 Hz, ^3J = 3.2 Hz, C**H**CH_3), 3.11-3.26 (m, 4H, C**H$_2$**C**H$_2$**), 3.70 (d, 1H, ^3J = 3.2 Hz, C**H**NH); ^{13}C NMR (50 MHz, D_2O): δ 11.5, 32.9, 41.4, 43.3, 45.5, 64.3, 174.0, 181.6; HRMS (ESI+): calcd. for $C_8H_{17}N_2O_4$, 205.1188; found, 205.1184.

2-(*N*-(2-aminoethyl)amino)-3-methylbutanedioic acid (3t)

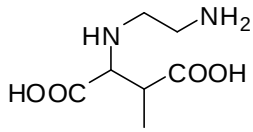

Conversion 96% (^{1}H NMR after 7 d). Yield 74%. Pale brown solid. ^{1}H NMR (200 MHz, D_2O): δ 1.00 (d, 3H, ^3J = 7.6 Hz, CHC**H$_3$**) 2.78 (dq, 1H, ^3J = 7.5 Hz, ^3J = 3.2 Hz, CH_3C**H**), 3.25-3.35 (m, 4H, C**H$_2$**C**H$_2$**), 3.80 (d, 1H, ^3J = 3.0 Hz, C**H**NH); ^{13}C NMR (50 MHz, D_2O): δ 11.7, 35.8, 40.8, 44.6, 64.3, 172.4, 181.2; HRMS (ESI+): calcd. for $C_7H_{15}N_2O_4$, 191.1032; found, 191.1026.

2-(3-aminopropyl-amino)-3-methylbutanedioic acid (3u)

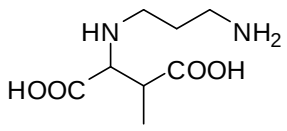

Conversion 80% (^{1}H NMR after 7 d). Yield 10%. Pale brown solid. ^{1}H NMR (200 MHz, D_2O): δ 0.96 (d, 3H, ^3J = 7.5 Hz, CHC**H$_3$**), 1.84-1.98 (m, 2H, CH_2C**H$_2$**CH_2), 2.71 (dq, 1H, ^3J = 7.6 Hz, ^3J = 3.2 Hz, CH_3C**H**), 2.86-3.04 (m, 4H, C**H$_2$**CH_2C**H$_2$**), 3.68 (d, 1H, ^3J = 3.0 Hz, C**H**NH); ^{13}C NMR (50 MHz, D_2O): δ 11.7, 24.2, 37.2, 41.3, 45.1, 64.2, 173.8, 181.6; HRMS (ESI+): calcd. for $C_8H_{17}N_2O_4$, 205.1188; found, 205.1184.

Chemical synthesis of 2-substituted fumarates

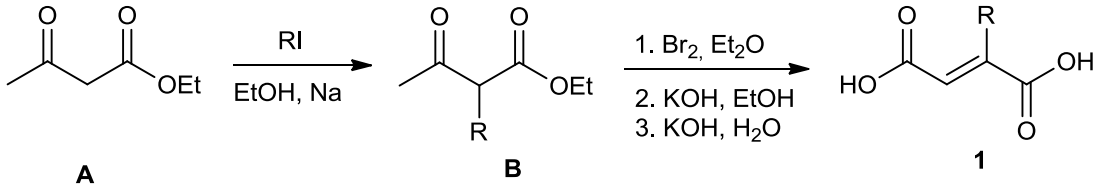

A **B** **1**

1c R = ethyl (from B)
1d R = propyl (from A)
1e R = butyl (from A)
1f R = pentyl (from B)
1g R = hexyl (from B)
1n R = benzyl (from B)

2-*n*-propylfumaric acid (1d)

Sodium (10 mmol, 230 mg) was dissolved in ethanol (6.0 ml). Ethyl acetoacetate (9.0 mmol, 1.14 ml) was added dropwise over 5 min at 5°C, followed by *n*-propyl iodide (12 mmol, 1.17 ml). The reaction was refluxed for 2 h and was then cooled to room temperature, poured on water (30 ml) and extracted with Et_2O (3 x 25 ml). Organic fractions, containing a mixture of mono- and dialkylated product, were dried and concentrated to ~15 ml. Bromine (4.0 g) was added slowly at room temperature, and the reaction mixture was refluxed for 3 h. The volatiles were evaporated, and the residue was slowly added to a solution of KOH (4.0 g) in ethanol (15 ml). The resultant mixture was refluxed for 30 min, after which 20 ml of water was added and the refluxing continued for another 20 min. The reaction mixture was washed with EtOAc (2 x 40 ml). The aqueous phase was acidified with aqueous HCl (12 N) to pH < 1 and extracted with Et_2O (4 x 50 ml). Collected organic fractions were dried, decolourized with activated carbon and the solvent was evaporated. The resultant residue was triturated with pentane to yield white crystals (100 mg, 7%). Mp: 173.5-174.7°C (lit.[16] 172-174°C); ^{1}H NMR (400 MHz, D_2O + K_2CO_3): δ 0.70 (t, 3H, ^3J = 7.6 Hz, C**H$_3$**), 1.19-1.25 (m, 2H, CH_3C**H$_2$**), 2.63 (t, 2H, ^3J = 7.2 Hz, C**H$_2$**C=C), 6.18 (s, 1H, vinyl **H**). ^{1}H NMR is consistent with literature data.[16]

2-ethylfumaric acid (1c)

Compound **1c** was prepared according to the same procedure as that used for the synthesis of **1d**, starting with commercially available ethyl 2-ethylacetoacetate. Yield: 33%. Yellow crystals; mp: 197-198°C (lit.[16] 195°C); ^{1}H NMR (400 MHz, D_2O): δ 0.89 (t, 3H, ^3J = 7.2 Hz, C**H$_3$**), 2.49 (d, 2H, ^3J = 7.2 Hz, C**H$_2$**), 6.57 (s, 1H, vinyl **H**). ^{1}H NMR is consistent with literature data.[16]

2-*n*-butylfumaric acid (1e)

Compound **1e** was prepared according to the same procedure as that used for the synthesis of **1d**. Yield: 24%. Yellow crystals; mp: 171.7-172.5°C (lit.[16] 170-171°C); ^{1}H NMR (400 MHz, D_2O + K_2CO_3): δ 0.71 (t, 3H, ^3J = 7.2 Hz, C**H$_3$**), 1.06-1.24 (m, 4H, CH_3C**H$_2$**C**H$_2$**), 2.31 (t, 2H, ^3J = 7.2 Hz, C**H$_2$**C=C), 6.17 (s, 1H, vinyl **H**). ^{1}H NMR is consistent with literature data.[16]

2-*n*-pentylfumaric acid (1f)

Compound **1f** was prepared according to the same procedure as that used for the synthesis of **1d**, starting with commercially available ethyl 2-*n*-pentylacetoacetate. Yield: 40%. Yellow crystals; mp: 160-162°C; ^{1}H NMR (400 MHz, DMSO-d_6): δ 0.83 (t, 3H, ^3J = 6.8 Hz, C**H$_3$**), 1.18-1.42 (m, 6H, CH_3(C**H$_2$**)**$_3$**), 2.62 (t, 2H, ^3J = 7.6 Hz, C**H$_2$**C), 6.55 (s, 1H, vinyl **H**); ^{13}C NMR (75 MHz, $CDCl_3$): δ 14.5, 22.4, 27.7, 28.9, 31.8, 127.5, 147.8, 167.4, 168.7; HRMS (ESI-): calcd. for $C_9H_{13}O_4$, 185.0808; found, 185.0804.

2-*n*-hexylfumaric acid (1g)

Compound **1g** was prepared according to the same procedure as that used for the synthesis of **1d**, starting with commercially available ethyl 2-*n*-hexylacetoacetate. Yield: 43%. Yellow crystals; mp: 161-162°C (lit.[17] 172-174°C); ^{1}H NMR (400 MHz, DMSO-d_6): δ 0.83 (t, 3H, ^3J = 6.8 Hz, C**H$_3$**), 1.19-1.38 (m, 8H, CH_3(C**H$_2$**)**$_4$**), 2.62 (t, 2H, ^3J = 7.6 Hz, C**H$_2$**C) 6.55 (s, 1H, vinyl **H**). ^{1}H NMR is consistent with literature data.[17]

2-benzylfumaric acid (1n)

Compound **1n** was prepared according to the same procedure as that used for the synthesis of **1d**, starting with commercially available ethyl 2-benzylacetoacetate. Yield: 10%. Yellow crystals; mp: 209-211°C; ^{1}H NMR (300 MHz, $CDCl_3$): δ 4.05 (s, 2H, C**H$_2$**C=C), 6.73 (s, 1H, vinyl **H**), 7.13-7.22 (m, 3H, Ar**H**), 7.22-7.31 (m, 2H, Ar**H**); ^{13}C NMR (75 MHz, $CDCl_3$): δ 32.3, 126.1, 127.6, 128.3, 128.4, 128.7, 128.9, 138.4, 144.7, 166.8, 167.6; HRMS (ESI+): calcd. for $C_{11}H_{11}O_4$, 207.0651; found, 207.0652.

2-(benzyloxy)-fumaric acid (1j)

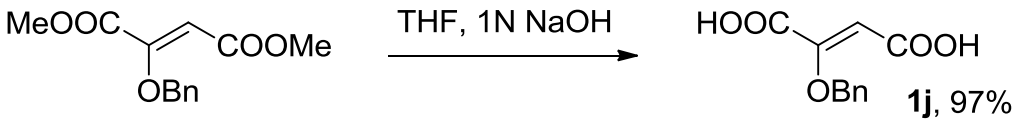

Dimethyl 2-(benzyloxy)-fumarate (1.12 mmol, 280 mg), prepared according to a published procedure.[18] was dissolved in tetrahydrofuran (3.0 ml). Aqueous NaOH (1 M, 3.0 ml) was added and the resultant mixture was stirred for 10 min at room temperature. The reaction mixture was poured on aqueous HCl (1 N, 20 mL) and extracted with ethyl acetate (3 x 20 ml). Collected organic phases were dried ($MgSO_4$) and the solvent was evaporated. The residue was dissolved in ethyl ether and the product was precipitated with pentane to give a white powder (240 mg, 97%). Mp: 132-133°C (decomp.); ^{1}H NMR (400 MHz, DMSO-d_6): δ 5.09 (s, 2H, PhC**H$_2$**), 6.06 (s, 1H, vinyl **H**), 7.30-7.41 (m, 5H, Ar**H**); ^{13}C NMR (75 MHz, $CDCl_3$): δ 74.3, 111.0, 128.5, 128.7, 129.0, 137.3, 154.4, 164.7, 166.0; HRMS (ESI-): calcd. for $C_{11}H_9O_5$, 221.0444; found, 221.0453.

Dimethyl 2-phenylthiofumarate (5)

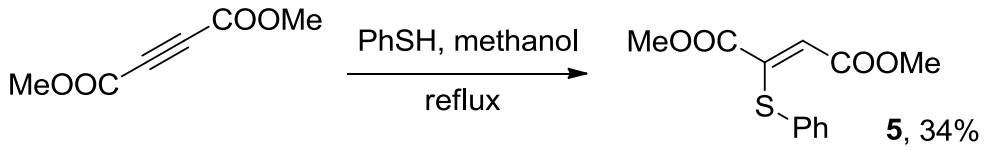

A solution of dimethyl acetylenedicarboxylate (5.0 mmol, 710 mg) and thiophenol (5.0 mmol, 510 μl) in methanol (15 ml) was heated to reflux for 2 h. TLC indicated full conversion of the starting compound. The solvent was evaporated and the product was purified by flash chromatography (Silicagel, 40-63 μm, Pentane/Et_2O, 95:5, v/v). Yield: 34%. Yellow oil; TLC (Pentane/Et_2O, 7:3 v/v): R_f = 0.48; ^{1}H NMR (400 MHz, $CDCl_3$): δ 3.35 (s, 3H, C**H**$_3$O), 3.79 (s, 3H, C**H**$_3$O), 6.38 (s, 1H, vinyl **H**), 7.31-7.46 (m, 5H, Ar**H**); ^{1}H NMR is in agreement with the literature data.[19]

General procedure for the hydrolysis of 2-substituted fumarate esters

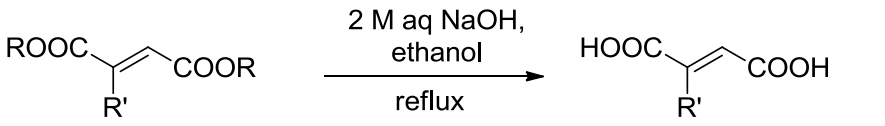

R = Me or Et
R' = EtS, EtO, PhS, PhO, BnS

1

1h R' = ethoxy, 80%
1i R' = phenoxy, 83%
1k R' = ethylthio, 85%
1l R' = phenylthio, 80%
1m R' = benzylthio, 80%

To a 0.5 M solution of R'-substituted fumarate ester in ethanol was added an equivolumous amount of 2 M aqueous NaOH. The resultant solution was stirred at reflux for 2 h. After cooling down to room temperature, the reaction mixture was washed with ethyl acetate and acidified to pH 1 with 30% aqueous HCl. The product was extracted with ethyl acetate. Collected organic phases were dried ($MgSO_4$) and the solvent was evaporated under reduced pressure to provide the desired product.

2-ethoxyfumaric acid (1h)

Compound **1h** was prepared from the respective diethyl ester, synthesized according to a previously reported protocol,[20] by the general hydrolysis procedure, and further purified by precipitation from Et_2O/pentane. Yield: 80%. White powder. Mp: 120-121°C (lit.[20] 117-118°C); ^{1}H NMR (400 MHz, acetone-d_6): δ 1.31 (t, 3H, ^3J = 7.2 Hz, C**H$_3$**), 4.21 (q, 2H, ^3J = 7.2 Hz, C**H$_2$**), 6.18 (s, 1H, vinyl **H**). ^{1}H NMR is in agreement with the literature data.[20]

2-phenoxyfumaric acid (1i)

Compound **1i** was prepared from the respective dimethyl ester, synthesized according to a previously reported protocol,[21] by the general hydrolysis procedure. Yield: 83%. White powder. Mp: 236-237°C; ^{1}H NMR (300 MHz, DMSO-d_6): δ 6.52 (s, 1H, vinyl **H**), 6.89 (d, 2H, ^3J = 8.1 Hz, *o*-Ph**H**), 7.04 (t, 1H, ^3J = 7.5 Hz, *p*-Ph**H**), 7.31 (app t, 2H, ^3J = 8.0 Hz, *m*-Ph**H**); ^{13}C NMR (75 MHz, DMSO-d_6): δ 116.4, 117.3, 123.4, 130.3, 149.4, 157.3, 163.7, 165.2; HRMS (ESI-): calcd. for $C_{10}H_7O_5$, 207.0288; found, 207.0298.

2-ethylthiofumaric acid (1k)

Compound **1k** was prepared from the respective dimethyl ester, synthesized according to a previously reported protocol,[22] by the general hydrolysis procedure. Yield: 85%. Yellow powder. Mp: 133-134°C; ^{1}H NMR (400 MHz, D_2O + K_2CO_3): δ 1.03 (t, 3H, ^3J = 7.2 Hz, C**H$_3$**), 2.55 (q, 2H, ^3J = 7.2 Hz, C**H$_2$**), 5.90 (s, 1H, vinyl **H**); ^{13}C NMR (75 MHz, D_2O + K_2CO_3): δ 14.7, 26.5, 122.6, 147.1, 173.4, 175.1; HRMS (ESI-): calcd. for $C_6H_7O_4S$, 175.0060; found, 175.0071.

2-phenylthiofumaric acid (1l)

Compound **1l** was prepared from the respective dimethyl ester **5** by the general hydrolysis procedure. Yield: 80%. Yellow powder. Mp: 158-159°C; ^{1}H NMR (400 MHz, DMSO-d_6): δ 6.39

(s, 1H, vinyl **H**), 7.34-7.40 (m, 5H, Ar**H**); ^{13}C NMR (75 MHz, DMSO-d_6): δ 121.7, 129.1, 129.8, 133.0, 148.4, 165.7, 166.7; HRMS (ESI-): calcd. for $C_{10}H_7O_4S$, 223.0060; found, 223.0070.

2-benzylthiofumaric acid (1m)

Compound **1m** was prepared from the respective dimethyl ester, which was synthesized according to a previously reported protocol,[22] by the general hydrolysis procedure. Yield: 80%. Yellow powder. Mp: 171-172°C (lit.[22] 162-164.5°C); ^{1}H NMR (400 MHz, DMSO-d_6): δ 4.10 (s, 2H, PhC**H$_2$**), 6.23 (s, 1H, vinyl **H**), 7.23-7.34 (m, 5H, Ar**H**). ^{1}H NMR is in agreement with the literature data.[22]

Preparative scale enzymatic synthesis of (substituted) aspartic acids 4a-4n

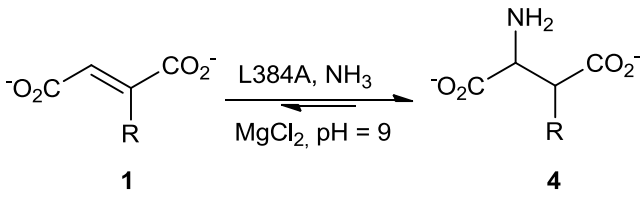

a R = H
b R = methyl
c R = ethyl
d R = propyl
e R = butyl
f R = pentyl
g R = hexyl
h R = ethoxy
i R = phenoxy
j R = benzyloxy
k R = ethylthio
l R = phenylthio
m R = benzylthio
n R = benzyl

L-Aspartic acid (**4a**) and its 3-substituted derivatives **4b-4n** were synthesized using the L384A mutant as catalyst in the ammonia addition to the unsaturated acids **1a-1n**. A solution of unsaturated acid (3.1 mmol), ammonium chloride (1.7 g, 31 mmol) and $MgCl_2$ (20 mM) was prepared in water (25 ml). The pH was adjusted to 9.0 by the addition of small aliquots of an aqueous NaOH (1 N) solution. The reactions were started by the addition of freshly purified enzyme (5 mg), and reaction mixtures were incubated at 22°C. An additional amount (5 mg) of enzyme was added to the individual mixtures after 2 d. ^{1}H NMR spectra were recorded 1 d, 3 d and 7 d after the first addition of enzyme. All reactions were terminated after 7 d. Subsequently, each reaction mixture was

lyophilized and crude product was dissolved in aqueous HCl (1 N, 20 mL). The amino acid products were purified by cation exchange chromatography using a Dowex column (15.0 g of Dowex 50W X8, 100-200 mesh), as described above for the synthesis of the *N*-substituted 3-methylaspartic acids **3n**-**3u**.

(*S*)-aspartic acid (4a)

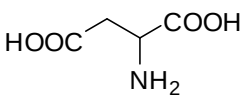

Conversion 99% (^{1}H NMR after 7 d). Yield 80%. White solid. ^{1}H NMR (500 MHz, D_2O): δ 2.68 (dd, 1H, ^2J = 17.5 Hz, ^3J = 8.1 Hz, CHC**H$_2$**), 2.78 (dd, 1H, ^2J = 17.5 Hz, ^3J = 3.8 Hz, CHC**H$_2$**), 3.88 (dd, 1H, ^3J = 8.0 Hz, ^3J = 3.9 Hz, C**H**NH_2); ^{13}C NMR (125 MHz, D_2O): δ 39.1, 54.7, 176.9, 180.1; HRMS (ESI+): calcd. for $C_4H_8NO_4$, 134.0447; found, 134.0449; HPLC (Chirex 3126-D-penicillamine, 2 mM aq. $CuSO_4$:isopropanol 90:10, flow 0.9 ml/min): (*S*)-aspartate, 8.2 min; (*R*)-aspartate, 9.9 min. The ^{1}H NMR signals for the enzymatically generated (*S*)-aspartic acid are in agreement with those found with an authentic standard.

3-methylaspartic acid (4b)

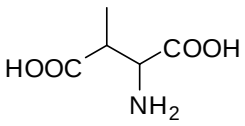

Conversion 73% (^{1}H NMR after 7 d). Yield 60%. White solid. Signals corresponding to two diastereoisomers (d.r. = 78:22) were observed in the ^{1}H NMR spectrum. ^{1}H NMR (500 MHz, D_2O): δ 1.13 (d, 3H, ^3J = 7.5 Hz, C**H$_3$**CH), 1.27 (d, 3H, ^3J = 7.5 Hz, C**H$_3$**CH), 2.86-2.94 (m, 2H, CH_3C**H**, CH_3C**H**), 3.67 (d, 1H, ^3J = 5.4 Hz, C**H**NH_2), 3.99 (d, 1H, ^3J = 3.2 Hz, C**H**NH_2); ^{13}C NMR (125 MHz, D_2O): δ 14.1, 17.8, 43.3, 44.2, 59.0, 60.0, 176.0, 176.4, 183.6, 183.9. HRMS (ESI+): calcd. for $C_5H_{10}NO_4$, 148.0604; found, 148.0605. The ^{1}H NMR spectrum is in agreement with the literature data.[1, 16]

3-ethylaspartic acid (4c)

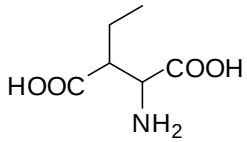

Conversion 73% (^{1}H NMR after 7 d). Yield 45%. White solid. ^{1}H NMR (500 MHz, D_2O): δ 0.90 (t, 3H, ^3J = 7.3 Hz, C**H**$_3$CH$_2$), 1.32-1.40 (m, 1H, C**H**$_2$CH$_3$), 1.46-1.55 (m, 1H, C**H**$_2$CH$_3$), 2.68 (app dt, 1H, ^3J = 10.4 Hz, ^3J = 3.5 Hz, C**H**CH$_2$), 3.89 (d, 1H, ^3J = 3.0 Hz, C**H**NH$_2$); ^{13}C NMR (125 MHz, D_2O): δ 14.4, 22.8, 51.1, 58.4, 175.7, 183.3 HRMS (ESI+): calcd. for $C_6H_{12}NO_4$, 162.0760; found, 162.0762. The ^{1}H NMR spectrum is in agreement with the literature data.[16]

3-propylaspartic acid (4d)

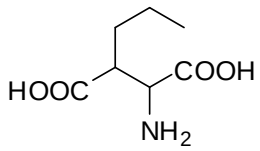

Conversion 66% (^{1}H NMR after 7 d). Yield 46%. White solid. ^{1}H NMR (500 MHz, D_2O): δ 0.77 (t, 3H, ^3J = 7.2 Hz, C**H**$_3$CH$_2$), 1.14-1.30 (m, 3H, C**H**$_2$C**H**$_2$CH$_3$), 1.38-1.46 (m, 1H, C**H**$_2$CH$_2$CH$_3$), 2.69-2.72 (m, 1H, CH$_2$C**H**), 3.80 (d, 1H, ^3J = 3.2 Hz, C**H**NH$_2$); ^{13}C NMR (50 MHz, D_2O): δ 15.7, 23.1, 31.5, 49.0, 58.5, 175.6, 183.4; HRMS (ESI+): calcd. for $C_7H_{14}NO_4$, 176.0923; found, 176.0917. The ^{1}H NMR spectrum is in agreement with the literature data.[16]

3-butylaspartic acid (4e)

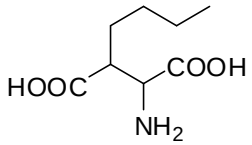

Conversion 57% (^{1}H NMR after 7 d). Yield 36%. White solid. Signals corresponding to two diastereoisomers (d.r. = 51:49) were observed in the ^{1}H NMR spectrum. ^{1}H NMR (500 MHz, D_2O): δ 0.83-0.91 (m, 3H + 3H, C**H**$_3$CH$_2$CH$_2$), 1.24-1.38 (m, 4H + 4H, CH$_2$C**H**$_2$C**H**$_2$CH$_3$), 1.52-1.59 (m, 1H + 1H, CHC**H**$_2$CH$_2$), 1.64-1.72 (m, 1H + 1H, CHC**H**$_2$CH$_2$), 2.78-2.85 (m, 1H + 1H, C**H**CH$_2$CH$_2$), 3.75 (d, 1H, ^3J = 4.6 Hz, C**H**NH$_2$), 4.91 (d, 1H, ^3J = 3.2 Hz, C**H**NH$_2$); ^{13}C NMR (50 MHz, D_2O): δ 13.0, 13.1, 21.6, 21.7, 26.2, 28.7, 29.2, 29.4, 46.5, 47.0, 55.6, 55.8, 172.9, 173.7, 180.0, 180.7; HRMS (ESI+): calcd. for $C_8H_{16}NO_4$, 190.1079; found, 190.1073.

3-pentylaspartic acid (4f)

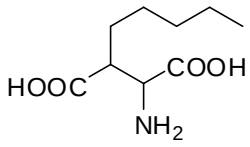

Conversion 52% (^{1}H NMR after 7 d). Yield 23%. White solid. ^{1}H NMR (200 MHz, DMSO-d_6): δ 0.85 (t, 3H, ^3J = 6.7 Hz, C**H**$_3$CH$_2$), 1.16-1.32 (m, 7H, CHC**H**$_2$(C**H**$_2$)$_3$CH$_3$), 1.40-1.50 (m, 1H, CHC**H**$_2$CH$_2$), 2.53-2.57 (m, 1H, C**H**CH$_2$), 3.41 (d, 1H, ^3J = 3.2 Hz, C**H**NH$_2$); ^{13}C NMR (50 MHz, DMSO-d_6): δ 14.4, 22.5, 27.6, 31.9, 40.2 46.9, 55.9, 170.7, 177.3 HRMS (ESI+): calcd. for $C_9H_{18}NO_4$, 204.1236; found, 204.1229.

3-hexylaspartic acid (4g)

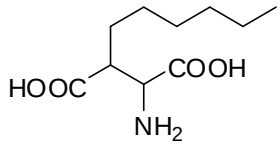

Conversion 53% (^{1}H NMR after 7 d). Yield 48%. White solid. ^{1}H NMR (200 MHz, DMSO-d_6): δ 0.86 (t, 3H, ^3J = 6.6 Hz, C**H**$_3$CH$_2$), 1.18-1.33 (m, 9H, CHC**H**$_2$(C**H**$_2$)$_4$CH$_3$), 1.47-1.53 (m, 1H, CHC**H**$_2$), 2.60-2.65 (m, 1H, C**H**CH$_2$), 3.44 (d, 1H, ^3J = 4.4 Hz, C**H**NH$_2$); ^{13}C NMR (50 MHz, DMSO-d_6): δ 14.4, 22.5, 27.7, 29.2, 31.6, 40.2, 46.3, 55.5, 170.3, 176.4; HRMS (ESI+): calcd. for $C_{10}H_{20}NO_4$, 218.1392; found, 218.1386.

3-ethoxyaspartic acid (4h)

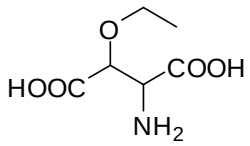

Conversion 45% (^{1}H NMR after 7 d). Yield 24%. White solid. Signals corresponding to two diastereoisomers (d.r. = 85:15) were observed in the ^{1}H NMR spectrum. Major diastereoisomer: ^{1}H NMR (500 MHz, D_2O): δ 1.04 (t, 3H, ^3J = 7.0 Hz, C**H**$_3$CH$_2$O), 3.33-3.40 (m, 1H, OC**H**$_2$CH$_3$), 3.51-3.60 (m, 1H, OC**H**$_2$CH$_3$), 3.87 (d, 1H, ^3J = 2.4 Hz, C**H**NH$_2$), 4.15 (d, 1H, ^3J = 2.4, C**H**OCH$_2$); ^{13}C NMR (50 MHz, D_2O): δ 14.1, 56.5, 66.4, 78.0, 171.8, 176.3; HRMS (ESI+): calcd. for $C_6H_{12}NO_5$, 178.0715; found, 178.0710.

3-phenoxyaspartic acid (4i)

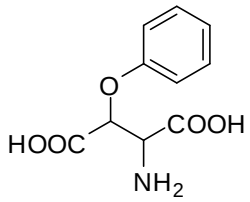

Conversion 46% (^{1}H NMR after 7 d). Yield 20%. White solid. ^{1}H NMR (200 MHz, D_2O): δ 4.03 (d, 1H, ^3J = 1.3 Hz, C**H**NH_2), 4.90 (br d, 1H, C**H**O), 6.78-7.29 (m, 5H, Ar**H**); ^{13}C NMR (50 MHz, D_2O): δ 56.5, 76.9, 114.9, 121.9, 129.8, 157.1, 171.9, 174.7; HRMS (ESI+): calcd. for $C_{10}H_{12}NO_5$, 226.0715; found, 226.0710.

3-benzyloxyaspartic acid (4j)

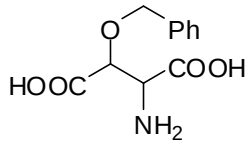

Conversion 65% (^{1}H NMR after 7 d). Yield 50%. White solid. ^{1}H NMR (200 MHz, DMSO-d_6): δ 3.75 (d, 1H, ^3J = 7.1 Hz, C**H**NH_2), 4.17 (d, 1H, ^3J = 7.2, C**H**O), 4.46 (d, 1H, ^2J = 11.2 Hz, C**H**$_2$Ar), 4.76 (d, 1H, ^2J = 11.2 Hz, C**H**$_2$Ar), 7.25-7.42 (m, 5H, Ar**H**); ^{13}C NMR (50 MHz, DMSO-d_6): δ 54.3, 72.6, 76.3, 127.8, 128.3, 128.4, 138.5, 169.0, 171.7; HRMS (ESI+): calcd. for $C_{11}H_{14}NO_5$, 240.0872; found, 240.0868; HPLC (Nucleosil chiral-1, 2 mM aq. $CuSO_4$:methanol 90:10, flow 1.0 ml/min): *threo*-DL-**4j**, R_{t-1} = 5.0 min; R_{t-2} = 6.9 min.

3-(ethylthio)aspartic acid (4k)

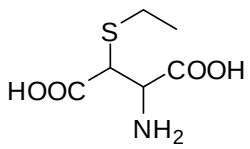

Conversion 81% (^{1}H NMR after 7 d). Yield 22%. White solid. Signals corresponding to two diastereoisomers (d.r. = 68:32) were observed in the ^{1}H NMR spectrum. ^{1}H NMR (500 MHz, D_2O): δ 1.12 (t, 3H, ^3J = 7.4 Hz, C**H**$_3$CH_2), 1.17 (t, 3H, ^3J = 7.4, C**H**$_3$CH_2), 2.49-2.61 (m, 2H + 2H, C**H**$_2$CH_3), 3.78 (d, 1H, ^3J = 3.0 Hz, SC**H**CH), 3.80 (d, 1H, ^3J = 3.9 Hz, SC**H**CH), 3.84 (d, 1H, ^3J = 3.9 Hz, C**H**NH_2), 4.05 (d, 1H, ^3J = 3.0, C**H**NH_2); ^{13}C NMR (50 MHz, D_2O): δ 13.6, 13.8, 25.6, 26.5, 48.0, 48.3, 55.4, 55.7, 171.7, 172.0, 175.7, 176.7; HRMS (ESI+): calcd. for $C_6H_{12}NO_4S$, 194.0487; found, 194.0482.

3-(phenylthio)aspartic acid (4l)

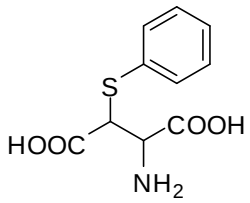

Conversion 45% (^{1}H NMR after 7 d). Yield 13%. White solid. Signals corresponding to two diastereoisomers (d.r. = 65:35) were observed in the ^{1}H NMR spectrum. Major diastereoisomer: ^{1}H NMR (500 MHz, D_2O): δ 3.60 (br d, 1H, SC**H**CH), 4.23 (br d, 1H, C**H**NH_2), 7.26-7.49 (m, 5H, Ar**H**); ^{13}C NMR (50 MHz, D_2O): δ 41.6, 53.5, 128.5, 129.6, 131.8, 132.4, 172.3, 174.6; HRMS (ESI+): calcd. for $C_{10}H_{12}NO_4S$, 242.0487; found, 242.0482.

3-(benzylthio)aspartic acid (4m)

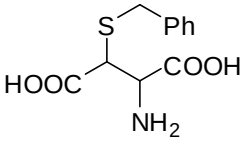

Conversion 55% (^{1}H NMR after 7 d). Yield 30%. White solid. Signals corresponding to two diastereoisomers (d.r. = 60:40) were observed in the ^{1}H NMR spectrum. ^{1}H NMR (500 MHz, DMSO-d_6): δ 3.47-3.90 (m, 4H + 4H, C**H$_2$**Ar, SC**H**CH, C**H**NH_2), 7.18-7.36 (m, 5H + 5H, Ar**H**); ^{13}C NMR (50 MHz, DMSO-d_6): δ 35.7, 35.9, 48.7, 49.2, 54.6, 55.2. 127.0, 127.2, 128.6, 128.7, 129.5, 129.6, 138.6, 139.1, 169.1, 170.2, 172.6, 173.2; HRMS (ESI+): calcd. for $C_{11}H_{13}NO_4S$, 256.0644; found, 256.0638.

3-benzylaspartic acid (4n)

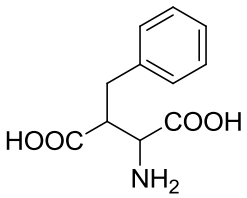

Conversion 90% (^{1}H NMR after 7 d). Yield 55%. White solid. ^{1}H NMR (500 MHz, D_2O): δ 2.74 (dd, 1H, ^2J = 13.3 Hz, ^3J = 4.3 Hz, ArC**H**$_2$CH), 2.83 (dd, 1H, ^2J = 13.1 Hz, ^3J = 11.4 Hz, ArC**H**$_2$CH), 3.06 (ddd, 1H, ^3J = 11.2 Hz, ^3J = 4.3 Hz, ^3J = 3.3 Hz, CH_2C**H**CH), 3.97 (d, 1H, ^3J = 3.1 Hz, C**H**NH_2), 7.22-7.35 (m, 5H, Ar**H**); ^{13}C NMR (125 MHz, D_2O): δ 35.7, 51.9, 58.4, 129.2, 131.3, 131.4, 141.5, 175.5, 182.3. HRMS (ESI+): calcd. for $C_{11}H_{14}NO_4$, 224.0917; found: 224.0919. ^{1}H NMR spectrum is in agreement with the literature data.[23]

Chemical synthesis of sulphur substituted aspartic acid derivatives

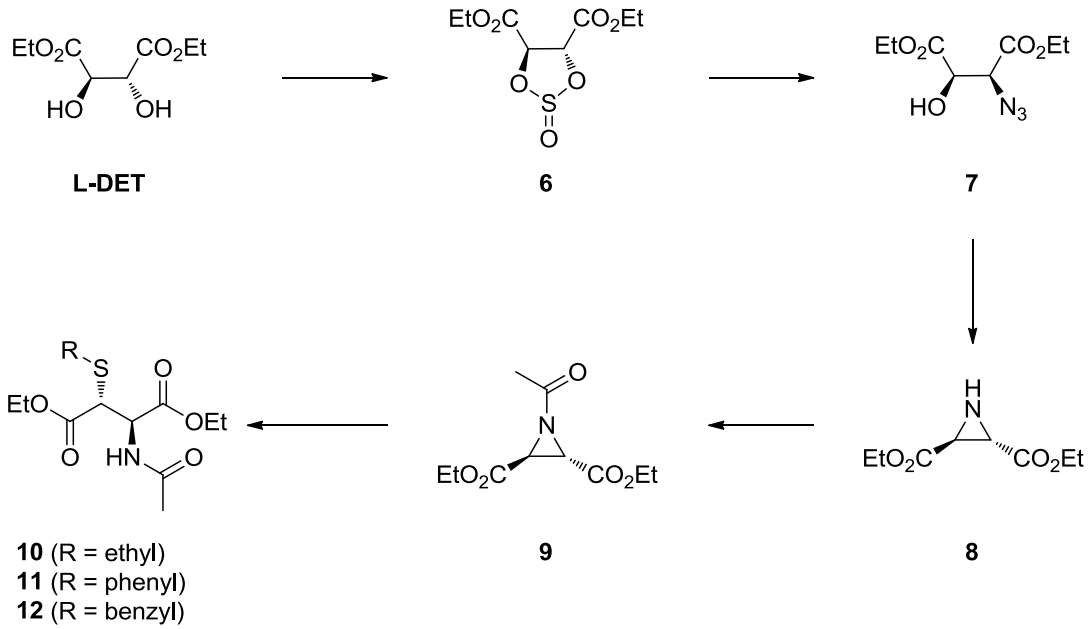

In order to determine the relative configuration of the products (**4k**-**4m**) of the L384A-catalyzed amination of 2-ethylthiofumarate (**1k**), 2-phenylthiofumarate (**1l**) and 2-benzylthiofumarate (**1m**), we have synthesized the reference molecules, *erythro*-**10**, *erythro*-**11** and *erythro*-**12**. The synthesis was mainly based on literature procedures.[24-26] Briefly, L-diethyl tartrate (L-DET) was converted to the cyclic sulphite **6**. Ring-opening of **6** was achieved with sodium azide in DMF to provide the azido alcohol **7**. Triphenyl phosphine was used to form the corresponding aziridinium **8**, which was subsequently protected as the acetyl derivative **9**. $BF_3{\cdot}(OEt)_2$ was used as Lewis acid to facilitate the nucleophilic attack on the aziridinium by either ethyl mercaptan, thiophenol, or benzyl mercaptan to provide the corresponding *N*-protected sulphur substituted aspartic acid analogues, *erythro*-**10**, *erythro*-**11** and *erythro*-**12**.

Diethyl (2*R*,3*R*)-2,3-O-sulfinyl-tartrate (6)

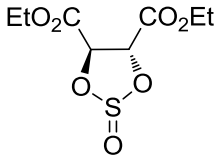

L-DET (7.36 ml, 43 mmol) was dissolved in dichloromethane (20 ml) and cooled to 0°C. $SOCl_2$ (3.62 ml, 52 mmol) was added to the solution drop-wise followed

by the addition of 10 drops of DMF. The reaction mixture was allowed to warm to room temperature and then heated at 50°C for 30 min. A fine stream of N_2 (g) was used to remove excess $SOCl_2$ and evolved HCl (g). Residual $SOCl_2$ was then removed *in vacuo* (50°C, 25 mbar) to give **6** as light yellow oil (10.6 g, 98%). TLC (EtOAc:Hexane, 1:1 v/v): R_f = 0.41; $[\alpha]_D^{20}$ = +161 (0.025 M in DCM); ^{1}H NMR (400 MHz, $CDCl_3$): δ 1.34 (app t, 7.1 Hz, 6H, $CH_2C\mathbf{H_3}$), 4.28-4.37 (m, 4H, $C\mathbf{H_2}CH_3$), 5.24 (d, J = 4.3 Hz, 1H, C**H**O), 5.71 (d, J = 4.3 Hz, 1H, C**H**O); ^{13}C NMR (75 MHz, $CDCl_3$): δ 14.2, 63.3, 79.4, 80.0, 166.6; HRMS (ESI+): calcd. for $C_8H_{13}O_7S$, 253.0374; found, 253.0376. Analytical data are in agreement with the literature.[24, 25]

Diethyl (2*R*,3*S*)-3-azido-3-deoxy-tartrate (7)

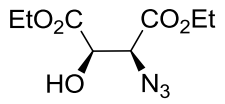

NaN_3 (7.37 g, 113.4 mmol) was added to a solution of **6** (10.57 g, 42 mmol) in DMF (24 ml) and stirred at room temperature until all the starting material was consumed (22 h, TLC, EtOAc:Hex 1:1 v/v). DCM (60 ml) and H_2O (36 ml) were added to the reaction mixture and the mixture was stirred for 2 h. The layers were separated and the aqueous layer was extracted with DCM (3 x 35 ml). The combined organic layers were washed with H_2O (5 x 100 ml) and brine (100 ml), dried (Na_2SO_4), filtered and the solvent was removed *in vacuo*. The crude oil was purified by flash column chromatography (silica gel, EtOAc:Hex 1:4 v/v) to give **7** as a colourless oil (6.2 g, 64%). TLC (EtOA:Hexane, 1:4 v/v): R_f = 0.16; $[\alpha]_D^{20}$ = +34.1 (7.2 mM in EtOH); ^{1}H NMR (400 MHz, $CDCl_3$): δ 1.30 (t, J = 7.1 Hz, 3H, $CH_2C\mathbf{H_3}$), 1.31 (t, J = 7.1 Hz, 3H, $CH_2C\mathbf{H_3}$), 3.28 (d, J = 5.4 Hz, 1H, C**H**N_3), 4.22-4.35 (m, 4H, $C\mathbf{H_2}CH_3$), 4.63 (dd, J = 5.4 Hz, J = 2.7 Hz, 1H, C**H**OH); ^{13}C NMR (75 MHz, $CDCl_3$): δ 14.2, 62.5, 62.9, 64.6, 72.2, 167.1, 170.9; HRMS (ESI+): calcd. for $C_8H_{14}O_5N_3$, 232.0928; found, 232.0925. Analytical data are in agreement with the literature.[24, 25]

Diethyl (2*S*,3*S*)-aziridine-2,3-dicarboxylate (8)

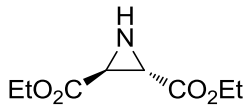

Triphenyl phosphine (12.20 g, 46.51 mmol) was slowly added over 30 min to a solution of **7** in DMF at 0°C. The ice bath was removed and the reaction mixture was stirred at room temperature for 90 min followed by another 270 min at 80°C. The solvent was removed *in vacuo* (77°C, 20 mbar), and the crude product was purified by flash column chromatography (silica gel, EtOAc:Hexane 1:3 v/v) to give **8** as a colourless oil (3.50 g, 72%). TLC (EtOAc:Hexane, 1:3 v/v): R_f = 0.25; $[\alpha]_D^{20}$ = +147.3 (9.2 mM in $CHCl_3$), ^{1}H NMR (400 MHz, $CDCl_3$): δ 1.30 (t, J = 7.1 Hz, 6H, $CH_2C\mathbf{H_3}$), 2.86 (s, 2H, C**H**NH), 4.24 (q, J = 7.0 Hz, 4H, $C\mathbf{H_2}CH_3$); ^{13}C NMR (75 MHz, $CDCl_3$): δ 14.3, 35.9, 62.2, 169.6; HRMS (ESI+): calcd. for $C_8H_{14}O_4N$, 188.0917; found, 188.0915. Analytical data are in agreement with the literature.[27]

Diethyl (2*S*,3*S*)-*N*-(acetyl)-aziridine-2,3-dicarboxylate (9)

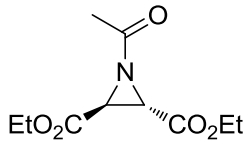

Pyridine (1.51 ml, 18.64 mmol) was added to **8** (3.49 g, 18.64 mmol) at room temperature and the mixture was stirred for 5 min. Acetic anhydride (2.64 ml, 27.96 mmol) was added drop wise to the reaction mixture and the mixture was heated at 60°C for 1 h. The reaction mixture was allowed to cool to room temperature and diluted with DCM (50 ml). The mixture was washed with H_2O (4 x 30 ml) and brine (30 ml), dried (Na_2SO_4), filtered and the solvent was removed *in vacuo*. The crude product was purified by flash column chromatography (silica gel, DCM: Et_2O, 8:2 v/v) to give **9** as a light yellow oil (3.19 g, 75%). TLC (DCM:Et_2O, 8:2 v/v): R_f = 0.66; $[\alpha]_D^{20}$ = +56.8 (0.025 M in $CHCl_3$); ^{1}H NMR (400 MHz, $CDCl_3$): δ 1.31 (app t, J = 7.1 Hz, 6H, $CH_2C\mathbf{H_3}$), 2.13 (s, 3H, $COC\mathbf{H_3}$), 3.42 (s, 2H, C**H**NCO), 4.20-4.30 (m, 4H, $C\mathbf{H_2}CH_3$); ^{13}C NMR (75 MHz, $CDCl_3$): δ 14.2, 24.0, 40.3, 62.6, 166.6, 177.8; HRMS (ESI+): calcd. for $C_{10}H_{16}O_5N_1$, 230.1023; found, 230.1022.

Diethyl *erythro*-(2*R*,3*R*)-2-acetamido-3-(ethylthio)succinate (10)

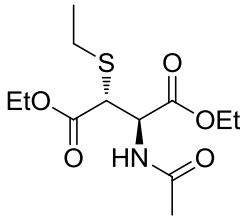

Ethanethiol (353 µl, 4.62 mmol) was added to a solution of **9** (530 mg, 2.31 mmol) in anhydrous $CHCl_3$ (20 ml). While stirring at room temperature, $BF_3{\cdot}(OEt)_2$ (477 µl, 2.31 mmol) was slowly added to the reaction mixture, which was then heated to 37°C for 3 h. The reaction was quenched with saturated aqueous $NaHCO_3$ (25 ml). The layers were separated and the organic layer was washed with saturated aqueous $NaHCO_3$ (20 ml). The organic layer was dried ($MgSO_4$) and the solvent was removed *in vacuo* to give **10** as a yellow oil (613 mg, 91%). TLC (DCM:Et_2O, 8:2 v/v): R_f = 0.47; $[\alpha]_D^{20}$ = +43.1 (0.034 M in EtOH); ^{1}H NMR (300 MHz, $CDCl_3$): δ 1.21-1.35 (m, 9H, CH_2CH_3), 2.08 (s, 3H, $COCH_3$), 2.68-2.82 (m, 2H, CH_2S), 3.95 (d, *J* = 4.5 Hz, 1H, CHS), 4.13-4.27 (m, 4H, CH_2CH_3), 5.14 (dd, *J* = 9.7 Hz; *J* = 4.5 Hz, 1H, CHNH), 6.63 (d, *J* = 9.4 Hz, 1H, CHNH); ^{13}C NMR (75.5 MHz, $CDCl_3$): δ 14.2, 14.4, 23.2, 27.0, 47.6, 53.0, 62.0, 62.1, 169.8, 170.5, 171.9; HRMS (ESI+): calcd. for $C_{12}H_{22}O_5NS$, 292.1213; found, 292.1212.

Diethyl *erythro*-(2*R*,3*R*)-2-acetamido-3-(phenylthio)-succinate (11)

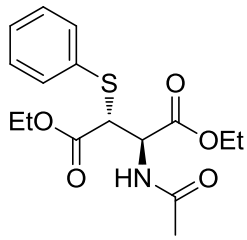

Thiophenol (450 µl, 4.36 mmol) was added to a solution of **9** (500 mg, 2.18 mmol) in anhydrous $CHCl_3$ (18.70 ml). While stirring at room temperature, $BF_3{\cdot}(OEt)_2$ (450 µl, 2.18 mmol) was slowly added to the reaction mixture, which was then heated at 37°C for 3 h. The reaction was quenched with saturated aqueous $NaHCO_3$ (20 ml). The layers were separated and the organic layer was washed with saturated aqueous $NaHCO_3$ (15 ml). The organic layer was dried ($MgSO_4$), the solvent was removed *in vacuo* and the crude oil was purified with flash column chromatography (silica gel, DCM: Et_2O, 8:2 v/v) to give **11** as a thick colourless oil (638 mg, 86%). TLC (DCM:Et_2O, 8:2 v/v): R_f = 0.40; $[\alpha]_D^{20}$ = +132.8 (3.9 mM in $CHCl_3$); ^{1}H NMR (400 MHz, $CDCl_3$): δ 1.18-1.25 (m, 6H, CH_2CH_3), 2.02 (s, 3H, $COCH_3$), 4.11-4.21 (m, 4H, CH_2CH_3), 4.28 (d, *J* = 4.2 Hz, 1H, CHS), 5.20 (dd, *J* = 9.4 Hz, *J* = 4.2 Hz, 1H, CHNH), 6.63 (d, *J* = 9.4 Hz, 1H, CHNH), 7.29-7.34 (m, 3H, ArH),

7.50-7.55 (m, 2H, Ar**H**); ^{13}C NMR (75 MHz, $CDCl_3$): δ 14.1, 14.2, 23.2, 52.5, 53.6, 62.1, 62.2, 128.7, 129.3, 133.0, 133.6, 169.6, 170.4, 171.0; HRMS (ESI+): calcd. for $C_{16}H_{22}O_5NS$, 340.1212; found, 340.1213.

Diethyl *erythro*-(2*R*,3*R*)-2-acetamido-3-(benzylthio)-succinate (12)

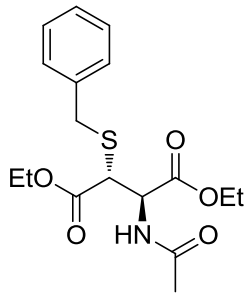

Benzyl mercaptan (512 µl, 4.36 mmol) was added to a solution of **9** (500 mg, 2.18 mmol) in anhydrous $CHCl_3$ (18.70 ml). While stirring at room temperature, $BF_3{\cdot}(OEt)_2$ (450 µl, 2.18 mmol) was slowly added to the reaction mixture, which was then heated at 37°C for 3 h. The reaction was quenched with saturated aqueous $NaHCO_3$ (20 ml). The layers were separated and the organic layer was washed with saturated aqueous $NaHCO_3$ (15 ml). The organic layer was dried ($MgSO_4$), the solvent was removed *in vacuo* and the crude oil was purified with flash column chromatography (silica gel, DCM:Et_2O, 8:2 v/v) to give **12** as a white solid (614 mg, 80%). Mp: 77-78°C; TLC (DCM:Et_2O, 8:2 v/v): R_f = 0.51; $[\alpha]_D^{20}$ = +29.4 (1.9 mM in $CHCl_3$); ^{1}H NMR (400 MHz, $CDCl_3$): δ 1.10 (t, *J* = 7.0 Hz, 3H, $CH_2C\mathbf{H_3}$), 1.30 (t, *J* = 7.1 Hz, 3H, $CH_2C\mathbf{H_3}$), 2.04 (s, 3H, $COC\mathbf{H_3}$), 3.80 (d, *J* = 4.4 Hz, 1H, C**H**S), 3.91 (iso(AB), *J* = 13.2 Hz, *J* = 4.5 Hz, 2H, $C\mathbf{H_2}$Ar), 4.09-4.24 (m, 4H, $C\mathbf{H_2}CH_3$), 5.06 (dd, *J* = 9.7 Hz, *J* = 4.4 Hz, 1H, C**H**NH), 6.53 (d, *J* = 9.6 Hz, 1H, CHN**H**), 7.82-7.36 (m, 5H, Ar**H**); ^{13}C NMR (75 MHz, $CDCl_3$): δ 14.2, 14.3, 23.3, 36.9, 46.9, 52.7, 61.1, 127.7, 128.8, 129.3, 136.7, 169.7, 170.4, 171.8; HRMS (ESI+): calcd. for $C_{17}H_{24}O_5NS$, 354.1369; found, 354.1369.

Procedure for determining the relative configuration of enzymatic products 4k-4m

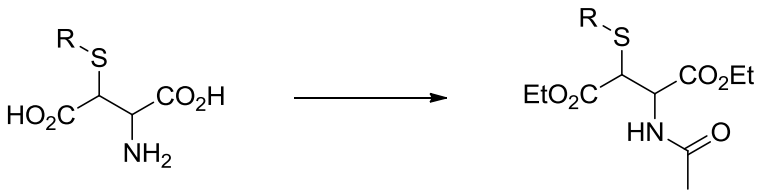

R = phenyl, benzyl, or ethyl

To determine the relative configuration of amino acid products **4k-4m**, synthesized using mutant L384A, these products were first esterified and acetylated (in separate reactions). Then, their ^{1}H NMR spectra were compared to those obtained with the respective reference molecules **10-12**, which suggested the relative configuration of **4k-4m**. The general procedure for the esterification and acetylation is as follows. Absolute ethanol (200 µl) was cooled in an ice-bath. Acetyl chloride (0.432 mmol) was added drop wise to generate HCl *in situ* and the mixture was stirred for 30 min. The acidic ethanol solution was added to either **4k**, **4l** or **4m** (0.108 mmol). The reaction mixture was heated to reflux for 4 h. The reaction mixture was allowed to cool down to room temperature and the solvent removed *in vacuo* to give an oily residue. The residue was dissolved in toluene (750 µl), pyridine (0.150 mmol) was added, and the solution was cooled to 0°C. Acetic anhydride (1.39 mmol) was added and the solution was stirred overnight. The reaction mixture was poured onto ice-diluted HCl (5 ml). The layers were separated and the organic layer was washed with H_2O (5 ml) and then dried over $MgSO_4$. After filtration and solvent removal under reduced pressure, the resulting residue was purified with flash column chromatography (silica gel, DCM: Et_2O, 8:2 v/v) to give the modified product.

Diethyl (*threo*/*erythro*)-2-acetamido-3-(ethylthio)-succinate

Yellow oil (15 mg, 22%). Isolated as a mixture of diastereoisomers (d.r. = 58:42, *threo*:*erythro*). The d.r. has changed compared to that of the unmodified enzymatic product (d.r. = 68:32), which suggests that some epimerization had occurred during the chemical esterification and acetylation

procedure. *Threo* isomer: ^{1}H NMR (300 MHz, $CDCl_3$): δ 1.20–1.32 (m, 9H, $CH_2C\mathbf{H_3}$), 2.03 (s, 3H, $COC\mathbf{H_3}$), 2.59-2.68 (m, 2H, $C\mathbf{H_2}S$), 3.86 (d, *J* = 5.3 Hz, 1H, C**H**S), 4.10-4.25 (m, 4H, $C\mathbf{H_2}CH_3$), 4.97 (dd, *J* = 7.9 Hz, *J* = 5.3 Hz, 1H, C**H**NH), 6.32 (d, *J* = 7.6 Hz, 1H, CHN**H**). *Erythro*-isomer: ^{1}H NMR signals are listed above.

Diethyl (*threo*/*erythro*)-2-acetamido-3-(phenylthio)-succinate

Yellow oil (35 mg, 23%). Isolated as a mixture of diastereoisomers (d.r. = 64:36, *threo*:*erythro*). The diastereomeric ratio is nearly identical to that of the unmodified enzymatic product (d.r. = 65:35), which suggests that no epimerization had occurred during the chemical esterification and acetylation procedure. *Threo* isomer: ^{1}H NMR (300 MHz, $CDCl_3$): δ 1.14–1.28 (m, 6H, $CH_2C\mathbf{H_3}$), 2.04 (s, 3H, $COC\mathbf{H_3}$), 4.08-4.22 (m, 4H, $C\mathbf{H_2}CH_3$), 4.29 (d, *J* = 4.4 Hz, 1H, C**H**S), 5.12 (dd, *J* = 8.2 Hz, *J* = 4.5 Hz, 1H, C**H**NH), 6.38 (d, *J* = 8.1 Hz, 1H, CHN**H**), 7.28–7.36 (m, 5H, Ar**H**). *Erythro*-isomer: ^{1}H NMR signals are listed above.

Diethyl (*threo*/*erythro*)-2-acetamido-3-(benzylthio)-succinate

Yellow oil (2 mg, 25%). Isolated as a mixture of diastereoisomers (d.r. = 59:41, *threo*:*erythro*). The diastereomeric ratio is nearly identical to that of the unmodified enzymatic product (d.r. = 60:40), which suggests that no epimerization had occurred during the chemical esterification and acetylation procedure. *Threo* isomer: ^{1}H NMR (300 MHz, $CDCl_3$): δ 1.18–1.34 (m, 6H, $CH_2C\mathbf{H_3}$), 1.99 (s, 3H, $COC\mathbf{H_3}$), 3.75 (d, *J* = 5.4 Hz, 1H, C**H**S), 3.82-3.86 (m, 2H, $C\mathbf{H_2}$Ar), 4.09–4.25 (m, 4H, $C\mathbf{H_2}CH_3$), 4.96 (dd, *J* = 8.1 Hz, *J* = 5.4 Hz, 1H, C**H**NH), 6.04 (d, *J* = 8.3 Hz, 1H, CHN**H**), 7.28–7.36 (m, 5H, Ar**H**). *Erythro*-isomer: ^{1}H NMR signals are listed above.

SUPPLEMENTARY RESULTS & DISCUSSION

Engineering of the amine binding pocket

Engineering of the amine binding pocket through saturation mutagenesis at position 172 did not result in MAL variants with the ability to catalyze methylamine addition to mesaconate. A closer inspection of the crystal structure of MAL complexed with its natural substrate *threo*-(2*S*,3*S*)-3-methylaspartate[11] provides a likely explanation for this finding. Residue Q172 not only forms a hydrogen bond with the amino group of the substrate but also with its C-1 carboxylate group. Hence, the replacement of Q172 with other residues will eliminate this critical interaction with the substrate's carboxylate group, thereby preventing the productive binding of mesaconate.

Additional mutagenesis experiments

The results may suggest that combining the Q73A and L384A mutations into one enzyme could yield a biocatalyst with the ability to process many different combinations of substituted amines and fumarates. However, the MAL double mutant (Q73A/L384A) is almost completely inactive (data not shown), which may be the result of a changed active site geometry, and thus not suitable for biocatalytic application. In future work, we therefore aim to construct a focused library by saturation mutagenesis at positions 73 and 384, screening of which may yield various active biocatalysts optimized for unique combinations of nucleophile and electrophile. The finding that at least six different substitutions at position 73 are allowed to give pronounced activity for methylamine addition to mesaconate argues in favor of this approach. It is important to note that not all nucleophile-electrophile combinations are likely to be productive as very bulky substituents on both the amine and fumarate substrates may sterically hinder the Michael-type addition. We also aim to develop MAL variants that lack specificity for the C-1 carboxylate group of the amino acid substrate, which, in contrast to the C-4 carboxylate group, appears not to play an essential role in the reaction mechanism.[6,11] If successful, these engineering efforts may further extent the substrate

scope of MAL to include not only various *N*,3-disubstituted aspartic acid analogs, but also β-amino acids and other monocarboxylic acids.

SUPPLEMENTARY FIGURES

Fig. S1a

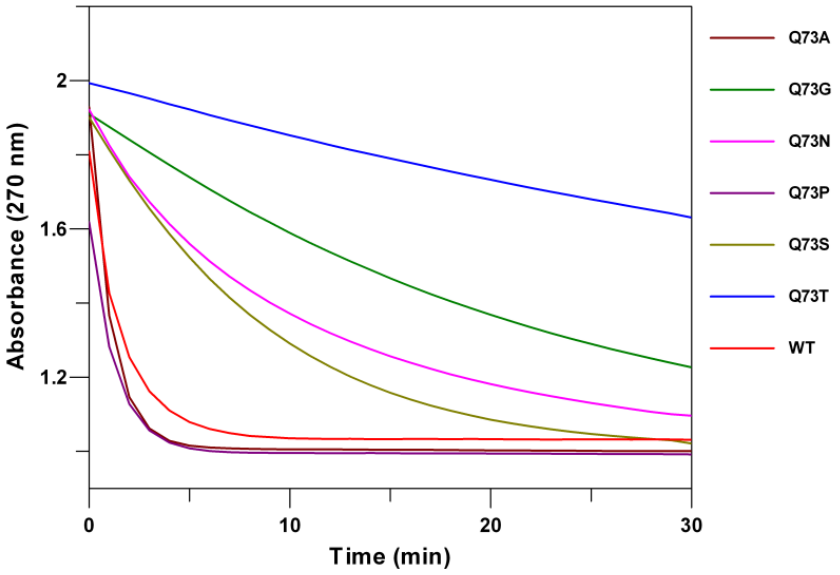

Fig. S1b

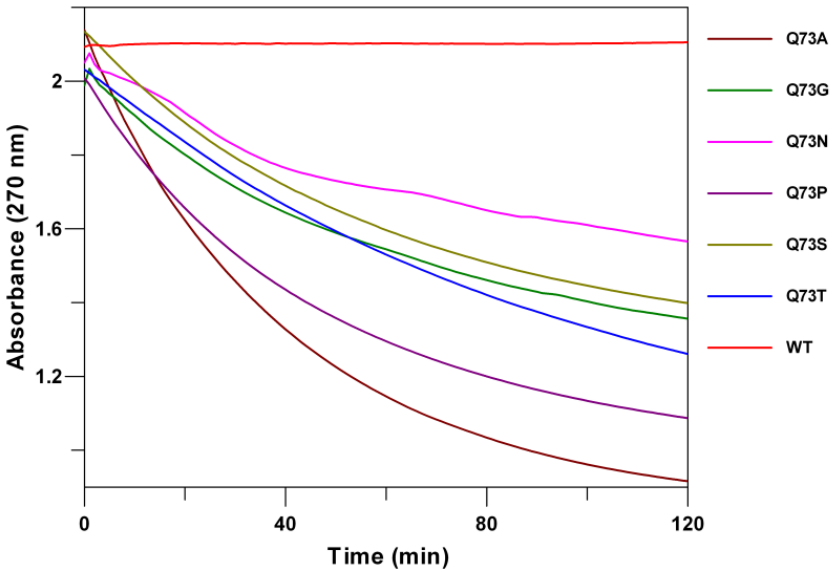

Supplementary Fig. 1. UV spectra monitoring the ammonia (**2a**, 400 mM) or methylamine (**2b**, 400 mM) additions to mesaconate (**1b**, 5 mM) catalyzed by wild-type MAL (WT) and the MAL mutants Q73A, Q73G, Q73N, Q73P, Q73S, and Q73T. (**a**) UV spectra monitoring the addition of **2a** to **1b** catalyzed by wild-type (15 µg/ml) or mutant (150 µg/ml) MAL. (**b**) UV spectra monitoring the addition of **2b** to **1b** catalyzed by wild-type (150 µg/ml) or mutant (150 µg/ml) MAL. The reactions were monitored by following the depletion of the absorbance of **1b** at 270 nm in 500 mM Tris-HCl buffer, pH 9.0, containing 20 mM $MgCl_2$.

Fig. S2a

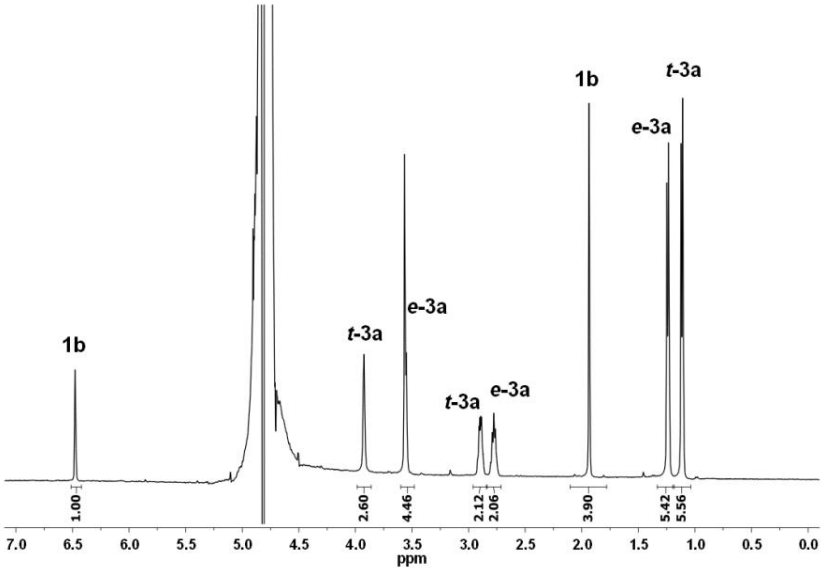

Fig. S2b

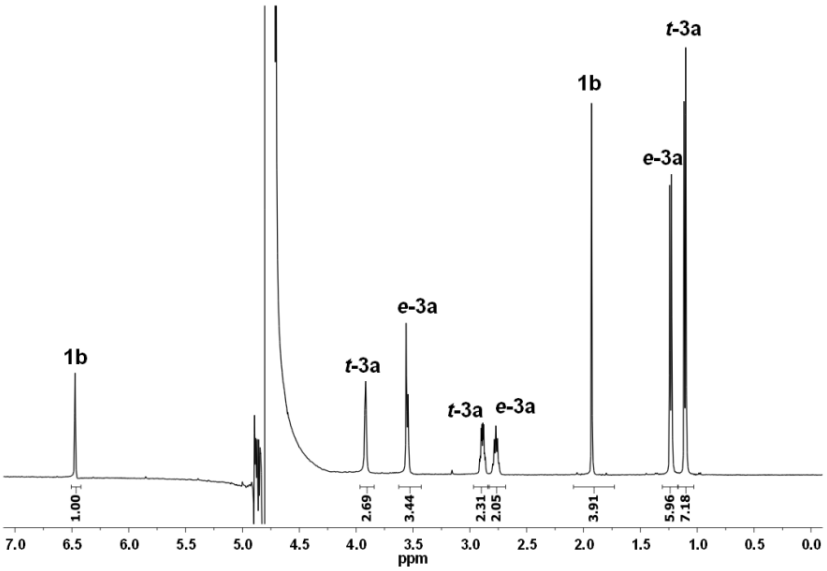

Fig. S2c

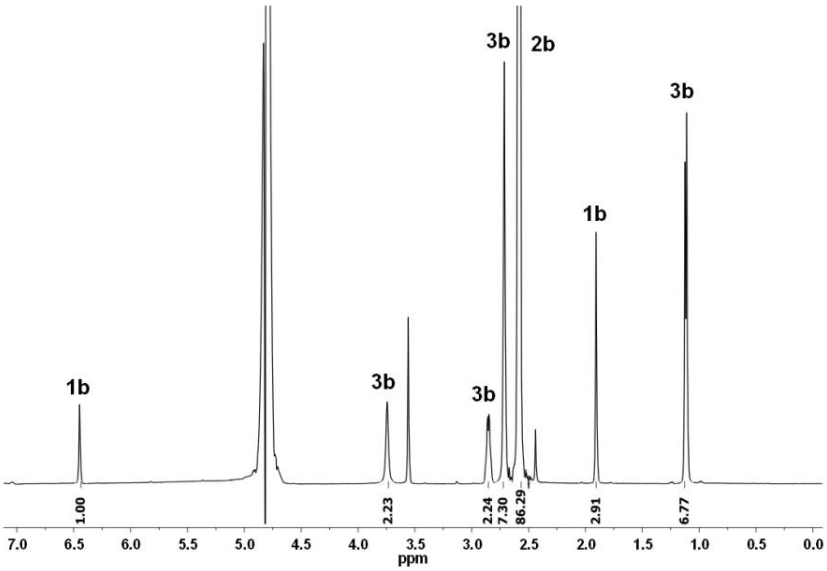

Fig. S2d

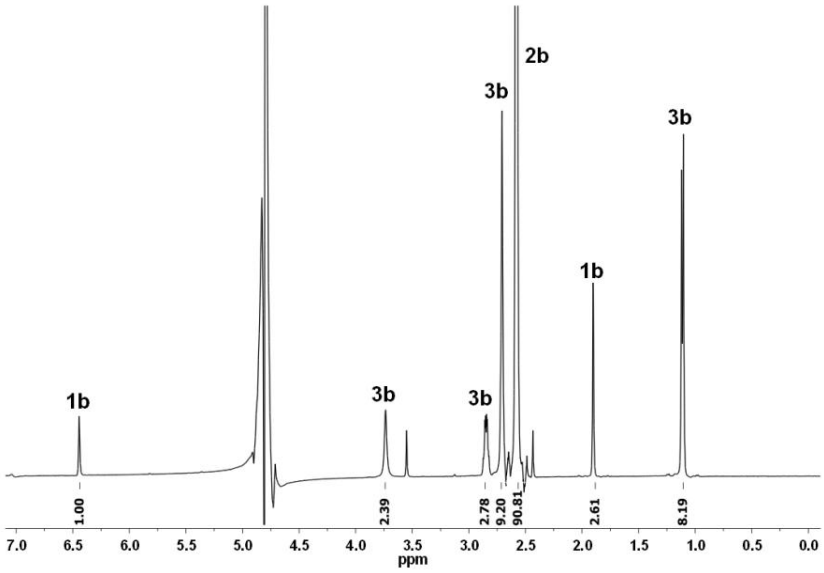

Supplementary Fig. 2. ^{1}H NMR spectroscopic analysis of the products of the ammonia and methylamine additions to mesaconate catalyzed by wild-type MAL and the Q73A mutant. (**a**) ^{1}H NMR spectrum monitoring the ammonia addition to mesaconate catalyzed by wild-type MAL. (**b**) ^{1}H NMR spectrum monitoring the ammonia addition to mesaconate catalyzed by mutant Q73A. (**c**) ^{1}H NMR spectrum monitoring the methylamine addition to mesaconate catalyzed by wild-type MAL. (**d**) ^{1}H NMR spectrum monitoring the methylamine addition to mesaconate catalyzed by mutant Q73A. The spectra were taken after 14 days of incubation at 22°C. In Figures 2a and 2b, the signals corresponding to mesaconate, *threo*-3-methylasparate and *erythro*-3-methylaspartate are labeled **1b**, ***t*-3a** and ***e*-3a**, respectively. In figures 2c and 2d, the signals corresponding to mesaconate, methylamine, and *threo*-*N*,3-dimethylaspartate are labelled **1b**, **2b** and **3b**, respectively. Impurity (Tris): δ = 3.5 (s).

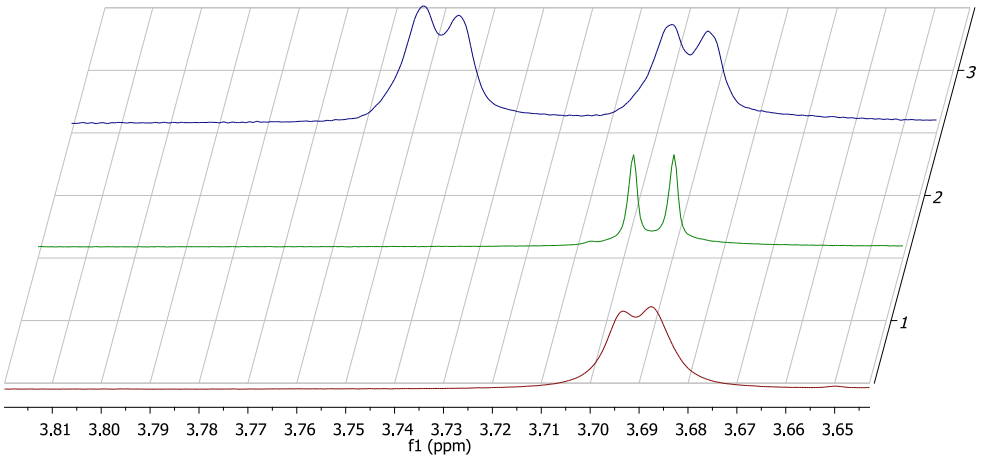

Supplementary Fig. 3. Identification of the relative configuration of the product, 2-(*cyclo*-pentylamino)-3-methylbutanedioic acid (**3j**), of the Q73A-catalyzed cyclopentylamine (**2j**) addition to mesaconate (**1b**) by using ^{1}H NMR spectroscopy and authentic standards. Spectrum 1: partial ^{1}H NMR spectrum of enzymatically synthesized **3j**. Spectrum 2: partial ^{1}H NMR spectrum of chemically synthesized *threo*-**3j**. Spectrum 3: partial ^{1}H NMR spectrum of a chemically synthesized mixture of *threo*- and *erythro*-**3j**. This analysis showed that the Q73A-catalyzed addition of **2j** to **1b** yields exclusively the *threo* isomer of **3j** (*de* >95%). Similar analyses were performed to determine the relative configuration of the other Q73A-synthesized amino acid products **3c-3i** and **3k-3m**.

Fig. S4a

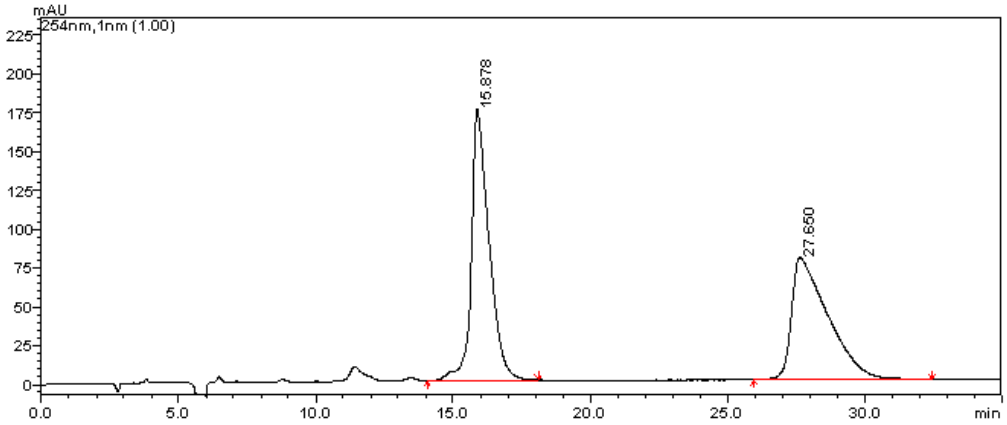

Fig. S4b

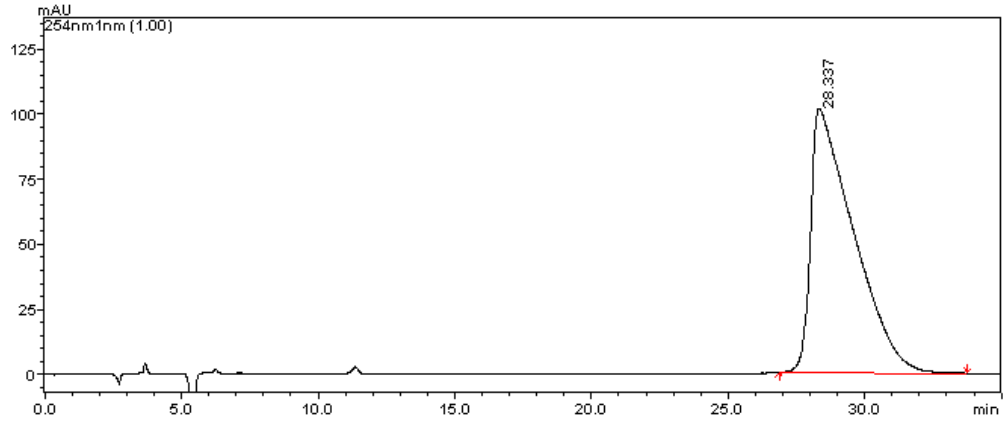

Supplementary Fig. 4. Determination of the *ee* value of the product, *threo*-2-(propylamino)-3-methylbutanedioic acid (**3d**), of the Q73A-catalyzed propylamine (**2d**) addition to mesaconate (**1b**) by using chiral HPLC. (**a**) Chromatogram of chemically synthesized *threo*-DL-**3d**. (**b**) Chromatogram of enzymatically prepared **3d**. This analysis showed that the Q73A-catalyzed addition of **2d** to **1b** is highly enantioselective, yielding **3d** with >99% *ee*. Similar analyses were performed to determine the *ee* value of the other Q73A-synthesized amino acid products **3c**, **3e**, **3h**, **3i**, and **3l**.

Fig. S5a

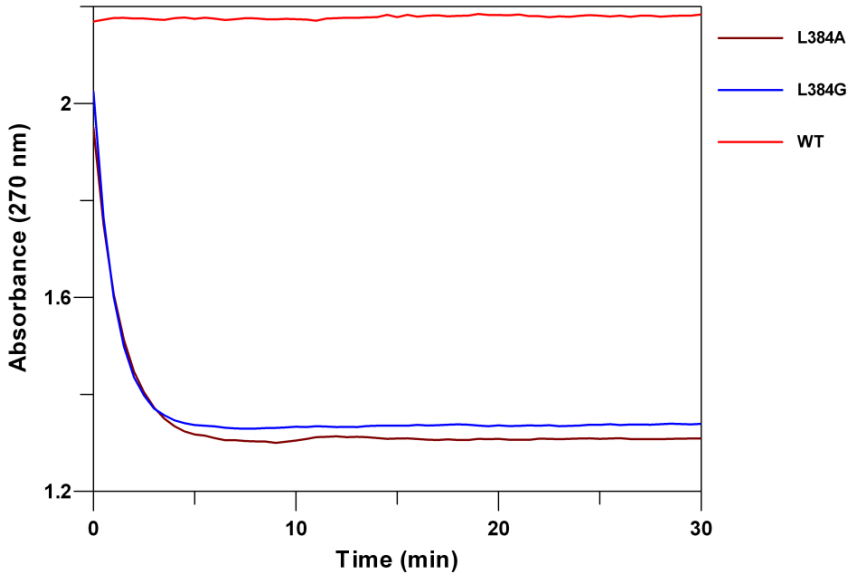

Fig. S5b

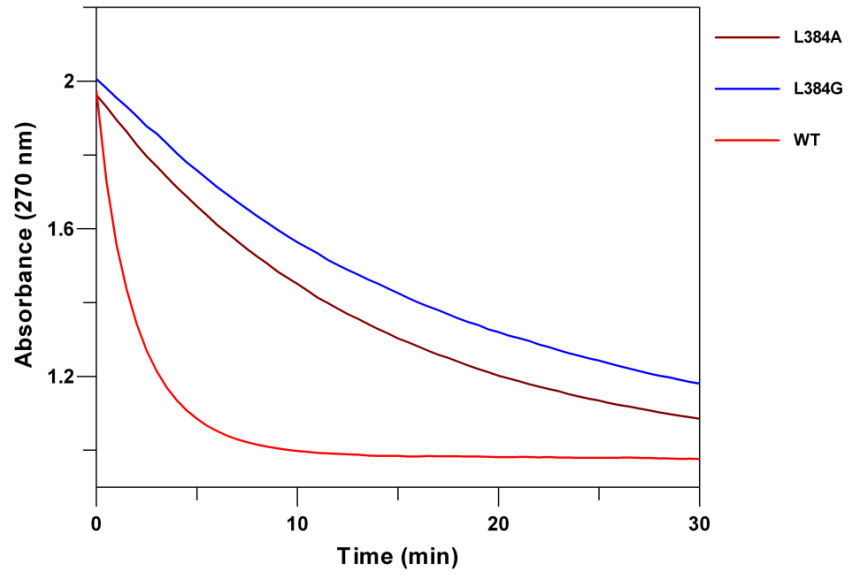

Supplementary Fig. 5. UV spectra monitoring the ammonia (**2a**, 400 mM) addition to mesaconate (**1b**, 5 mM) or 2-hexylfumarate (**1g**, 3 mM) catalyzed by wild-type MAL and the MAL mutants L384G and L384A. (**a**) UV spectra monitoring the addition of **2a** to **1g** catalyzed by wild-type (150 µg/ml) or mutant (150 µg/ml) MAL. (**b**) UV spectra monitoring the addition of **2a** to **1b** catalyzed by wild-type (15 µg/ml) or mutant (150 µg/ml) MAL. The amination reactions were monitored by following the depletion of the absorbance of either **1b** or **1g** at 270 nm in 500 mM Tris-HCl buffer, pH 9.0, containing 20 mM $MgCl_2$.

SUPPLEMENTARY TABLES

Supplementary Table 1. Apparent kinetic parameters for wild-type MAL and the Q73A mutant using ammonia (**2a**) or methylamine (**2b**) as nucleophiles in the addition to mesaconate[a].

Enzyme	Substrate	k_{cat} (s^{-1})	K_m (mM)	k_{cat}/K_m (M^{-1} s^{-1})
MAL	**2a**	50 ± 4	46 ± 5	1.0×10^3
Q73A	**2a**	0.6 ± 0.1	270 ± 40	2.2
MAL	**2b**	-	-	<0.01
Q73A	**2b**	0.8 ± 0.1	580 ± 30	1.4

[a]The steady state kinetic parameters were determined at 30°C in 500 mM Tris buffer, pH 9.0, containing 20 mM $MgCl_2$ and 1.5 mM mesaconic acid. Errors are standard deviations from each fit.

Supplementary Table 2. Apparent kinetic parameters for the wild-type MAL- and L384A-catalyzed amination of fumarate (**1a**), mesaconate (**1b**), 2-ethylfumarate (**1c**), 2-*n*-propylfumarate (**1d**), 2-*n*-butylfumarate (**1e**), 2-*n*-pentylfumarate (**1f**) and 2-*n*-hexylfumarate (**1g**).

Substrate	MAL k_{cat} (s^{-1})	MAL K_m (mM)	MAL k_{cat}/K_m ($M^{-1}s^{-1}$)	L384A k_{cat} (s^{-1})	L384A K_m (mM)	L384A k_{cat}/K_m ($M^{-1}s^{-1}$)
1a	104 ± 5	9.4 ± 1.6	1.1×10^4	> 6	> 60	1.0×10^2
1b	61 ± 1[b]	0.7 ± 0.02[b]	8.7×10^4	> 16	> 60	2.6×10^2
1c	194 ± 10	7.6 ± 0.7	2.6×10^4	> 8	> 50	1.6×10^2
1d	> 5.5	> 50	1.1×10^2	36 ± 4	25 ± 3	1.4×10^3
1e	-	-	-	32 ± 3	11 ± 1	2.9×10^3
1f	-	-	-	21 ± 1	2.0 ± 0.4	1.0×10^4
1g	-	-	-	36 ± 2	4.6 ± 0.5	7.8×10^3

[a]The steady state kinetic parameters were determined at 30°C in 500 mM Tris buffer, pH 9.0, containing 20 mM $MgCl_2$ and 400 mM NH_4Cl. Errors are standard deviations from each fit. [b]These kinetic parameters were obtained from Raj *et al*.[1]

Supplementary Table 3. Data collection and refinement statistics.

	Q73A	**L384A**
Data collection		
Space group	$P2_12_12_1$	$P2_12_12_1$
Cell dimensions *a*, *b*, *c* (Å)	66.8, 109.7, 110.1	66.6, 109.8, 110.8
Resolution (Å)	38.9 – 2.00 (2.11 – 2.00)*	39.0 – 1.90 (2.00 – 1.90)
No. of observations	216949 (23742)	280019 (32561)
No. of unique reflections	54091 (7596)	61377 (8172)
R_{merge} (%)	15.6 (57.7)	14.4 (64.2)
R_{pim} (%)	8.4 (36.6)	7.4 (35.3)
Completeness (%)	98.0 (95.4)	94.2 (87.2)
Mean I/σ (I)	6.9 (2.1)	9.8 (2.3)
Refinement		
R/Rfree (%)	19.8 / 24.9	16.2 / 21.0
No. of atoms in asymmetric unit		
Protein (chain A, B)	3218, 3220	3223, 3223
Water	535	796
Magnesium ions	2	2
Chloride ions	1	1
Glycerol	30	30
Propanamide	-	10
B-factors		
Protein (chain A, B)	15.2, 13.9	13.6, 13.0
Ligands / ions	21.5 / 13.3	21.8 / 13.3
Water	14.1	16.2
Geometry		
RMSD bond lengths (Å)	0.011	0.010
RMSD bond angles (°)	1.3	1.3
Ramachadran favored (%)	95.5	97.1
Ramachandran outliers (%)	0	0
Molprobity score	1.85	1.52
Protein Data Bank code	3ZVH	3ZVI

*Values in parentheses are for highest-resolution shell.

Supplementary Table 4. The primers used for library construction.

Primer	Nucleotide sequence (from 5' to 3')
Fwd-Q73X	GGAGATTGTGCTGCAGTT**NNS**TACTCAGGAGCAGGCGGA
Rev-Q73X	CCGCCTGCTCCTGAGTA**SNN**AACTGCAGCACAATCTCC
Fwd-Q172X	CCTGTATTTGCT**NNS**TCAGGTGATGATAGATACG
Rev-Q172X	CGTATCTATCATCACCTGA**SNN**AGCAAATACAGG
Fwd-F170X	CAATGCAGTTCCTGTA**NNS**GCTCAGTCAGGTGATGATAGATAC
Rev-F170X	GTATCTATCATCACCTGACTGAGC**SNN**TACAGGAACTGCATTG
Fwd-Y356X	GCTAACGGAATGGGAGCT**NNS**TGTGGAGGAACTTGTAACG
Rev-Y356X	CGTTACAAGTTCCTCCACA**SNN**AGCTCCCATTCCGTTAGC
Fwd-L384X	GGAGCTAGACAGGTT**NNS**GCTAAACCAGGTATGGG
Rev-L384X	CCCATACCTGGTTTAGC**SNN**AACCTGTCTAGCTCC

Supplementary Table 5. Molar absorption coefficients of (2-substituted) fumaric acids at 240 and 270 nm. The extinction coefficients were measured in 500 mM Tris-HCl buffer, pH 9.0, at 30°C.

Substrate	ε ($M^{-1} cm^{-1}$) 240 nm	ε ($M^{-1} cm^{-1}$) 270 nm
fumarate[a]	2.53×10^3	5.55×10^2
mesaconate[a]	3.85×10^3	4.83×10^2
2-ethylfumarate[a]	3.32×10^3	4.31×10^2
2-*n*-propylfumarate	3.73×10^3	4.63×10^2
2-*n*-butylfumarate	3.66×10^3	6.60×10^2
2-*n*-pentylfumarate	3.94×10^3	7.29×10^2
2-*n*-hexylfumarate	3.22×10^3	7.42×10^2

[a]These values were obtained from Botting *et al*.[28]

SUPPLEMENTARY REFERENCES

1. Raj, H. *et al*. Alteration of the diastereoselectivity of 3-methylaspartate ammonia lyase by using structure-based mutagenesis. *Chembiochem* **10**, 2236-2245 (2009).

2. Ho, S.N., Hunt, H.D., Horton, R.M., Pullen, J.K. & Pease, L.R. Site-directed mutagenesis by overlap extension using the polymerase chain reaction. *Gene* **77**, 51-59 (1989).

3. Kamerbeek, N.M., Fraaije, M.W. & Janssen, D.B. Identifying determinants of NADPH specificity in Baeyer-Villiger monooxygenase. *Eur. J. Biochem.* **271**, 2107-2116 (2004).

4. Kabsch, W. Automatic processing of rotation diffraction data from crystals of initially unknown symmetry and cell constants. *J. Appl. Crystallogr.* **26**, 795-800 (1993).

5. Evans, P. Scaling and assessment of data quality. *Acta Crystallogr. D Biol. Crystallogr.* **62**, 72-82 (2006).

6. Asuncion, M., Blankenfeldt, W., Barlow, J.N., Gani, D. & Naismith, J.H. The structure of 3-methylaspartase from *Clostridium tetanomorphum* functions via the common enolase chemical step. *J. Biol. Chem.* **277**, 8306-8311 (2002).

7. McCoy, A.J. *et al*. Phaser crystallographic software. *J. Appl. Crystallogr.* **40**, 658-674 (2007).

8. Emsley, P. & Cowtan, K. Coot: model-building tools for molecular graphics. *Acta Crystallogr. D Biol. Crystallogr.* **60**, 2126-2132 (2004).

9. Murshudov, G.N., Vagin, A.A. & Dodson, E.J. Refinement of macromolecular structures by the maximum-likelihood method. *Acta Crystallogr. D Biol. Crystallogr.* **53**, 240-255 (1997).

10. Davis, I.W. *et al*. MolProbity: all-atom contacts and structure validation for proteins and nucleic acids. *Nucleic Acids Res.* **35**, W375-383 (2007).

11. Levy, C.W. *et al.* Insights into enzyme evolution revealed by the structure of methylaspartate ammonia lyase. *Structure* **10**, 105-113 (2002).

12. Brooks, B.R. *et al*. CHARMM: A program for macromolecular energy, minimization, and dynamics calculations. *J. Comput. Chem.* **4**, 187-217 (1983).

13. MacKerell, A.D., Jr., *et al*. *The Encyclopedia of Computational Chemistry* (ed Schleyer *et al*.), pp. 271-277 (John Wiley & Sons, Chichester, 1998).

14. Erickson, J.A., Jalaie, M., Robertson, D.H., Lewis, R.A. & Vieth, M. Lessons in molecular recognition: the effects of ligand and protein flexibility on molecular docking accuracy. *J. Med. Chem.* **47**, 45-55 (2004).

15. Wu, G., Robertson, D.H., Brooks, C.L., 3rd & Vieth, M. Detailed analysis of grid-based molecular docking: A case study of CDOCKER-A CHARMm-based MD docking algorithm. *J. Comput. Chem.* **24**, 1549-1562 (2003).

16. Akhtar, M., Botting, N.P., Cohen, M.A. & Gani, D. Enantiospecific synthesis of 3-substituted aspartic acids via enzymic amination of substituted fumaric acids. *Tetrahedron* **43**, 5899-5908 (1987).

17. Jawaid, S., Farrugia, L.J. & Robins, D.J. Asymmetric synthesis of 2-substituted butane-1,4-diols by hydrogenation of homochiral fumaramide derivatives. *Tetrahedron: Asymmetry* **15**, 3979-3988 (2004).

18. Fan, M.-J., Li G.-Q. & Liang, Y.-M. DABCO catalyzed reaction of various nucleophiles with activated alkynes leading to the formation of alkenoic acid esters, 1,4-dioxane, morpholine, and piperazinone derivatives. *Tetrahedron* **62**, 6782-6791 (2006).

19. Gotthardt, H. & Reiter, F. Neue, ungewöhnliche photochemische reaktionen von 3-aminosydnonen. *Chem. Ber.* **114**, 1737-1745 (1981).

20. Sahoo, M.K., Mhaske, S.B. & Argade, N.P. Facile routes to alkoxymaleimides/maleic anhydrides. *Synthesis*, 346-349 (2003).

21. Kianmehr, E., Tabatabai, K., Abbasi, A. & Mehr, H.S. Diastereoselective O-vinylation of phenols using DMAD under mild reaction conditions. *Synth. Commun.* **38**, 2529-2539 (2008).

22. Meindertsma, A.F., Pollard, M.M., Feringa, B.L., de Vries, J.G. & Minnaard, A.J. Asymmetric hydrogenation of alkyl(vinyl)thioethers: a promising approach to α-chiral thioethers. *Tetrahedron: Asymmetry* **18**, 2849-2858 (2007).

23. Mavencamp, T.L., Rhoderick, J.F., Bridges, R.J. & Esslinger, C.S. Synthesis and preliminary pharmacological evaluation of novel derivatives of L-β-*threo*-benzylaspartate as inhibitors of the neuronal glutamate transporter EAAT-3. *Bioorg. Med. Chem.* **16**, 7740-7748 (2008).

24. Calderon, F., Doyaguez, E.G. & Fernandez-Mayoralas, A. Synthesis of azasugars through a proline-catalyzed reaction. *J. Org. Chem.* **71**, 6258-6261 (2006).

25. Breuning, A., Vicik, R. & Schirmeister, T. An improved synthesis of aziridine-2,3-dicarboxylates via azido alcohols—epimerization studies. *Tetrahedron: Asymmetry* **14**, 3301-3312 (2003).

26. Antolini, L. *et al*. Stereoselective synthesis of *erythro* β-substituted aspartates. *J. Org. Chem.* **62**, 8784-8789 (1997).

27. Legters, J., Lambertus, T. & Zwanenburg, B. Synthesis of naturally occurring (2*S*,3*S*)-(+)-aziridine-2,3-dicarboxylic acid. *Tetrahedron* **47**, 5287-5294 (1991).

28. Botting, N.P., Akhtar, M., Cohen, M.A. & Gani, D. Substrate specificity of the 3-methylaspartate ammonia-lyase reaction: observation of differential relative reaction rates for substrate-product pairs. *Biochemistry* **27**, 2953-2955 (1988).

PART TWO

BIOCATALYTIC APPLICATIONS

OF ENGINEERED

METHYLASPARTATE AMMONIA LYASES

Chapter 4

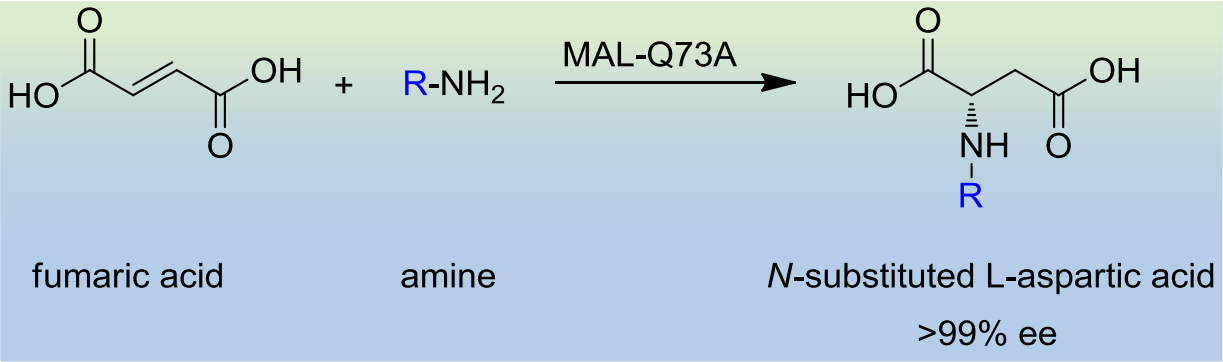

Enantioselective synthesis of *N*-substituted aspartic acids using an engineered variant of methylaspartate ammonia lyase

Vinod Puthan Veetil,[a,*] **Hans Raj,[a,*]** Marianne de Villiers,[a] Pieter G. Tepper,[a] Frank J. Dekker,[b] Wim J. Quax,[a] and Gerrit J. Poelarends[a]

[a] *Department of Pharmaceutical Biology, Groningen Research Institute of Pharmacy, University of Groningen, Antonius Deusinglaan 1, 9713 AV Groningen, The Netherlands.*

[b] *Department of Pharmaceutical Gene Modulation, Groningen Research Institute of Pharmacy, University of Groningen, Antonius Deusinglaan 1, 9713 AV Groningen, The Netherlands*

**These authors contributed equally to this work*.

Published in *ChemCatChem* (2013) 5, 1325-1327.

ABSTRACT

We report the synthesis of a large variety of *N*-substituted aspartic acids by the addition of structurally diverse amines to fumaric acid, catalyzed by a previously engineered variant of methylaspartate ammonia lyase. The enzyme-catalyzed additions are highly enantioselective, only yielding the L-enantiomers of the corresponding amino acid products (>99% *ee*).

INTRODUCTION

N-substituted aspartic acids are important building blocks for pharmaceuticals, artificial sweeteners, synthetic enzymes, and peptidomimetics.[1-4] In such applications the optical purity of the compounds is paramount. The most common synthetic route to *N*-substituted aspartic acids is via the direct Michael-type addition of amines to maleic acid, maleic anhydride, or the ester or amide derivatives of maleic acid.[5-8] Recently, a novel one-step method for the preparation of *N*-substituted aspartic acids from maleic anhydride and amines via the monolithium salt of maleic acid was reported.[9] However, the products of all these reactions are racemic mixtures and further separation steps are needed to get an optically pure amino acid. A general method for the synthesis of enantiomerically pure *N*-substituted aspartic acids is the reductive amination of carbonyl compounds with enantiopure aspartic acid.[10, 11] However, this method is limited by the availability of the corresponding carbonyl compounds and the formation of multiple undesired side-products. In addition to these chemical synthesis routes, two classes of ammonia lyases, aspartate ammonia lyases (E.C 4.3.1.1) and 3-methylaspartate ammonia lyases (EC 4.3.1.2),[12] have recently been explored for the enzymatic synthesis of enantiopure *N*-substituted aspartic acids (Scheme 1).[13, 14]

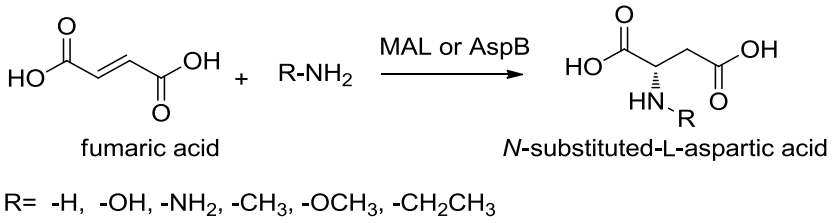

Scheme 1. Biocatalytic synthesis of a few *N*-substituted-L-aspartic acids.

Aspartate ammonia lyases play a key role in microbial nitrogen metabolism by catalyzing the reversible amination of fumaric acid to produce L-aspartic acid.[12, 15, 16] These enzymes are highly enantioselective and have been used in industry for the production of L-aspartic acid, which in turn is an ingredient in the synthesis of the artificial sweetener aspartame.[17, 18] The aspartate ammonia lyase from *Bacillus* species YM55-1 (AspB) is highly active, thermostable and lacks allosteric

regulation by substrate or metal ions.[19-21] AspB processes different amines in the addition reaction and has been used to synthesize *N*-substituted-L-aspartic acids with high enantiomeric excess (>97% *ee*).[14] However, the enzyme only accepts a few small amines such as hydroxylamine, hydrazine, methylamine and methoxylamine in the addition reaction, yielding a limited number of aspartic acid derivatives (Scheme 1). To overcome this limitation, we have attempted to broaden the amine scope of AspB by rational design and structure-guided saturation mutagenesis. However, we were unsuccessful in these engineering attempts, which may have to do with complex loop movement upon substrate binding,[22, 23] making protein engineering of AspB (and other aspartate ammonia lyases) a formidable challenge.

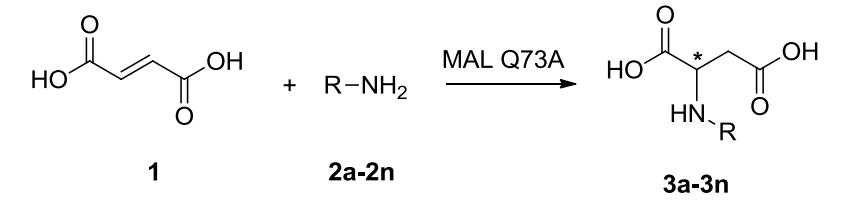

a R = H **f** R = pentyl **k** R = 3-aminopropyl

b R = methyl **g** R = cyclobutyl **l** R = 3-hydroxypropyl

c R = ethyl **h** R= (cyclopropyl)methyl **m** R = ethoxy

d R = propyl **i** R = cyclopropyl **n** R = 2-methoxyethyl

e R = butyl **j** R = 2-aminoethyl

Scheme 2. Biocatalytic synthesis of a large variety of *N*-substituted aspartic acids by MAL-Q73A catalyzed addition of various amines to fumaric acid.

3-Methylaspartate ammonia lyases catalyze the reversible addition of ammonia to mesaconic acid (2-methylfumaric acid) to give *threo*-(2*S*,3*S*)-3-methylaspartic acid and *erythro*-(2*S*,3*R*)-3-methylaspartic acid as products.[12, 24-28] These enzymes are part of glutamate catabolic pathways in anaerobic bacteria and require the presence of Mg^{2+} and K^{+} ions for full activity. The methylaspartate ammonia lyase from *Clostridium tetanomorphum* (MAL) accepts fumaric acid as well as a range of 2-substituted fumaric acids (ethyl-, propyl-, isopropyl- and halo-derivatives) in

the ammonia addition reaction.[29, 30] MAL also accepts hydrazine, hydroxylamine, methylamine, methoxylamine and ethylamine in the addition reaction. The MAL-catalyzed additions of these amines to fumaric acid were highly enantioselective and yielded the corresponding *N*-substituted-L-aspartic acids as the only product (Scheme 1).[13] Unfortunately, like AspB, MAL has a very narrow amine scope and only accepts these small amines as substrates. Interestingly, previous protein engineering work on MAL, which involved structure-guided saturation mutagenesis and activity screening, has resulted in the MAL variant Q73A, which accepts many structurally distinct amines in the addition to mesaconic acid.[31] In the present study, we have exploited the synthetic potential of this engineered MAL variant for the preparation of a large variety of *N*-substituted aspartic acids by the addition of structurally diverse amines to fumaric acid. The enzyme-catalyzed additions are highly enantioselective, only yielding the L-enantiomers of the amino acid products (>99% *ee*).

To test MAL-Q73A as catalyst in amine additions to fumaric acid (Scheme 2), the enzyme was incubated with fumaric acid (**1**, 86 mM) and various amines (**2a**-**2n**, 0.5 to 5 M) in separate reaction mixtures (15 mL final volume; pH 9.0) at 22°C. The reactions were started by the addition of a freshly purified MAL-Q73A enzyme (32 mg, 0.05 mol%) and the progress of the reactions was monitored by UV-Vis and ^{1}H NMR spectroscopy. Interestingly, the MAL-Q73A enzyme was found to efficiently catalyze the addition of amines **2a**-**2n** to fumaric acid (Table 1). With only 0.05 mol% of biocatalyst, excellent (91-100%) conversions were achieved within 0.5-48 h at 22°C. The single amino acid products (**3a**-**3n**) were isolated in fair to good yields and identified by ^{1}H NMR, ^{13}C NMR, and HRMS as the corresponding *N*-substituted aspartic acids.

Table 1. Conversions and yields of isolated products determined for MAL-Q73A catalyzed addition of amines to fumaric acid.

Entry	Amine (M)[a]	Product	Conv. (%) (h)[b]	Yield (%)[c]	*e.e.* (%)[d]
a	**2a** (5)	**3a**	100 (0.5)	79	>99
b	**2b** (3)	**3b**	100 (2.5)	96	>99
c	**2c** (3)	**3c**	100 (24)	75	>99
d	**2d** (3)	**3d**	99 (3)	53	>99
e	**2e** (2)	**3e**	97 (24)	33	>99
f	**2f** (0.5)	**3f**	91 (48)	14	>99
g	**2g** (2)	**3g**	99 (13)	74	>99
h	**2h** (3)	**3h**	96 (24)	28	>99
i	**2i** (2)	**3i**	100 (48)	48	n.d.[e]
j	**2j** (3)	**3j**	99 (2.5)	67	n.d.
k	**2k** (3)	**3k**	100 (9)	61	n.d.
l	**2l** (3)	**3l**	99 (13)	57	n.d.
m	**2m** (3)	**3m**	100 (0.5)	61	n.d.
n	**2n** (3)	**3n**	100 (9)	53	n.d.

[a]Molar concentration of amine used; [b]Hours of incubation; [c]Isolated product yield; [d]The enantiomeric excess of the isolated product was determined by chiral HPLC using authentic standards with known L- or D-configuration; [e]n.d. = not determined.

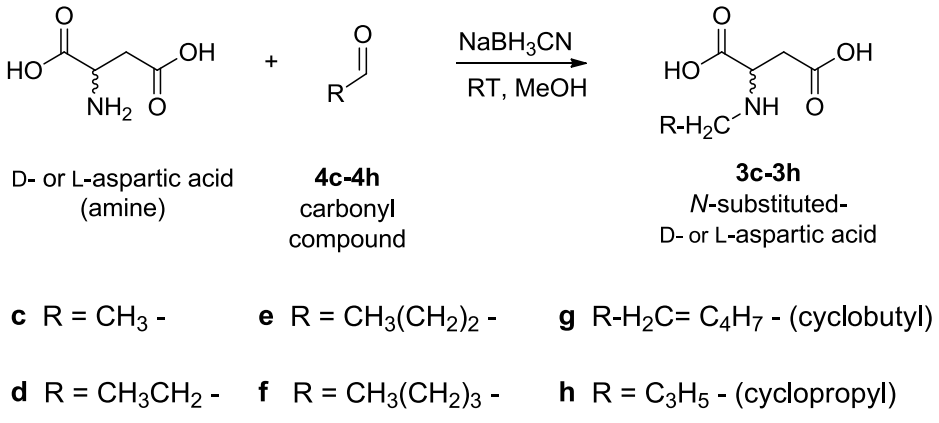

Scheme 3. Reductive amination using D- or L-aspartic acid to obtain enantiopure *N*-substituted aspartic acids with D or L configuration.

For eight selected products (**3a-3h**), the absolute configuration and enantiomeric excess were determined by high-performance liquid chromatography (HPLC) on a chiral stationary phase using authentic standards with known L or D configuration. Whereas the L- and D-enantiomers of **3a** and **3b** are commercially available, those for **3c-3h** were chemically synthesised using pure L- and D-aspartic acid in reductive amination of the corresponding carbonyl compounds (Scheme 3).[10, 11] Chiral HPLC analysis revealed that in all cases (entries a-h, Table 1) the absolute configuration of the enzymatically prepared amino acid product is L, whereas no D-enantiomers were observed. This demonstrates that the high enantioselectivity (*ee* values are >99%) of the MAL-Q73A catalyzed addition reactions is not influenced by the different substituents on the amine substrate. The absolute configuration of products **3i-3n** has not been determined by comparison to enantiopure authentic standards with L or D configuration, but we assume the absolute configuration to be L for all amino acid products **3a-3n**.

In conclusion, we have demonstrated the potential of the MAL-Q73A enzyme for application in the asymmetric synthesis of a large variety of valuable *N*-substituted L-aspartic acids, given that the product yields may be further improved by optimizing isolation procedures. This attractive biocatalytic methodology for the enantioselective synthesis of a wide range of *N*-substituted L-aspartic acids appears to be a simple, environmentally friendly alternative for existing chemical methods.

ACKNOWLEDGEMENTS

We thank Dr. Wiktor Szymański (Center for Systems Chemistry, University of Groningen), Dr. Jandré de Villiers (Department of Pharmaceutical Biology, University of Groningen), and André Boltjes (Department of Pharmaceutical Gene Modulation, University of Groningen) for helpful discussions. This research was financially supported by VENI grant 700.54.401 and ECHO grant 700.59.042 (both to G.J.P.) from the Division of Chemical Sciences of the Netherlands Organisation of Scientific Research (NWO-CW).

REFERENCES

1. M. Kahn, *Synlett.* **1993**, *11*, 821-826.
2. M. Hamada, T. Takeuchi, S. Kondo, Y. Ikeda, H. Naganawa, *J. Antibiot. (Tokyo).* **1970**, *23*, 170-171.
3. K. Burger, J. Spengler, *Eur. J. Org. Chem.* **2000**, *31*, 199-204.
4. C. Nofre, J. -M. Tinti, *United States Patent* **1996**, number: 5,480,668.
5. Y. Liwschitz, A. Zilkha, Y. Amiel, *J. Am. Chem. Soc.* **1956**, *78*, 3067-3069.
6. A. Zilkha, M. D. Bachi, *J. Org. Chem.* **1959**, *24*, 1096-1098.
7. R. Laliberte, L. Berlinguet, *Can. J. Chem.* **1962**, *40*, 163-165.
8. C. J. Abshire, L. Berlinguet, *Can. J. Chem.* **1966**, 2354-2355.
9. P. S. Piispanen, P. M. Pihko, *Tetrahedron Lett.* **2005**, *46*, 2751-2755.
10. Y. Ohfune, N. Kurokawa, N. Higuchi, M. Saito, M. Hashimoto, T. Tanaka, *Chem. Lett.* **1984**, 441-444.
11. R. F. Borch, M. D. Bernstein, H. D. Durst, *J. Am. Chem. Soc.* **1971**, *93*, 2897-2904.
12. M. de Villiers, V. Puthan Veetil, H. Raj, J. de Villiers, G. J. **Poelarends,** *ACS Chem. Biol.* ***2012****, 7*, 1618-1628.
13. M. S. Gulzar, M. Akhtar, D. Gani, *J. Chem. Soc., Perkin Trans. I.* **1997**, 649-656.
14. B. Weiner, G. J. Poelarends, D. B. Janssen, B. L. Feringa, *Chemistry* **2008**, *14*, 10094-10100.
15. R. E. Viola, *Adv. Enzymol. Relat. Areas Mol. Biol.* **2000**, *74*, 295-341.
16. T. Mizobata, Y. Kawata in *Industrial Enzymes: structure, function and applications* (Eds.: J. Polaina, A. P. MacCabe), Springer, New York, **2000**, pp. 549-565.
17. M. Wubbolts in *Enzyme catalysis in organic synthesis: a comprehensive handbook* (Eds.: K. Drauz, H. Waldmann), Wiley-VCH, Weinheim, **2002**, pp. 866-872.
18. A. Liese, K. Seelbach, A. Bulcholz, J. Haberland, in *Industrial biotransformations* (Eds.: A. Liese, K. Seelbach, C. Wandrey), Wiley-VCH, Weinheim, **2006**, pp. 494-501.

19. Y. Kawata, K. Tamura, M. Kawamura, K. Ikei, T. Mizobata, J. Nagai, M. Fujita, S. Yano, M. Tokushige, N. Yumoto, *Eur. J. Biochem.* **2000**, *267*, 1847-1857.

20. T. Fujii, H. Sakai, Y. Kawata, Y. Hata, *J. Mol. Biol.* **2003**, *328*, 635-654.

21. V. Puthan Veetil, H. Raj, W. J. Quax, D. B. Janssen, G. J. Poelarends, *FEBS J.* **2009**, *276*, 2994-3007.

22. G. Fibriansah, V. Puthan Veetil, G. J. Poelarends, A. -M. W. H. Thunnissen, *Biochemistry* **2011**, *50*, 6053-6062.

23. V. Puthan Veetil, G. Fibriansah, H. Raj, A. -M. W. H. Thunnissen, G. J. **Poelarends,** *Biochemistry* ***2012****, 51*, 4237-4243.

24. H. A. Barker, R. D. Smyth, R. M. Wilson, H. Weissbach, *J. Biol. Chem.* **1959**, *234*, 320-328.

25. S. K. Goda, N. P. Minton, N. P. Botting, D. Gani, *Biochemistry* **1992**, *31*, 10747-10756.

26. M. Asuncion, W. Blankenfeldt, J. N. Barlow, D. Gani, J. H. Naismith, *J. Biol. Chem.* **2002**, *277*, 8306-8311.

27. H. Raj, B. Weiner, V. Puthan Veetil, C. R. Reis, W. J. Quax, D. B. Janssen, B. L. Feringa, G. J. Poelarends, *ChemBioChem* **2009**, *10*, 2236-45.

28. H. Raj, V. Puthan Veetil, W. Szymanski, F. J. Dekker, W. J. Quax, B. L. Feringa, D. B. Janssen, G. J. Poelarends, *Appl. Microbiol. Biotechnol.* **2012**, *94*, 385-397.

29. M. Akhtar, N. P. Botting, M. A. Cohen, D. Gani, *Tetrahedron* **1987**, *43*, 5899-5908.

30. N. P. Botting, M. Akhtar, M. A. Cohen, D. Gani, *Biochemistry* **1988**, *27*, 2953-2955.

31. H. Raj, W. Szymański, J. de Villiers, H. J. Rozeboom, V. Puthan Veetil, C. R. Reis, M. de Villiers, F. J. Dekker, S. de Wildeman, W. J. Quax, A. -M. W. H., Thunnissen, B. L. Feringa, D. B. Janssen, G. J. Poelarends, *Nat. Chem.* **2012**, *4*, 478-484.

Supplementary Information

Materials and general methods

All reagents were purchased from Sigma-Aldrich Chemical Co. (St. Louis, MO) or Merck (Darmstadt, Germany) and used without further purification. L-aspartic acid, D-aspartic acid, *N*-methyl-DL-aspartic acid and *N*-methyl-D-aspartic acid were purchased from Sigma-Aldrich. Flash chromatography was carried out on Silicagel (300-400 nm) using CH_2Cl_2/MeOH: 40/60 (v/v) as solvent. NMR spectra were recorded on either a Varian 500 (500 MHz) or on a Varian 200 (200 MHz) spectrometer. High resolution mass spectrometry (HRMS) measurements were performed on a LTQ-Orbitrap XL mass spectrometer (Thermo Fisher Scientific, Bremen, Germany). HPLC analysis was performed using a Shimadzu VP HPLC system. The MAL-Q73A enzyme was overproduced and purified to homogeneity by following a previously described protocol.[1]

General procedure for biocatalytic synthesis of *N*-substituted aspartic acids using MAL-Q73A

N-substituted aspartic acids were synthesized using the MAL-Q73A enzyme. For each substrate pair, a solution (15 mL) of fumaric acid (0.15 g, 86mM), amine (0.5-5 M) and $MgCl_2$ (20 mM) was prepared. The pH was adjusted to 9.0 by addition of aqueous HCl or NaOH. The reactions were started by the addition of freshly purified MAL-Q73A enzyme (32 mg, 0.05 mol%) and reaction mixtures were incubated at 22°C. The progress of each reaction was monitored by UV-Vis and ^{1}H NMR (500 MHz) spectroscopy. The reaction was stopped by incubating the reaction mixture at 100°C for 10 min. The excess of amine was removed from the reaction mixture by purification using anion-exchange chromatography. A Dowex column (50 g anion-exchange resin, Dowex 1X8 chloride, 50-100 mesh) was prepared by pre-treatment with a solution of aqueous HCl (2 N, 4 column volumes), aqueous NaOH (1 M, 2 column volumes) and distilled water (4 column

volumes). The reaction mixture was basified (with ~10 mL of 1 M NaOH) and loaded onto the column, the column was washed with distilled water to remove unbound amine (2 column volumes), and the product was eluted with aqueous HCl (2 N, 2 column volumes). The ninhydrine positive fractions were pooled and concentrated under reduced pressure, followed by lyophilization. The crude product was re-dissolved in water (20 mL) and further purified by cation-exchange chromatography to remove the unreacted fumaric acid, if present. A Dowex column (50 g cation-exchange resin, Dowex 50W X8, 100-200 mesh) was prepared by pre-treatment with aqueous NH_3 (2 M, 4 column volumes), aqueous HCl (1 N, 2 column volumes) and distilled water (4 column volumes). The crude product solution was loaded onto the column, the column was washed with water (2 column volumes) and the product was eluted with aqueous NH_3 (2 M, 2 column volumes). The ninhydrine positive fractions were pooled and concentrated under reduced pressure, followed by lyophilization. The purified products were obtained as diammonium salts and identified by ^{1}H NMR, ^{13}C NMR and HRMS.

L-aspartic acid (L-3a)

Conversion 100% (after 0.5 h). Yield 79%. White solid. ^{1}H NMR (500 MHz, D_2O): δ 2.68 (dd, 1H, J = 17.5 Hz, 8.6 Hz, CHC**H**$_2$), 2.80 (dd, 1H, J = 17.5 Hz, 3.8 Hz, CHC**H**$_2$), 3.89 (dd, 1H, J = 8.6 Hz, 3.8 Hz, C**H**CH_2); ^{13}C NMR (125 MHz, D_2O): δ 39.1, 54.7, 176.8, 180.0; HRMS: m/z calc. for $C_4H_8NO_4$, 134.0453 $[M+H]^+$; found: 134.0448.

***N*-methyl-L-aspartic acid (L-3b)**

Conversion 100% (after 2.5 h). Yield 96%. White solid. ^{1}H NMR (500 MHz, D_2O): δ 2.70-2.75 (m, 4H CHC**H**$_2$NHC**H**$_3$), 2.82 (dd, 1H, J = 17.6 Hz, 4.1 Hz, CHC**H**$_2$), 3.73 (dd, 1H, J = 7.7 Hz, 4.1 Hz, C**H**CH_2); ^{13}C NMR (125 MHz, D_2O): δ 34.3, 37.8, 63.2, 175.9, 179.8; HRMS: m/z calc. for $C_5H_{10}NO_4$, 148.0610 $[M+H]^+$; found: 148.0604.

***N*-ethyl-L-aspartic acid (L-3c)**

Conversion 100% (after 24 h). Yield 75%. White solid. ^{1}H NMR (500 MHz, D_2O): δ 1.30 (t, 3H, J = 7.3 Hz, C**H$_3$**CH$_2$), 2.71 (dd, 1H, J = 17.5 Hz, 8.0 Hz, CHC**H$_2$**), 2.82 (dd, 1H, J = 17.5 Hz, 3.4 Hz, CHC**H$_2$**), 3.09-3.16 (m, 2H, CH$_3$C**H$_2$**), 3.81 (dd, 1H, J = 7.6 Hz, 3.8 Hz, C**H**CH$_2$); ^{13}C NMR (125 MHz, D_2O): δ 13.4, 38.2, 44.5, 61.4, 176.0, 179.5; HRMS: m/z calc. for $C_6H_{12}NO_4$, 162.0766 $[M+H]^+$; found: 162.0761.

***N*-propyl-L-aspartic acid (L-3d)**

Conversion 99% (after 3 h). Yield 53%. White solid. ^{1}H NMR (500 MHz, D_2O): δ 0.97 (t, 3H, J = 7.5 Hz, CH$_2$CH$_2$C**H$_3$**), 1.68-1.76 (m, 2H, CH$_2$C**H$_2$**CH$_3$), 2.69 (dd, 1H, J = 17.6 Hz, 8.5 Hz, CHC**H$_2$**), 2.82 (dd, 1H, J = 17.5 Hz, 4.0 Hz, CHC**H$_2$**), 2.98-3.06 (m, 2H, NHC**H$_2$**CH$_2$), 3.79 (dd, 1H, J = 8.4 Hz, 4.0 Hz, C**H**CH$_2$); ^{13}C NMR (125 MHz, D_2O): δ 12.8, 21.9, 38.0, 50.8, 61.8, 175.9, 179.7; HRMS: m/z calc. for $C_7H_{14}NO_4$, 176.0923 $[M+H]^+$; found: 176.0917.

***N*-butyl-L-aspartic acid (L-3e)**

Conversion 97% (after 24 h). Yield 33%. White solid. ^{1}H NMR (500 MHz, D_2O): δ 0.93 (t, 3H, J = 7.4 Hz, CH$_2$CH$_2$C**H$_3$**), 1.38-1.43 (m, 2H, CH$_2$C**H$_2$**CH$_3$), 1.66-1.72 (m, 2H, C**H$_2$**CH$_2$CH$_3$), 2.69 (dd, 1H, J = 17.5 Hz, 8.5 Hz, CHC**H$_2$**), 2.81 (dd, 1H, J = 17.5 Hz, 4.0 Hz, CHC**H$_2$**), 3.04-3.11 (m, 2H, NHC**H$_2$**CH$_2$), 3.80 (dd, 1H, J = 8.4 Hz, 4.0 Hz, C**H**CH$_2$); ^{13}C NMR (125 MHz, D_2O): δ 15.3, 21.7, 30.3, 38.1, 49.0, 61.9, 175.9, 179.8, HRMS: m/z calc. for $C_8H_{16}NO_4$. 190.1079 $[M+H]^+$; found: 190.1074.

***N*-pentyl-L-aspartic acid (L-3f)**

Conversion 91% (after 48 h). Yield 14%. White solid. ^{1}H NMR (500 MHz, D_2O): δ 0.89 (t, 3H, J = 7.0 Hz, CH$_2$CH$_2$C**H$_3$**), 1.31-1.39 (m, 4H, CH$_2$C**H$_2$**C**H$_2$**CH$_3$), 1.69-1.75 (m, 2H, C**H$_2$**CH$_2$CH$_2$CH$_3$), 2.69 (dd, 1H, J = 17.5 Hz, 8.1 Hz, CHC**H$_2$**), 2.82 (dd, 1H, J = 17.5 Hz, 4.4 Hz, CHC**H$_2$**), 3.03-3.12

(m, 2H, NHC**H₂**CH₂), 3.77 (dd, 1H, *J* = 8.1 Hz, 4.4 Hz, C**H**CH₂); ^{13}C NMR (125 MHz, D₂O): *δ* 13.0, 21.3, 25.2, 27.7, 35.4, 46.5, 59.2, 173.2, 177.1; HRMS: m/z calc. for $C_9H_{18}NO_4$, 204.1236 $[M+H]^+$; found: 204.1230.

N-cyclobutyl-L-aspartic acid (L-3g)

Conversion 99% (after 13 h). Yield 74%. White solid. ^{1}H NMR (500 MHz, D₂O): *δ* 1.81-1.92 (m, 2H, CH₂C**H₂**CH₂), 2.18–2.31 (m, 4H, C**H₂**CH₂C**H₂**), 2.68 (dd, 1H, *J* = 17.5 Hz, 7.5 Hz, CHC**H**₂), 2.78 (dd, 1H, *J* = 17.6 Hz, 4.6 Hz, CHC**H**₂), 3.71 (dd, 1H, *J* = 7.5 Hz, 4.5 Hz, C**H**CH₂COOH), 3.82 (p, 1H, *J* = 8.2 Hz, NHC**H**(CH₂)₂); ^{13}C NMR (50 MHz, D₂O): *δ* 12.2, 24.1, 33.5, 48.7, 55.2, 171.2, 174.8; HRMS: m/z calc. for $C_8H_{14}NO_4$, 188.0923 $[M+H]^+$; found: 188.0918.

N-(cyclopropyl)methyl-L-aspartic acid (L-3h)

Conversion 96% (after 24 h). Yield 28%. White solid. ^{1}H NMR (500 MHz, D₂O): *δ* 0.31-0.41 (m, 2H, CH₂C**H₂**), 0.65-0.70 (m, 2H, C**H₂**CH₂) 1.07-1.15 (m, 1H, CH₂C**H**(CH₂)₂), 2.67 (dd, 1H, *J* = 17.5 Hz, 8.8 Hz, CHC**H**₂), 2.80 (dd, 1H, *J* = 17.5 Hz, 4.0 Hz, CHC**H**₂), 2.93 (dd, 1H, *J* = 12.9 Hz, 7.4 Hz, NHC**H**₂), 3.01 (dd, 1H, *J* = 12.9 Hz, 7.4 Hz, NHC**H**₂), 3.86 (dd, 1H, *J* = 8.8 Hz, 4.0 Hz, C**H**CH₂); ^{13}C NMR (125 MHz, D₂O): *δ* 6.0, 6.2, 9.6, 38.3, 54.1, 61.4, 175.9, 179.9; HRMS: m/z calc. for $C_8H_{14}NO_4$, 188.0923 $[M+H]^+$; found: 188.0917.

N-cyclopropylaspartic acid (3i)

Conversion 100% (after 48 h). Yield 48%. White solid. ^{1}H NMR (500 MHz, D₂O): *δ* 0.85-0.97 (m, 4H, C**H₂**C**H₂**), 2.66-2.82 (m, 2H, CH₂C**H**CH₂, CHC**H**₂), 2.89 (dd, 1H, *J* = 17.6 Hz, 4.2 Hz, CHC**H**₂), 3.96 (dd, 1H, *J* = 8.1 Hz, 4.4 Hz, C**H**CH₂); ^{13}C NMR (125 MHz, D₂O): *δ* 3.0, 3.2, 29.0, 35.3, 60.5, 173.4, 177.2; HRMS: m/z calc. for $C_7H_{12}NO_4$, 174.0766 $[M+H]^+$; found: 174.0761.

N-(2-aminoethyl)aspartic acid (3j)

Conversion 99% (after 2.5 h). Yield 67%. White solid. ^{1}H NMR (500 MHz, D_2O): δ 2.53 (dd, 1H, J = 16.9 Hz, 8.8 Hz, CHC**H**$_2$), 2.70 (dd, 1H, J = 16.9 Hz, 3.9 Hz, CHC**H**$_2$), 3.17-3.25 (m, 4H, NHC**H$_2$**C**H$_2$**NH$_2$), 3.66 (dd, 1H, J = 8.8 Hz, 3.9 Hz, C**H**CH$_2$); ^{13}C NMR (125 MHz, D_2O): δ 39.4, 40.0, 46.4, 62.7, 178.2, 180.6; HRMS: m/z calc. for $C_6H_{13}N_2O_4$, 177.0875 $[M+H]^+$; found: 177.0870.

N-(3-aminopropyl)aspartic acid (3k)

Conversion 100% (after 9 h). Yield 61%. White solid. ^{1}H NMR (500 MHz, D_2O): δ 2.08–2.14 (m, 2H, CH$_2$C**H$_2$**CH$_2$NH$_2$), 2.65 (dd, 1H, J = 17.5 Hz, 8.7 Hz, CHC**H**$_2$), 2.79 (dd, 1H, J = 17.5 Hz, 3.9 Hz, CHC**H**$_2$), 3.10 (t, 2H, J = 7.7 Hz, CH$_2$CH$_2$C**H$_2$**NH$_2$), 3.13–3.22 (m, 2H, NHC**H$_2$**CH$_2$CH$_2$), 3.81 (dd, 1H, J = 8.7 Hz, 3.9 Hz, C**H**CH$_2$); ^{13}C NMR (125 MHz, D_2O): δ 26.5, 38.3, 39.2, 46.1, 62.1, 175.7, 179.9; HRMS: m/z calc. for $C_7H_{15}N_2O_4$, 191.1032 $[M+H]^+$; found: 191.1026.

N-(3-hydroxypropyl)aspartic acid (3l)

Conversion 99% (after 13 h). Yield 57%. White solid. ^{1}H NMR (200 MHz, D_2O): δ 1.90-2.03 (m, 2H, CH$_2$C**H$_2$**CH$_2$OH), 2.69 (dd, 1H, J = 17.5 Hz, 7.9 Hz, CHC**H**$_2$), 2.83 (dd, 1H, J = 17.5 Hz, 4.3 Hz, CHC**H**$_2$), 3.12-3.31 (m, 2H, NHC**H$_2$**CH$_2$CH$_2$), 3.71-3.84 (m, 3H, NHC**H$_2$**CH$_2$CH$_2$, C**H**CH$_2$); ^{13}C NMR (50 MHz, D_2O): δ 25.8, 33.3, 42.5, 57.0, 57.3, 171.0, 175.0; HRMS: m/z calc. for $C_7H_{14}NO_5$, 191.0872 $[M+H]^+$; found: 191.0867.

N-ethoxyaspartic acid (3m)

Conversion 100% (after 0.5 h). Yield 61%. White solid. ^{1}H NMR (500 MHz, D_2O): δ 1.05 (t, 3H, J = 7.0, C**H$_3$**CH$_2$O), 2.26 (dd, 1H, J = 15.7 Hz, 8.7 Hz, CHC**H**$_2$), 2.49 (dd, 1H, J = 15.7 Hz, 5.0 Hz, CHC**H**$_2$), 3.68-3.76 (m, 3H, CH$_3$C**H$_2$**O, C**H**CH$_2$); ^{13}C NMR (125 MHz, D_2O): δ 15.8, 39.9, 65.4, 71.9, 181.2, 181.3; HRMS: m/z calc. for $C_6H_{12}NO_5$, 178.0715 $[M+H]^+$; found: 178.0712.

N-(2-methoxy)ethylaspartic acid (3n)

Conversion 100% (after 9 h). Yield 53%. White solid. ^{1}H NMR (500 MHz, D_2O): δ 2.69 (dd, 1H, J = 18.0 Hz, 7.3 Hz, CHC**H**$_2$), 2.82 (dd, 1H, J = 18.0 Hz, 4.9 Hz, CHC**H**$_2$), 3.17-3.29 (m, 2H, NHC**H$_2$**CH_2), 3.40 (s, 3H, CH_2OC**H$_3$**), 3.67 (t, 2H, J = 5.0 Hz, CH_2C**H$_2$**OCH_3), 3.79 (dd, 1H, J = 7.2 Hz, J = 4.8 Hz, C**H**CH_2); ^{13}C NMR (50 MHz, D_2O): δ 34.3, 46.0, 58.1, 58.4, 66.8, 172.2, 175.1; HRMS: m/z calc. for $C_7H_{14}NO_5$, 192.0872 $[M+H]^+$; found: 192.0867.

Chemical synthesis of enantiopure *N*-substituted aspartic acids

N-substituted aspartic acids were prepared by the method of Ohfune *et al*.[2] The preparation of *N*-pentyl-L-aspartic acid is given here as an example. To a suspension of L-aspartic acid (666 mg, 5 mmol) and $NaBH_3CN$ (471 mg, 7.5 mmol) in MeOH (15 mL) was added pentaldehyde (0.64 ml, 6 mmol). The reaction mixture was stirred for 18 h at room temperature. The mixture was then filtered and the filtrate was evaporated. Subsequently, the residue was washed with ethyl acetate (3 x 10 mL) and dried under vacuum. A white precipitate was formed, which was dissolved in 1-2 mL of 1 N HCl. The solution was triturated with acetone and the white precipitate formed was filtered and dried to obtain the product *N*-pentyl-L-aspartic acid. For products **3c**, **3g** and **3h** silica chromatography (CH_2Cl_2/MeOH: 40/60, v/v) was used to further purify the product. For analysis by NMR spectroscopy, the amino acid products were dissolved in 0.2 M NaOH in D_2O. In similar manner, the L- and D- enantiomers of **3c-3h** were successfully synthesized and purified. All chemically synthesized compounds were characterized by ^{1}H NMR and ^{13}C NMR spectroscopy and HRMS analysis.

N-ethyl-L-aspartic acid (L-3c)

Yield 5%. White solid. ^{1}H NMR (200 MHz, D_2O): δ 1.06 (t, 3H, J = 7.3 Hz, C**H$_3$**CH_2), 2.30 (dd, 1H, J = 11.1 Hz, 4.8 Hz, CHC**H**$_2$), 2.44-2.59 (m, 3H, CH_3C**H$_2$**, CHC**H**$_2$), 3.40 (dd, 1H, J = 8.2 Hz,

5.6 Hz, C**H**CH_2); ^{13}C NMR (50 MHz, D_2O): δ 13.7, 41.5, 41.5, 61.2, 179.8, 181.7; HRMS: m/z calc. for $C_6H_{12}NO_4$, 162.0766 $[M+H]^+$; found: 162.0762.

N-ethyl-D-aspartic acid (D-3c)

Yield 5%. White solid. ^{1}H NMR (200 MHz, D_2O): δ 1.02 (t, 3H, J = 7.2 Hz, C**H$_3$**CH_2), 2.27 (dd, 1H, J = 15.0 Hz, 8.2 Hz, CHC**H**$_2$), 2.41–2.59 (m, 3H, CH_3C**H$_2$**, CHC**H**$_2$), 3.36 (dd, 1H, J = 8.2 Hz, 5.7 Hz, C**H**CH_2); ^{13}C NMR (50 MHz, D_2O): δ 13.7, 41.5, 41.6, 61.2, 179.8, 181.8; HRMS: m/z calc. for $C_6H_{12}NO_4$, 162.0766 $[M+H]^+$; found: 162.0762.

N-propyl-L-aspartic acid (L-3d)

Yield 43%. White solid. ^{1}H NMR (200 MHz, D_2O): δ 1.02 (t, 3H, J = 7.4 Hz, CH_2CH_2C**H$_3$**), 1.68-1.87 (m, 2H, CH_2C**H$_2$**CH_3), 2.92–2.98 (m, 2H, CHC**H$_2$**), 3.04-3.15 (m, 2H, NHC**H$_2$**CH_2), 3.94 (dd, 1H, J = 6.8 Hz, 4.9 Hz, C**H**CH_2); ^{13}C NMR (50 MHz, D_2O): δ 10.1, 19.2, 34.5, 48.5, 58.3, 172.6, 175.3; HRMS: m/z calc. for $C_7H_{14}NO_4$, 176.0923 $[M+H]^+$; found: 176.0918.

N-propyl-D-aspartic acid (D-3d)

Yield 34%. White solid. ^{1}H NMR (200 MHz, D_2O): δ 1.02 (t, 3H, J = 7.4 Hz, CH_2CH_2C**H$_3$**), 1.68-1.88 (m, 2H, CH_2C**H$_2$**CH_3), 3.04-3.09 (m, 2H, CHC**H$_2$**), 3.12-3.17 (m, 2H, NHC**H$_2$**CH_2), 4.03 (dd, 1H, J = 6.8 Hz, 4.9 Hz, C**H**CH_2); ^{13}C NMR (50 MHz, D_2O): δ 10.1, 19.1, 34.0, 48.7, 57.7, 172.1, 174.1; HRMS: m/z calc. for $C_7H_{14}NO_4$, 176.0923 $[M+H]^+$, found: 176.0918.

N-butyl-L-aspartic acid (L-3e)

Yield 14%. White solid. ^{1}H NMR (200 MHz, D_2O): δ 0.98 (t, 3H, J = 7.3 Hz, CH_2CH_2C**H$_3$**), 1.36-1.55 (m, 2H, CH_2C**H$_2$**CH_3), 1.68-1.83 (m, 2H, C**H$_2$**CH_2CH_3), 2.73 (dd, 1H, J = 17.5 Hz, 8.0 Hz, CHC**H**$_2$), 2.88 (dd, 1H, J = 17.5 Hz, 4.4 Hz, CHC**H**$_2$), 3.10-3.18 (m, 2H, NHC**H$_2$**CH_2), 3.85 (dd, 1H, J = 8.0 Hz, 4.4 Hz, C**H**CH_2); ^{13}C NMR (50 MHz, D_2O): δ 13.2, 19.8, 30.8, 41.6, 46.9, 61.4, 179.9, 181.9; HRMS: m/z calc. for $C_8H_{16}NO_4$, 190.1079 $[M+H]^+$; found: 190.1074.

***N*-butyl-D-aspartic acid (D-3e)**

Yield 18%. White solid. ^{1}H NMR (200 MHz, D_2O): δ 0.97 (t, 3H, J = 7.3 Hz, $CH_2CH_2C\mathbf{H_3}$), 1.36-1.55 (m, 2H, $CH_2C\mathbf{H_2}CH_3$), 1.67-1.83 (m, 2H, $C\mathbf{H_2}CH_2CH_3$), 2.71 (dd, 1H, J = 17.5 Hz, 8.2 Hz, $CHC\mathbf{H}_2$), 2.86 (dd, 1H, J = 17.5 Hz, 4.4 Hz, $CHC\mathbf{H}_2$), 3.06-3.19 (m, 2H, $NHC\mathbf{H_2}CH_2$), 3.84 (dd, 1H, J = 8.1 Hz, 4.3 Hz, $C\mathbf{H}CH_2$); ^{13}C NMR (50 MHz, D_2O): δ 13.2, 19.8, 30.8, 41.6, 46.9, 61.4, 179.9, 181.8; HRMS: m/z calc. for $C_8H_{16}NO_4$, 190.1079 $[M+H]^+$; found: 190.1074.

***N*-pentyl-L-aspartic acid (L-3f)**

Yield 25%. White solid. ^{1}H NMR (200 MHz, D_2O): δ 0.92 (t, 3H, J = 7.0 Hz, $CH_2CH_2C\mathbf{H_3}$), 1.33-1.43 (m, 4H, $CH_2C\mathbf{H_2}C\mathbf{H_2}CH_3$), 1.68-1.79 (m, 2H, $C\mathbf{H_2}CH_2CH_2CH_3$), 2.78 (dd, 1H, J = 17.6 Hz, 7.7 Hz, $CHC\mathbf{H}_2$), 2.91 (dd, 1H, J = 17.6 Hz, 4.6 Hz, $CHC\mathbf{H}_2$), 3.07-3.16 (m, 2H, $NHC\mathbf{H_2}CH_2$), 3.86 (dd, 1H, J = 7.6 Hz, 4.6 Hz, $C\mathbf{H}CH_2$); ^{13}C NMR (50 MHz, D_2O): δ 13.0, 21.4, 25.2, 27.7, 35.0, 46.7, 58.9, 173.0, 176.4; HRMS: m/z calc. for $C_9H_{18}NO_4$, 204.1236 $[M+H]^+$; found: 204.1229.

***N*-pentyl-D-aspartic acid (D-3f)**

Yield 20%. White solid. ^{1}H NMR (200 MHz, D_2O): δ 0.92 (t, 3H, J = 7.1 Hz, $CH_2CH_2C\mathbf{H_3}$), 1.33-1.44 (m, 4H, $CH_2C\mathbf{H_2}C\mathbf{H_2}CH_3$), 1.68-1.79 (m, 2H, $C\mathbf{H_2}CH_2CH_2CH_3$), 2.77 (dd, 1H, J = 17.6 Hz, 7.7 Hz, $CHC\mathbf{H}_2$), 2.91 (dd, 1H, J = 17.6 Hz, 4.6 Hz, $CHC\mathbf{H}_2$), 3.08-3.16 (m, 2H, $NHC\mathbf{H_2}CH_2$), 3.86 (dd, 1H, J = 7.7 Hz, 4.6 Hz, $C\mathbf{H}CH_2$); ^{13}C NMR (50 MHz, D_2O): δ 13.0, 21.4, 25.2, 27.7, 35.1, 46.7, 58.9, 173.1, 176.5; HRMS: m/z calc. for $C_9H_{18}NO_4$, 204.1236 $[M+H]^+$; found: 204.1229.

***N*-cyclobutyl-L-aspartic acid (L-3g)**

Yield 5%. White solid. ^{1}H NMR (200 MHz, D_2O): δ 1.50-1.85 (m, 4H, $\mathbf{CH_2}CH_2C\mathbf{H_2}$), 2.07-2.19 (m, 2H, $CH_2C\mathbf{H_2}CH_2$), 2.26 (dd, 1H, J = 15.1 Hz, 8.3 Hz, $CHC\mathbf{H}_2$), 2.45 (dd, 1H, J = 15.0 Hz, 5.6 Hz, $CHC\mathbf{H}_2$), 3.20 (m, 1H, $NHC\mathbf{H}(CH_2)_2$), 3.34 (dd, 1H, J = 8.2 Hz, 5.6 Hz, $C\mathbf{H}CH_2$); ^{13}C NMR

(50 MHz, D_2O): δ 14.3, 29.8, 29.9, 41.7, 52.0, 59.3, 179.8, 182.1; HRMS: m/z calc. for $C_8H_{14}NO_4$, 188.0923 $[M+H]^+$; found: 188.0918.

N-cyclobutyl-D-aspartic acid (D-3g)

Yield 5%. White solid. ^{1}H NMR (200 MHz, D_2O): δ 1.49-1.84 (m, 4H, **CH$_2$**CH$_2$C**H$_2$**), 2.07-2.17 (m, 2H, CH$_2$C**H$_2$**CH$_2$), 2.26 (dd, 1H, *J* = 15.1 Hz, 8.3 Hz, CHC**H**$_2$), 2.45 (dd, 1H, *J* = 15.1 Hz, 5.6 Hz, CHC**H**$_2$), 3.19 (m, 1H, NHC**H**(CH$_2$)$_2$), 3.34 (dd, 1H, *J* = 8.2 Hz, 5.6 Hz, C**H**CH$_2$); ^{13}C NMR (50 MHz, D_2O): δ 14.3, 29.8, 29.9, 41.7, 52.0, 59.3, 179.8, 182.1; HRMS: m/z calc. for $C_8H_{14}NO_4$, 188.0923 $[M+H]^+$; found: 188.0918.

N-(cyclopropyl)methyl-L-aspartic acid (L-3h)

Yield 5%. White solid. ^{1}H NMR (200 MHz, D_2O): δ 0.03-0.14 (m, 2H, CH$_2$C**H$_2$**), 0.33-0.53 (m, 2H, C**H$_2$**CH$_2$) 0.78-0.99 (m, 1H, CH$_2$C**H**(CH$_2$)$_2$), 2.19-2.52 (m, 4H, CHC**H$_2$**, NHC**H$_2$**), 3.40 (dd, 1H, *J* = 8.4 Hz, 5.5 Hz, C**H**CH$_2$); ^{13}C NMR (50 MHz, D_2O): δ 0.0, 0.6, 7.5, 39.2, 49.9, 58.7, 177.4, 179.3; HRMS: m/z calc. for $C_8H_{14}NO_4$, 188.0923 $[M+H]^+$; found: 188.0920.

N-(cyclopropyl)methyl-D-aspartic acid (D-3h)

Yield 5%. White solid. ^{1}H NMR (200 MHz, D_2O): δ 0.04-0.18 (m, 2H, CH$_2$C**H$_2$**), 0.36-0.48 (m, 2H, C**H$_2$**CH$_2$) 0.78-1.00 (m, 1H, CH$_2$C**H**(CH$_2$)$_2$), 2.20-2.53 (m, 4H, CHC**H$_2$**, NHC**H$_2$**), 3.41 (dd, 1H, *J* = 8.4 Hz, 5.5 Hz, C**H**CH$_2$); ^{13}C NMR (50 MHz, D_2O): δ 0.0, 0.6, 7.5, 39.2, 49.9, 58.7, 177.4, 179.3; HRMS: m/z calc. for $C_8H_{14}NO_4$, 188.0923 $[M+H]^+$; found: 188.0920.

Chiral HPLC analysis of the purified amino acid products

Chiral HPLC was performed using a Chirex 3126-D-penicillamine column (250 mm x 4.6 mm, Phenomenex, USA) with 2 mM $CuSO_4$ solution:isopropanol (90:10, v/v) as eluent at 25°C at a flow rate of 0.9 mL min^{-1}. First, racemic mixtures of *N*-substituted aspartic acids were prepared by

mixing the D- and L-enantiomers in equimolar amounts. These mixtures were then separated by chiral HPLC. The peak assignments were carried out by chiral HPLC analysis of the pure enantiomers. Finally, samples of the enzymatically prepared amino acids were injected on the chiral stationary phase to determine their absolute configuration and enantiomeric excess.

Table S1. Retention times of racemic mixtures of *N*-substituted aspartic acids as determined by chiral HPLC analysis.

Entry	Product	L-enantiomer r. t.[1] (min)	D-enantiomer r. t.[1] (min)
A	**3a**	8.2	9.9
B	**3b**	15.1	12.2
C	**3c**	20.4	10.7
D	**3d**	35.5	17.9
E	**3e**	82.6	42.5
F	**3f**	253.0	133.5
G	**3g**	55.9	30.2
H	**3h**	24.6	15.6

[1]r.t., retention time.

SUPPLEMENTARY REFERENCES

1. Raj, H., Szymański, W., de Villiers, J., Rozeboom, H. J., Puthan Veetil, V., Reis, C. R., de Villiers, M., Dekker, F. J., de Wildeman, S., Quax, W. J., Thunnissen, A. M. W. H., Feringa, B. L., Janssen, D. B., and Poelarends G. J. (2012) Engineering methylaspartate ammonia lyase for the asymmetric synthesis of unnatural amino acids. *Nat. Chem. 4*, 478-484.

2. Ohfune, Y., Kurokawa, N., Higuchi, N., Saito, M., Hashimoto, M., and Tanaka, T. (1984) An efficient one-step reductive *N*-monoalkylation of α-amino acids. *Chem. Lett.*, 441-444.

Chapter 5

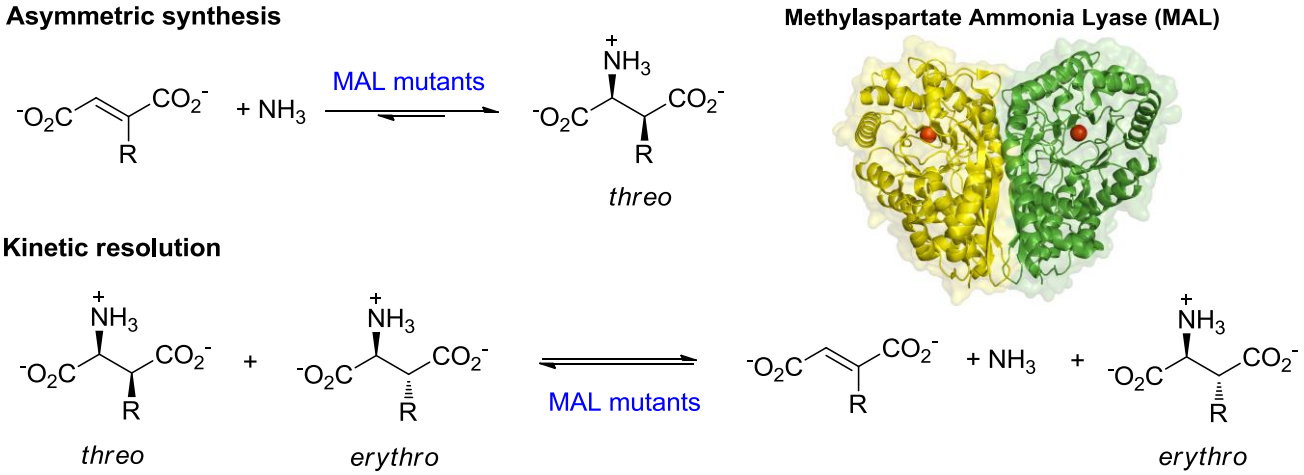

Kinetic resolutions and stereoselective synthesis of 3-substituted aspartic acids using engineered methylaspartate ammonia lyases

Hans Raj,[a] Wiktor Szymanski,[b] Jandré de Villiers,[a] Vinod Puthan Veetil,[a] Wim J. Quax,[a] Keiko Shimamoto,[c] Dick B. Janssen,[d] Ben L. Feringa,[b] and Gerrit J. Poelarends[a]

[a] *Department of Pharmaceutical Biology, Groningen Research Institute of Pharmacy, University of Groningen, Antonius Deusinglaan 1, 9713 AV Groningen, The Netherlands.*
[b] *Center for Systems Chemistry, Stratingh Institute for Chemistry, University of Groningen, Nijenborgh 4, 9747 AG Groningen, The Netherlands*
[c] *Suntory Foundation for Life Sciences, Wakayamadai, Shimamotocho, Mishima-gun, Osaka 618-8503, Japan.*
[d] *Department of Biochemistry, Groningen Biomolecular Sciences and Biotechnology Institute, University of Groningen, Nijenborgh 4, 9747 AG Groningen, The Netherlands.*

Published in *Chem. Eur. J.* (2013) 19, 11148-11152.

ABSTRACT

We describe kinetic resolutions and asymmetric synthesis of various valuable 3-substituted aspartic acids, which were obtained in fair to good yields with dr values of up to >98:2 and ee values of up to >99%, using engineered methylaspartate ammonia lyases. These biocatalytic methodologies for the selective preparation of aspartic acid derivatives appear to be attractive alternatives for existing chemical methods.

INTRODUCTION

Optically pure aspartic acid derivatives are highly valuable as tools for biological research and as chiral building blocks for pharmaceuticals, nutraceuticals, and peptidomimetics.[1, 2] The preparation of these amino acids remains a difficult and laborious task with conventional organic synthesis, and the use of a biocatalytic methodology can be an important and highly competitive alternative option.[3-7] In recent years, the enzyme 3-methylaspartate ammonia lyase (MAL) has gained a lot of interest because of its potential for application in the asymmetric synthesis of substituted aspartic acids.[7] MAL catalyzes the reversible addition of ammonia to mesaconate (**1a**) to give L-*threo*-(2*S*,3*S*)-3-methylaspartate (L-*threo*-**2a**) and L-*erythro*-(2*S*,3*R*)-3-methylaspartate (L-*erythro*-**2a**) as products (Scheme 1).[8] In addition to mesaconate, MAL also accepts fumarate as well as a few 2-substituted fumarates (ethyl-, ethoxy-, ethylthio-, propyl-, isopropyl- and halo-derivatives) in the ammonia addition reaction.[9-11] However, the enzyme has a narrow electrophile scope, and only displays amination activity towards fumarate derivatives with a small substituent at the C2 position. Interestingly, recent protein engineering work on MAL, which involved structure-guided saturation mutagenesis and activity screening, has resulted in the MAL variant L384A, which has a very broad electrophile scope in the ammonia addition reaction, including fumarate derivatives with large alkyl, aryl, alkoxy, aryloxy, alkylthio and arylthio substituents at the C2 position.[11] The synthetic potential of both wild-type MAL and the L384A mutant has been demonstrated by their use as biocatalyst in the asymmetric synthesis of various 3-substituted aspartic acids. Unfortunately, however, the MAL- and L384A-catalyzed amination of fumarate derivatives gives varying degrees of diastereoselectivity, with several amination reactions yielding an undesired mixture of *threo* and *erythro* isomers of the corresponding 3-substituted aspartic acids.[11] Obviously, this irregular pattern of diastereoselectivities limits the use of these enzymes in stereoselective amino acid synthesis.

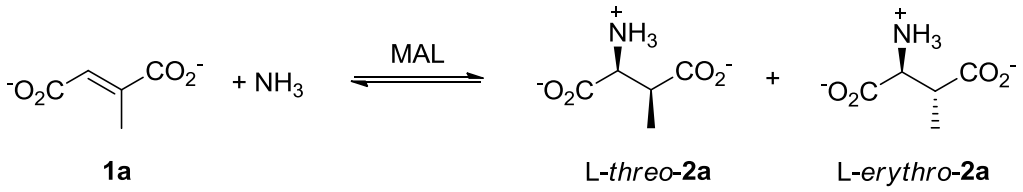

Scheme 1. MAL-catalyzed amination of mesaconate (**1a**) to yield L-*threo*-(2*S*,3*S*)-3-methylaspartate (L-*threo*-**2a**) and L-*erythro*-(2*S*,3*R*)-3-methylaspartate (L-*erythro*-**2a**).

In previous work, we have shown that an alanine substitution at position His-194 in MAL resulted in a mutant enzyme with strongly enhanced diastereoselectivity in the amination of mesaconate.[12] In the present study, we have exploited the high diastereo- and enantioselectivity of the H194A mutant in kinetic resolutions and asymmetric synthesis of various 3-substituted aspartic acids. In addition, we have combined the high stereoselectivity of the H194A mutant with the broad electrophile scope of the L384A mutant by generating the double mutant H194A/L384A, which has the unique ability to catalyze the diastereoselective amination of 2-butylfumarate to give exclusively *threo*-3-butylaspartic acid.

To demonstrate the synthetic usefulness of the H194A mutant, a preparative-scale reaction using 0.05 mol% biocatalyst, ammonia (5 M) and mesaconate (1.0 g, 7.7 mmol, 77 mM) was performed (Scheme 2). Under these optimized conditions, the reaction was complete within 30 min at 25°C, achieving a final conversion of >95% (Table 1, entry 1). The amino acid product was purified (90% isolated yield) and identified as the *threo* isomer of 3-methylaspartic acid (d.r. >98:2) by comparison of its ^{1}H NMR signals to those of authentic standards with known *threo* or *erythro* configuration. No other regio- or diastereoisomer was observed. The absolute configuration of the product was determined by high-performance liquid chromatography (HPLC) on a chiral stationary phase using authentic standards with known L-*threo* or D-*threo* configuration (Figure 1). This analysis revealed that the product has the L-*threo* configuration (Figure 1C) and is present as a single enantiomer (e.e. >99%). These results demonstrate the potential of the H194A mutant for

application in the diastereo- and enantioselective synthesis of L-*threo*-(2*S*,3*S*)-3-methylaspartic acid (L-*threo*-**2a**, Scheme 2).

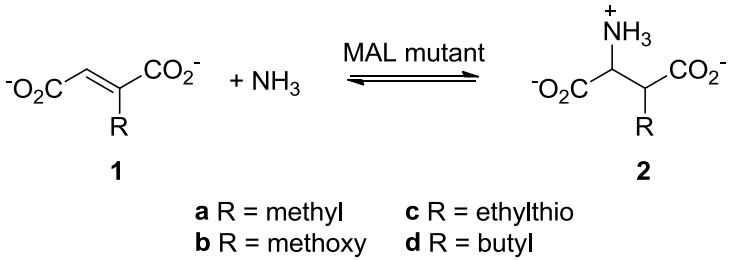

Scheme 2. H194A- or H194A/L384A-catalyzed amination of fumarate derivatives **1a-1d** to yield the 3-substituted aspartic acids **2a-2d**.

Table 1. Preparative-scale synthesis of 3-substituted aspartic acids using MAL wild-type or mutants as biocatalyst in ammonia additions to fumarate derivatives **1a-1d**.

Entry	Substrate	Enzyme	Product	Conv. (%)	Yield (%)[b]	d.r.[c]	*e.e.* (%)
1	**1a**	H194A	**2a**	>95 (0.5 h)[a]	90	>98:2[d]	>99[f]
2	**1a**	WT	**2a**	>95 (24 h)[a]	87	51:49[d]	>99[f,g]
3	**1b**	H194A	**2b**	82 (7 d)[a]	41	>98:2[d]	ND
4	**1c**	H194A	**2c**	80 (24 h)[a]	26	>98:2[d]	ND
5	**1c**	L384A	**2c**	85 (72 h)[a]	43	47:53[d]	ND
6	**1d**	H194A/L384A	**2d**	68 (24 h)[a]	40	>98:2[e]	ND

[a]Reaction time. [b]Yield of isolated product after cation exchange chromatography. [c]Diastereomeric ratio (*threo*-isomer:*erythro*-isomer). [d]The relative configuration of the isolated product was assigned by ^{1}H NMR spectroscopy using reference compounds with known *threo* or *erythro* configuration. [e]The purified product could be tentatively assigned the *threo* configuration on the basis of analogy. [f]The enantiomeric excess of the isolated product was determined by chiral HPLC using authentic standards with known absolute configuration. [g]Both the *threo* and *erythro* isomers have the L-configuration. ND, not determined.

Having established that the H194A mutant is highly diastereoselective, we have exploited this biocatalyst for the kinetic resolution of a mixture of L-*threo* and L-*erythro* isomers of 3-methylaspartic acid (L-*threo*-**2a** and L-*erythro*-**2a**, respectively, in Scheme 3). As these two diastereoisomers are not commercially available, they were first synthesized using wild-type MAL as catalyst (Scheme 1). The preparative-scale reaction mixture contained 0.05 mol% biocatalyst, ammonia (5 M) and mesaconate (1.0 g, 7.7 mmol, 77 mM). The reaction was stopped after 24 h, resulting in a final conversion of >95% (Table 1, entry 2). The two amino acid products were purified (87% isolated yield), giving an ~1:1 mixture of L-*threo*-**2a** and L-*erythro*-**2a** (Figure 1B). Subsequently, this mixture of diastereoisomers was incubated with the H194A mutant to achieve selective deamination of L-*threo*-**2a** (Scheme 3). After 2 h of incubation, ~15% of the starting amount of L-*threo*-**2a** was still present. To achieve better conversion of L-*threo*-**2a**, the amino acid mixture was purified (to remove ammonia and mesaconate) and then incubated again with the H194A enzyme. After 2 h, the reaction was stopped, resulting in a final conversion of the starting material of >45% (Table 2, entry 1). The remaining amino acid product was purified (44% isolated yield) and its identity verified by ^{1}H NMR spectroscopy and chiral HPLC (Figure 1D) as L-*erythro*-(2*S*,3*R*)-3-methylaspartic acid (d.r. = 95:5).

Next, the high enantioselectivity of the H194A mutant was exploited for the kinetic resolution of a racemic mixture of DL-*threo*-3-methylaspartic acid (165 mg, 1.12 mmol, 112 mM). With 0.05 mol% of biocatalyst, the reaction (Scheme 4) was complete within 60 min, achieving >45% conversion of the starting material (Table 2, entry 2). The remaining amino acid product was purified (44% isolated yield) and its identity verified by ^{1}H NMR spectroscopy and chiral HPLC as D-*threo*-(2*R*,3*R*)-3-methylaspartic acid (D-*threo*-**2a**, e.e. >99%). Taken together, the results demonstrate the usefulness of the H194A mutant for the preparation of various stereoisomers of the natural substrate 3-methylaspartic acid.

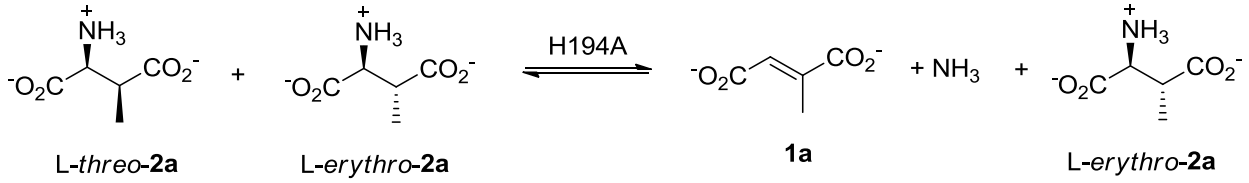

Scheme 3. Kinetic resolution of a mixture of L-*threo*-3-methylaspartate (L-*threo*-**2a**) and L-*erythro*-3-methylaspartate (L-*erythro*-**2a**) using the H194A mutant as biocatalyst.

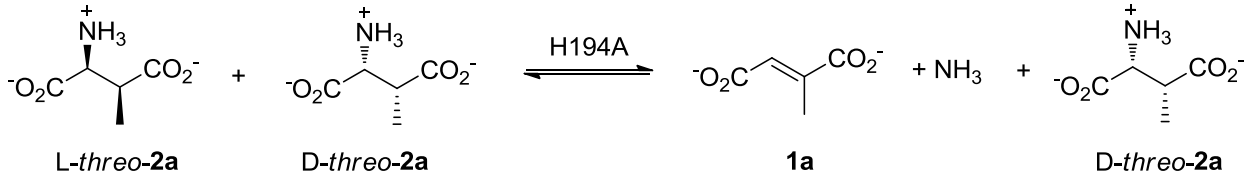

Scheme 4. Kinetic resolution of a racemic mixture of DL-*threo*-3-methylaspartate using the H194A mutant as biocatalyst.

Table 2. Kinetic resolutions of stereoisomeric mixtures of amino acids **2a** and **2c** using the MAL-H194A mutant as biocatalyst.

Entry	Substrate	Product	Conv. (%)	Yield (%)[b]	d.r.[c]	*e.e.* (%)
1	L-*threo*- and L-*erythro*-**2a**	L-*erythro*-**2a**	>45 (2 h)[a]	44	5:95[d]	>99[e]
2	L-*threo*- and D-*threo*-**2a**	D-*threo*-**2a**	>45 (1 h)[a]	44	>97:3[d]	>99[e]
3	*threo*- and *erythro*-**2c**	*erythro*-**2c**	>45 (3 h)[a]	40	5:95[d]	ND

[a]Reaction time. [b]Yield of isolated product after cation exchange chromatography. [c]Diastereomeric ratio (*threo*-isomer:*erythro*-isomer). [d]The relative configuration of the isolated product was assigned by ^{1}H NMR spectroscopy using reference compounds with known *threo* or *erythro* configuration. [e]The enantiomeric excess of the isolated product was determined by chiral HPLC using authentic standards with known absolute configuration. ND, not determined.

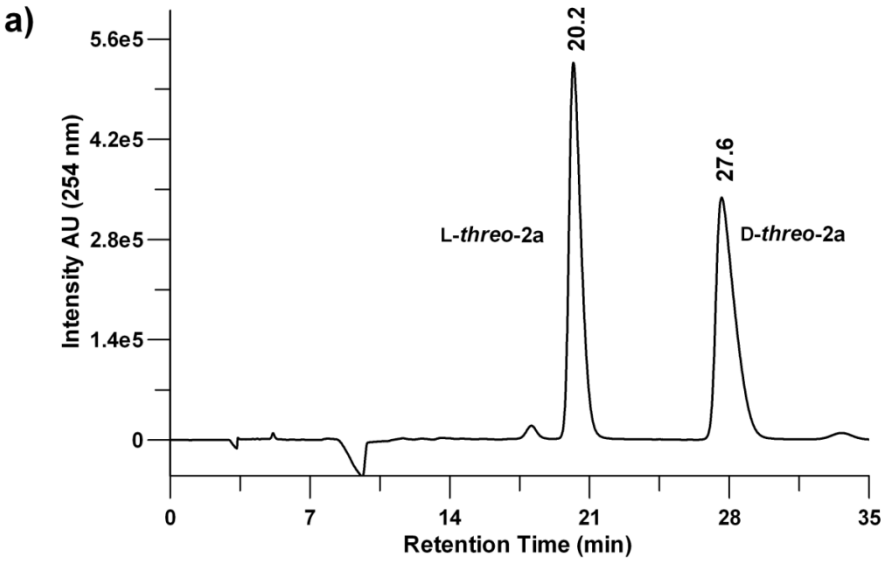
a)
5.6e5
4.2e5
2.8e5
1.4e5
0
Intensity AU (254 nm)
20.2
27.6
L-threo-2a
D-threo-2a
0
7
14
21
28
35
Retention Time (min)

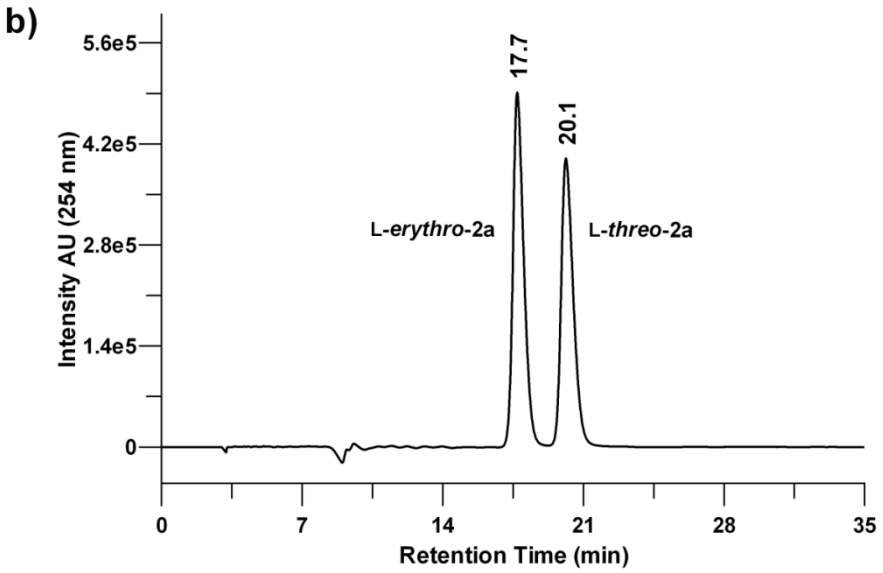
b)
5.6e5
4.2e5
2.8e5
1.4e5
0
Intensity AU (254 nm)
17.7
20.1
L-erythro-2a
L-threo-2a
0
7
14
21
28
35
Retention Time (min)

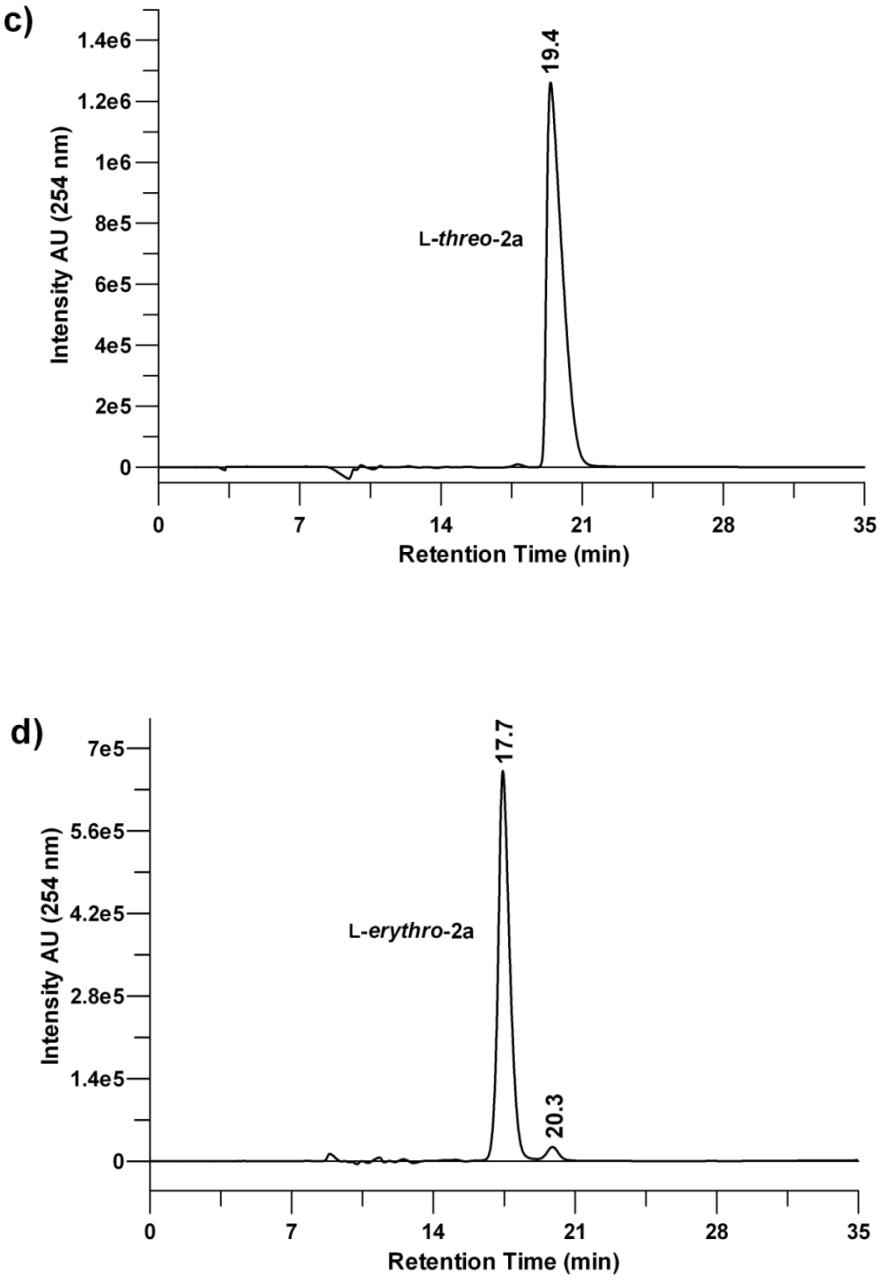

Figure 1. Separation of stereoisomers of 3-methylaspartic acid by HPLC on a chiral stationary phase. (a) Chromatogram of a commercially available racemic mixture of L-*threo*-3-methylaspartic acid (L-*threo*-**2a**) and D-*threo*-3-methylaspartic acid (D-*threo*-**2a**). (b) Chromatogram of a ~1:1 mixture of L-*threo*-3-methylaspartic acid (L-*threo*-**2a**) and L-*erythro*-3-methylaspartic acid (L-*erythro*-**2a**), which was prepared with wild-type MAL as biocatalyst. (c) Chromatogram of L-*threo*-3-methylaspartic acid (L-*threo*-**2a**), which was prepared with the H194A mutant as biocatalyst. (d) Chromatogram of L-*erythro*-3-methylaspartic acid (L-*erythro*-**2a**), which was prepared with the H194A mutant as biocatalyst.

To investigate the potential of the H194A mutant for the stereoselective synthesis of valuable unnatural amino acids, the amination of 2-methoxyfumarate (**1b** in Scheme 2) was selected as a model reaction for three reasons. First, substrate **1b** shows close structural resemblance to mesaconate (**1a**), the natural substrate of MAL. Second, the presumed product of the amination reaction is 3-methoxyaspartic acid (**2b** in Scheme 2), which is an important inhibitor of the excitatory amino-acid transporters EAAT1-5.[2a] Third, the selective chemical preparation of L-*threo*-3-methoxyaspartic acid, the **2b** isomer with the most potent inhibitory properties, is a highly challenging multiple-step synthesis procedure.[13] To test whether H194A is able to catalyze the selective amination of **1b**, a preparative-scale reaction using 0.05 mol% biocatalyst, ammonia (5 M) and 2-methoxyfumarate (100 mg, 0.685 mmol, 68.5 mM) was performed. The reaction was stopped after 7 d at 25°C, achieving a final conversion of 82% (Table 1, entry 3). The single amino acid product was purified (41% isolated yield) and identified as the desired *threo* isomer of 3-methoxyaspartic acid (d.r. >98:2) by comparison of the ^{1}H NMR signals (Figure 1A, Supplementary Information) to those of chemically synthesized L-*threo*-3-methoxyaspartic acid.[13] In contrast to the excellent diastereoselectivity of the H194A mutant, the wild-type MAL-catalyzed amination of **1b** (using the same preparative-scale reaction conditions) yielded an undesired mixture of *threo* and *erythro* isomers of **2b** (Figure 1B, Supplementary Information).

To further explore the electrophile scope of the H194A mutant, its ability to catalyze the amination of 2-ethylthiofumarate (**1c**) and 2-butylfumarate (**1d**) was tested (Scheme 2). Whereas **1c** is a known substrate for both wild-type MAL and the L384A mutant, the larger compound **1d** is only accepted as substrate by the L384A mutant.[11] Like wild-type MAL, the H194A mutant only shows activity with **1c**, indicating that its substrate scope is also limited to fumarate derivatives with a small substituent at the C2 position (**1a**-**1c** in Scheme 2). A preparative-scale reaction [using 0.05 mol% biocatalyst, 5 M ammonia and 57 mM **1c** (100 mg, 0.57 mmol)] was stopped after 24 h, yielding a final conversion of 80% (Table 1, entry 4). The single amino acid product was purified (26% isolated yield) and identified as the desired *threo* isomer of 3-(ethylthio)aspartic acid (d.r.

>98:2) by comparison of the ^{1}H NMR signals to those of chemically synthesized authentic standards with known *threo* or *erythro* configuration.[11] Thus, unlike wild-type MAL and the L384A mutant which both catalyze the amination of **1c** to yield an undesired mixture of diastereoisomers of **2c**, the H194A mutant has exciting potential for the diastereoselective synthesis of *threo*-**2c**.

Next, the high diastereoselectivity of the H194A mutant was exploited for the kinetic resolution of a mixture of *threo*- and *erythro*-**2c**. Because these two diastereoisomers are not commercially available, they were first synthesized using the L384A mutant as catalyst (0.05 mol%) in a preparative-scale reaction, using ammonia (5 M) and **1c** (100 mg, 0.57 mmol, 57 mM). The reaction was stopped after 72 h, resulting in a final conversion of 85% (Table 1, entry 5). The two amino acid products were purified (43% isolated yield), giving an ~1:1 mixture of *threo*-**2c** and *erythro*-**2c**. Subsequently, this mixture of diastereoisomers was incubated with the H194A mutant to achieve selective deamination of *threo*-**2c**. The reaction was complete in 3 h, resulting in >45% conversion of the starting material (Table 2, entry 3). The product was purified (40% isolated yield) and its identity verified by ^{1}H NMR spectroscopy as *erythro*-3-(ethylthio)aspartic acid (d.r. = 95:5).

The preceding results suggest that combining the high stereoselectivity of the H194A mutant with the broad electrophile scope of the L384A mutant could yield a new biocatalyst with the unique ability to catalyze the diastereoselective amination of 2-butylfumarate (**1d**, Scheme 2) and other fumarate derivatives with a large substituent at the C2 position. Accordingly, we have constructed the double mutant H194A/L384A and tested its synthetic usefulness in a preparative-scale reaction, using 0.05 mol% biocatalyst, ammonia (5 M) and 2-butylfumarate (125 mg, 0.87 mmol, 58.2 mM). The reaction was stopped after 24 h, resulting in 68% conversion (Table 1, entry 6). The amino acid product was purified (40% isolated yield), identified as a single diastereoisomer (d.r. >98:2) of 3-butylaspartic acid by ^{1}H NMR spectroscopy (**2d**, Scheme 2), and could be tentatively assigned the *threo* configuration on the basis of analogy.[11] Whereas the L384A-

catalyzed amination of **1d** yields an undesired mixture of diastereoisomers of **2d**,[11] the H194A/L384A mutant has striking potential for application in the diastereoselective synthesis of *threo*-3-butylaspartic acid.

We have also tested 2-phenylthio- and 2-benzylthiofumarate, which are both aminated by the L384A mutant with poor diastereoselectivity,[11] as potential substrates for the H194A/L384A mutant. Unfortunately, the double mutant showed very low-level amination activity with these fumarate derivatives, preventing the enzymatic synthesis of the corresponding amino acids. We have therefore initiated studies to enhance the catalytic activity of the H194A/L384A mutant by directed evolution. If these studies are successful, they may lead to a new biocatalytic methodology that provides simple and environmentally friendly access to a broad range of 3-substituted aspartic acids with a very high diastereomeric excess.

In summary, we have demonstrated the potential of the H194A and H194A/L384A mutants for application in stereo- and regioselective amination reactions as well as kinetic resolutions of stereoisomeric mixtures to prepare a variety of 3-substituted aspartic acids with a very high diastereo- and enantiomeric excess. These attractive biocatalytic methodologies for the selective preparation of 3-substituted aspartic acids appear to be simple, environmentally friendly alternatives for existing chemical methods. This is best illustrated by the H194A-catalyzed synthesis of *threo*-3-methoxyaspartic acid, an important inhibitor of excitatory amino acid transporters (EAAT1-5) in the brain.[2a, 13]

ACKNOWLEDGEMENTS

We thank Dr. Marianne de Villiers (Department of Pharmaceutical Biology, University of Groningen, The Netherlands) for her insightful discussions and critical reading of the manuscript. We thank Pieter van der Meulen (Molecular Dynamics group, University of Groningen) for his assistance in acquiring the NMR spectra. This research was financially supported by VENI grant 700.54.401 and ECHO grant 700.59.042 (both to G.J.P.) from the Division of Chemical Sciences of

the Netherlands Organisation of Scientific Research (NWO-CW), and by the Netherlands Ministry of Economic Affairs and the B-Basic partner organizations (www.b-basic.nl) through B-Basic, a public-private NWO-ACTS programme. Financial support from NRSC-C Catalysis (B.L.F., W.S.) is also gratefully acknowledged.

REFERENCES

1. a) M. Kahn, *Synlett*. **1993**, *11*, 821-826; b) M. Hamada, T. Takeuchi, S. Kondo, Y. Ikeda, H. Naganawa, *J. Antibiot.(Tokyo)* **1970**, *23*, 170-171; c) K. Burger, J. Spengler, *Eur. J. Org. Chem.* **2000**, *31*, 199-204; d) C. Nofre, J. -M. Tinti, *United States Patent* **1996**, number: 5,480,668.
2. a) K. Shimamoto, *Chem. Rec.* **2008**, *8*, 182-199; b) K. Shimamoto, R. Sakai, K. Takaoka, N. Yumoto, T. Nakajima, S. G. Amara, Y. Shigeri, *Mol. Pharmacol*. **2004**, *65*, 1008-1015; c) T. L. Mavencamp, J. F. Rhoderick, R. J. Bridges, C. S. Esslinger, *Bioorg. Med. Chem.* **2008**, *16*, 7740-7748; d) C. S. Esslinger *et al.*, *Neuropharmacology* **2005**, *49*, 850-861; e) R. J. Bridges, C. S. Esslinger, *Pharmacol. Ther.* **2005**, *107*, 271-285.
3. T. Sonke, B. Kaptein, H. E. Schoemaker in *Amino Acids, Peptides and Proteins in Organic Chemistry, Vol. 1*, (Ed. A. B. Hughes), Wiley-VCH, **2009**, 77-117.
4. a) H. E. Schoemaker, D. Mink, M. G. Wubbolts, *Science* **2003**, *299*, 1694-1697; b) R. Wohlgemuth, *Curr. Opin. Biotechnol*. **2010**, *21*, 713-724; c) S. Panke, M. Held, M. Wubbolts, *Curr. Opin. Biotechnol.* **2004**, *15*, 272-279; d) S. Panke, M. Wubbolts, *Curr. Opin. Chem. Biol.* **2005**, *9*, 188-194.
5. a) M. H. Heberling, B. Wu, S. Bartsch, D. B. Janssen, *Curr. Opin. Chem. Biol.* **2013**, http://dx.doi.org/10.1016/j.cbpa.2013.02.013; b) U. T. Bornscheuer, G. W. Huisman, R. J. Kazlauskas, S. Lutz, J. C. Moore, K. Robins, *Nature* **2012**, *485*, 185-194; c) J. A. Gerlt, P. C. Babbitt, M. P. Jacobson, S. C. Almo, *J. Biol. Chem.* **2012**, *287*, 29-34; d) M. H. Meyer, E.

Eichhorn, S. Hanlon, S. Lütz, M. Schürmann, R. Wohlgemuth, R. Coppolecchia. *Catal. Sci. Technol.* **2013**, *3*, 29–40; e) K. Faber, W. Kroutil, *Curr. Opin. Chem. Biol.* **2005**, *9*, 181-187.

6. a) N. J. Turner, *Nat. Chem. Biol*. **2009**, *5*, 567-573; b) N. J. Turner, *Curr. Opin. Chem. Biol.* **2011**, *15*, 234-240.
7. M. de Villiers, V. Puthan Veetil, H. Raj, J. de Villiers, G. J. Poelarends, *ACS Chem. Biol.* **2012**, *7*, 1618-1628.
8. a) H. A. Baker, R. D. Smyth, R. M. Wilson, H. Weissbach, *J. Biol. Chem.* **1959**, *234*, 320-328; b) H. J. Bright, L. L. Ingraham, R. E. Lundin, *Biochim. Biophys. Acta.* **1964**, *81*, 576-584; c) S. K. Goda, N. P. Minton, N. P. Botting, D. Gani, *Biochemistry* **1992**, *31*, 10747-10756.
9. H. Raj, V. Puthan Veetil, W. Szymanski, F. J. Dekker, W. J. Quax, B. L. Feringa, D. B. Janssen, G. J. Poelarends, *Appl. Microbiol. Biotechnol*. **2012**, *94*, 385-397.
10. a) M. Akhtar, N. P. Botting, M. A. Cohen, D. Gani, *Tetrahedron* **1987**, *43*, 5899-5908; b) N. P. Botting, M. Akhtar, M. A. Cohen, D. Gani, *Biochemistry* **1988**, *27*, 2953-2955; c) M. S. Gulzar, M. Akhtar, D. Gani, *J. Chem. Soc. Perkin Trans.* **1997**, *1*, 649-656.
11. H. Raj, W. Szymanski, J. de Villiers, H. J. Rozeboom, V. Puthan Veetil, C. R. Reis, M. de Villiers, F. J. Dekker, S. de Wildeman, W. J. Quax, A. -M.W.H. Thunnissen, B. L. Feringa, D. B. Janssen, G. J. Poelarends, *Nat. Chem.* **2012**, *4*, 478-484.
12. H. Raj, B. Weiner, V. Puthan Veetil, C. R. Reis, W. J. Quax, D. B. Janssen, B. L. Feringa, G. J. Poelarends, *Chembiochem* **2009**, *10*, 2236-2245.
13. K. Shimamoto, Y. Shigeri, Y. Yasuda-Kamatani, B. Lebrun, N. Yumoto, T. Nakajima, *Bioorg. Med. Chem. Lett.* **2000**, *10*, 2407-2410.

Supplementary Information

Materials and general methods

Mesaconic acid (**1a**), DL-*threo*-3-methylaspartic acid (DL-*threo*-**2a**), and other chemicals were purchased from Sigma-Aldrich unless stated otherwise. The fumaric acid derivatives **1b-1d** and L-*threo*-3-methoxyaspartic acid (L-*threo*-**2b**) were prepared according to previously described experimental procedures.[1, 2] The sources for the biochemicals, buffers, solvents, components of Luria-Bertani (LB) media as well as the materials, enzymes, and reagents used in the molecular biology procedures are reported elsewhere.[3, 4] Oligonucleotides for DNA amplification were synthesized by Operon Biotechnologies (Cologne, Germany). *Escherichia coli* strain XL1-Blue (Stratagene, La Jolla, CA) was used for cloning and isolation of plasmids. *E. coli* strain TOP10 (Invitrogen) and the pBAD/*Myc*-His A expression vector (Invitrogen) were used for recombinant protein production. DNA sequencing was performed by Macrogen (Seoul, Korea). Protein was analyzed by polyacrylamide gel electrophoresis (PAGE) using sodium dodecyl sulfate (SDS) gels containing polyacrylamide (10%). The gels were stained with Coomassie brilliant blue. Protein concentrations were determined by the Waddell method.[5]

Construction, expression and purification of MAL wild-type and mutants

The construction of the H194A and L384A mutants has been reported elsewhere.[1, 3] The double mutant H194A/L384A was constructed by the overlap extension PCR method[6] using plasmid pBAD(MAL-His), which contains the wild-type MAL gene under the transcriptional control of the *araBAD* promoter, as the template and the primers that have previously been used for the construction of the individual mutants.[1, 3] The final PCR products were gel-purified, digested with *Nde*I and *Hin*dIII restriction enzymes, and cloned in frame with both the initiation ATG start codon and the sequence that codes for the polyhistidine region of the expression vector pBAD*N*/*Myc*-His A.[3] The mutant gene was completely sequenced (with overlapping reads) to verify that only the

intended mutations had been introduced. Wild-type MAL and the mutant enzymes were overproduced in *E. coli* TOP10 cells harboring the appropriate expression vector and purified to near homogeneity as described before.[3, 4]

Preparative-scale enzymatic synthesis of aspartic acid derivatives

The 3-substituted aspartic acids (**2a-2d**) were synthesized using wild-type MAL or MAL mutants as catalyst in the ammonia additions to unsaturated acids **1a-1d**. The general procedure is as follows. A solution of NH_4Cl (5 M), unsaturated acid (0.57-7.7 mmol, 57-77 mM), and $MgCl_2$ (20 mM) was prepared in water (10-100 mL), and the pH was adjusted to 9.0 by the addition of small aliquots of an aq. NaOH solution. The reactions were started by the addition of freshly purified enzyme (0.05 mol%), and the reaction mixtures were incubated at 25°C. The progress of each reaction was monitored by UV-Vis and ^{1}H NMR spectroscopy. The reactions were stopped (reaction times are given in the main text) by incubating the reaction mixture at 100°C for 10 min, and the enzyme was removed by filtration. The individual reaction mixtures were lyophilized, after which the amino acid product was purified using cation exchange chromatography (Dowex, 50W X8, 100-200 mesh size, Merck) by following a previously described protocol.[1, 4] The ninhydrin-positive fractions were collected and concentrated under reduced pressure, followed by lyophilization to give the purified amino acid product as diammonium salt.

L-*threo*-(2*S*,3*S*)-3-methylaspartic acid (L-*threo*-2a)

Product L-*threo*-**2a** was synthesized using the H194A mutant as catalyst in the ammonia addition to mesaconate (**1a**). Conversion >95%. Yield 90% (1.25 g). White solid. ^{1}H NMR (300 MHz, D_2O): δ 1.15 (d, 3H, ^3J = 7.5 Hz, CHC**H$_3$**), 2.97 (dq, 1H, ^3J = 3.3 Hz, ^3J = 7.6 Hz, C**H**CH_3), 4.01 (d, 1H, ^3J = 3.0 Hz, C**H**NH); ^{13}C NMR (75 MHz, D_2O): δ 11.7, 41.0, 56.5, 173.5, 181.3. HRMS (ESI+) m/z calc. for $C_5H_{10}NO_4$: 148.0610 $[M+H]^+$, found: 148.0604. HPLC (Chirex 3126-D-penicillamine, 2mM aq. $CuSO_4$:*iso*-propanol; 90:10, flow rate 0.9 ml/min): R_t = 19.4 min.

threo-3-methoxyaspartic acid (*threo*-2b)

Product *threo*-**2b** was synthesized using the H194A mutant as catalyst in the ammonia addition to 2-methoxyfumarate (**1b**). Conversion 82%. Yield 41% (55 mg). White solid. ^{1}H NMR (500 MHz, D_2O): δ 3.38 (s, 3H, OC**H$_3$**), 4.00 (d, 1H, ^{3}J = 2.4 Hz, C**H**NH_2), 4.18 (d, 1H, ^{3}J = 2.4 Hz, C**H**OCH_3); ^{13}C NMR (75 MHz, D_2O): δ 56.4, 58.3, 80.0, 171.8, 175.8. HRMS (ESI+) m/z calc. for $C_5H_{10}NO_5$: 164.0599 $[M+H]^+$, found: 164.0553.

threo-3-(ethylthio)aspartic acid (*threo*-2c)

Product *threo*-**2c** was synthesized using the H194A mutant as catalyst in the ammonia addition to 2-ethylthiofumarate (**1c**). Conversion 80%. Yield 26% (35 mg). Yellow solid. ^{1}H NMR (500 MHz, D_2O): δ 1.24 (t, 3H, ^{3}J = 7.4 Hz, CH_2C**H$_3$**), 2.60-2.73 (m, 2H, S**H$_2$**CH_3), 3.92 (d, 1H, ^{3}J = 3.0 Hz, CH_2SC**H**), 4.18 (d, 1H, ^{3}J = 3.0 Hz, C**H**NH_2); ^{13}C NMR (125 MHz, D_2O): δ 13.8, 26.5, 48.3, 55.3, 171.7, 176.5. HRMS (ESI+) m/z calc. for $C_6H_{12}NO_4S$: 194.0487 $[M+H]^+$, found: 194.0481.

threo-3-butylaspartic acid (*threo*-2d)

Product *threo*-**2d** was synthesized using the H194A/L384A mutant as catalyst in the ammonia addition to 2-butylfumarate (**1d**). Conversion 68%. Yield 40% (78 mg). Pale brown solid. ^{1}H NMR (500 MHz, D_2O): δ 0.85 (t, 3H, ^{3}J = 6.7 Hz, CH_2C**H$_3$**), 1.25-1.37 (m, 5H, C**H**(C**H$_2$**)**$_2$**CH_3), 1.52-1.59 (m, 1H, CHC**H**$_2CH_2$), 2.80-2.83 (m, 1H, CHC**H**CH_2), 3.92 (d, 1H, ^{3}J = 3.1 Hz, C**H**NH_2); ^{13}C NMR (125 MHz, D_2O): δ 15.7, 24.3, 28.9, 31.9, 49.2, 58.5, 175.6, 183.2. HRMS (ESI+) m/z calc. for $C_8H_{16}NO_4$: 190.1079 $[M+H]^+$, found: 190.1073.

Kinetic resolutions of isomeric mixtures of aspartic acid derivatives

L-*erythro*-(2*S*,3*R*)-3-methylaspartic acid (L-*erythro*-2a)

Product L-*erythro*-**2a** was prepared using the H194A mutant in the kinetic resolution of a mixture of L-*threo*- and L-*erythro*-**2a**. First, a mixture of L-*threo*- and L-*erythro*-**2a** was synthesized using wild-type MAL as catalyst in the ammonia addition to mesaconate (**1a**). This was done according to the general preparative-scale enzymatic synthesis procedure described above, and yielded ~1.2 g (87% yield) of ~1:1 mixture of L-*threo*- and L-*erythro*-**2a**. This stereoisomeric mixture was dissolved in water (30 mL), containing 1 mM KCl and 20 mM $MgCl_2$ (final pH of 9.0). The reaction was started by the addition of freshly purified H194A enzyme (0.05 mol%), and the reaction mixture was incubated at 25°C. The progress of the reaction was monitored by UV-Vis and ^{1}H NMR spectroscopy. After 2 h, the reaction was stopped and the product of the reaction was purified using cation exchange chromatography (Dowex, 50W X8, 100-200 mesh size, Merck) by following a previously reported protocol.[1] ^{1}H NMR analysis revealed that the purified product consisted of about 15% L-*threo*-**2a** and 85% L-*erythro*-**2a**. To achieve better resolution, the product was incubated for a second time with the H194A enzyme. The reaction was stopped after 2 h (>45% conversion of the starting material), and the amino acid product was purified using the same cation-exchange protocol, giving an overall yield of 44% (530 mg). The final purified product was obtained as a white solid in the form of a diammonium salt, and contained <5% of L-*threo*-**2a**. The analytical data for L-*erythro*-**2a** are as follows. ^{1}H NMR (500 MHz, D_2O): δ 1.26 (d, 3H, ^3J = 7.5, CHC**H$_3$**), 2.84-2.95 (m, 1H, C**H**CH_3), 3.66 (d, 1H, ^3J = 5.3 Hz, C**H**NH); ^{13}C NMR (125 MHz, D_2O): δ 15.1, 41.5, 57.3, 173.8, 181.0. HRMS (ESI+) m/z calc. for $C_5H_{10}NO_4$: 148.0610 $[M+H]^+$, found: 148.0604. HPLC (Chirex 3126-D-pencillamine, 2 mM aq. $CuSO_4$:*iso*-propanol; 90:10, flow rate 0.9 ml/min): R_t = 17.7 min.

Erythro-3-(ethylthio)aspartic acid (*erythro*-2c)

Product *erythro*-**2c** was prepared using the H194A mutant in the kinetic resolution of a mixture of *threo*- and *erythro*-**2c**. First, a mixture of *threo*- and *erythro*-**2c** was synthesized using the L384A mutant as catalyst in the ammonia addition to 2-ethylthiofumarate (**1c**). This was done according to the general preparative-scale enzymatic synthesis procedure described above, and yielded 55 mg (43% yield) of ~1:1 mixture of *threo*- and *erythro*-**2c**. This stereoisomeric mixture was dissolved in water (10 mL), containing 1 mM KCl and 20 mM $MgCl_2$ (final pH of 9.0). The reaction was started by the addition of freshly purified H194A enzyme (0.05 mol%), and the reaction mixture was incubated at 25°C. The progress of the reaction was monitored by UV-Vis and ^{1}H NMR spectroscopy. After 3 h (>45% conversion of the starting material), the reaction was stopped and the product of the reaction was purified using cation exchange chromatography (40% yield, 20 mg). The final purified product was obtained as a yellow solid in the form of a diammonium salt, and contained only a trace amount of *threo*-**2c**. The analytical data for *erythro*-**2c** are as follows. ^{1}H NMR (500 MHz, D_2O): δ 1.23 (t, 3H, ^3J = 7.3 Hz, SCHC**H$_3$**), 2.54-2.64 (m, 2H, SC**H$_2$**CH_3), 3.29 (d, 1H, ^3J = 9.9 Hz, C**H**NH), 3.37 (d, 1H, ^3J = 9.9 Hz, C**H**NH); ^{13}C NMR (125 MHz, D_2O): δ 13.9, 25.6, 42.0, 54.0, 178.3, 184.5. HRMS (ESI+) m/z calc. for $C_6H_{12}NO_4S$: 194.0487 $[M+H]^+$, found: 194.0482.

D-*threo*-(2*R*,3*R*)-3-methylaspartic acid (D-*threo*-2a)

Product D-*threo*-**2a** was prepared using the H194A mutant in the kinetic resolution of a racemic mixture of L-*threo*- and D-*threo*-**2a**. The racemic mixture of DL-*threo*-**2a** (165 mg, 1.12 mmol) was dissolved in water (10 mL), containing $MgCl_2$ (20 mM) and KCl (1 mM). The pH of the solution was adjusted to 9.0 using aq. NaOH. The reaction was started by the addition of freshly purified H194A enzyme (0.05 mol%) and the reaction mixture was incubated at 25°C. After 1 h, the reaction was stopped by incubating at 100°C for 10 min and the product was purified using cation exchange chromatography. Conversion of the starting material >45%. Yield 44% (90 mg). The

product was obtained as a white solid in the form of a diammonium salt. ^{1}H NMR (500 MHz, D_2O): δ 1.14 (d, 3H, ^{3}J = 7.5 Hz, CHC**H$_3$**), 2.96 (dq, 1H, ^{3}J = 3.2 Hz, ^{3}J = 7.5 Hz, C**H**CH_3), 4.01 (d, 1H, ^{3}J = 3.1 Hz, C**H**NH); ^{13}C NMR (125 MHz, D_2O): δ 11.8, 41.4, 56.5, 173.8, 181.6. HRMS (ESI+) m/z calc. for $C_5H_{10}NO_4$: 148.0610 $[M+H]^+$, found: 148.0604. HPLC (Chirex 3126-D-penicillamine, 2mM aq. $CuSO_4$:*iso*-propanol; 90:10, flow rate 0.9 ml/min): R_t = 27.6 min.

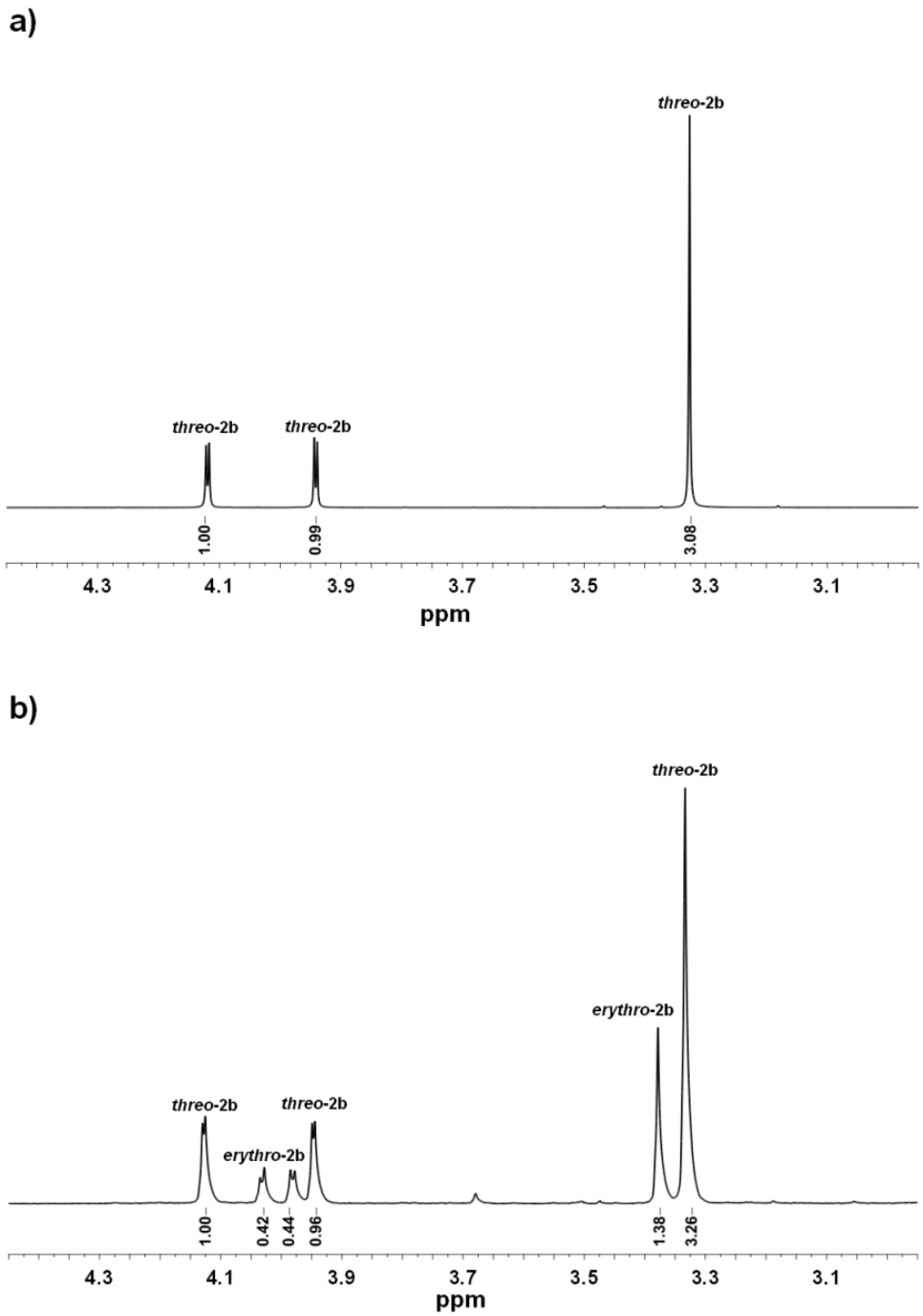

Supporting Figure 1. (**a**) ^{1}H NMR spectrum of purified *threo*-3-methoxyaspartic acid, which was prepared using H194A as biocatalyst. (**b**) ^{1}H NMR spectrum of purified 3-methoxyaspartic acid (a mixture of diastereosiomers), which was synthesized using wild-type MAL as biocatalyst.

SUPPLEMENTARY REFERENCES

1. H. Raj, W. Szymanski, J. de Villiers, H. J. Rozeboom, V. Puthan Veetil, C. R. Reis, M. de Villiers, F. J. Dekker, S. de Wildeman, W. J. Quax, A. -M. W. H. Thunnissen, B. L. Feringa, D. B. Janssen, G. J. Poelarends, *Nat. Chem.* **2012**, *4*, 478-484.
2. a) M. K. Sahoo, S. B. Mhaske, N. P. Argade, *Synthesis* **2003**, *3*, 346-349; b) A. F. Meindertsma, M. M. Pollard, B. L. Feringa, J. G. de Vries, A. J. Minnaard, *Tetrahedron: Asymmetry* **2007**, *18*, 2849-2858; c) E. Kianmehr, K. Tabatabai, A. Abbasi, H. S. Mehr, *Synth. Commun.* **2008**, *38*, 2529-2539; d) S. Jawaid, L. J. Farrugia, D. J. Robins, *Tetrahedron: Asymmetry* **2004**, *15*, 3979-3988; e) M.-J. Fan, G.-Q. Li, Y.-M. Liang, *Tetrahedron* **2006**, *62*, 6782-6791; f) K. Shimamoto, Y. Shigeri, Y. Yasuda-Kamatani, B. Lebrun, N. Yumoto, T. Nakajima, *Bioorg. Med. Chem. Lett.* **2000**, *10*, 2407-2410.
3. H. Raj, B. Weiner, V. Puthan Veetil, C. R. Reis, W. J. Quax, D. B. Janssen, B. L. Feringa, G. J. Poelarends, *Chembiochem* **2009**, *10*, 2236-2245.
4. H. Raj, V. Puthan Veetil, W. Szymanski, F. J. Dekker, W. J. Quax, B. L. Feringa, D. B. Janssen, G. J. Poelarends, *Appl. Microbiol. Biotechnol.* **2012**, *94*, 385-397.
5. W. J. Waddell, *J. Lab. Clin. Med.* **1956**, *48*, 311-314.
6. S. N. Ho, H. D. Hunt, R. M. Horton, J. K. Pullen, L. R. Pease, *Gene* **1989**, *77*, 51-59.

PART THREE

CATALYTIC MECHANISM AND CHARACTERIZATION OF A THERMOSTABLE METHYLASPARTATE AMMONIA LYASE

Chapter 6

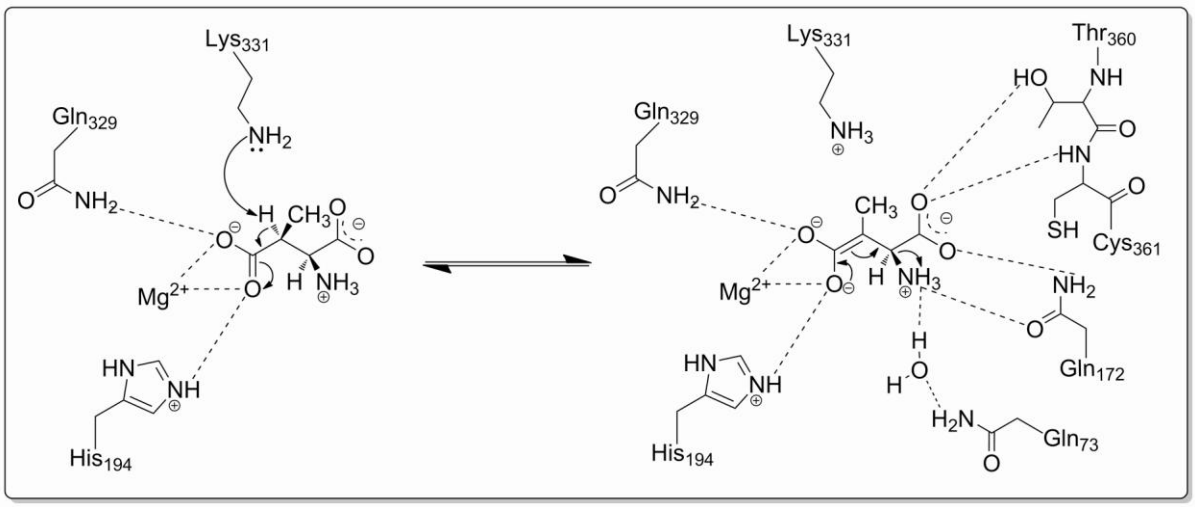

The roles of active site residues in the catalytic mechanism of methylaspartate ammonia lyase

Hans Raj and Gerrit J. Poelarends

Department of Pharmaceutical Biology, Groningen Research Institute of Pharmacy, University of Groningen, Antonius Deusinglaan 1, 9713 AV Groningen, The Netherlands.

Published in *FEBS Open Bio.* (2013) 3, 285-290.

ABSTRACT

Methylaspartate ammonia lyase (MAL) catalyzes the reversible addition of ammonia to mesaconate to yield L-*threo*-(2*S*,3*S*)-3-methylaspartate and L-*erythro*-(2*S*,3*R*)-3-methylaspartate as products. In the proposed minimal mechanism for MAL, Lys-331 acts as the (*S*)-specific base catalyst and abstracts the 3*S*-proton from L-*threo*-3-methylaspartate, resulting in an enolate anion intermediate. This enolic intermediate is stabilized by coordination to the essential active site Mg^{2+} ion and hydrogen bonding to the Gln-329 residue. Collapse of this intermediate results in the release of ammonia and the formation of mesaconate. His-194 likely acts as the (*R*)-specific base catalyst and abstracts the 3*R*-proton from the L-*erythro* isomer of 3-methylaspartate, yielding the enolic intermediate. In the present study, we have investigated the importance of the residues Gln-73, Phe-170, Gln-172, Tyr-356, Thr-360, Cys-361 and Leu-384 for the catalytic activity of MAL. These residues, which are part of the enzyme surface lining the substrate binding pocket, were subjected to site-directed mutagenesis and the mutant enzymes were characterized for their structural integrity, ability to catalyze the amination of mesaconate, and regio- and diastereoselectivity. Based on the observed properties of the mutant enzymes, combined with previous structural studies and protein engineering work, we propose a detailed catalytic mechanism for the MAL-catalyzed reaction, in which the side chains of Gln-73, Gln-172, Tyr-356, Thr-360, and Leu-384 provide favorable interactions with the substrate, which are important for substrate binding and activation. This detailed knowledge of the catalytic mechanism of MAL can serve as a guide for future protein engineering experiments.

INTRODUCTION

The enzyme methylaspartate ammonia lyase (MAL) catalyzes the reversible addition of ammonia to mesaconate (**1**) to yield L-*threo*-(2*S*,3*S*)-3-methylaspartate (**2**) and L-*erythro*-(2*S*,3*R*)-3-methylaspartate (**3**) as products (Scheme 1).[1, 2] MAL is used by the bacterium *Clostridium tetanomorphum* H1 as part of a catabolic pathway that converts L-glutamate, via **2**, to yield acetyl-CoA.[1-3] In recent years, MAL has gained a lot of interest because of its potential for application in the asymmetric synthesis of a wide variety of aspartic acid derivatives.[4-8] These non-proteinogenic amino acids are highly valuable as tools for biological research and as chiral building blocks for pharma- and nutraceuticals.[9-14]

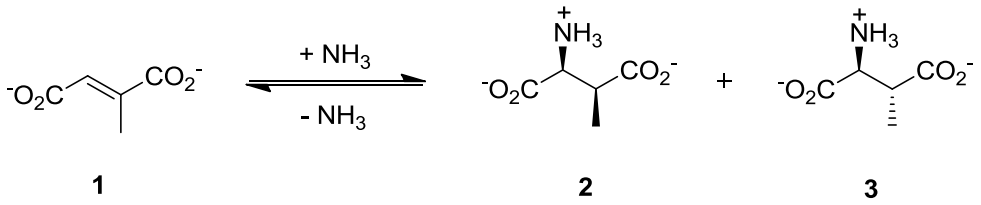

Scheme 1. MAL catalyzed reversible amination of mesaconate (**1**) to yield L-*threo*-(2*S*,3*S*)-3-methylaspartate (**2**) and L-*erythro*-(2*S*,3*R*)-3-methylaspartate (**3**).

The structure of MAL and that of the isozyme from *Citrobactor amalonaticus* have been solved by X-ray crystallography.[15, 16] On the basis of these structural studies,[15-17] combined with kinetic isotope measurements[18, 19] and mutagenesis experiments,[20] a minimal mechanism has emerged for the MAL-catalyzed reaction. In this proposed mechanism, an (*S*)-specific (Lys-331) or (*R*)-specific (His-194) catalytic base abstracts the C3 proton of the respective stereoisomer of 3-methylaspartate to generate an enolate anion intermediate that is stabilized by a hydrogen bond interaction with Gln-329 and coordination to the essential active site Mg^{2+} ion.[20] Collapse of the enolic intermediate results in the elimination of ammonia and yields **1**. This mechanism, however, is far from complete and the importance of other residues for the catalytic activity of MAL has not been investigated yet.

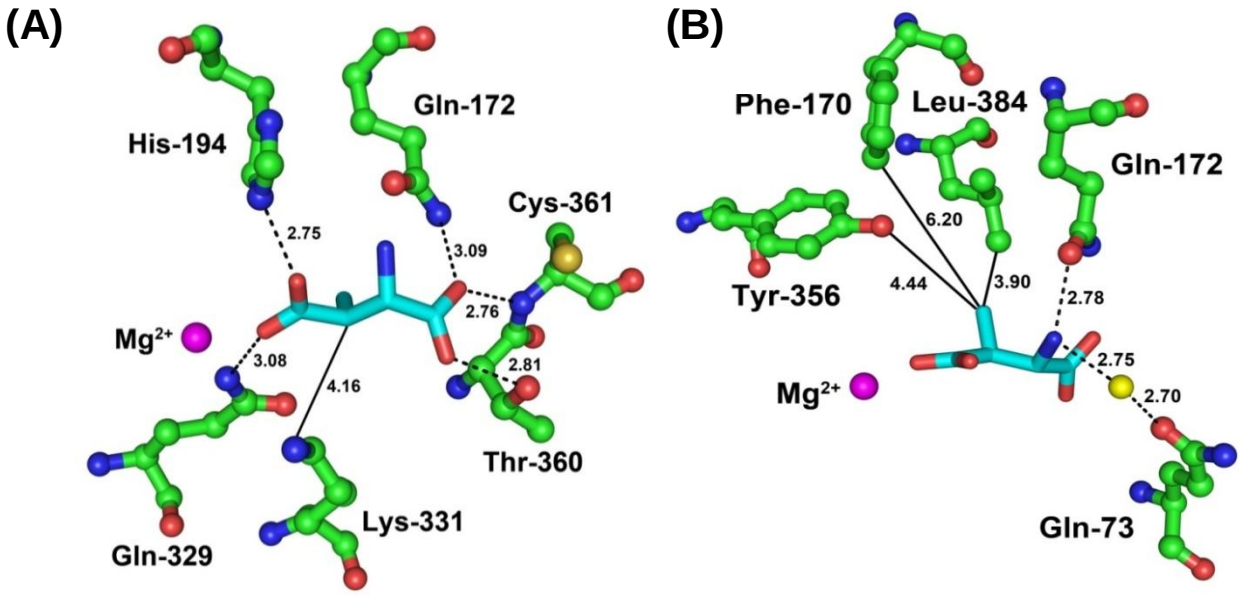

Figure 1. Crystal structure of MAL in complex with the natural substrate L-*threo*-(2*S*,3*S*)-3-methylaspartate.[16] (**a**) Close-up of the active site showing the hydrogen-bond interactions between the substrate's carboxylate groups (C1 and C4) and the side chains of His-194, Gln-329, Gln-172 and Thr-360, or the main chain NH of Cys-361. The carbon atoms of the active site residues are shown in green, and those of the substrate in cyan. Hydrogen bonds are represented as dashed lines. The distance (in Ångstroms) between the C3 atom of the substrate and side chain of Lys-331 is shown (atoms connected by a solid line). The magnesium ion is shown as a magenta sphere. (**b**) Close-up of the active site showing the hydrogen-bond interactions between the substrate's amino group and the side chains of Gln-73 (via a water molecule) and Gln-172, as well as the observed distances (in Ångstroms, atoms connected by solid lines) between the substrate's methyl group and the side chains of Leu-384, Phe-170 and Tyr-356. The magnesium ion and water molecule are shown as magenta and yellow spheres, respectively. Colour scheme as in (**a**). The figures were prepared with Pymol (http://www.pymol.org).[30]

The crystal structure of MAL complexed with its natural substrate **2** shows that the surface of the enzyme lining the substrate binding pocket is provided, in part, by residues Gln-73, Phe-170, Gln-172, Tyr-356, Thr-360, Cys-361 and Leu-384 (Figure 1).[16] In the present study, we performed site-directed mutagenesis experiments on all these residues to provide insight into their roles in the catalytic mechanism for the MAL-catalyzed reaction. The mutant enzymes were characterized for their structural integrity, ability to catalyze the amination of mesaconate, and regio- and diastereoselectivity. Based on the observed properties of the mutant enzymes, combined with previous structural studies and recent enzyme engineering work, we present a detailed catalytic

mechanism for the MAL-catalyzed reaction, with important roles for Gln-73, Gln-172, Tyr-356, Thr-360, and Leu-384 in substrate binding and activation.

RESULTS

Production, purification and characterization of the MAL mutants

The surface of the protein lining the substrate binding site is provided by the residues shown in Figure 1.[16] In a previous study, the roles of residues His-194, Gln-329 and Lys-331 in the catalytic mechanism of the MAL-catalyzed reaction have been investigated by site-directed mutagenesis.[20] The residues selected for mutagenesis in the present study were Gln-73, Phe-170, Gln-172, Tyr-356, Thr-360, Cys-361 and Leu-384 (Figure 1). Similar to wild-type MAL, all mutant proteins were constructed as His_6-tagged fusion proteins, produced in *E. coli* TOP10 cells, and purified to >95% homogeneity (as assessed by SDS-PAGE) using a one-step Ni-based immobilized metal affinity chromatography procedure.[20] This yielded about 20-30 mg of homogenous protein per liter of cell culture.

Each MAL mutant was analyzed by non-denaturing PAGE (data not shown). The mutant enzymes were found to migrate comparably with the wild-type enzyme, which suggests that the homodimeric association of the mutants was still intact. The structural integrity of each mutant was also assessed by circular dichroism (CD) spectroscopy. The CD spectra of the mutants were comparable to that of wild-type MAL, suggesting that the mutations did not result in any major conformational changes (data not shown).

Residues that interact with the substrate's 1-carboxylate group

The crystal structure of MAL in complex with **2** shows that the 1-carboxylate group of the substrate has hydrogen-bonding interactions with the main chain NH of Cys-361, the oxygen atom (Oγ) of Thr-360, and the nitrogen atom (Nε2) of Gln-172 (Figure 1a).[16] Residue Gln-172 also interacts, via hydrogen-bonding, with the 2-amino group of the substrate (Figure 1b).[16] To investigate the

importance of these residues for the catalytic activity and regio- and diastereoselectivity of MAL, six single site-directed mutants were constructed in which Thr-360 was replaced with either an alanine or a serine (T360A and T360S), Cys361 with either an alanine or a lysine (C361A and C361K), and Gln-172 with either an alanine or an asparagine (Q172A and Q172N). The amination activities of the mutants were assayed using **1** as the substrate.

The mutation of Thr-360 to an alanine has a large effect on the catalytic efficiency of MAL. For the T360A mutant, a ~100-fold decrease in k_{cat} and a ~22-fold increase in K_m was observed, which results in a ~2200-fold decrease in k_{cat}/K_m (Table 1). Hence, the major effect of this mutation is on the value of k_{cat}. The mutation of Thr-360 to another residue with an aliphatic hydroxyl group (serine), however, has a less drastic effect on the catalytic efficiency. For the T360S mutant, the k_{cat}/K_m is reduced only approximately 3.5-fold (Table 1).

Obviously, mutations at position 361 cannot eliminate the main chain NH interaction with the substrate. As might therefore be expected, the removal of the side chain at this position, by the substitution of Cys-361 with an alanine, has hardly any effect on the catalytic efficiency of MAL. For the C361A mutant, there is a ~2.2-fold decrease in k_{cat} and an approximately 4.2-fold increase in K_m. As a result, the k_{cat}/K_m is reduced only ~9-fold (Table 1). However, the introduction of a new side chain at position 361, by mutation of Cys-361 to a lysine, essentially abolished enzymatic activity (Table 1). Under the conditions of the kinetic assay, no activity could be detected for this mutant.

Table 1. Apparent kinetic parameters for the amination of mesaconate (**1**) catalyzed by wild-type or mutant MAL[a]

Enzyme	k_{cat} (s^{-1})	K_m for 1 (mM)	k_{cat}/K_m (M^{-1} s^{-1})
MAL[b]	61 ± 1	0.7 ± 0.02	8.7×10^4
T360A	0.6 ± 0.1	15 ± 2.5	40
T360S	35 ± 1	1.4 ± 0.3	2.5×10^4
C361A	27.5 ± 2.5	2.9 ± 0.5	9.5×10^3
C361K	ND	ND	<0.1
Q172A	> 20	> 60	3.4×10^2
Q172N	ND	ND	<0.1
Q73A	0.7 ± 0.1	0.2 ± 0.02	3.5×10^3
Q73N	ND	ND	<0.1
F170A	10 ± 1	0.9 ± 0.1	1.1×10^4
Y356A	> 0.7	> 60	12
L384A	>16	> 60	2.7×10^2

[a] The steady state kinetic parameters were determined in 500 mM Tris-HCl buffer (pH 9.0) containing 20 mM $MgCl_2$ and 400 mM NH_4Cl at 30ºC. Errors are standard deviations from each fit. ND, not determined. [b] These kinetic parameters were obtained from Raj et al.[20]

The mutation of Gln-172 to an alanine (i.e., removal of the functional side chain) has a large effect on the values of K_m and k_{cat}/K_m. For the Q172A mutant, a plot of various concentrations of **1** versus the initial rates measured at each concentration remained linear up to 60 mM. Hence, the Q172A mutant could not be saturated. Accordingly, only the k_{cat}/K_m was determined, and this parameter is reduced ~255-fold compared to that of wild-type MAL (Table 1). Because the increase

in K_m for the Q172A mutant is >85-fold, the k_{cat} must be >20 s^{-1}. Surprisingly, the mutation of Gln-172 to an asparagine, which has a side chain with a similar functional group, essentially abolished enzymatic activity (Table 1).

The amination of **1** catalyzed by wild-type MAL and the mutants was also monitored by ^{1}H NMR spectroscopy to identify the products of the reaction. This spectroscopic analysis showed that the ammonia additions to **1** catalyzed by the MAL mutants lead to the same amino acid product (i.e., 3-methylaspartate) as the corresponding wild-type MAL-catalyzed reaction. This demonstrates that the mutations at positions 172, 360 and 361 do not affect the regioselectivity of MAL. However, varying diastereomeric product ratios were observed. Consistent with the fact that MAL catalyzes the fast *anti*-addition and the much slower *syn*-addition of ammonia to **1**,[20] leading to the *threo* and *erythro* isomers of 3-methylaspartate, respectively, the ^{1}H NMR spectra recorded after 2 h predominantly showed the formation of **2**, whereas the signals corresponding to **3** mainly appeared in later spectra (Table 2). After 7 days of incubation, the Q172A, T360A, T360S, and C361A mutant-catalyzed amination reactions resulted in 74%, 82%, 85%, and 78% conversion of **1** into the amino acid product with a diastereomeric ratio (d.r.) of 89:11, 54:46, 51:49, and 53:47, respectively (Table 2). The reactions catalyzed by the Q172N and C361K mutants, which have low-level amination activities, resulted in ~70% conversion of **1** into 3-methylaspartate with a d.r. of >95:5 (Table 2).

Table 2. Conversions and diastereomeric product ratios for the ammonia additions to mesaconate catalyzed by wild-type and mutant MAL[a]

Enzyme	Con. (%) 2 h	d.r. (*threo:erythro*)[b] after 2 h	Con. (%) 7 d	d.r. (*threo:erythro*)[b] after 7 d
MAL	73	89:11	81	51:49
T360A	38	93:7	82	54:46
T360S	76	86:14	85	51:49
C361A	47	>95:5	78	53:47
C361K	10	>95:5	70	>95:5
Q172A	16	>95:5	74	89:11
Q172N	6	>95:5	68	>95:5
Q73A	37	91:9	71	69:31
Q73N	18	>95:5	74	>95:5
F170A	63	>95:5	83	55:45
Y356A	24	>95:5	74	80:20
L384A	61	>95:5	75	86:14

[a] Reactions were monitored by ^{1}H NMR spectroscopy. [b] The d.r. [defined as *threo*-3-methylaspartate (**2**):*erythro*-3-methylaspartate (**3**)] of the amino acid product was determined by comparison of its ^{1}H NMR signals in the crude reaction mixture to those of authentic standards of **2** and **3**.

Residues that interact with the substrate's 2-amino group

The crystal structure of MAL in complex with **2** shows that the 2-amino group of the substrate has hydrogen-bonding interactions with the oxygen atom (Oε1) of Gln-172 and, via a water molecule, with the nitrogen atom (Nε2) of Gln-73 (Fig. 1b).[16] The importance of Gln-172 for the catalytic

activity of MAL is described above. To investigate the importance of the Gln-73 residue for the catalytic activity and regio- and diastereoselectivity of MAL, this residue was mutated to either an alanine or an asparagine. These mutations are expected to completely remove the functional side chain (Q73A) or to replace the side chain with another one that has a similar functional group (Q73N). The replacement of Gln-73 with an alanine resulted in an active enzyme with a 87-fold reduction in k_{cat} and a 3.5-fold decrease in K_m, resulting in a ~25-fold lower k_{cat}/K_m compared to wild-type MAL (Table 1). Hence, the major effect of this mutation is on the value of k_{cat}. Surprisingly, the Q73N mutant showed very low-level amination activity, preventing the measurement of kinetic parameters (Table 1).

The ammonia additions to **1** catalyzed by the Q73A and Q73N mutants were also monitored by ^{1}H NMR spectroscopy to identify the amino acid products of these reactions. After a 7 days incubation period, the Q73A- and Q73N-catalyzed amination reactions resulted in 71% and 74% conversion of **1** into 3-methylaspartate with d.r. values of 69:31 and >95:5, respectively (Table 2). No other amino acid products were observed, indicating that the regioselectivity of the enzyme is not influenced by the mutations at position 73.

Residues lining the binding site for the substrate's 3-methyl group

The crystal structure of MAL in complex with **2** suggests that the side chains of Phe-170, Tyr-356 and Leu-384 are involved in the formation of the binding pocket for the 3-methyl group of the substrate (Figure 1b).[16] To study the importance of these residues for the catalytic activity and regio- and diastereoselectivity of MAL, each residue was replaced with an alanine. The mutation of Phe-170 to an alanine resulted in a mutant enzyme with a ~6-fold decrease in k_{cat} and a ~1.3-fold higher K_m, which results in an approximately 8-fold decrease in k_{cat}/K_m (Table 1). The substitutions of Tyr-356 and Leu-384 to an alanine, however, have a larger effect on the catalytic efficiencies of MAL (Table 1). For both the Y356A and L384A mutants, saturation by substrate **1** (up to 60 mM) could not be achieved and therefore only the k_{cat}/K_m was determined. A 7250- and 320-fold

reduction in k_{cat}/K_m was observed for the Y356A and L384A mutants, respectively. Hence, it is clear that the mutations at positions Tyr-356 and Leu-384 largely influence the K_m for **1** (Table 1).

The amination reactions catalyzed by the F170A, Y356A and L384A mutants were also followed by ^{1}H NMR spectroscopy. After an incubation period of 7 days, the F170A-, Y356A- and L384A-catalyzed reactions resulted in about 83%, 74% and 75% conversion of **1** into 3-methylaspartate with d.r. values of 55:45, 80:20 and 86:14, respectively (Table 2). No other amino acid products were observed, which indicates that the regioselectivity of the enzyme is also not influenced by the mutations at positions 170, 356 and 384.

DISCUSSION

On the basis of previous kinetic isotope measurements,[18, 19] structural studies,[15, 16] and mutagenesis experiments,[20] a minimal mechanism has emerged for the MAL-catalyzed reaction. In this proposed mechanism, Lys-331 acts as the (*S*)-specific base catalyst and abstracts the 3*S*-proton from L-*threo*-3-methylaspartate (**2**), resulting in an enolate anion intermediate (**4** in Scheme 2). This enolic intermediate is stabilized by coordination to the essential active site Mg^{2+} ion.[21] Residues His-194 and Gln-329 are thought to assist the Mg^{2+} ion in binding the substrate's 4-carboxylate group and stabilizing the enolate intermediate. Collapse of this intermediate results in the release of ammonia and the formation of mesaconate (**1**). In addition to its proposed role in binding the 4-carboxylate group of the substrate, His-194 is believed to also act as the (*R*)-specific base catalyst and abstracts the 3*R*-proton from the L-*erythro* isomer of 3-methylaspartate, yielding the enolic intermediate **4**. The strongest support for this catalytic role of His-194 comes from the observation that the H194A mutant of MAL is highly diastereoselective and can be used as biocatalyst in the synthesis of exclusively the *threo* isomers of various 3-substituted aspartic acids.[20, 22] In the present study, guided by the crystal structure of MAL complexed with the natural substrate **2**, we have selected seven other active site residues for site-directed mutagenesis to provide further insight into the catalytic mechanism of MAL. The obtained results allow us to present of a full catalytic

mechanism for the MAL-catalyzed reaction, detailed knowledge of which can serve as an important guide for future protein engineering experiments.

The crystal structure of MAL in complex with **2** shows that the 1-carboxylate group of the substrate has hydrogen-bond interactions with the main chain NH of Cys-361, Oγ of Thr-360, and Nε2 of Gln-172 (Figure 1a).[16] To examine the role of Gln-172 and Thr-360 in the mechanism of the MAL-catalyzed reaction, we have mutated these two residues. Complete removal of the functionality at position Thr-360 by replacement with an alanine leads to a ~2200-fold decrease in k_{cat}/K_m with a ~22-fold increase in the K_m for **1**. The same substitution at position Gln-172 also results in a reduced catalytic efficiency with a large increase (>85-fold) in the K_m for **1**. These observations, combined with the increase in activity and decrease in K_m observed with a serine mutation at position Thr-360, support a role for the side chains of Thr-360 and Gln-172 in assisting the main chain NH of Cys-361 to bind and position the substrate (**1**, **2** or **3**) through hydrogen-bond interactions with its 1-carboxylate group.

The crystal structure of MAL in complex with **2** shows that the 2-amino group of the substrate has hydrogen-bond interactions with Oε1 of Gln-172 and, via a water molecule, with Nε2 of Gln-73 (Figure 1b).[16] This suggests roles for the functional groups of these residues in binding the amino group of **2** (or **3**) in the deamination reaction or ammonia in the reverse addition to **1**. Examination of the kinetic properties of the amination reaction catalyzed by the Q73A mutant, which is the only mutation at this position that resulted in an enzyme with significant activity, shows that there is only a minor effect on the value of K_m for **1** (Table 1), suggesting that Gln-73 indeed does not play a role in binding this substrate. One potential explanation for the loss in activity (i.e., reduced k_{cat} value) of the Q73A mutant is that Gln-73 could bind and position ammonia in a favorable orientation for amination of **1**. Support for this view is provided by a recent study in which engineering of the amine binding pocket (i.e., saturation mutagenesis at positions Gln-73 and Gln-172), followed by screening of mutants for enhanced activity towards methylamine addition to **1**, also yielded mutant

Q73A.[23] Interestingly, the Q73A mutation moved the specificity of MAL away from ammonia and towards alkylamines. For example, a comparison of k_{cat}/K_m values shows that wild-type MAL is ~500-fold more efficient in ammonia addition to **1** than the Q73A mutant, whereas the Q73A mutant is at least 140-fold more efficient in the addition of methylamine to **1**. These observations clearly indicate that Gln-73 is one of the residues that influences the amine specificity of MAL, strongly supporting the proposed role for Gln-73 in binding the amino group of **2** (or **3**) in the deamination reaction or ammonia in the reverse addition to **1**.

The crystal structure of MAL complexed with **2** suggests that the enzyme surface lining the binding site for the 3-methyl group of the substrate is composed almost entirely of side chains, including those of Phe-170, Tyr-356 and Leu-384 (Figure 1b).[16] To assess their role in catalysis, we have mutated these residues to an alanine. Examination of the kinetic properties for the Y356A and L384A mutants shows that there is a significant reduction in catalytic efficiency and a large increase (>85-fold) in the K_m for **1**, suggesting that these residues play a major role in binding the methyl group of the substrate. By contrast to these observations, examination of the kinetic properties for the F170A mutant shows that there is only a small effect of replacing Phe-170 to an alanine on the values of K_m and k_{cat}/K_m, suggesting that Phe-170 is not directly involved in binding the methyl group of the substrate. Consistent with the observed distances between the substrate's methyl group and the side chains of Leu-384, Phe-170 and Tyr-356 (Figure 1b),[16] our results suggest that additional stabilization of the substrate in the active site is provided by favorable van der Waals packing interactions between the substrate's methyl group and the side chains of Tyr-356 and Leu-384, while the side chain of Phe-170 is likely too far away to provide a stabilizing interaction. Strong support for the interaction between Leu-384 and the methyl group of the substrate also comes from a recent protein engineering study, in which position Leu-384 was randomized, followed by screening of mutants for amination activity towards 2-hexylfumarate.[23] This approach yielded mutants L384G and L384A, and both mutations moved the specificity of MAL away from mesaconate and towards the unnatural substrate 2-hexylfumarate. Intriguingly, the

L384A mutant was shown to exhibit a broad substrate scope, including fumarate derivatives with alkyl, aryl, alkoxy, aryloxy, alkylthio and arylthio substituents at the C2 position. These observations indicate that Leu-384 is one of the residues that influences the substrate (i.e., fumarate) specificity of MAL, supporting a role for Leu-384 in assisting Tyr-356 to bind and position the substrate through van der Waals interactions with its methyl group.

Notably, all mutants described in this study retained the high regioselectivity of the wild-type enzyme, producing 3-methylaspartate as single amino acid product in the amination reaction. Hence, altering the regioselectivity of MAL probably requires the synergistic effects encountered by multiple simultaneous mutations. However, although all mutants exclusively produce 3-methylaspartate, varying diastereomeric ratios (i.e., mixtures of L-*threo* and L-*erythro* isomers of 3-methylasparate) were observed. Whereas the amination reactions catalyzed by most mutants provided a mixture of *threo* and *erythro* isomers, the amination reactions catalyzed by the C361K, Q172N, and Q73N mutants provided a single diastereoisomer having the *threo* configuration (Table 2). It is important to emphasize that the latter mutants have very low-level amination activities. Given that for wild-type MAL the rate of *anti*-addition is approximately 100-fold higher than the rate for *syn*-addition,[20, 24-26] and assuming that for these mutants both rates are equally reduced by the mutation, the amount of *syn*-addition product (i.e., the *erythro* isomer) formed in the reaction mixture might be too low to detect by ^{1}H NMR spectroscopy. Hence, these mutant enzymes do not necessarily have altered diastereoselectivities.

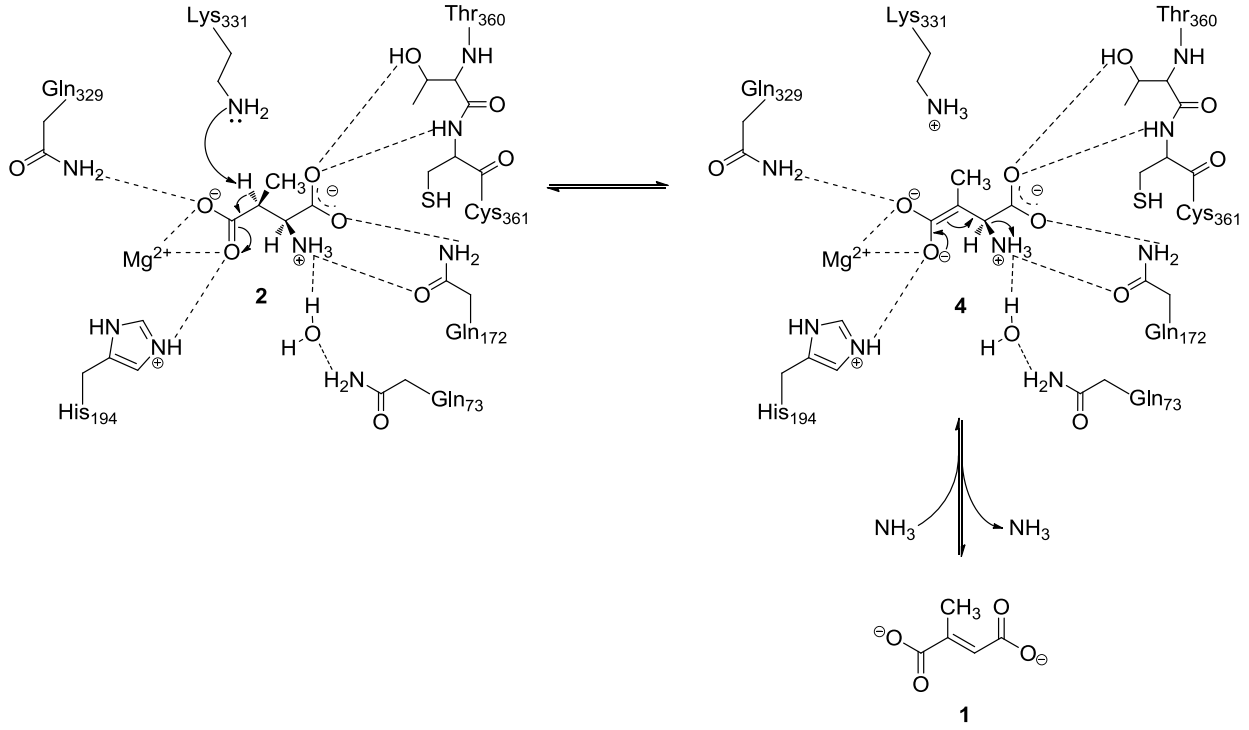

Scheme 2. A schematic representation of the proposed catalytic mechanism of the MAL-catalyzed reaction.

On the basis of the results described in this study, the previously proposed minimal mechanism for the MAL-catalyzed deamination reaction can now be extended (Scheme 2). As described above, residues Lys-331, His-194 and Gln-329 and the Mg^{2+} ion play important roles in formation and stabilization of the enolate anion intermediate **4**. In the next step, this enolic intermediate collapses and eliminates ammonia to form the mesaconate (**1**) product. Residues Gln-73 (via a water molecule) and Gln-172 could position and 'lock' the amino group in a favorable orientation for deamination, whereas Thr-360 and Cys-361, assisted by Gln-172, play important roles in binding the substrate's 1-carboxylate group. In addition, residues Tyr-356 and Leu-384 provide stabilizing interactions with the substrate's 3-methyl group. Together, these interactions are important for the optimal positioning and activation of the substrate, and are important determinants of the substrate specificity of MAL. This detailed understanding of the catalytic mechanism of MAL can serve as an important guide for future engineering experiments that aim to further expand the substrate scope of this fascinating enzyme.

MATERIALS AND METHODS

Materials

Mesaconic acid and other chemicals were purchased from Sigma-Aldrich Chemical Co. (St Louis, MO, USA), unless stated otherwise. The sources for the media components, buffers, solvents, pre-packed PD-10 Sephadex G-25 columns, and molecular biology reagents, including PCR purification, gel extraction, and Miniprep kits, are reported elsewhere.[20, 23, 26] Oligonucleotides for DNA amplification were synthesized by Operon Biotechnologies (Cologne, Germany).

Bacterial strains, plasmids and growth conditions

Escherichia coli strain XL1-Blue (Stratagene, La Jolla, CA) was used for cloning and isolation of plasmids. *E. coli* strain TOP10 (Invitrogen) was used in combination with the pBAD/*Myc*-His A vector (Invitrogen) for recombinant protein production. *E. coli* cells were grown in Luria-Bertani (LB) medium. When required, Difco agar (15 g/L), ampicillin (Ap, 100 μg/mL), and/or arabinose (0.004% w/v) were added to the medium.

General methods

Techniques for restriction enzyme digestions, ligation, transformation, and other standard molecular biology manipulations were based on methods described elsewhere[27] or as suggested by the manufacturer. PCR was carried out in a DNA thermal cycler (model GS-1) obtained from Biolegio (Nijmegen, The Netherlands). DNA sequencing was performed by Macrogen (Seoul, Korea). Protein was analyzed by polyacrylamide gel electrophoresis (PAGE) under either denaturing conditions using sodium dodecyl sulfate (SDS) or native conditions on gels containing polyacrylamide (10%). The gels were stained with Coomassie brilliant blue. Protein concentrations were determined by the Waddell method.[28] Kinetic data were obtained on a V-650 spectrophotometer from Jasco (IJsselstein, The Netherlands). The kinetic data were fitted by nonlinear regression data analysis by using the Grafit program (Erithacus, Software Ltd., Horley,

UK) obtained from Sigma Chemical Co. The CD spectra were recorded on a model 62A-DS spectropolarimeter from AVIV Biomedical Inc. (Lakewood, NJ, USA). ^{1}H NMR spectra were recorded on a Varian Inova 500 (500 MHz) spectrometer using a pulse sequence for selective presaturation of the water signal. Chemical shifts for protons are reported in parts per million scale (δ scale) downfield form tetramethylsilane and are referenced to protium (H_2O: δ = 4.80).

Construction, expression and purification of MAL mutants

The MAL mutants were generated by the overlap extension PCR method[29] using plasmid pBAD(MAL-His), which contains the wild-type MAL gene under the transcriptional control of the *araBAD* promoter,[20] as the template. The final PCR products were gel-purified, digested with *Nde*I and *Hin*dIII restriction enzymes, and ligated in frame with both the initiation ATG start codon and the sequence that codes for the polyhistidine region of the expression vector pBAD*N*/*Myc*-His A. All mutant genes were completely sequenced (with overlapping reads) to verify that only the intended mutation had been introduced. Wild-type MAL and the mutant enzymes were overproduced in *E. coli* TOP10 cells and purified to near homogeneity by following a previously described protocol.[20]

Circular dichroism spectroscopy

Circular dichroism (CD) spectra of the purified wild-type MAL and the purified mutants were measured in Tris-HCl buffer (5 mM, pH 8.0), containing $MgCl_2$ (2 mM) and KCl (0.1 mM), at a concentration of approximately 3.0 μM in a CD cell with an optical path length of 1.0 mm.

Kinetic assay

The amination of **1** catalyzed by wild-type or mutant MAL was monitored by following the depletion of **1** at 240 nm or 270 nm in 500 mM Tris-HCl buffer (pH 9.0), containing 20 mM $MgCl_2$

and 400 mM NH_4Cl, at 30°C as described previously.[20] The concentration of **1** used in the assay varied in the range 0.1 to 60 mM.

Product analysis by ^{1}H NMR spectroscopy

The amino acid products of the amination of **1** catalyzed by wild-type or mutant MAL were identified by ^{1}H NMR spectroscopy. Reaction mixtures consisted of 500 µL of a 1 M stock solution of NH_4Cl in water (pH 9.0, containing 20 mM $MgCl_2$), 100 µL of a 500 mM stock solution of **1** in water (pH 9.0, containing 20 mM $MgCl_2$), and 100 µL of D_2O. Reactions were started by the addition of 200 µg of freshly purified enzyme, and the reaction mixtures were incubated at 25°C. ^{1}H NMR spectra were recorded 2 h and 7 days after the addition of enzyme. Given that MAL catalyzes the fast *anti*-addition and much slower *syn*-addition of ammonia to **1**,[20, 24, 25] leading to *threo*-(2*S*,3*S*)-3-methylaspartate (**2**) and *erythro*-(2*S*,3*R*)-3-methylaspartate (**3**), respectively, we allowed the amination reactions to run for 7 days to detect the formation of low amounts of *erythro* product isomer, if present. Product amounts were estimated by integration of the signals corresponding to **2** and **3** (if present). The ^{1}H NMR signals for **1**, **2** and **3** have been reported previously.[20]

ACKNOWLEDGEMENTS

We gratefully acknowledge Gea K. Schuurman-Wolters (Department of Biochemistry, University of Groningen) for her assistance in acquiring the CD spectra. We thank Pieter van der Meulen (Molecular Dynamics group, University of Groningen) for his assistance in acquiring the NMR spectra. We thank Dr. Wiktor Szymanski (Center for Systems Chemistry, Stratingh Institute of Chemistry, University of Groningen), Dr. Jandre de Villiers (Department of Pharmaceutical Biology, University of Groningen) and Dr. Vinod Puthan Veetil (Department of Pharmaceutical Biology, University of Groningen) for their insightful discussions. This research was financially supported by a VENI (700.54.401) grant (to G.J.P.) from the Division of Chemical Sciences of the Netherlands Organisation of Scientific Research (NWO-CW).

REFERENCES

1. Barker HA, Smyth RD, Wilson RM & Weissbach H (1959) The purification and properties of β-methylaspartase. *J Biol Chem* **234**, 320-328.
2. Goda SK, Minton NP, Botting NP & Gani D (1992) Cloning, sequencing, and expression in *Escherichia coli* of the *Clostridium tetanomorphum* gene encoding β-methylaspartase and characterization of the recombinant protein. *Biochemistry* **31**, 10747-10756.
3. Kato Y & Asano Y (1997) 3-Methylaspartate ammonia-lyase as a marker enzyme of the mesaconate pathway for (*S*)-glutamate fermentation in Enterobacteriaceae. *Arch Microbiol* **168**, 457-463.
4. Akhtar M, Botting NP, Cohen MA & Gani D (1987) Enantiospecific synthesis of 3-substituted aspartic acids via enzymic amination of substituted fumaric acids. *Tetrahedron* **43**, 5899-5908.
5. Botting NP, Akhtar M, Cohen MA & Gani D (1988) Substrate specificity of the 3-methylaspartate ammonia-lyase reaction: observation of differential relative reaction rates for substrate-product pairs. *Biochemistry* **27**, 2953-2955.
6. Gulzar MS, Akhtar M & Gani D (1997) Preparation of *N*-substituted aspartic acids via enantiospecific conjugate addition of *N*-nucleophiles to fumaric acids using methylaspartase: synthetic utility and mechanistic implications. *J Chem Soc Perkin Trans* **I**, 649-656.
7. de Villiers M, Puthan Veetil V, Raj H, de Villiers J & Poelarends GJ (2012) Catalytic mechanisms and biocatalytic applications of aspartate and methylaspartate ammonia lyases. *ACS Chem Biol* **7**, 1618-1628.
8. Heberling MM, Wu B, Bartsch S & Janssen DB (2013) Priming ammonia lyases and aminomutases for industrial and therapeutic applications. *Curr Opin Chem Biol* **17**, 250-260.
9. Shimamoto K, Sakai R, Takaoka K, Yumoto N, Nakajima T, Amara SG & Shigeri Y (2004) Characterization of novel L-*threo*-β-benzyloxyaspartate derivatives, potent blockers of the glutamate transporters. *Mol Pharmacol* **65**, 1008-1015.

10. Shimamoto K (2008) Glutamate transporter blockers for elucidation of the function of excitatory neurotransmission systems. *Chem Rec* **8**, 182-199.
11. Mavencamp TL, Rhoderick JF, Bridges RJ & Esslinger CS (2008) Synthesis and preliminary pharmacological evaluation of novel derivatives of L-β-*threo*-benzylaspartate as inhibitors of the neuronal glutamate transporter EAAT3. *Bioorg Med Chem* **16**, 7740-7748.
12. Kahn M (1993) Peptide secondary structure mimetics: Recent advances and future challenges. *Synlett* **11**, 821-826.
13. Burger K & Spengler J (2000) A new approach to *N*-methylaspartic, *N*-methylglutamic, and *N*-methyl-α-aminoadipic acid derivatives. *Eur J Org Chem* **31**, 199-204.
14. Nofre C & Tinti J-M (1996) *N*-substituted derivatives of aspartame useful as sweetening agents. United States Patent No. 5480668.
15. Asuncion M, Blankenfeldt W, Barlow JN, Gani D & Naismith JH (2002) The structure of 3-methylaspartase from *Clostridium tetanomorphum* functions via the common enolase chemical step. *J Biol Chem* **277**, 8306-8311.
16. Levy CW, Buckley PA, Sedelnikova S, Kato Y, Asano Y, Rice DW & Baker PJ (2002) Insights into enzyme evolution revealed by the structure of methylaspartate ammonia lyase. *Structure* **10**, 105-113.
17. Babbitt PC, Hasson MS, Wedekind JE, Palmer DR, Barrett WC, Reed GH, Rayment I, Ringe D, Kenyon GL & Gerlt JA (1996) The enolase superfamily: a general strategy for enzyme-catalyzed abstraction of the α-protons of carboxylic acids. *Biochemistry* **35**, 16489-16501.
18. Bright HJ, Ingraham LL & Lundin RE (1964) The mechanism of the methylaspartate ammonia-lyase reaction: deuterium exchange. *Biochim Biophys Acta* **81**, 576-584.
19. Bright H (1964) The mechanism of the β-methylaspartase reaction. *J Biol Chem* **239**, 2307-2315.

20. Raj H, Weiner B, Puthan Veetil V, Reis CR, Quax WJ, Janssen DB, Feringa BL & Poelarends GJ (2009) Alteration of the diastereoselectivity of 3-methylaspartate ammonia lyase by using structure-based mutagenesis. *ChemBioChem* **10**, 2236-2245.

21. Bright HJ (1967) Divalent metal activation of β-methylaspartase. The importance of ionic radius. *Biochemistry* **6**, 1191-1203.

22. Raj H, Szymański W, de Villiers J, Puthan-Veetil V, Quax WJ, Shimamoto K, Janssen DB, Feringa BL & Poelarends GJ (2013) Kinetic resolutions and stereoselective synthesis of 3-substituted aspartic acids using engineered methylaspartate ammonia lyases. Manuscript submitted for publication.

23. Raj H, Szymański W, de Villiers J, Rozeboom HJ, Puthan Veetil V, Reis CR, de Villiers M, Dekker FJ, de Wildeman S, Quax WJ, Thunnissen A-MWH, Feringa BL, Janssen DB & Poelarends GJ (2012) Engineering methylaspartate ammonia lyase for the asymmetric synthesis of unnatural amino acids. *Nat Chem* **4**, 478-484.

24. Archer CH, Thomas NR & Gani D (1993) Syntheses of (2*S*,3*R*)-3-methylaspartic and (2*S*,3*R*)[3-^{2}H]-3-methylaspartic acids - slow substrates for a *syn*-elimination reaction catalyzed by methylaspartase. *Tetrahedron-Asymmetry* **4**, 1141-1152.

25. Archer CH & Gani D (1993) Kinetics and mechanism of *syn*-elimination of ammonia from (2*S*,3*R*)-3-methylaspartic acid by methylaspartase. *J Chem Soc Chem Comm* **2**, 140-142.

26. Raj H, Puthan Veetil V, Szymański W, Dekker FJ, Quax WJ, Feringa BL, Janssen DB & Poelarends GJ (2012) Characterization of a thermostable methylaspartate ammonia lyase from *Carboxydothermus hydrogenoformans*. *Appl Microbiol Biotechnol* **94**, 385-397.

27. Sambrook J, Fritsch EF & Maniatis T (1989) *Molecular Cloning: A Laboratory Manual*. 2nd ed., Cold Spring Harbor Laboratory Press, Cold Spring Harbor, NY.

28. Waddell WJ (1956) A simple ultraviolet spectrophotometric method for the determination of protein. *J Lab Clin Med* **48**, 311-314.

29. Ho SN, Hunt HD, Horton RM, Pullen JK & Pease LR (1989) Site-directed mutagenesis by overlap extension using the polymerase chain reaction. Gene **77**, 51-59.

30. DeLano WL (2002) *The PyMOL molecular graphics system*. DeLano Scientific, San Carlos, CA, USA (http://www.pymol.org).

Chapter 7

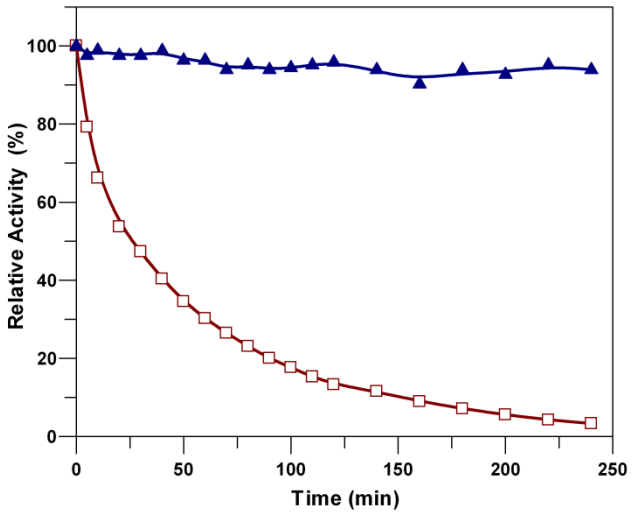

Characterization of a thermostable methylaspartate ammonia lyase from *Carboxydothermus hydrogenoformans*

Hans Raj,[a] Vinod Puthan Veetil,[a] Wiktor Szymanski,[b,c] Frank J. Dekker,[d] Wim J. Quax,[a] Ben L. Feringa,[b] Dick B. Janssen,[c] and Gerrit J. Poelarends[a]

Departments of [a]Pharmaceutical Biology and [d]Pharmaceutical Gene Modulation, Groningen Research Institute of Pharmacy, University of Groningen, Antonius Deusinglaan 1, 9713 AV Groningen, The Netherlands.

[b]Center for Systems Chemistry, Stratingh Institute for Chemistry, University of Groningen, Nijenborgh 4, 9747 AG Groningen, The Netherlands.

[c]Department of Biochemistry, Groningen Biomolecular Sciences and Biotechnology Institute, University of Groningen, Nijenborgh 4, 9747 AG Groningen, The Netherlands.

Published in *Appl. Microbiol. Biotechnol.* (2012) 94, 385-397.

ABSTRACT

Methylaspartate ammonia lyase (MAL; EC 4.3.1.2) catalyzes the reversible addition of ammonia to mesaconate to give (2*S*,3*S*)-3-methylaspartate and (2*S*,3*R*)-3-methylaspartate as products. MAL is of considerable biocatalytic interest because of its potential use for the asymmetric synthesis of substituted aspartic acids, which are important building blocks for synthetic enzymes, peptides, chemicals, and pharmaceuticals. Here, we have cloned the gene encoding MAL from the thermophilic bacterium *Carboxydothermus hydrogenoformans* Z-2901. The enzyme (named *Ch*-MAL) was overproduced in *Escherichia coli* and purified to homogeneity by immobilized metal affinity chromatography. *Ch*-MAL is a dimer in solution, consisting of two identical subunits (~49 kDa each), and requires Mg^{2+} and K^{+} ions for maximum activity. The optimum pH and temperature for the deamination of (2*S*,3*S*)-3-methylaspartic acid are 9.0 and 70°C (k_{cat} = 78 s^{-1} and K_m = 16 mM). Heat inactivation assays showed that *Ch*-MAL is stable at 50°C for >4 h, which is the highest thermal stability observed among known MALs. *Ch*-MAL accepts fumarate, mesaconate, ethylfumarate and propylfumarate as substrates in the ammonia addition reaction. The enzyme also processes methylamine, ethylamine, hydrazine, hydroxylamine and methoxylamine as nucleophiles that can replace ammonia in the addition to mesaconate, resulting in the corresponding *N*-substituted methylaspartic acids with excellent diastereomeric excess (>98% de). This newly identified thermostable MAL appears to be a potentially attractive biocatalyst for the stereoselective synthesis of aspartic acid derivatives on large (industrial) scale.

INTRODUCTION

Enantiomerically pure amino acids constitute a significant part of the chiral building blocks for a range of natural products, pharmaceuticals, and agrochemicals.[1-3] The synthesis of enantiomerically pure amino acids still remains a challenging task with traditional chemical catalysts.[4, 5] In some cases, the use of biocatalysts is an attractive alternative option.[6] Recently, the ammonia lyases and aminomutases (which exhibit ammonia lyase activity) have gained a lot of interest for the asymmetric synthesis of chiral α- and β-amino acids, with the advantage that they use readily available unsaturated acids as substrates.[7-12] However, most known ammonia lyases show low stability and therefore they are not compatible with the harsh reaction conditions that are usually required for industrial processes, such as high temperature, high pH and high ammonia concentrations needed to catalyze the reverse reactions.[7] Hence, there is a clear application for the discovery and characterization of novel ammonia lyases with increased stability.

3-Methylaspartate ammonia lyase (MAL; EC 4.3.1.2) catalyzes the reversible amination of mesaconate (**1**) to give (2*S*,3*S*)-3-methylaspartate (**2**) as a major product and (2*S*,3*R*)-3-methylaspartate (**3**) as a minor product (Scheme 1).[13, 14] MAL was discovered initially in *Clostridium tetanomorphum*, and subsequently also in several other anearobic bacteria, where the enzyme forms part of the glutamate catabolic pathway that converts (*S*)-glutamic acid via **2** to finally yield acetyl-CoA.[15] Recently, it has been shown that MAL also forms part of the methylaspartate cycle in haloarchaea, in which acetyl-CoA is oxidized to glyoxylate via methylaspartate. This is a novel pathway of carbon assimilation in addition to the already known glyoxylate cycle and ethylmalonyl-CoA pathway.[16]

Microbial genome and metagenome sequencing projects have revealed that there is a large diversity of protein sequences that based on sequence similarities to *C. tetanomorphum* MAL (*Ct*-MAL) might be classified as putative MALs. However, so far MALs have been isolated and characterized from only a few different organisms, including *C. tetanomorphum*, *Bacterium*

cadaveris, *Morganella morganii*, *Citrobactor amalonaticus*, *Escherichia coli* and *Fusobacterium varium*.[13, 15, 17-20] The best studied MALs are those from *C. tetanomorphum* and *C. amalonaticus*, for both of which the structures have been solved by X-ray crystallography.[21, 22] Based on these structural studies[21, 22] and recent mutagenesis experiments,[26] a mechanism has emerged for the MAL-catalyzed deamination reaction. In this proposed mechanism, a (*S*)- or (*R*)-specific catalytic base (Lys-331 and His-194, respectively; *Ct*-MAL numbering) abstracts the C-3 proton of the respective stereoisomer of 3-methylaspartate to generate an enolate anion intermediate that is stabilized by coordination to the essential active site Mg^{2+} ion. Collapse of this intermediate eliminates ammonia and yields the product, mesaconate.

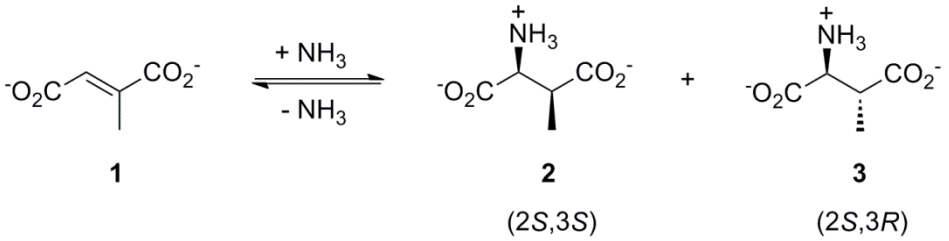

Scheme 1. MAL-catalyzed reversible amination of mesaconate to yield (2*S*,3*S*)- and (2*S*,3*R*)-3-methylaspartate.

Ct-MAL has been shown to accept a range of different nucleophiles (amines) and electrophiles (substituted fumarates). The broad substrate scope of *Ct*-MAL has been exploited for the stereoselective synthesis of various *N*-, *3*-, and *N,3*-(di)substituted aspartic acids.[23-25] A recent mutagenesis study on *Ct*-MAL has shown that the H194A, Q329A and K331A mutants display distinct diastereoselectivities and may be useful for the diastereoselective synthesis of (2*S*,3*S*)-3-methylaspartic acid.[26] Its broad substrate scope, high activity and stereoselectivity make *Ct*-MAL an attractive biocatalyst for organic synthesis. However, the enzyme is not stable upon long-term storage (at +4 or -80°C) and rapidly loses activity at elevated temperatures.[13] Hence, in order to

use the MAL reaction for biocatalytic applications, it is essential to identify putative MAL isozymes with increased stability.

In this study, we screened the microbial genomes available in the NCBI database for homologues of *Ct*-MAL with the aim to identify MALs from thermophilic microorganisms. Here, we report the identification of a MAL enzyme (designated *Ch*-MAL) from the thermophilic bacterium *Carboxydothermus hydrogenoformans* Z-2901, which was isolated from a hot spring in Russia and grows at very high temperatures,[27, 28] that shares significant sequence identity (53%) with *Ct*-MAL. The gene encoding *Ch*-MAL was cloned, and the corresponding enzyme overproduced, purified, and subjected to kinetic and biochemical characterization. *Ch*-MAL shows optimal activity at 70°C and pH 9.0, and is stable at 50°C for >4 h, which is the highest thermal stability observed among reported MALs. Like *Ct*-MAL, *Ch*-MAL has a broad substrate scope, accepting various substituted fumarates and amines, and exhibits high activity and diastereoselectivity. This makes *Ch*-MAL an attractive enzyme for biocatalytic applications, as well as a promising scaffold for engineering to yield highly stable and efficient enzymes for the asymmetric synthesis of new aspartic acid derivatives.

RESULTS

Identification of a thermostable MAL

A sequence similarity search in the NCBI microbial genome database was performed with the BLASTP program using the *Ct*-MAL amino acid sequence as the query. This search yielded several bacterial proteins that shared high sequence identity (>50%) with *Ct*-MAL. The top 20 hits included a sequence from the thermophilic bacterium *C. hydrogenoformans* Z-2901, which was isolated from a hot spring in Kunashir Island (Russia) and grows optimally at 78°C.[27, 28] This bacterial protein (designated *Ch*-MAL) is annotated as a putative methylaspartate ammonia lyase and was selected for further study.

The *Ch*-MAL protein is predicted to be 420 amino acids in length. Unlike the *Ct*-MAL gene, the gene encoding *Ch*-MAL is not located next to a gene encoding a putative glutamate mutase.[15] In fact, the genomic context of the gene encoding *Ch*-MAL does not provide any clues about the biological function of this protein in *C. hydrogenoformans* Z-2901. The sequence of *Ch*-MAL is 53% identical and 73% similar to that of *Ct*-MAL. A sequence alignment shows that nine of the ten active site residues of *Ct*-MAL are conserved in *Ch*-MAL[22] (Figure S1, Supporting Information). The non-conserved residue, Thr-360, is replaced by Ser-359 in *Ch*-MAL. As there are no significant active site differences between *Ch*-MAL and *Ct*-MAL, a catalytic mechanism, with important roles for Lys-331 and His-194 (*Ct*-MAL numbering) as the *S*- and *R*-specific base/acid catalysts, similar to that of *Ct*-MAL[26] may be expected for *Ch*-MAL. To obtain insight into the functional properties of this *Ct*-MAL homologue, *Ch*-MAL was overproduced, purified and subjected to kinetic and biochemical characterization (see below).

Expression and purification of *Ch*-MAL

The gene coding for *Ch*-MAL was amplified from genomic DNA of *C. hydrogenoformans* Z-2901 and cloned into the expression vector pBAD*N*/*Myc*-His A, resulting in the construct pBAD(*Ch*-MAL). The *Ch*-MAL encoding gene in pBAD(*Ch*-MAL) is under transcriptional control of the *araBAD* promoter and the recombinant enzyme was produced upon induction with arabinose in *E. coli* TOP10 as a C-terminal His_6-tag fusion protein. Optimal expression of the *Ch*-MAL gene was achieved when the TOP10 cells were cultivated at 22°C in an auto-induction medium[31] in the presence of 0.05% (w/v) arabinose. The recombinant enzyme was purified by a one-step Ni-sepharose affinity chromatography protocol, which typically provides ~200 mg of homogeneous enzyme per liter of culture. The purified *Ch*-MAL has a molecular mass of ~50 kDa when analyzed by SDS-PAGE. *Ch*-MAL was further analyzed by electrospray ionization mass spectrometry (ESI-MS) and gelfiltration chromatography. Analysis of *Ch*-MAL by ESI-MS showed, upon

deconvolution, one major peak that corresponds to a mass of 49291 (± 3) Da. A comparison of this value to the calculated mass (49288 Da) indicates that, in contrast to Cys-361 in *Ct*-MAL,[22] no oxidation of the active site cysteine (Cys-360) in *Ch*-MAL had occurred upon purification. Gel filtration chromatography resulted in elution of *Ch*-MAL as a single symmetrical peak, which corresponds to a native molecular mass of ~100 kDa. A comparison of this value to that of the subunit mass suggests that, like *Ct*-MAL (22), *Ch*-MAL is a homodimeric protein.

Ammonia lyase activity of *Ch*-MAL

To examine whether *Ch*-MAL exhibits ammonia lyase activity, the enzyme was incubated with **2** (in 500 mM Tris-HCl buffer, pH 9.0) and the reaction was monitored by a previously described spectroscopic assay.[26] The results show that *Ch*-MAL deaminates **2** to yield **1**, and maximum activity is achieved in the presence of both Mg^{2+} (≥20 mM) and K^{+} (≥1 mM) ions in the assay buffer. Having established that *Ch*-MAL exhibits methylaspartate ammonia lyase activity, kinetic parameters were measured (at 30°C) and compared to those previously measured for *Ct*-MAL (Table 1). *Ch*-MAL catalyzes the deamination of **2** with a catalytic efficiency (k_{cat}/K_m) of 3.5×10^3 M^{-1} s^{-1}, which is ~25-fold lower than the value measured for the same reaction catalyzed by *Ct*-MAL.

Optimum pH and temperature for the ammonia lyase activity of *Ch*-MAL

The optimum pH for the *Ch*-MAL–catalyzed deamination of **2** was determined at 30°C in Tris-HCl buffers (500 mM, containing 20 mM $MgCl_2$ and 1 mM KCl) with pH values ranging from 6.0-9.5. The *Ch*-MAL enzyme is active in the complete pH range tested and shows maximum activity at pH 9.0 (Figure 1a). A similar pH optimum was found for *Ct*-MAL (Figure 1a). The optimum temperature for the deamination of **2** by *Ch*-MAL was determined in Tris-HCl buffer (500 mM, pH 9.0, containing 20 mM $MgCl_2$ and 1 mM KCl) at different temperatures ranging from 10 to 90°C.

Ch-MAL was active at all temperatures analyzed, and showed the highest activity at 70°C (Figure 1b). For comparison, *Ct*-MAL was found to be active at temperatures ranging from 10 to 70°C with maximum activity at 50°C (Figure 1b). The observation that *Ch*-MAL shows maximum activity at 70°C, prompted us to measure kinetic parameters at this temperature. At 70°C, *Ch*-MAL catalyzes the deamination of **2** with a k_{cat} of 78 s^{-1} and a K_m of 16 mM, which results in a k_{cat}/K_m that is slightly higher (1.4-fold) than that measured at 30°C (Table 1). The observed 4.9-fold increase in k_{cat} confirms that *Ch*-MAL is more active at elevated temperatures. At 70°C, *Ct*-MAL is almost completely inactive (Figure 1b).

Table 1. Kinetic parameters for the *Ct*-MAL and *Ch*-MAL catalyzed deamination of (2*S*,3*S*)-3-methylaspartic acid (2)[a].

Enzyme	k_{cat} **(s^{-1})**	K_m **(mM)**	k_{cat}/K_m **($M^{-1}s^{-1}$)**
Ct-MAL (at 30°C) [b]	89 ± 4	1.0 ± 0.1	8.9×10^4
Ch-MAL (at 30°C)	16 ± 1	4.6 ± 0.4	3.5×10^3
Ch-MAL (at 70°C)	78 ± 4	16 ± 3	4.9×10^3

[a] The steady state kinetic parameters were determined in Tris-HCl buffer (500 mM, pH 9.0) containing $MgCl_2$ (20 mM) and KCl (1 mM) at 30°C or 70°C. [b] These kinetic data were obtained from Raj *et al*.[26] Errors are standard deviations from each fit.

Thermostability of *Ch*-MAL

The preceding results demonstrate that *Ch*-MAL and *Ct*-MAL have different temperature-activity profiles, with *Ch*-MAL being active at higher temperatures. To compare the thermostability of these two MALs, they were incubated at 50°C (in separate incubations) and samples were withdrawn every 5 min to measure residual ammonia lyase activity. Interestingly, *Ch*-MAL stayed fully active

upon incubation at 50°C. Even after 4 h of incubation, the enzyme retained more than 95% of its initial activity towards **2** (Figure 2). In contrast, the ammonia lyase activity of *Ct*-MAL decreased rapidly upon incubation at 50°C, and within 30 min half of its initial activity was lost. After 4 h, *Ct*-MAL retained only ~4% of its initial activity towards **2**. Hence, in contrast to *Ct*-MAL, *Ch*-MAL is highly stable at 50°C.

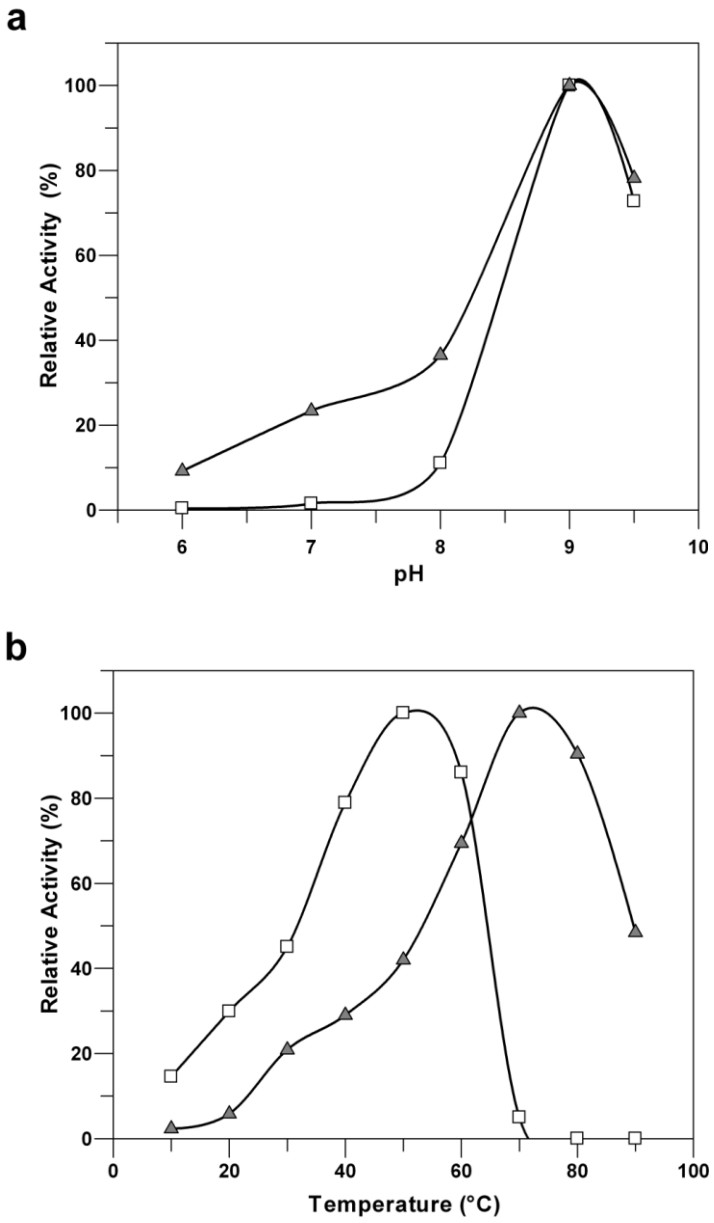

Figure 1. Effect of (**a**) pH and (**b**) temperature on the deamination activity of *Ch*-MAL (filled triangles) and *Ct*-MAL (empty squares).

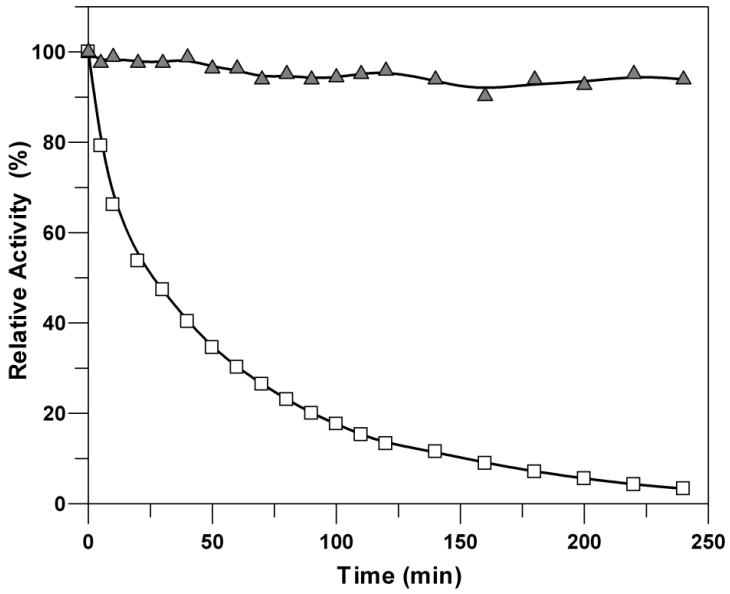

Figure 2. The thermostability of *Ch*-MAL (filled triangles) and *Ct*-MAL (empty squares) upon incubation at 50°C.

Amination activity of *Ch*-MAL

The rate of amination of **1** by *Ch*-MAL was monitored by following the depletion of **1** at 270 nm in Tris-HCl buffer (500 mM, pH 9.0) containing $MgCl_2$ (20 mM) and NH_4Cl (400 mM) at 30°C.[24, 26] *Ch*-MAL catalyzes the amination of **1** with an apparent k_{cat}/K_m value of 2.5×10^4 M^{-1} s^{-1}, which is only 3.5-fold lower than the value measured for the same reaction catalyzed by *Ct*-MAL (Table 2). The *Ch*-MAL-catalyzed amination of **1** was also monitored by ^{1}H NMR spectroscopy to verify that the products of the reaction are **2** and **3** (Scheme 1). The *Ch*-MAL catalyzed amination of **1** indeed yields **2** and **3**, as indicated by signals in the NMR spectra consistent with the structures of these amino acid products (Figure 3a). Although the ^{1}H NMR spectra showed signals for both **2** and **3**, those corresponding to **2** predominated in the initial spectra whereas signals for **3** increased in the later spectra. Hence, **2** is the kinetically preferred product. After a 14 day-incubation period at 22°C, a final conversion of ~76% was achieved, giving a ~1:1 ratio of **2**:**3** (Figure 3a) (Table 3). For comparison, the *Ct*-MAL-catalyzed amination of **1** was also followed by ^{1}H NMR spectroscopy,

showing the same kinetic profile of product (**2** and **3**) formation (Figure 3b) (Table 3). These results suggest that, like *Ct*-MAL, *Ch*-MAL likely catalyzes the rapid *anti*-addition and the much slower *syn*-addition of ammonia to **1**, yielding **2** and **3**, respectively.[23, 26]

Table 2. Apparent kinetic parameters for the *Ch*-MAL and *Ct*-MAL catalyzed amination of mesaconate (**1**)[a].

Enzyme	k_{cat} (s^{-1})	K_m for 1 (mM)	k_{cat}/K_m ($M^{-1}s^{-1}$)
Ct-MAL[b]	61 ± 1	0.7 ± 0.02	8.7×10^4
Ch-MAL	15 ± 1	0.6 ± 0.1	2.5×10^4

[a] The steady state kinetic parameters were determined in Tris-HCl buffer (500 mM, pH 9.0) containing $MgCl_2$ (20 mM) and NH_4Cl (400 mM) at 30°C. [b] These kinetic data were obtained from Raj *et al.*[26] Errors are standard deviations from each fit.

Electrophile scope of *Ch*-MAL

It has previously been determined that *Ct*-MAL accepts fumarate and several of its 2-substituted derivatives as alternative substrates.[23, 24] These observations prompted us to examine whether *Ch*-MAL also catalyzes the amination of these electrophiles. The *Ch*-MAL-catalyzed addition reactions were monitored by ^{1}H NMR spectroscopy. To identify the products of the reactions and to establish their relative configuration (*threo* or *erythro*), we compared the ^{1}H NMR spectra of the products of the *Ch*-MAL-catalyzed addition reactions to those obtained for the same reactions catalyzed by *Ct*-MAL, the products of which have previously been identified and their absolute configuration assigned.[23] Representative conversions for each reaction are summarized in Table 3. Both MALs efficiently catalyze the amination of fumarate and ethylfumarate (in addition to the natural substrate

methylfumarate). While *Ct*-MAL has reasonable activity towards propylfumarate, this compound is a poor substrate for *Ch*-MAL. Butylfumarate is not accepted as substrate by either MAL.

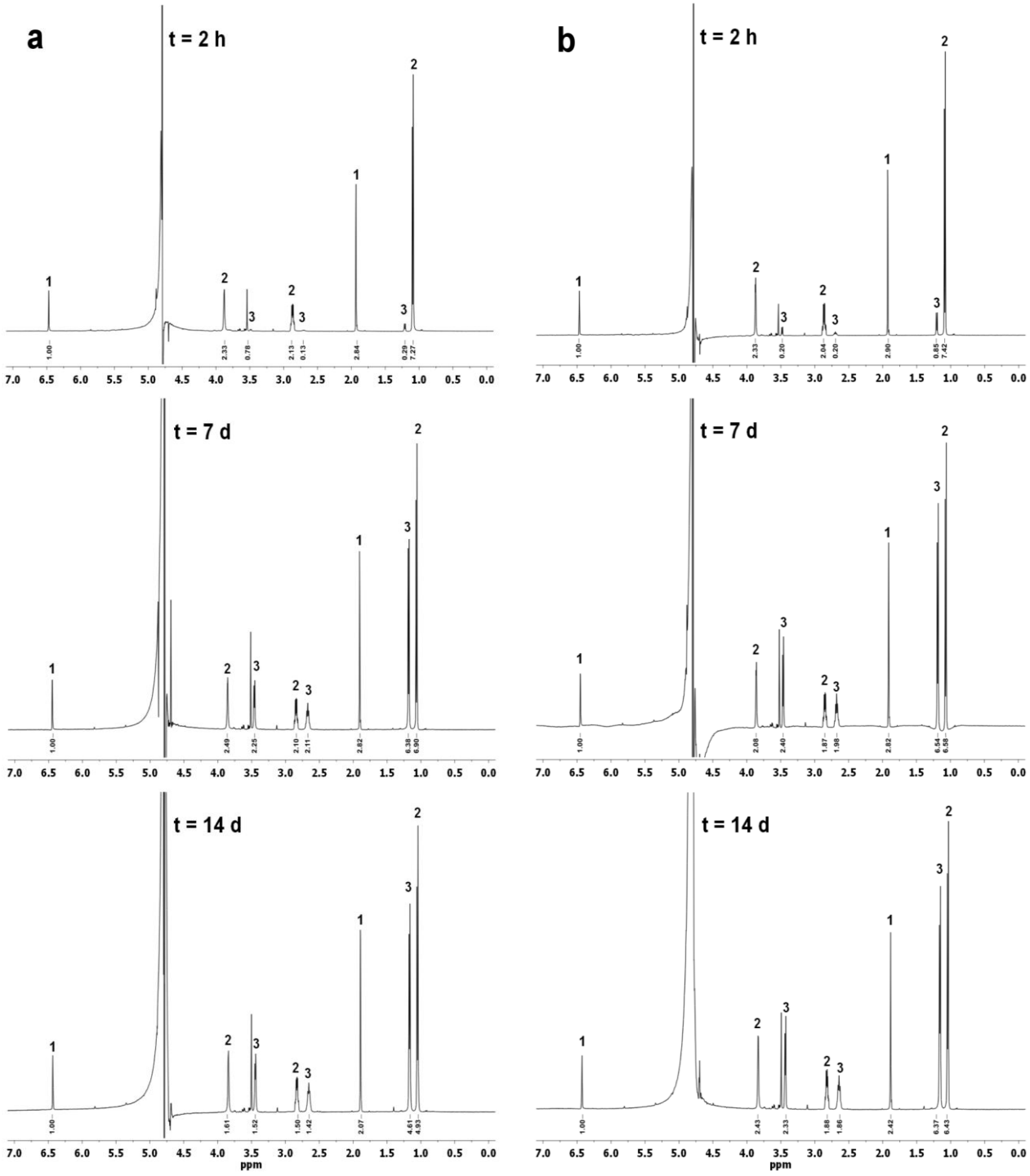

Figure 3. ^{1}H NMR spectra monitoring the amination of **1** by (**a**) *Ch*-MAL and (**b**) *Ct*-MAL. The ^{1}H NMR signals for **1**, **2**, and **3** were previously reported.[26] Impurity (Tris): $\delta = 3.5$ (s).

Table 3. Addition of ammonia to various electrophiles catalyzed by *Ch*-MAL or *Ct*-MAL.

Electrophile	***Ch*-MAL** **% conversion (days of incubation)**	***Ch*-MAL** ***ee*[a] or d.r.[b] of product**	***Ct*-MAL** **% conversion (days of incubation)**	***Ct*-MAL** ***ee*[a] or d.r.[b] of product**
Fumarate	99 (7)	*ee* >99%	99 (7)	*ee* >99%
Methylfumarate	76 (14)	d.r. = 52:48	81 (14)	d.r. = 51:49
Ethylfumarate	65 (14)	d.r. = 95:5	71 (14)	d.r. = 72:28
Propylfumarate	~7 (14)	d.r. = 100:0	61 (14)	d.r. = 100:0

[a] The enantiomeric excess of the (*S*)-aspartic acid product was determined by chiral HPLC. [b] The diastereomeric ratio (*threo*:*erythro*) of the 3-substituted aspartic acid products was determined by ^{1}H NMR spectroscopy.

Fumarate appears to be the best non-natural substrate for *Ch*-MAL, showing ~97% conversion after 2 h of incubation. The ^{1}H NMR spectrum recorded 7 days after the addition of enzyme showed the nearly complete disappearance of the signals corresponding to fumarate and the formation of new signals corresponding to the expected product, aspartate (Figure S2). The absolute configuration of this product was determined by using chiral HPLC, with authentic (*R*)-and (*S*)-aspartate for comparison, and found to be (*S*)-aspartate (>99% ee). Ethylfumarate is also a good substrate for *Ch*-MAL, showing ~60% conversion after 2 h of incubation. After a 14-day incubation period, a final conversion of ~65% was achieved and the spectrum showed signals corresponding to the expected products *threo*-(2*S*,3*S*)-3-ethylaspartate (P1) and *erythro*-(2*S*,3*R*)-3-ethylaspartate (P2). The ratio of S:P1:P2 was determined to be 35:60:5 (Figure S3). Propylfumarate is a poor substrate for *Ch*-MAL; the spectrum recorded after 14 days of incubation showed only ~7%

conversion of substrate with formation of *threo*-(2*S*,3*S*)-3-propylaspartate as the expected product (Figure S4). The tentative assignment of the absolute configuration of the 3-ethylaspartate and 3-propylasparate products was made on the basis of analogy to the known configuration of the products of the corresponding *Ct*-MAL catalyzed reactions.[23]

Nucleophile scope of *Ch*-MAL

We next screened *Ch*-MAL for its ability to add different unnatural amines to mesaconate (**1**). The reactions were followed by using ^{1}H NMR spectroscopy. The products were identified (and their relative configuration established) by comparing the ^{1}H NMR spectra of the *Ch*-MAL-catalyzed addition reactions to those obtained for the same reactions catalyzed by *Ct*-MAL, the products of which have previously been identified and their absolute configuration assigned.[25] Representative conversions for each reaction are summarized in Table 4. Both MALs efficiently catalyze the addition of hydroxylamine and hydrazine (in addition to the natural nucleophile, ammonia) to mesaconate. Methylamine, ethylamine and methoxylamine are also processed by both MALs, but at a much lower catalytic rate. Propylamine is not accepted as alternative nucleophile by either MAL.

Hydroxylamine and hydrazine seem to be the best alternative nucleophiles for *Ch*-MAL, showing ~80% and ~60% conversion after 2 h of incubation, respectively. For both these amines, ^{1}H NMR spectra recorded 7 days after the addition of enzyme showed the nearly complete disappearance of the signals corresponding to mesaconate (**1**) and the formation of new signals corresponding to the expected products, *threo*-(2*S*,3*S*)-*N*-hydroxy-3-methylaspartate and *threo*-(2*S*,3*S*)-2-hydrazino-3-methylaspartate, respectively (Figures S8 and S9) (Table 4). Methylamine and ethylamine are also accepted as substrates, showing ~12% and <1% conversion after 2 h of incubation, respectively. After a 14 day-incubation period, respective conversions of ~70% and ~30% were achieved (Table 4) and the ^{1}H NMR spectra showed signals corresponding to the expected products, *threo*-(2*S*,3*S*)-*N*,3-dimethylaspartate and *N*-ethyl-3-methylaspartate, respectively

(Figures S5 and S6). The relative configuration of the latter product has not been determined. Methoxylamine is a poor substrate for *Ch*-MAL. The spectrum recorded after 14 days of incubation showed only ~9% conversion of substrate with formation of *threo*-(2*S*,3*S*)-*N*-methoxy-3-methylaspartate as the expected product (Figure S7). The tentative assignment of the absolute configuration of the amino acid products was again made on the basis of analogy.

Table 4. Addition of various amines to mesaconate catalyzed by *Ch*-MAL or *Ct*-MAL[a].

Amine	***Ch*-MAL % conversion (days of incubation)**	***Ct*-MAL % conversion (days of incubation)**
Ammonia	76 (14)	81 (14)
Methylamine[b]	70 (14)	64 (14)
Ethylamine[b]	30 (14)	14 (14)
Methoxylamine[b]	9 (14)	67 (14)
Hydroxylamine[b]	99 (7)	96 (7)
Hydrazine[b]	100 (7)	100 (7)

[a] Reactions were followed by ^{1}H NMR spectroscopy. [b] The enzyme showed high diastereoselectivity in the formation of the corresponding amino acid product (>98% de).

Preparative scale synthesis of *threo*-(2*S*,3*S*)-*N*,3-dimethylaspartic acid

In order to demonstrate the potential of *Ch*-MAL for chemical synthesis, the enzyme was used to synthesize *threo*-(2*S*,3*S*)-*N*,3-dimethylaspartic acid at preparative scale. Accordingly, *Ch*-MAL was incubated with methylamine (1.04 g, 15.4 mmol) and mesaconate (0.2 g, 1.54 mmol) at 50°C, and the reaction was monitored by ^{1}H NMR spectroscopy (Figure 4a); after 8 days of incubation, a final conversion of ~75% was achieved. The product was purified using a Dowex cation exchange

column, giving a final yield of 61% (white solid), and identified as *threo*-(2*S*,3*S*)-*N*,3-dimethylaspartic acid by ^{1}H NMR (Figure 4b),^{13}C NMR and HRMS.[25] The enzyme showed high diastereoselectivity in the formation of *threo*-(2*S*,3*S*)-*N*,3-dimethylaspartic acid (>98% de, as assessed by ^{1}H NMR spectroscopy).

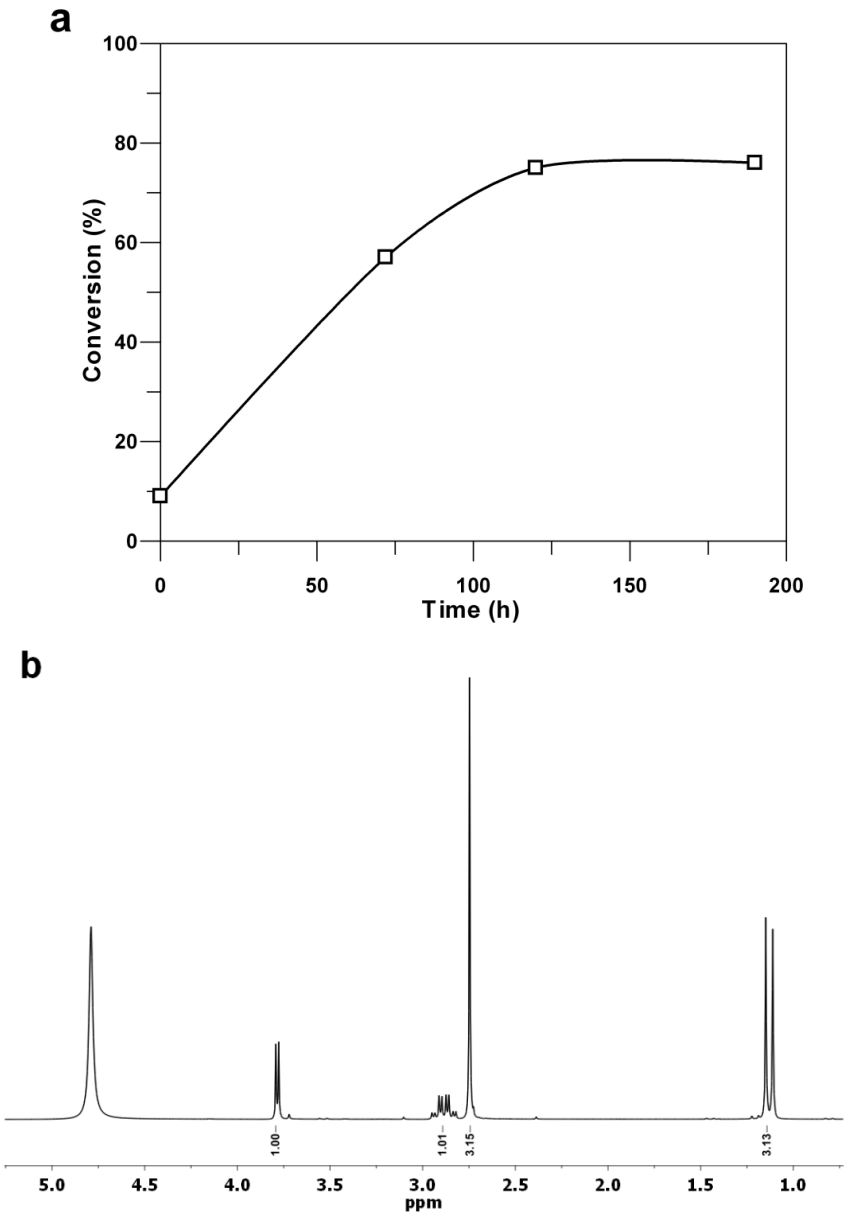

Figure 4. Enzymatic synthesis of *threo*-(2*S*,3*S*)-*N*,3-dimethylaspartic acid. (**a**) Progress curve of the *Ch*-MAL-catalyzed methylamine addition to mesaconate (**1**) as monitored by ^{1}H NMR spectroscopy. (**b**) ^{1}H NMR spectrum of purified *threo*-(2*S*,3*S*)-*N*,3-dimethylaspartic acid. The ^{1}H NMR signals for this amino acid are reported elsewhere.[25]

DISCUSSION

The thermophilic, Gram-positive bacterium *C. hydrogenoformans* Z-2901 has attracted much interest because of its unique biology: it grows at very high temperature, it lives almost entirely on a diet of carbon monoxide, and it converts water to hydrogen gas as part of its metabolism. The genome sequence of this extreme thermophile contains two open reading frames coding for putative MALs.[28] It can be anticipated that the MALs from *C. hydrogenoformans* exhibit increased thermostability compared to known MALs from mesophilic hosts.[13, 15, 17-20]

Herein, we have described the cloning, recombinant expression and purification of *Ch*-MAL from *C. hydrogenoformans* Z-2901, which provided an opportunity to characterize the substrate specificity and thermostability of a MAL isozyme from an extreme thermophile. The enzyme can be highly overproduced in *E. coli* in a soluble and active form and rapidly purified with the help of a C-terminal hexahistidine tag. The thermostability, activity and substrate specificity of *Ch*-MAL were compared to *Ct*-MAL, the best studied MAL from a mesophilic host. As might be expected, *Ch*-MAL and *Ct*-MAL have different temperature-activity profiles, with *Ch*-MAL being active at much higher temperature. *Ch*-MAL catalyzes the deamination of (2*S*,3*S*)-3-methylaspartate (**2**, Scheme 1) with a k_{cat}/K_m of 3.5 $\times 10^3$ M^{-1} s^{-1} at 30°C and 4.9 $\times 10^3$ M^{-1} s^{-1} at 70°C, which is somewhat lower (18- to 25-fold) than the value measured for the same conversion catalyzed by *Ct*-MAL at 30°C. The lower catalytic efficiency of the *Ch*-MAL catalyzed reaction results mainly from a higher K_m value, which suggests less optimal binding of **2** in the active site of *Ch*-MAL. A comparison of the kinetic parameters for the *Ch*-MAL and *Ct*-MAL catalyzed amination of **1** (Table 2) shows similar catalytic efficiencies for both enzymes. These results indicate that *Ch*-MAL functions as an effective 3-methylaspartate ammonia lyase, catalyzing the reversible addition of ammonia to mesaconate to give (2*S*,3*S*)-3-methylaspartate and (2*S*,3*R*)-3-methylaspartate as products. Activity measurements further showed that *Ch*-MAL is highly thermostable and retains >95% of its initial activity after heating for 4 h at 50°C. Importantly, and in contrast to *Ct*-MAL,[13]

Ch-MAL can be stored at 4°C for several months without significant loss of activity. Thus, *Ch*-MAL indeed exhibits enhanced stability compared to *Ct*-MAL and other MALs from mesophilic hosts.[13, 15, 17-20]

Ch-MAL has been shown to catalyze the regioselective addition of ammonia to several substituted fumarates, resulting in the corresponding 3-substituted aspartic acids with the *threo*-isomers being the kinetically preferred products (Table 3). Also, the enzyme is highly enantioselective in the addition of ammonia to fumarate, leading to the formation of (*S*)-aspartic acid with >99% ee. While *Ch*-MAL efficiently processes fumarate and small substituted fumarates such as methylfumarate and ethylfumarate, it displays low (propylfumarate) or no (butylfumarate) activity with larger substrates. This suggests that the binding pocket for the C-2 alkyl substituent in *Ch*-MAL is designed to bind small alkyl chains and excludes large groups. A similar electrophile scope and isomer preference was found for *Ct*-MAL (Table 3). *Ch*-MAL (and *Ct*-MAL) also accepts various unnatural amines in the addition to mesaconate, yielding the corresponding *N*-substituted methylaspartic acids (Table 4). The enzyme efficiently processes small substituted amines such as hydroxylamine and hydrazine, but displays low (methylamine, ethylamine and methoxylamine) or no (propylamine) activity with larger amine nucleophiles. These observations suggest that the amine binding pocket of *Ch*-MAL (and *Ct*-MAL) is designed to bind small amine compounds and excludes large nucleophiles. In contrast to the enzyme-catalyzed ammonia addition reactions, both MALs showed high diastereoselectivity in the amine additions to mesaconate, resulting in the formation of the *N*-substituted methylaspartic acids with high diastereomeric access (>98% de, as assessed by ^{1}H NMR spectroscopy).[23, 24, 25]

In conclusion, *Ch*-MAL from *C. hydrogenoformans* Z-2901 can be overproduced in *E. coli* and purified in high yield. This MAL is a promising new biocatalyst because it is highly thermostable and accepts various substituted fumarates and amines to produce a range of aspartic acid derivatives. These chiral amino acids are important building blocks for synthetic enzymes,

peptides, chemicals, and pharmaceuticals.[32, 33, 34] To further enlarge the substrate scope of MAL and improve its stereoselectivity in the amination reactions, protein engineering experiments, guided by the previously published crystal structure of *C. amalonaticus* MAL in complex with substrate **2**,[21] have been initiated in our laboratory. If successful, these efforts may help to increase the number and diversity of enzyme applications in industry.

MATERIALS AND METHODS

Materials

All chemicals were purchased from Sigma-Aldrich unless stated otherwise. The sources for the media components, buffers, solvents, Pre-packed PD-10 Sephadex G-25 columns, and molecular biology reagents, including PCR purification, gel extraction, and Miniprep kits, are reported elsewhere.[26] Oligonucleotides for DNA amplification were synthesized by Operon Biotechnologies (Cologne, Germany).

Bacterial strains, plasmids, and growth conditions

E. coli strain TOP10 (Invitrogen) was used for cloning, isolation of plasmids and, in combination with the pBAD/*Myc*-His A vector (Invitrogen), for recombinant protein production. The genomic DNA of *C. hydrogenoformans Z*-2901, the source of the *Ch*-MAL gene, was kindly provided by Professor Frank Robb (Center of Marine Biotechnology, University of Maryland, USA). *E. coli* TOP10 cells were grown in Luria-Bertani (LB) medium containing 100 µg/mL ampicillin (Ap). *Ct*-MAL was produced in *E. coli* TOP10 and purified to homogeneity by using a previously published protocol.[26]

General methods

BLASTP searches of the National Center for Biotechnology Information (NCBI) databases were performed using the *Ct*-MAL amino acid sequence (GenBank: AAB24070.1) as the query

sequence. Amino acid sequences were aligned using a version of the CLUSTALW multiple-sequence alignment routines available in the computational tools at the EMBL-EBI website. Techniques for restriction enzyme digestions, ligation, transformation, and other standard molecular biology manipulations were based on methods described elsewhere[29] or as suggested by the manufacturer. PCR was carried out in a DNA thermal cycler (model GS-1) obtained from Biolegio (Nijmegen, The Netherlands). DNA sequencing was performed by Macrogen (Seoul, Korea). Proteins were analyzed by sodium dodecyl sulfate polyacrylamide gel electrophoresis (SDS-PAGE) under denaturing conditions on gels containing polyacrylamide (10%). The gels were stained with Coomassie brilliant blue. Protein concentrations were determined by the Waddell method.[30] Kinetic data were obtained on a V-650 spectrophotometer from Jasco (IJsselstein, The Netherlands). High Performance Liquid Chromatography (HPLC) was performed using a Waters 510 HPLC Pump (Waters Corporation, USA) in combination with a variable wavelength UV detector 875-UV (Jasco) and a BD112 recorder (Kipp and Zonen, The Netherlands). ^{1}H NMR spectra were recorded on a Varian Inova 500 (500 MHz) spectrometer using a pulse sequence for selective suppression of the proton signals for water by presaturation methods. ^{1}H chemical shifts (δ) are reported in parts per million (ppm) downfield from tetramethylsilane and are calibrated on protons in the NMR solvents (H_2O: $\delta = 4.79$).

Construction of the expression vector for the production of *Ch*-MAL

The *Ch*-MAL gene was amplified from genomic DNA of *C. hydrogenoformans* Z-2901 (28) using two synthetic primers and high fidelity Phusion polymerase by following the protocol supplied with the polymerase (Finnzymes, Espoo, Finland). The forward primer (5'-G GAG CGG TGG **CAT ATG** AGA ATA AAA GAT G -3') contains an *Nde*I restriction site (in bold) followed by 13 bases corresponding to the coding sequence of the *Ch*-MAL gene. The reverse primer (5'- CC TTC CGG **AAG CTT** ACC AAC TTT TTT CTG AAA TGT GAC C -3') contains a *Hin*dIII restriction site (in

bold) followed by 25 bases corresponding to the complementary sequence of the *Ch*-MAL gene. The resulting PCR product and the pBAD*N*/*Myc*-His A vector were digested with *Nde*I and *Hin*dIII restriction enzymes, purified, and ligated using T4 DNA ligase. Aliquots of the ligation mixture were transformed into competent *E. coli* TOP10 cells. Transformants were selected at 37°C on LB/Ap plates. Plasmid DNA was isolated from several colonies and analyzed by restriction analysis for the presence of the insert. The cloned *Ch*-MAL gene was sequenced to verify that no mutations had been introduced during the amplification of the gene.

Expression and purification of *Ch*-MAL

The *Ch*-MAL enzyme was produced in *E. coli* TOP10 using the pBAD*N* expression system. Fresh TOP10 cells containing the appropriate expression plasmid were collected from a LB/Ap plate using a sterile loop and used to inoculate LB/Ap medium (15 mL). After growth for 8 h at 37°C, a sufficient quantity of the culture was used to inoculate 1 L of fresh auto-induction (ZYM) medium (10 g/L tryptone, 5 g/L yeast extract, 25 mM Na_2HPO_4 buffer, 25 mM KH_2PO_4, 5 mM Na_2SO_4, pH 6.7), containing 0.5% (v/v) glycerol, 0.05% (w/v) glucose, $MgSO_4$ (2 mM), ampicillin (100 µg/mL) and arabinose (0.05% w/v), in a 3 L Erlenmeyer flask to an initial A_{600} of ~0.1.[31] Cultures were grown for 24 h at 22°C with vigorous (170 rpm) shaking. Cells were harvested by centrifugation (6000*g*, 15 min). Protein purification was performed using an immobilized metal affinity chromatography (IMAC) procedure as previously described.[26] The elution buffer was exchanged against Tris-HCl buffer (50 mM, pH 8.0), containing $MgCl_2$ (2 mM) and KCl (0.1 mM), using a pre-packed PD-10 Sephadex G-25 gel filtration column. The purified enzyme was stored at +4°C or −80°C until further use. At both temperatures, the enzyme can be stored for several months without significant loss of activity.

Determination of the molecular mass of *Ch*-MAL

The native molecular mass of *Ch*-MAL was determined by gel filtration chromatography. The purified enzyme (1 mg/mL) was applied to a Superdex 200 column (10/300; GE Healthcare, USA), previously equilibrated with Tris-HCl buffer (50 mM, pH 8.0), containing $MgCl_2$ (2 mM) and KCl (0.1 mM). The column was eluted with the same buffer at a flow rate of 0.5 mL/min. The column was calibrated with the reference proteins aldolase (MW 158 kDa), bovine-serum albumin (MW 66.7 kDa) and ovalbumin (MW 44 kDa) (GE Healthcare). The subunit molecular mass of *Ch*-MAL was determined by mass spectrometry using an API 3000 triple-quadrapole mass spectrometer (Applied Biosystems/MDS Sciex) connected to a LC system via a TurboIonSpray source. For this, the Tris-HCl buffer of the protein sample was exchanged to NH_4CO_2H (5 mM, pH 7.0) using a Nanosep centrifugal device (PALL Life Sciences). Data were collected and analyzed by using Analyst 1.5.1 data acquisition software (Applied Biosystems/MDS Sciex).

Enzyme assays

The rate of the MAL-catalyzed amination of **1** was monitored by following the depletion of **1** at 270 nm ($\varepsilon = 482\ M^{-1}\ cm^{-1}$) in Tris-HCl buffer (500 mM, pH 9.0) containing $MgCl_2$ (20 mM) and NH_4Cl (400 mM) at 30°C.[26] The rate of the MAL-catalyzed deamination of **2** was monitored by following the formation of **1** at 240 nm ($\varepsilon = 3850\ M^{-1}\ cm^{-1}$) in Tris-HCl buffer (500 mM, pH 9.0), containing $MgCl_2$ (20 mM) and KCl (1 mM), at either 30°C or 70°C.[24, 26] At 70°C, the pH of the Tris buffer was adjusted to the desired pH of 9.0. Like *Ct*-MAL, *Ch*-MAL requires both Mg^{2+} and K^+ ions for its deamination activity, whereas for the amination activity only Mg^{2+} is needed. Optimal activity was obtained with 20 mM $MgCl_2$ and 1 mM KCl, and these concentrations were used for all enzyme assays.

Determination of pH and temperature optima of MAL

The pH optima of *Ch*-MAL and *Ct*-MAL were determined in Tris-HCl buffer (500 mM), containing $MgCl_2$ (20 mM) and KCl (1 mM), with pH values ranging from 6.0 to 9.5 at 30°C. A sufficient quantity of enzyme was added and its activity assayed using **2** (15 mM) as the substrate. Stock solutions of **2** were made in Tris buffer (500 mM) and the pH of the stock solutions were adjusted to the desired pH (6.0-9.5). The normalized initial reaction rates were plotted against pH.

The temperature optima for *Ch*-MAL and *Ct*-MAL were determined in Tris-HCl buffer (500 mM, pH 9.0), containing $MgCl_2$ (20 mM) and KCl (1 mM), using a temperature range of 10 to 90°C. At each temperature, the pH of the Tris buffer was adjusted to the desired pH (9.0). A sufficient quantity of enzyme was added and its activity assayed using **2** (15 mM) as the substrate. Stock solutions of **2** were made in Tris-HCl buffer (500 mM, pH adjusted to 9.0). The normalized initial reaction rates were plotted against temperature.

Thermostability assay

The thermostability of *Ch*-MAL or *Ct*-MAL was examined in Tris-HCl buffer (500 mM, pH 9.0), containing $MgCl_2$ (20 mM) and KCl (1 mM). An appropriate amount of enzyme was incubated in the assay buffer (25 mL) at 50°C. Samples (1 mL) were withdrawn every 5 min and the residual activity was measured using **2** (15 mM) as the substrate. The initial reaction rates were plotted against time.

Product analysis of the amination of 1 by MAL

^1H NMR spectra monitoring the *Ch*-MAL- or *Ct*-MAL-catalyzed amination of **1** were recorded according to a protocol reported elsewhere,[26] with the following modifications. Reaction mixtures consisted of NH_4Cl (500 µL of 1 M stock solution in water, pH 9.0, containing 20 mM $MgCl_2$), D_2O (100 µL), and **1** (100 µL of a 500 mM stock solution in water, pH 9.0). Reactions were

initiated by the addition of 10-15 µL of freshly purified enzyme (400 µg of either *Ct*-MAL or *Ch*-MAL), and each reaction mixture was incubated at 22°C. ^{1}H NMR spectra were recorded 2 h, 7 days, and 14 days after the addition of enzyme. Product amounts were estimated by integration of the signals corresponding to **2** and **3**. The ^{1}H NMR signals for **1**, **2** and **3** were previously reported.[26]

Procedure for the nucleophile screening

The nucleophile scope of *Ch*-MAL was examined by using ^{1}H NMR spectroscopy. *Ch*-MAL was incubated (in separate reactions) with different amines in the presence of **1**. The reaction mixtures consisted of amine (500 µL of a 1 M stock solution in water, pH 9.0, containing 20 mM $MgCl_2$), **1** (100 µL of a 500 mM stock solution in water, pH 9.0), and D_2O (100 µL). Reactions were initiated by the addition of 10-15 µL of freshly purified *Ch*-MAL (400 µg), and each reaction mixture was incubated at 22°C. ^{1}H NMR spectra were recorded 2 h, 7 days, and 14 days after the addition of enzyme. To identify the products of the reactions and to assign their relative (*threo* or *erythro*) configuration, the ^{1}H NMR spectra were compared to those generated for the same reactions catalyzed by *Ct*-MAL (performed as described above for *Ch*-MAL) as well as to previously published ^{1}H NMR spectral data.[23, 25] Relative product distributions were estimated by integration of the corresponding signals.

Synthesis of 2-substituted fumaric acids

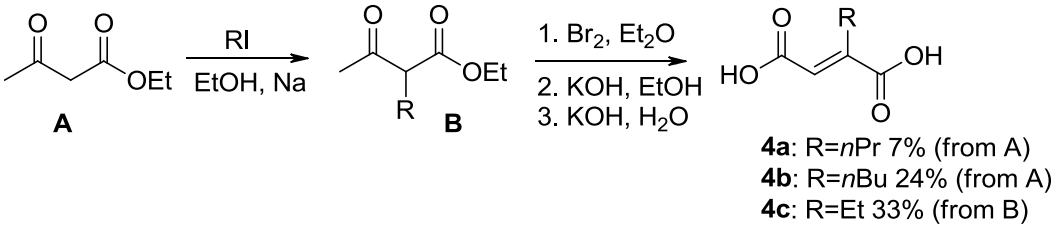

4a: 2-Propylfumaric acid. The synthesis of **4a** (and **4b** and **4c**) is largely based on a previously published protocol.[23] Accordingly, sodium (10 mmol, 230 mg) was dissolved in ethanol (6.0 mL). Ethyl acetoacetate (9.0 mmol, 1.14 mL) was added dropwise over 5 min at 5°C, followed by *n*-propyl iodide (12 mmol, 1.17 mL). The reaction mixture was refluxed for 2 h and was then cooled to room temperature, poured on water (30 mL) and extracted with Et_2O (3 x 25 mL). Organic fractions, containing a mixture of mono- and dialkylated product, were dried and concentrated to ~15 mL volume. Bromine (4.0 g) was added slowly at room temperature, and the reaction mixture was refluxed for 3 h. The volatiles were evaporated, and the residue was slowly added to a solution of KOH (4.0 g) in ethanol (15 mL). The resultant mixture was heated at reflux for 30 min, after which 20 mL of water was added and the refluxing continued for another 20 min. The reaction mixture was washed with EtOAc (2 x 40 mL). The aqueous phase was acidified with aqueous HCl (12 N) to pH < 1 and extracted with Et_2O (4 x 50 mL). The collected organic fractions were dried, decolourized with activated carbon and the solvent was evaporated. The resultant residue was triturated with pentane to yield white crystals (100 mg, 7%). Mp. 173.5-174.7°C (lit. 172-174°C, (23)); ^{1}H NMR (400 MHz, D_2O + K_2CO_3): δ 0.70 (t, 3H, ^3J = 7.6 Hz, C**H$_3$**), 1.19-1.25 (m, 2H, CH_3C**H$_2$**), 2.63 (t, 2H, ^3J = 7.2 Hz, C**H$_2$**C=C), 6.18 (s, 1H, vinyl **H**). ^{1}H NMR consistent with literature data.[23]

4b: 2-Butylfumaric acid was prepared according to the same procedure as 2-propylfumaric acid. Yield: 24%. Yellow crystals; Mp. 171.7-172.5°C (lit.[23] 170-171°C); ^{1}H NMR (400 MHz, D_2O + K_2CO_3): δ 0.71 (t, 3H, ^3J = 7.2 Hz, C**H$_3$**), 1.06-1.24 (m, 4H, CH_3C**H$_2$C H$_2$**), 2.31 (t, 2H, ^3J = 7.2 Hz, C**H$_2$**C=C), 6.17 (s, 1H, vinyl **H**). ^{1}H NMR consistent with literature data.[23]

4c: 2-Ethylfumaric acid was prepared according to the same procedure as 2-propylfumaric acid, starting with commercially available ethyl 2-ethylacetoacetate. Yield: 33%. Yellow crystals; Mp. 197-198°C (lit.[23] 195°C); ^{1}H NMR (400 MHz, D_2O): δ 0.89 (t, 3H, ^3J = 7.2 Hz, C**H$_3$**), 2.49 (d, 2H, ^3J = 7.2 Hz, C**H$_2$**), 6.57 (s, 1H, vinyl **H**). ^{1}H NMR consistent with literature data.[23]

Procedure for the electrophile screening

The electrophile scope of *Ch*-MAL was analyzed by ^{1}H NMR spectroscopy. In separate experiments, *Ch*-MAL was incubated with fumarate (or substituted fumarates) and ammonia. Reaction mixtures consisted of NH_4Cl (500 µL of 1 M stock solution in water, pH 9.0, containing 20 mM $MgCl_2$), D_2O (100 µL), and (substituted) fumarate (100 µL of a 500 mM stock solution in water, pH 9.0). Reactions were initiated by the addition of 10-15 µL of freshly purified *Ch*-MAL (400 µg), and each reaction mixture was incubated at 22°C. ^{1}H NMR spectra were recorded 2 h, 7 days, and 14 days after the addition of enzyme. To identify the products of the reactions and to assign their relative (*threo* or *erythro*) configuration, the ^{1}H NMR spectra were compared to those obtained for the same reactions catalyzed by *Ct*-MAL (performed as described above for *Ch*-MAL) as well as to previously published ^{1}H NMR spectral data.[23, 25] Product amounts were estimated by integration of the corresponding signals.

The enantiomeric excess of the product of the MAL-catalyzed addition of ammonia to fumarate (i.e., aspartate) was determined by chiral HPLC using a Chirex 3126-(D)-pencillamine column (250 mm x 4.6 mm, Phenomenex, USA) with 2 mM $CuSO_4$ solution-methanol (90:10) as

eluent at a flow rate of 1 mL/min. Retention times were as follows: (*S*)-aspartate, 23.4 min; (*R*)-aspartate, 31 min.

Preparative scale synthesis of *threo*-(2*S*,3*S*)-*N*,3-dimethylaspartic acid

Purified *Ch*-MAL was used for the synthesis of *threo*-(2*S*,3*S*)-*N*,3-dimethylaspartic acid. A solution (20 mL) of **1** (0.2 g, 1.54 mmol), methylamine (1.04 g, 15.4 mmol) and $MgCl_2$ (20 mM) was prepared. The pH was adjusted to 9.0 by the addition of small aliquots of an aqueous NaOH (1M) solution. The reaction was started by the addition of *Ch*-MAL (10 mg), and the reaction mixture was incubated at 50°C. The progress of the reaction was monitored by using ^{1}H NMR (500 MHz) spectroscopy. After 8 days, the reaction was terminated and the reaction mixture was lyophilized, after which the product was purified using cation exchange chromatography (Dowex, 50W X8, 100-200 mesh size, Merck). A Dowex column (15.0 g resin per 1 g of mesaconate) was prepared by pre-treatment of the resin with a solution of aqueous NH_3 (2 M, 4 column volumes), aqueous HCl (1 N, 2 column volumes) and distilled water (4 column volumes). The lyophilized reaction mixture was suspended in aqueous HCl (1 N, 20 mL) and loaded on the column. The column was washed with distilled water (1 column volume) and the product was eluted with aqueous NH_3 (2 M, 2 column volumes). The ninhydrin positive fractions were pooled and concentrated under reduced pressure, followed by lyophilization. The product was obtained as a white solid in 61% (152 mg) yield. ^{1}H NMR (200 MHz, D_2O): δ 1.13 (d, 3H, ^3J = 7.6 Hz, CHC**H$_3$**), 2.75 (s, 3H, C**H$_3$**NH), 2.82-2.95 (dq, 1H, ^3J = 7.6 Hz, ^3J = 3.0 Hz, C**H**CH_3), 3.79 (d, 1H, ^3J = 3.0 Hz, C**H**NH); ^{13}C NMR (50 MHz, D_2O): δ 11.7, 33.0, 40.8, 65.4, 172.2, 180.9. HRMS (ESI+) m/z calc. for $C_6H_{12}NO_4$: 162.0766 $[M+H]^+$, found: 162.0760.

ACKNOWLEDGMENTS

We are grateful to Professor Frank Robb (Center of Marine Biotechnology, University of Maryland, USA) for the kind gift of genomic DNA of *C. hydrogenoformans* Z-2901. We thank Dr. Jandré de Villiers, Dr. Marianne de Villiers, and Dr. Edzard Geertsema (Department of Pharmaceutical Biology, University of Groningen, The Netherlands) for their insightful discussions and critical reading of the manuscript. We thank Pieter van der Meulen (Molecular Dynamics group, University of Groningen) for his assistance in acquiring the NMR spectra. We gratefully thank Annie van Dam and Margot Jeronimus-Stratingh (University of Groningen) for their expert assistance in acquiring the protein MS spectra. This research was financially supported by VENI (700.54.401) and VIDI (700.56.421) grants (to GJP) from the Division of Chemical Sciences of the Netherlands Organisation of Scientific Research (NWO-CW), and by the Netherlands Ministry of Economic Affairs and the B-Basic partner organizations (www.b-basic.nl) through B-Basic, a public-private NWO-ACTS programme.

REFERENCES

1. Schulze, B., and Wubbolts, M. G. (1999) Biocatalysis for industrial production of fine chemicals. *Curr. Opin. Biotechnol. 10*, 609-615.
2. Pollard, D. J., and Woodley, J. M. (2007) Biocatalysis for pharmaceutical intermediates: the future is now. *Trends Biotechnol. 25*, 66-73.
3. Panke, S., Held, M., and Wubbolts, M. (2004) Trends and innovations in industrial biocatalysis for the production of fine chemicals. *Curr. Opin. Biotechnol. 15*, 272-279.
4. Schoemaker, H. E., Mink, D., and Wubbolts, M. G. (2003) Dispelling the myths-biocatalysis in industrial synthesis. *Science 299*, 1694-1697.

5. Weiner, B., Szymanski, W., Janssen, D. B., Minnaard, A. J., and Feringa, B. L. (2010) Recent advances in the catalytic asymmetric synthesis of beta-amino acids. *Chem. Soc. Rev. 39*, 1656-1691.

6. Wohlgemuth, R. (2010) Biocatalysis-key to sustainable industrial chemistry. *Curr. Opin. Biotechnol. 21*, 713-724.

7. Turner, N. J. (2010) Ammonia lyases and aminomutases as biocatalysts for the synthesis of α-amino and β-amino acids. *Curr. Opin. Chem. Biol.* 15, 234-240.

8. Verkuijl, B. J., Szymanski, W., Wu, B., Minnaard, A. J., Janssen, D. B., de Vries, J. G., and Feringa, B. L. (2010) Enantiomerically pure beta-phenylalanine analogues from alpha-beta-phenylalanine mixtures in a single reactive extraction step. *Chem. Commun. (Camb) 46*, 901-903.

9. Szymanski, W., Wu, B., Weiner, B., de Wildeman, S., Feringa, B. L., and Janssen, D. B. (2009) Phenylalanine aminomutase-catalyzed addition of ammonia to substituted cinnamic acids: a route to enantiopure alpha- and beta-amino acids. *J. Org. Chem. 74*, 9152-9157.

10. Wu, B., Szymanski, W., Wietzes, P., de Wildeman, S., Poelarends, G. J., Feringa, B. L., and Janssen, D. B. (2009) Enzymatic synthesis of enantiopure alpha- and beta-amino acids by phenylalanine aminomutase-catalysed amination of cinnamic acid derivatives. *Chembiochem. 10*, 338-344.

11. Wu, B., Szymanski, W., Wijma, H. J., Crismaru, C. G., de Wildeman, S., Poelarends, G. J., Feringa, B. L., and Janssen, D. B. (2010) Engineering of an enantioselective tyrosine aminomutase by mutation of a single active site residue in phenylalanine aminomutase. *Chem. Commun. (Camb) 46*, 8157-8159.

12. Weiner, B., Poelarends, G. J., Janssen, D. B., and Feringa, B. L. (2008) Biocatalytic enantioselective synthesis of *N*-substituted aspartic acids by aspartate ammonia lyase. *Chemistry. 14*, 10094-10100.

13. Barker, H. A., Smyth, R. D., Wilson, R. M., and Weissbach, H. (1959) The purification and properties of beta-methylaspartase. *J. Biol. Chem. 234*, 320-328.

14. Goda, S. K., Minton, N. P., Botting, N. P., and Gani, D. (1992) Cloning, sequencing, and expression in E*scherichia coli* of the *Clostridium tetanomorphum* gene encoding beta-methylaspartase and characterization of the recombinant protein. *Biochemistry 31*, 10747-10756.

15. Kato, Y., and Asano, Y. (1997) 3-methylaspartate ammonia-lyase as a marker enzyme of the mesaconate pathway for (S)-glutamate fermentation in *Enterobacteriaceae*. *Arch. Microbiol. 168*, 457-463.

16. Khomyakova, M., Bukmez, O., Thomas, L. K., Erb, T. J., and Berg, I. A. (2011) A methylaspartate cycle in *haloarchaea*. *Science 331*, 334-337.

17. Asano, Y., and Kato, Y. (1994) Crystalline 3-methylaspartase from a facultative anaerobe, *Escherichia coli* strain YG1002. *FEMS Microbiol. Lett. 118*, 255-258.

18. Kato, Y., and Asano, Y. (1995) Purification and properties of crystalline 3-methylaspartase from two facultative anaerobes, *Citrobacter sp*. strain YG-0504 and M*organella morganii* strain YG-0601. *Biosci. Biotechnol. Biochem. 59*, 93-99.

19. Kato, Y., and Asano, Y. (1995) 3-methylaspartate ammonia-lyase from a facultative anaerobe, strain YG-1002. *Appl. Microbiol. Biotechnol. 43*, 901-907.

20. Kato, Y., and Asano, Y. (1998) Cloning, nucleotide sequencing, and expression of the 3-methylaspartate ammonia-lyase gene from C*itrobacter amalonaticus* strain YG-1002. *Appl. Microbiol. Biotechnol. 50*, 468-474.

21. Levy, C. W., Buckley, P. A., Sedelnikova, S., Kato, Y., Asano, Y., Rice, D. W., and Baker, P. J. (2002) Insights into enzyme evolution revealed by the structure of methylaspartate ammonia lyase. *Structure 10*, 105-113.

22. Asuncion, M., Blankenfeldt, W., Barlow, J. N., Gani, D., and Naismith, J. H. (2002) The structure of 3-methylaspartase from C*lostridium tetanomorphum* functions via the common enolase chemical step. *J. Biol. Chem. 277*, 8306-8311.

23. Akhtar, M., Botting, N. P., Cohen, M. A., and Gani, D. (1987) Enantiospecific synthesis of 3-susbtituted aspartic acid via enzymatic amination of substituted fumaric acid derivatives. *Tetrahedron 43*, 5899-5908.

24. Botting, N. P., Akhtar, M., Cohen, M. A., and Gani, D. (1988) Substrate specificity of the 3-methylaspartate ammonia-lyase reaction: Observation of differential relative reaction rates for substrate-product pairs. *Biochemistry 27*, 2953-2955.

25. Gulzar, M. S., Akhtar, M. and Gani, D. (1997) Preparation of *N*-substituted aspartic acids viaenantiospecific conjugate addition of *N*-nucleophiles to fumaric acids using methylaspartase: synthetic utility and mechanistic implications. *J. Chem. Soc. Perkin Trans. I* 649-656.

26. Raj, H., Weiner, B., Veetil, V. P., Reis, C. R., Quax, W. J., Janssen, D. B., Feringa, B. L., and Poelarends, G. J. (2009) Alteration of the diastereoselectivity of 3-methylaspartate ammonia lyase by using structure-based mutagenesis. *Chembiochem. 10*, 2236-2245.

27. Svetlichny, V.A., Sokolova, T.G., Gerhardt, M., Ringpfeil, M., Kostrikina, N.A., and Zavarzin, G.A. (1991) *Carboxydothermus hydrogenoformans* gen. nov., sp. nov., a CO-utilizing thermophilic anaerobic bacterium from hydrothermal environments of Kunashir Island. *Syst Appl Microbiol. 14*, 254-260.

28. Wu, M., Ren, Q., Durkin, A. S., Daugherty, S. C., Brinkac, L. M., Dodson, R. J., Madupu, R., Sullivan, S. A., Kolonay, J. F., Haft, D. H., Nelson, W. C., Tallon, L. J., Jones, K. M., Ulrich, L. E., Gonzalez, J. M., Zhulin, I. B., Robb, F. T., and Eisen, J. A. (2005) Life in hot carbon monoxide: the complete genome sequence of *Carboxydothermus hydrogenoformans* Z-2901. *PLoS Genet. 1*, e65.

29. Sambrook, J., E.F. Fritsch, and T. Maniatis. (1989) Molecular cloning : a laboratory manual. 2nd ed., Cold spring Harbor Laboratory Press, New York.

30. Waddell, W. J. (1956) A simple ultraviolet spectrophotometric method for the determination of protein. *J. Lab. Clin. Med. 48*, 311-314.

31. Studier, F. W. (2005) Protein production by auto-induction in high density shaking cultures. *Protein Expr. Purif. 41*, 207-234.

32. Kahn, M. (1993) Peptide secondary structure mimetics: recent advances and future challenges. *Synlett. 11*, 821-826.

33. Burger, K., and Spengler, J. (2000) A new approach to *N*-methylaspartic, *N*-methylglutamic, and *N*-methyl-α-aminoadipic acid derivatives. *Eur J Org Chem. 31*, 199-204.

34. Hughes, E., Burke, R. M., and Doig, A. J. (2000) Inhibition of toxicity in the β-amyloid peptide fragment β-(25-35) using *N*-methylated derivatives: a general strategy to prevent amyloid formation. *J. Biol. Chem. 275*, 25109-25115.

Supplementary Information

Figure S1. Amino acid sequence alignment of the MAL proteins from *Clostridium tetanomorphum* (*Ct*-MAL) and *Carboxydothermus hydrogenoformans* Z-2901 (*Ch*-MAL). Identical residues are shaded in gray. The ten active site residues of *Ct*-MAL are indicated by an asterisk.

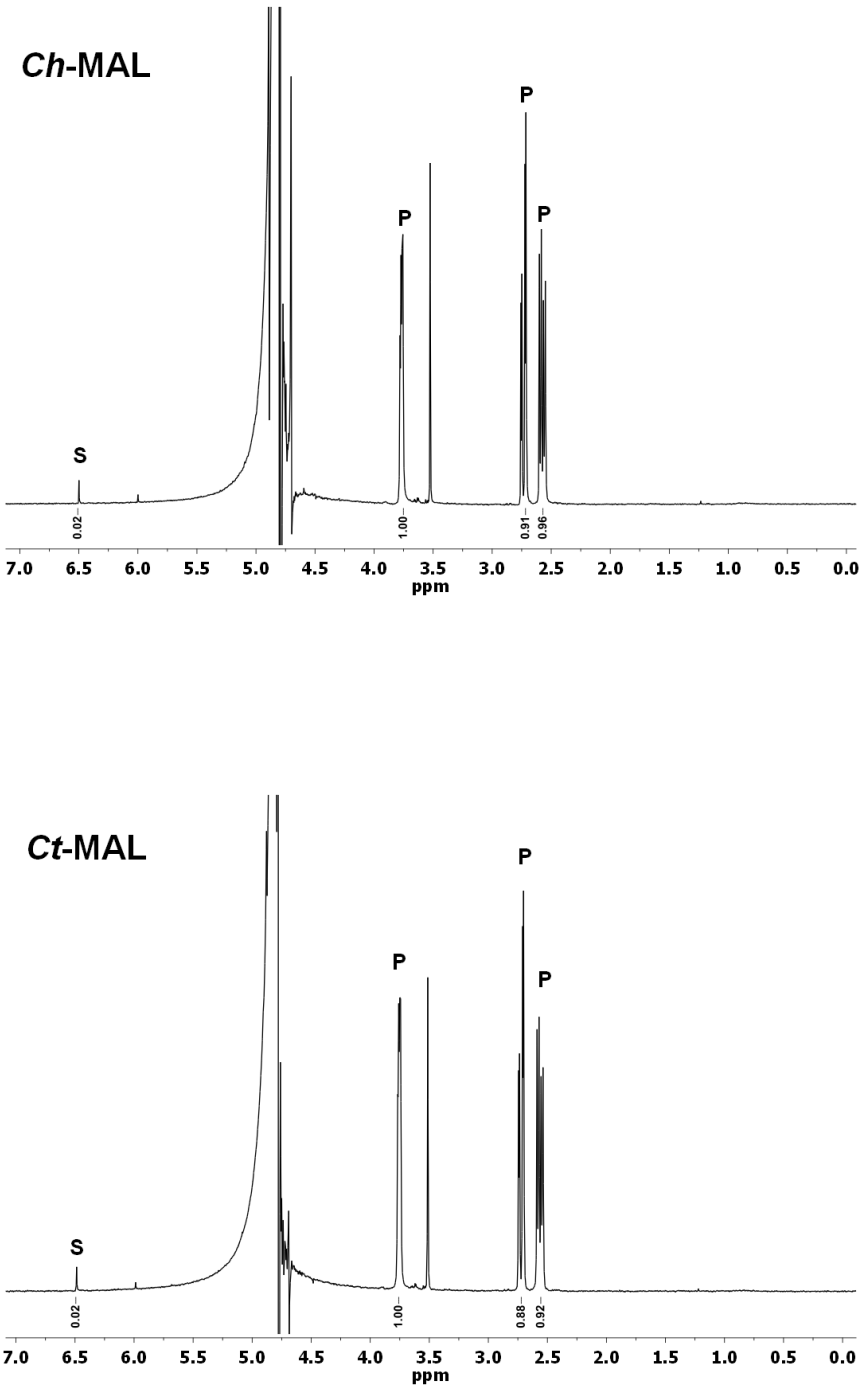

Figure S2. ^{1}H NMR spectra monitoring the *Ch*-MAL and *Ct*-MAL catalyzed amination of fumarate. The spectra were taken after 7 days of incubation at 22°C. For both *Ch*-MAL and *Ct*-MAL, the ratio of S:P = 1:99, respectively. S, fumarate; P, (*S*)-aspartic acid. The ^{1}H NMR signals for the enzymatically generated (*S*)-aspartic acid are identical to those found with an authentic standard. Impurity (Tris): δ = 3.5 (s).

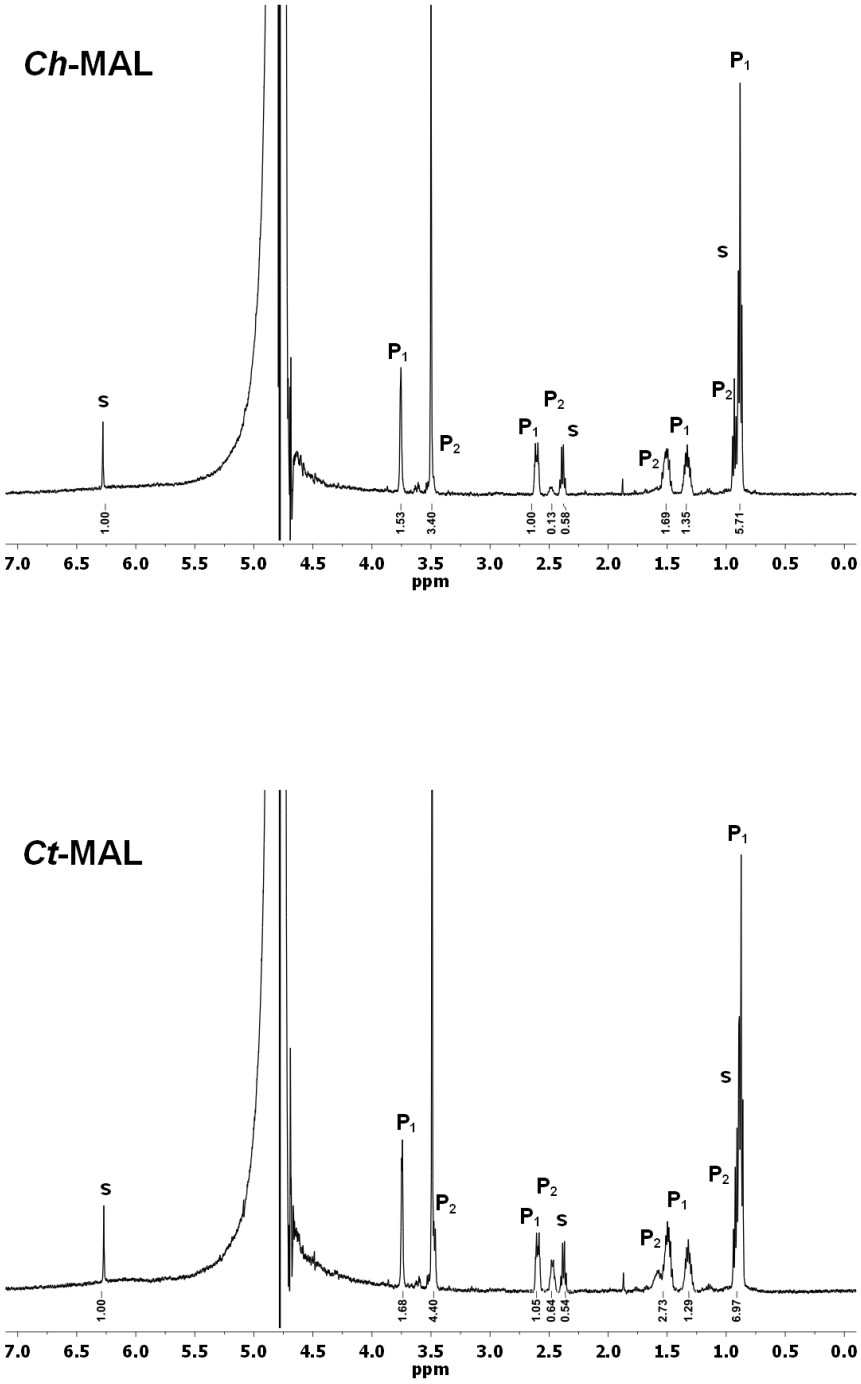

Figure S3. ^{1}H NMR spectra monitoring the *Ch*-MAL and *Ct*-MAL catalyzed ammonia addition to 2-ethylfumarate. The spectra were taken after 14 days of incubation at 22°C. For *Ch*-MAL and *Ct*-MAL, the ratio of S:P_1:P_2 = 35:60:5 and S:P_1:P_2 = 29:48:23, respectively. S, 2-ethylfumarate; P_1, *threo*-(2*S*,3*S*)-3-ethylaspartate (major diastereoisomer); P_2, *erythro*-(2*S*,3*R*)-3-ethylaspartate (minor diastereoisomer). The ^{1}H NMR signals for 2-ethylfumarate and (2*S*,3*S*)-3-ethylaspartate are reported elsewhere.[1] Impurity (Tris): δ = 3.5 (s).

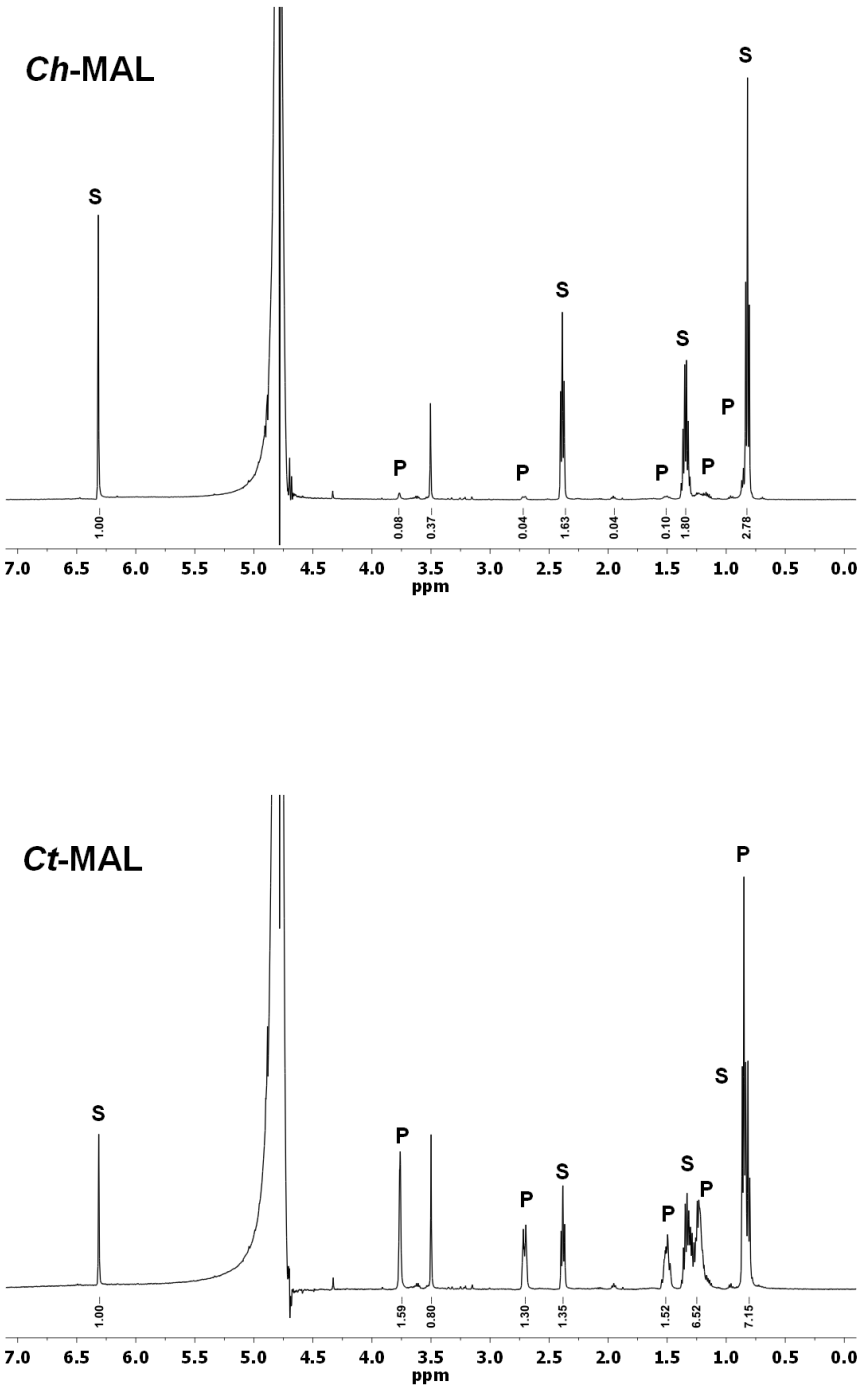

Figure S4. ^{1}H NMR spectra monitoring the *Ch*-MAL and *Ct*-MAL catalyzed ammonia addition to 2-propylfumarate. The spectra were taken after 14 days of incubation at 22°C. For *Ch*-MAL and *Ct*-MAL, the ratio of S:P = 93:7 and S:P = 39:61, respectively. S, 2-propylfumarate; P, *threo*-(2*S*,3*S*)-3-propylaspartate. ^{1}H NMR consistent with literature data.[1] Impurity (Tris): δ = 3.5 (s).

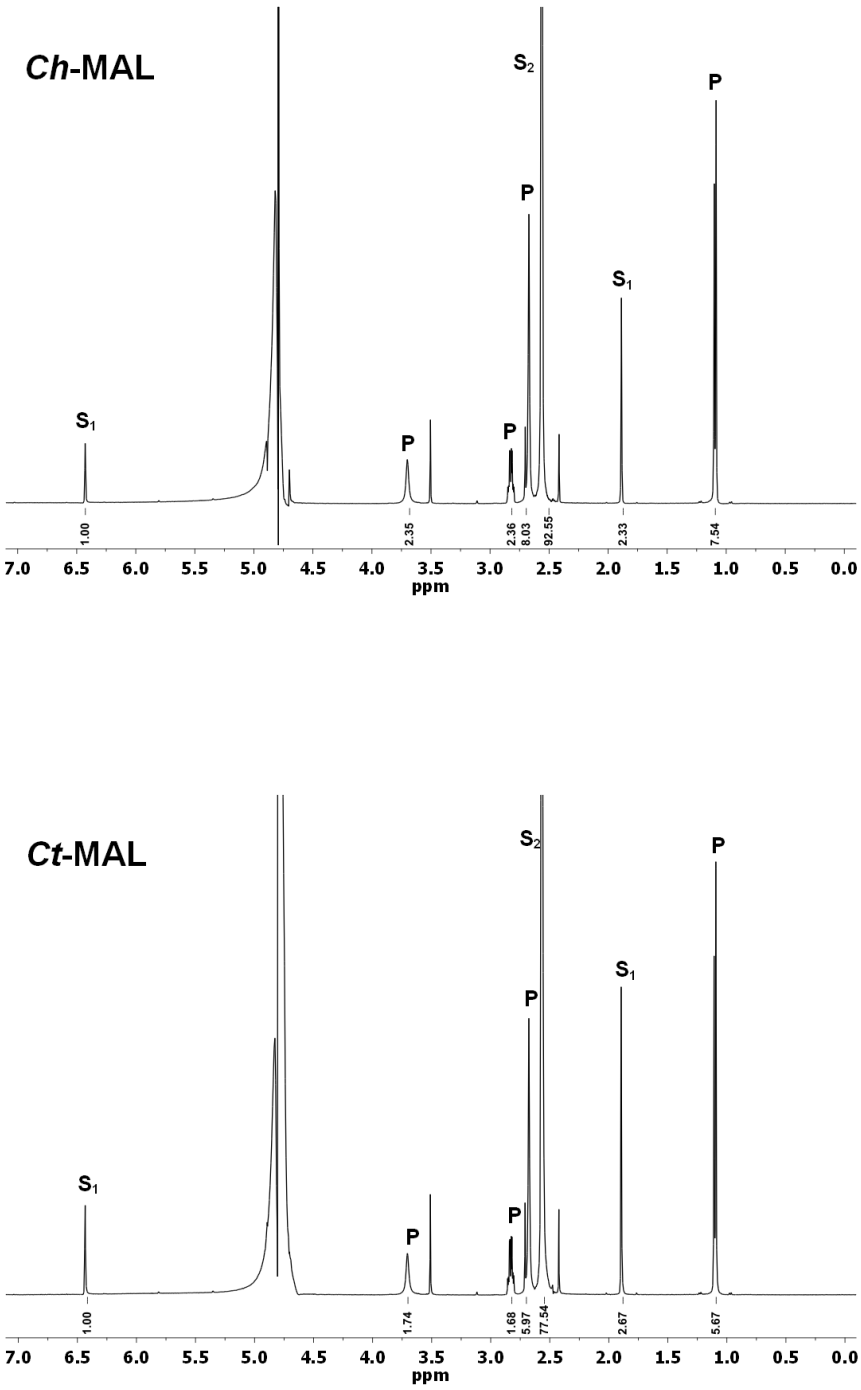

Figure S5. ^{1}H NMR spectra monitoring the *Ch*-MAL and *Ct*-MAL catalyzed methylamine addition to mesaconate. The spectra were taken after 14 days of incubation at 22°C. For *Ch*-MAL and *Ct*-MAL, the ratio of S_1:P = 30:70 and S_1:P = 36:64, respectively. S_1, mesaconate; S_2, methylamine; P, *threo*-(2*S*,3*S*)-*N*,3-dimethylaspartate. The ^{1}H NMR signals for (2*S*,3*S*)-*N*,3-dimethylaspartate are reported elsewhere.[2] Impurity (Tris): δ = 3.5 (s).

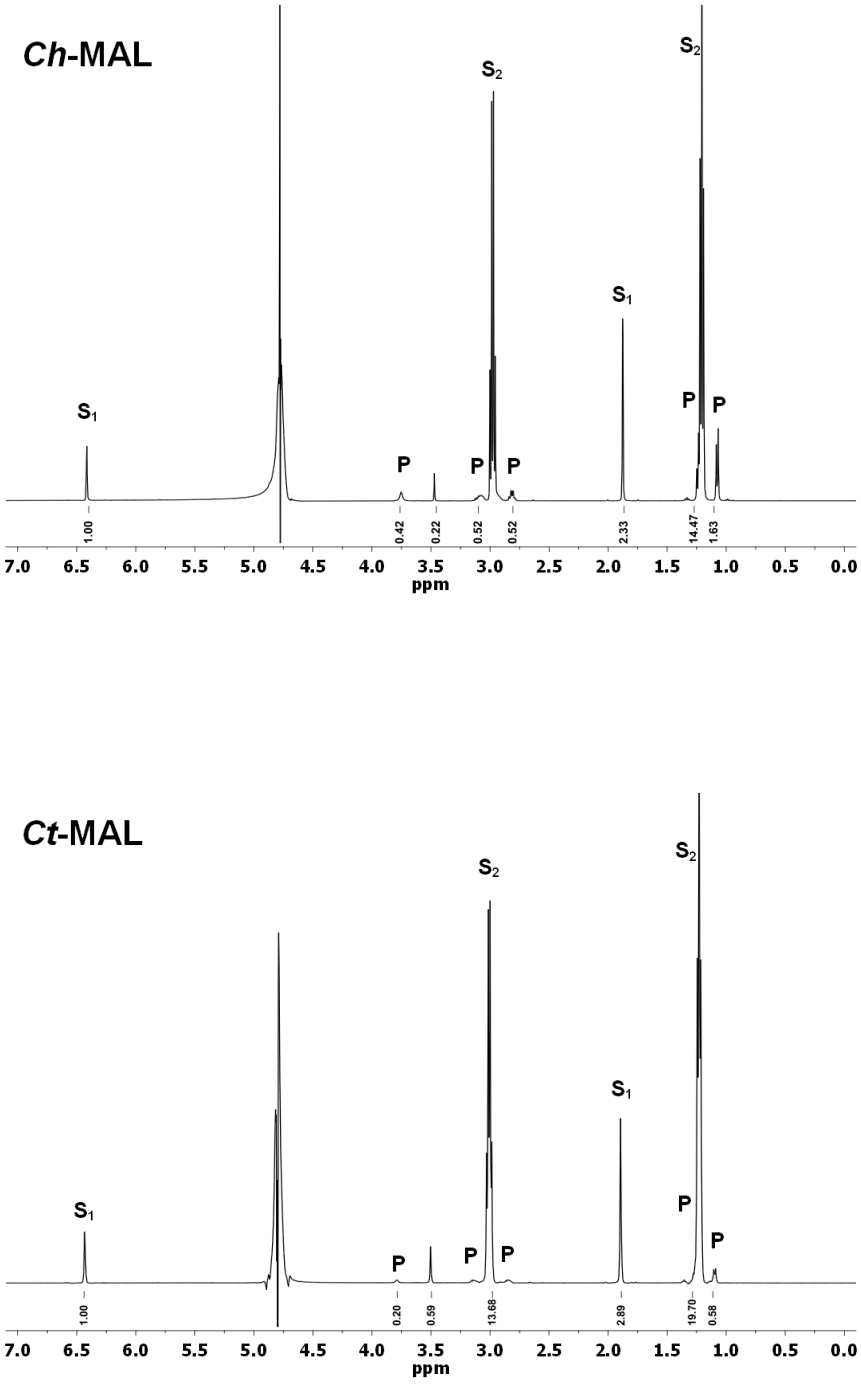

Figure S6. ^{1}H NMR spectra monitoring the *Ch*-MAL and *Ct*-MAL catalyzed ethylamine addition to mesaconate. The spectra were taken after 14 days of incubation at 22°C. For *Ch*-MAL and *Ct*-MAL, the ratio of S_1:P = 70:30 and S_1:P = 86:14, respectively. S_1, mesaconate; S_2, ethylamine; P, tentatively identified as 2-ethylamino-3-methylaspartic acid, the enzymatic synthesis of which has not been reported before. Impurity (Tris): δ = 3.5 (s).

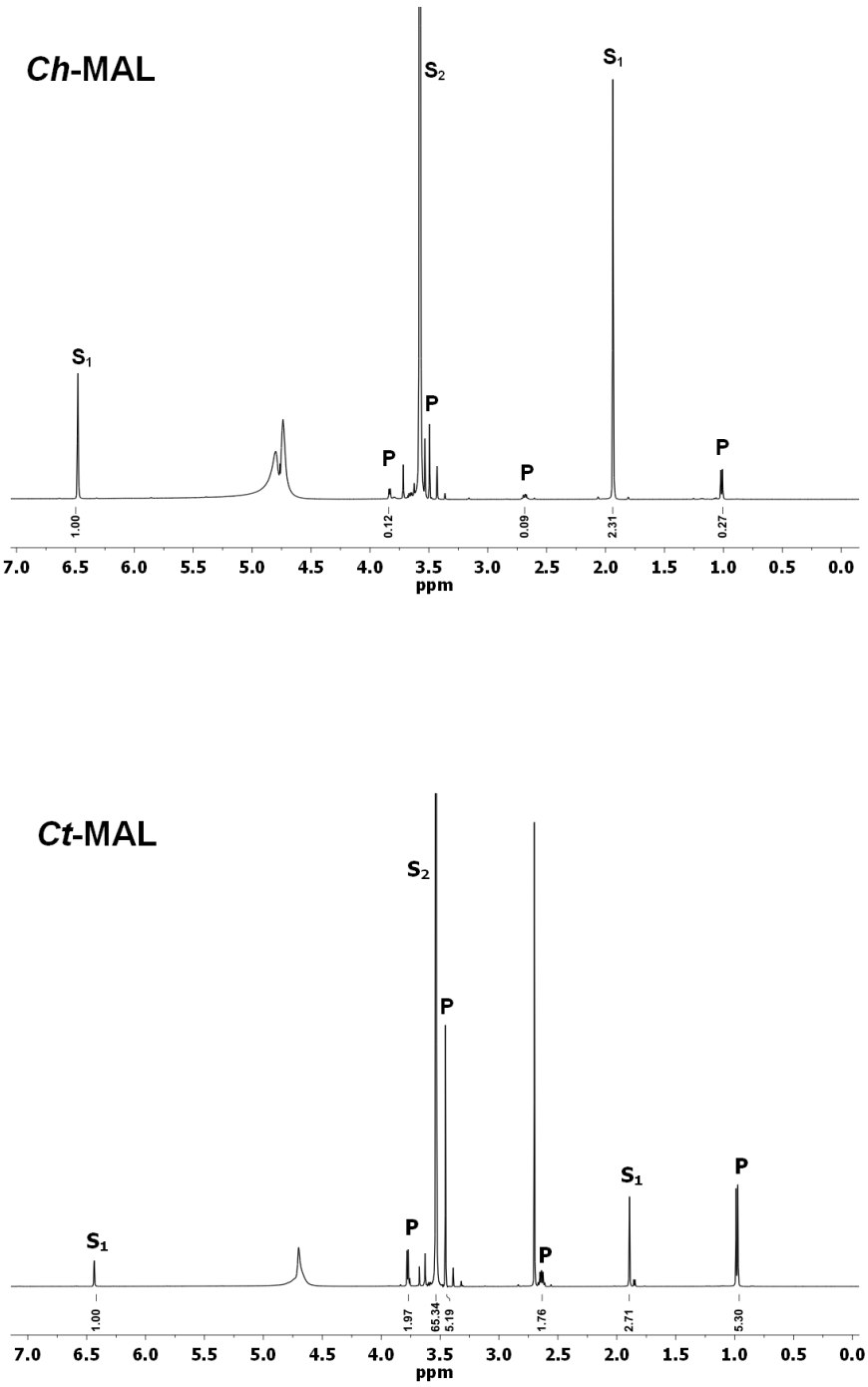

Figure S7. ^{1}H NMR spectra monitoring the *Ch*-MAL and *Ct*-MAL catalyzed methoxylamine addition to mesaconate. The spectra were taken after 14 days of incubation at 22°C. For *Ch*-MAL and *Ct*-MAL the ratio of S_1:P = 91:9 and S_1:P = 33:67, respectively. S_1, mesaconate; S_2, methoxylamine; P, *threo*-(2*S*,3*S*)-*N*-methoxy-3-methylaspartate. The ^{1}H NMR signals for (2*S*,3*S*)-*N*-methoxy-3-methylaspartate are reported elsewhere.[2] Impurities (Tris): δ = 3.5 (s); (DMSO): δ = 2.6 (s).

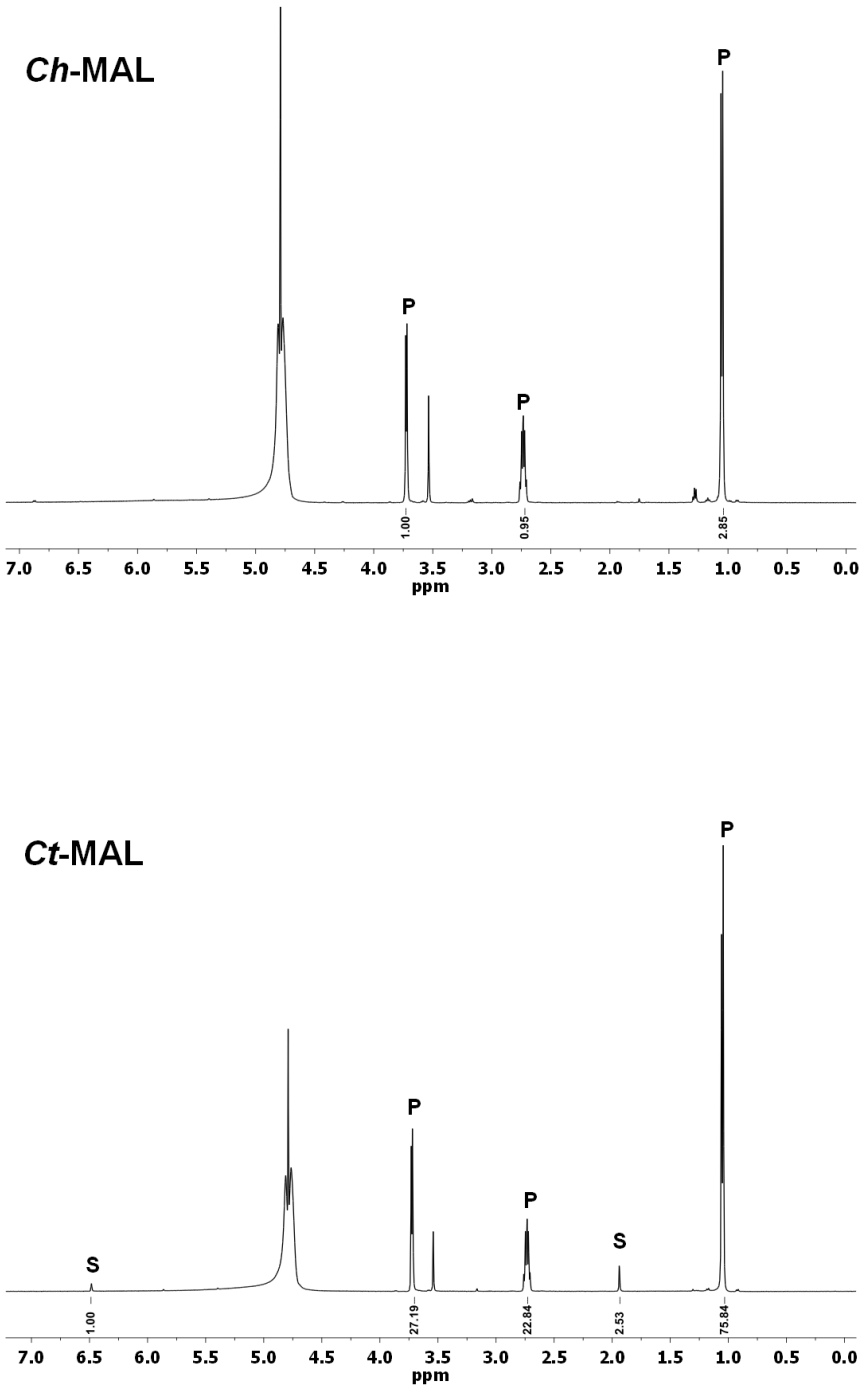

Figure S8. ^{1}H NMR spectra monitoring the *Ch*-MAL and *Ct*-MAL catalyzed hydroxylamine addition to mesaconate. The spectra were taken after 7 days of incubation at 22°C. For *Ch*-MAL and *Ct*-MAL the ratio of S:P = 1:99 and S:P = 4:96, respectively. S, mesaconate; P, *threo*-(2*S*,3*S*)-*N*-hydroxy-3-methylaspartate. The ^{1}H NMR signals for (2*S*,3*S*)-*N*-hydroxy-3-methylaspartate are reported elsewhere.[2] Impurity (Tris): δ = 3.5 (s).

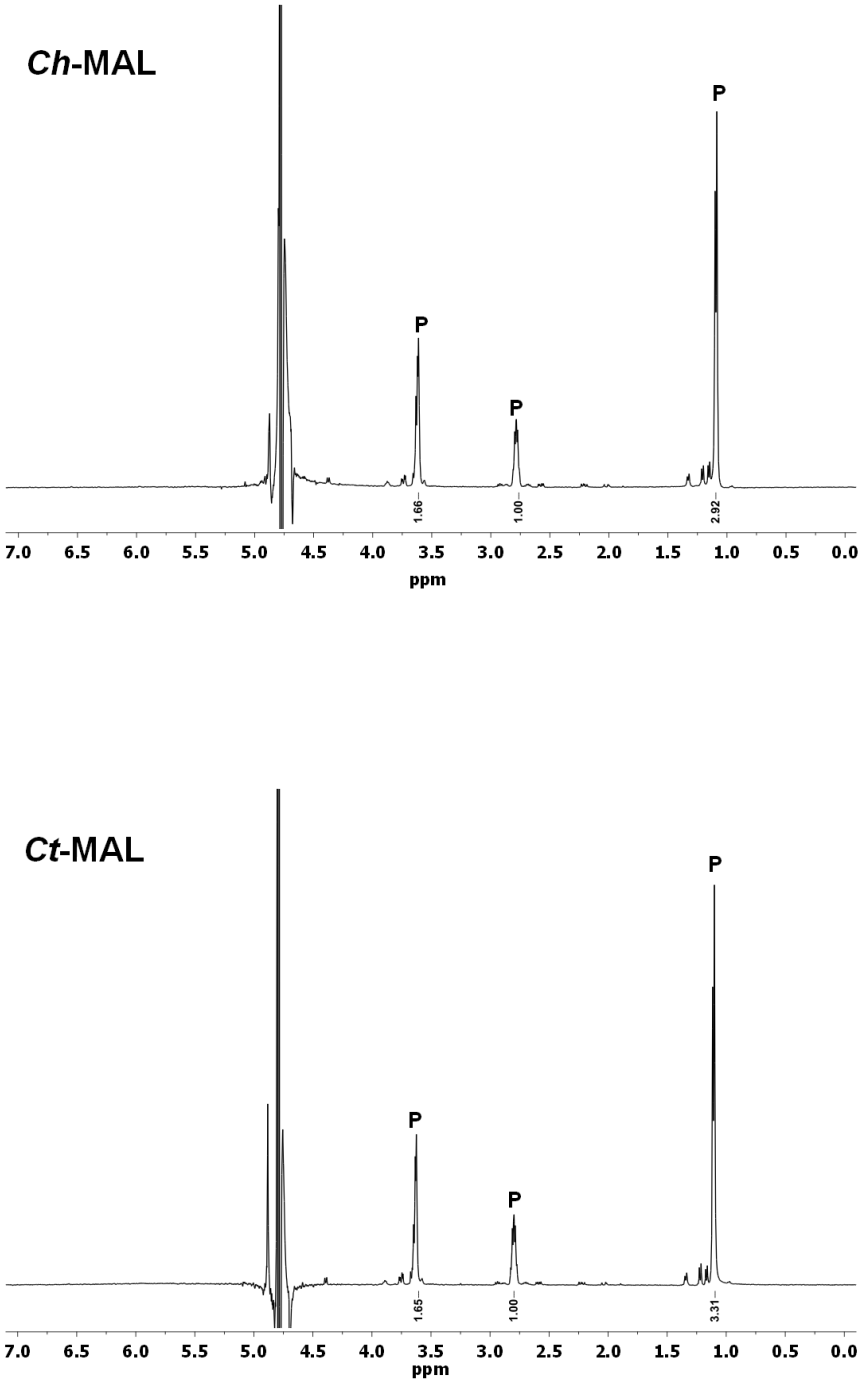

Figure S9. ^{1}H NMR spectra monitoring the *Ch*-MAL and *Ct*-MAL catalyzed hydrazine addition to mesaconate. The spectra were taken after 7 days of incubation at 22°C. For both *Ch*-MAL and *Ct*-MAL complete conversion of substrate to product was achieved. P, *threo*-(2*S*,3*S*)-2-hydrazino-3-methylaspartate. The ^{1}H NMR signals for (2*S*,3*S*)-2-hydrazino-3-methylaspartate are reported elsewhere.[2]

SUPPLEMENTARY REFERENCES

1. Akhtar, M., Botting, N. P., Cohen, M. A., and Gani, D. (1987) Enantiospecific synthesis of 3-susbtituted aspartic acid via enzymatic amination of substituted fumaric acid derivatives. *Tetrahedron 43*, 5899-5908.
2. Gulzar, M. S., Akhtar, M. and Gani, D. (1997) Preparation of *N*-substituted aspartic acids via enantiospecific conjugate addition of *N*-nucleophiles to fumaric acids using methylaspartase: synthetic utility and mechanistic implications. *J. Chem. Soc. Perkin Trans. I* 649-656.

PART FOUR

SUMMARY AND PERSPECTIVES

Chapter 8

Summary, concluding remarks and future perspectives

INTRODUCTION

Optically pure aspartic acid derivatives are highly valuable as tools for biological research and as chiral building blocks for pharmaceuticals and neutraceuticals. The preparation of these amino acids by traditional organic synthesis still remains a challenging task. In some cases, the use of a biocatalytic methodology can be an important, environmentally attractive, and highly competitive alternative option. Aspartate ammonia lyases (aspartases) and methylaspartate ammonia lyases (MALs) have been explored for producing optically pure L-aspartic acid and its derivatives. In industry, aspartases have been used for the preparation of enantiopure L-aspartic acid, an important starting compound for the synthesis of the artificial sweetener aspartame. Unfortunately, the substrate scope of aspartases is limited to fumarate and a few small substituted amines, yielding a limited number of L-aspartic acid derivatives. All our engineering attempts to broaden the substrate scope of aspartases were unsuccessful. Recently, the three-dimensional structure of an aspartase (AspB) in complex with L-aspartate was determined, showing that binding of the substrate in the active site triggers a complex loop movement. This large (~10 Å) loop movement is essential for catalysis as the loop closes over the active site to form the complete catalytic machinery of the enzyme. This makes the engineering of the substrate specificity of aspartases a formidable challenge.

MAL catalyzes the reversible addition of ammonia to mesaconate to give L-*threo*-(2*S*,3*S*)-3-methylaspartate and L-*erythro*-(2*S*,3*R*)-3-methylaspartate as products. MAL is a homodimeric enzyme that forms part of the glutamate catabolic pathway in anaerobic bacteria, and requires Mg^{2+} and K^{+} ions for full catalytic activity. The MAL from the anaerobic bacterium *Clostridium tetanomorphum* is the best characterized MAL with regard to substrate scope and biochemical properties. It accepts a few small amines as alternative nucleophiles that can replace ammonia in the addition to mesaconate, yielding a limited number of *N*-substituted methylaspartic acids. MAL also accepts a few fumarate derivatives with short 2-alkyl substituents as alternative electrophiles in the ammonia addition reaction, yielding a small set of 3-substituted aspartic acids. Hence, the

biocatalytic applicability of MAL is limited by its poor diastereoselectivity and narrow substrate scope. Interestingly, the crystal structure of MAL in complex with the natural substrate shows that the catalytic machinery of MAL is intact and, unlike aspartases, it does not undergo a large conformational change upon substrate binding, thereby making it more amenable to protein engineering. In **Chapter 1**, we have reviewed the properties, structures, catalytic mechanisms and biocatalytic applications of aspartate and methylaspartate ammonia lyases.

The aim of the work described in this thesis was to engineer MAL in order to enhance its diastereoselectivity and to broaden its substrate scope, and to explore the newly designed biocatalysts for their usefulness in the stereoselective synthesis of a wide variety of valuable aspartic acid derivatives. In addition, we aimed to clone and characterize a MAL from a thermophilic bacterium, with a view to obtain a thermostable MAL that could be exploited for large scale amino acid synthesis and as template in future engineering experiments.

Engineering the stereoselectivity and substrate specificity of MAL

We have focused our studies on MAL from the anaerobic bacterium *Clostridium tetanomorphum*, which is the best characterized MAL to this date, and further exploited it as template in our engineering experiments. The crystal structure of MAL from *Citrobacter amalonaticus* in complex with L-*threo*-(2*S*,3*S*)-3-methylaspartate provided the essential information about the residues that interact with the substrate (Figure 1). It was suggested that MAL operates via a general-base mechanism, where Lys-331 abstracts the 3*S*-proton and His-194 abstracts the 3*R*-proton from the respective isomer of 3-methylaspartic acid (Figure 1a). In **Chapter 2**, we have investigated the importance of the Lys-331 and His-194 residues for the activity and diastereoselectivity of MAL by site-directed mutagenesis. Kinetic studies have shown that mutations at the Lys-331 and His-194 positions have a profound effect on the k_{cat} and k_{cat}/K_m values, implying that these residues are mechanistically important. Product analysis by ^{1}H NMR spectroscopy showed that the K331A and H194A mutants have altered diastereoselectivity in the amination of mesaconate, with a preference

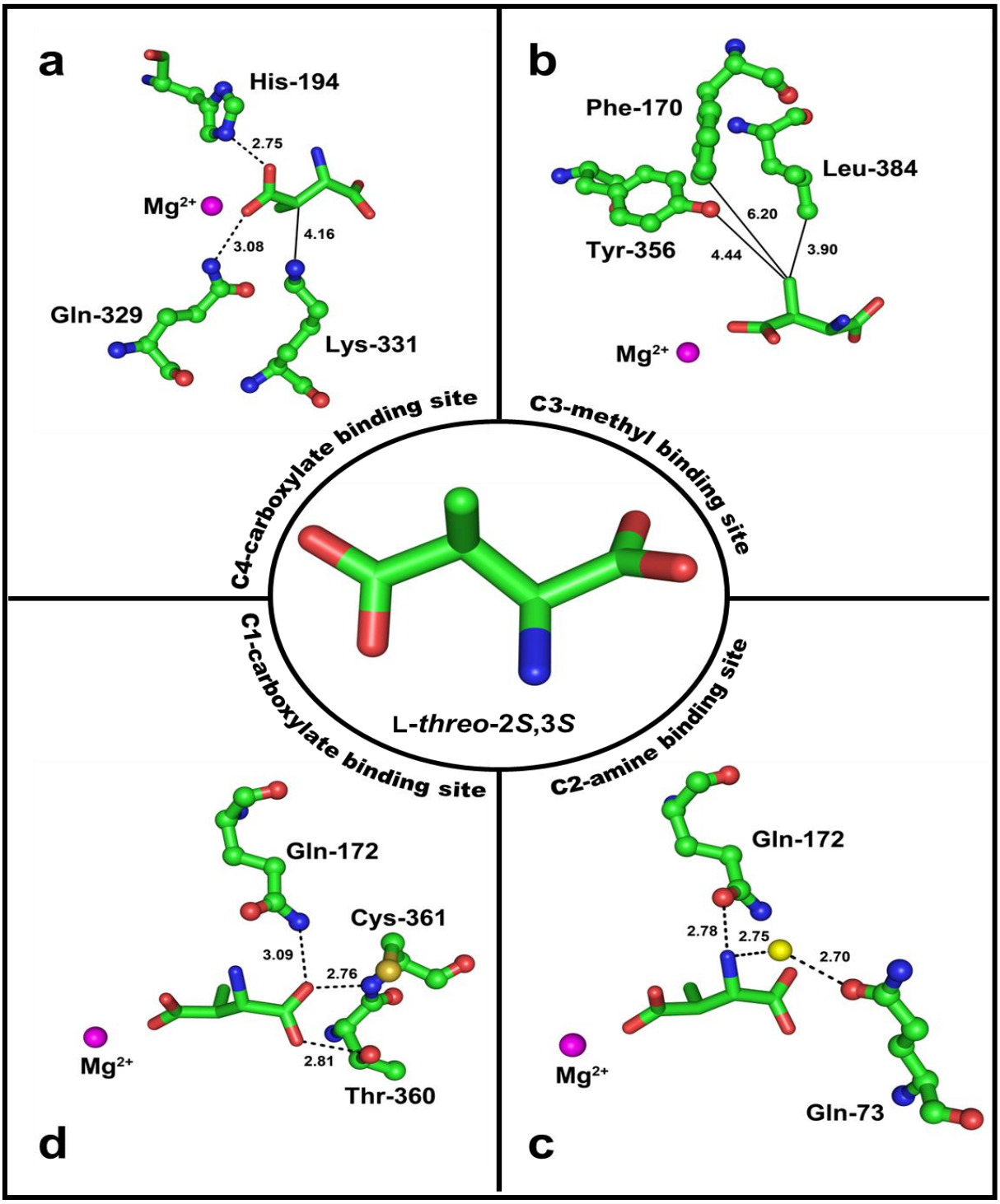

Figure 1. Crystal structure of MAL in complex with the natural substrate L-*threo*-(2*S*,3*S*)-3-methylaspartate. A close-up of the active site showing hydrogen bond interactions (dashed lines) or observed distances (solid lines) between (**a**) the substrate's C4 carboxylate group and the side chains of His-194, Gln-329 and Lys-331; (**b**) the substrate's C3 methyl group and side chains of Phe-170, Tyr-356 and Leu-384; (**c**) the substrate's C2 amino group and side chains of Gln-73 and Gln-172; and (**d**) the substrate's C1-carboxylate group and side chains of Gln-172, Thr-360 and Cys-361. The carbon atoms of the active site residues and the substrate are shown in green. The magnesium ion and water molecule are shown as magenta and yellow spheres, respectively. The figure was prepared using PyMOL (www.pymol.org).

for the formation of L-*threo*-3-methylaspartic acid, suggesting that these residues play an important role in controlling the stereoselectivity of MAL. It has been suggested that the high diastereoselectivity of the H194A mutant can be exploited for the stereoselective synthesis of the *threo* isomers of various 3-substituted aspartic acids.

In **Chapter 3**, we describe the engineering of MAL to broaden its substrate scope. Guided by the crystal structure of MAL in complex with the substrate, we selected the residues lining the substrate binding pocket of the enzyme (Figure 1). To enlarge the nucleophile scope of MAL, the residues which are involved in the formation of the substrate's amine binding pocket were selected and subjected to saturation mutagenesis (Figure 1c). Mutants were screened for their ability to catalyze methylamine addition to mesaconate. This approach resulted in a single active site mutant (Q73A) with strongly improved activity for the methylamine addition reaction. Furthermore, the Q73A mutant exhibits a very broad nucleophile scope, including structurally diverse linear and cyclic alkylamines, in the addition to mesaconate. The enzyme-catalyzed amine addition reactions are highly diastereoselective, only yielding the *threo* isomers of the corresponding *N*-substituted methylaspartic acids (*de* >95%). Likewise, to expand the electrophile scope of MAL, the residues lining the substrate's methyl-binding pocket were subjected to saturation mutagenesis (Figure 1b). Mutants were screened for their ability to catalyze ammonia addition to 2-hexylfumarate. This approach resulted in a single active site mutant (L384A), which showed pronounced amination activity towards 2-hexylfumarate. Interestingly, the L384A mutant exhibits a very broad electrophile scope including fumarate derivatives with alkyl, aryl, alkoxy, aryloxy, alkylthio and arylthio substituents at the C2 position. However, while providing high regioselectivities, the L384A mutant-catalyzed amination reactions provided varying degrees of diastereoselectivity. Structural analysis of the Q73A and L384A mutants showed that both mutants have an enlarged active site that accommodates the new substrates. These engineered MALs have exciting potential for applications in the asymmetric synthesis of various *N*- or 3-substituted aspartic acids.

Biocatalytic applications of the engineered MAL mutants

Next, we demonstrated the preparative usefulness of the engineered MAL mutants. The use of the Q73A mutant for the enantioselective synthesis of a large variety of *N*-substituted aspartic acids by the addition of structurally diverse amines to fumaric acid is described in **Chapter 4**. The purified enzyme was incubated with fumaric acid and various amines in separate reaction mixtures. Interestingly, by using only 0.05 mol% of biocatalyst, excellent (91-100%) conversions were achieved within 0.5-48 h. The single amino acid products were isolated and identified by ^{1}H NMR, ^{13}C NMR, and HRMS as the corresponding *N*-substituted aspartic acids. To establish the absolute configurations and enantiopurity of these amino acid products, authentic standards with known L- or D- configuration were synthesized by reductive amination. Comparative chiral HPLC analysis of the amino acid products and authentic standards showed that the enzyme-catalyzed amine additions are highly enantioselective, only yielding the L-enantiomers of the corresponding amino acid products (>99% *ee*).

In **Chapter 5**, we describe kinetic resolutions and asymmetric synthesis of various 3-substituted aspartic acids using the H194A and H194A/L384A mutant enzymes as biocatalysts. First, we established that the H194A-catalyzed reaction is highly regio-, enantio- and diastereoselective by demonstrating the preparative usefulness of the H194A enzyme in the selective synthesis of L-*threo*-(2*S*,3*S*)-3-methylaspartic acid. Then, we exploited the high regio- and stereoselectivity of the H194A mutant in kinetic resolutions and asymmetric synthesis to produce various 3-substituted aspartic acids, including *threo*-3-methoxyaspartic acid, an important inhibitor of excitatory glutamate transporters (EAAT2 and EAAT5) in the brain. We also showed that the biocatalytic applicability of the H194A mutant can be broadened by combining the high stereoselectivity of the H194A mutant with the broad electrophile scope of the L384A mutant by generating the double mutant H194A/L384A, which allowed the selective synthesis of *threo*-3-butylaspartic acid. Thus, these engineered MALs have potential for application in the stereoselective preparation of various 3-substituted aspartic acids.

Detailed catalytic mechanism of MAL

In **Chapter 6**, we describe the roles of active site residues in the catalytic mechanism of MAL. Based on the crystal structure of MAL in complex with L-*threo*-(2*S*,3*S*)-3-methylaspartic acid (Figure 1), we selected seven active site residues (Gln-73, Phe-170, Gln-172, Tyr-356, Thr-360, Cys-361, Leu-384) lining the substrate binding pocket and investigated their importance for the activity and diastereoselectity of MAL. The selected residues were subjected to site-directed mutagenesis and the mutant enzymes were characterized for their structural integrity, by using CD spectroscopy and native PAGE, and ability to catalyze the amination of mesaconate, using both kinetic assays and ^{1}H NMR spectroscopy. Based on the observed properties of the mutant enzymes, combined with previous kinetic isotope measurements, structural studies and protein engineering work, we propose a detailed catalytic mechanism for the MAL catalyzed reaction. In this proposed mechanism, Lys-331 acts as the primary base that abstracts the 3*S*-proton from L-*threo*-3-methylaspartate, resulting in an enolate anion intermediate. This enolic intermediate is stabilized by the essential Mg^{2+} ion and the Gln-329 residue. Collapse of this intermediate results in the release of ammonia and the formation of mesaconate. Similarly, His-194 acts as the secondary base and abstracts the 3*R*-proton from the L-*erythro* isomer of 3-methylaspartic acid, yielding the enolic intermediate. The side chains of the active site residues that form the C1 carboxylate-binding pocket (Gln-172, Thr-360 and Cys-361), the C2 amino-binding pocket (Gln-73 and Gln-172) and C3 methyl-binding pocket (Phe-170, Tyr-356 and Leu-384) provide additional interactions, which are essential for substrate binding and activation. This detailed knowledge of the catalytic mechanism of MAL can serve as a guide for future engineering experiments.

Cloning and characterization of a thermostable methylaspartate ammonia lyase

In **Chapter 7**, we describe the cloning, heterologous expression, and purification of a methylaspartate ammonia lyase (designated *Ch*-MAL) from the thermophilic bacterium *Carboxydothermus hydrogenoformans* Z-2901. *Ch*-MAL is a homodimer in solution and shows

optimal activity at 70°C and pH 9.0. Heat-inactivation assays showed that the purified enzyme is stable at 50°C for several hours, which is the highest thermal stability observed among known MALs. *Ch*-MAL accepts fumarate, 2-methylfumarate, 2-ethylfumarate, and 2-propylfumarate as substrates in the ammonia addition reaction. The enzyme also processes methylamine, ethylamine, hydrazine, hydroxylamine, or methoxylamine as an alternative nucleophile that can replace ammonia in the addition to mesaconate, resulting in the corresponding *N*-substituted methylaspartic acids with a very high diastereomeric excess. The high thermostability and stereoselectivity, and the broad substrate scope, make *Ch*-MAL an attractive biocatalyst for large scale, asymmetric synthesis of aspartic acid derivatives and a promising template for future engineering experiments.

Conclusions and future perspectives

In the work described in this thesis, we have engineered both the stereoselectivity and substrate specificity of MAL. The structure-guided engineering of MAL led to the identification of three single-active-site mutants: one shows strongly enhanced diastereoselectivity (H194A), one exhibits a very broad nucleophile scope (Q73A), and one accepts a wide range of electrophiles (L384A). The usefulness of these engineered MALs for the selective synthesis of various substituted aspartic acids has convincingly been demonstrated. This is perhaps best illustrated by the L384A-catalyzed synthesis of L-*threo*-(2*S*,3*S*)-3-benzyloxyaspartic acid (L-TBOA in Figure 2), an important inhibitor of excitatory glutamate transporters in the brain. Compared to the difficult and laborious 15-steps chemical synthesis of L-TBOA, our 3-steps chemo-enzymatic synthesis of L-TBOA (*de* >98% and *ee* >99%) provides a simple and environmentally friendly method to produce this important compound.

Next, there is a need to develop second generation MAL-based biocatalysts, which have an even larger substrate scope and are more robust than the first generation MAL-based biocatalysts. For instance, the L384A mutant enzyme exhibits a broad electrophile scope, but shows poor diastereoselectivity. To improve the stereoselectivity of this mutant enzyme, we constructed the

double mutant L384A\H194A, where we combined the broad electrophile scope of the L384A mutant with the high stereoselectivity of the H194A mutant. Unfortunately, the double mutant shows very low-level amination activity. Therefore, we have initiated studies to improve the catalytic activity of the double mutant. If successful, the newly engineered second generation biocatalyst may be highly useful for the stereoselective synthesis of a wide variety of 3-substituted aspartic acids.

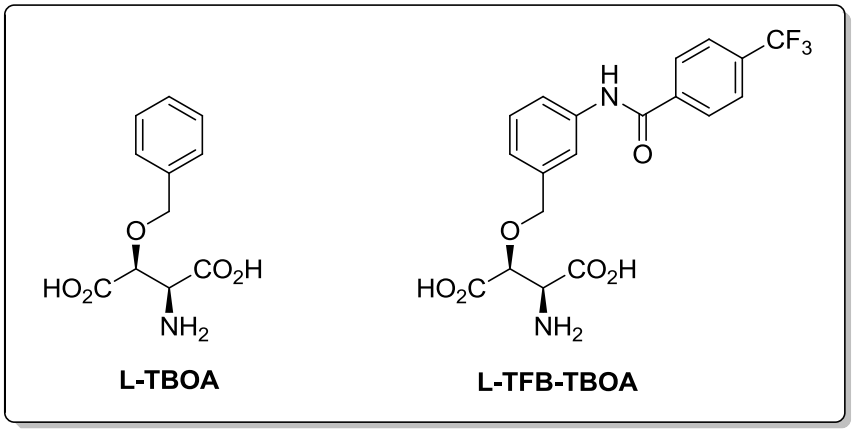

Figure 2. Structures of L-TBOA and L-TFB-TBOA.

Similarly, the nucleophile scope of the Q73A mutant is mainly confined to relatively small (C1-C7) primary amines. To synthesize large and complex *N*-substituted aspartic acids, which can be used as building blocks for low-calorie sweeteners, such as the aspartame derivatives advantame and neotame (Figure 3), the nucleophile scope of MAL-Q73A needs to be broadened to also include large and branched primary amines. Likewise, to synthesize large L-TBOA derivatives such as L-TFB-TBOA (Figure 2), which is the most potent inhibitor of excitatory glutamate transporters in the brain, MAL-L384A needs to be engineered to accept very large 2-aryloxy fumarates. To further expand the nucleophile or electrophile scope of MAL, *in silico* mutagenesis combined with substrate docking can be an attractive strategy to reduce the sequence space that has to be covered to identify valuable mutants. The catalytic activity of the designed mutants can be further improved by random mutagenesis (e.g., error-prone PCR) and activity screening.

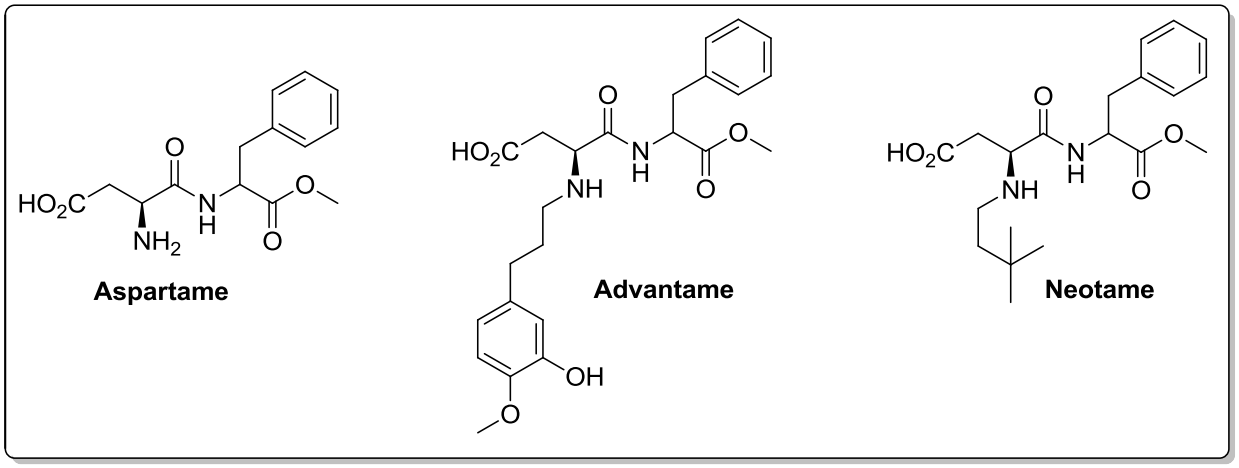

Figure 3. Structures of aspartame, advantame, and neotame.

The results presented in this thesis suggested that combining the broad nucleophile scope of the Q73A mutant with the broad electrophile scope of the L384A mutant could yield a new enzyme with the ability to process many different combinations of substituted amines and fumarates. However, the MAL double mutant (Q73A/L384A) is almost completely inactive and thus not suitable for amino acid synthesis. In future work, we therefore aim to construct a focused library by saturation mutagenesis at positions 73 and 384, screening of which may yield various active biocatalysts optimized for unique combinations of nucleophile and electrophile. It is important to note that not all nucleophile-electrophile combinations are likely to be productive as very large substituents on both the amine and fumarate substrates may sterically hinder the addition reaction.

Until now, we were successful in engineering the stereoselectivity and substrate specificity of MAL for the production of a wide range of α-amino acids. The next highly challenging step will be to engineer MAL for the synthesis of various β-amino acids. Unfortunately, the redesign of the binding pocket for the substrate's C1 carboxylate group by saturation mutagenesis at positions Gln-172, Thr-360 and Cys-361 (Figure 1d) did not result in mutants with amination activity towards unsaturated monocarboxylic acids. Therefore, we have started an engineering programme that aims to engineer MAL for the asymmetric synthesis of β-amino acids by targeting multiple sites at the

same time, with a view to benefit from synergistic effects encountered by multiple simultaneous mutations. This approach requires a robust and sensitive screening assay, for example detection of the desired activity by HPLC from a pool of 100-500 clones (so-called cluster screening).

Chapter 9

Samenvatting, conclusies en toekomstperspectief

INTRODUCTIE

Optisch zuivere asparaginezuurderivaten zijn uitermate waardevol voor biologisch onderzoek en zijn tevens belangrijke chirale bouwstenen voor farmaceutica en nutraceutica (een hypogram van de woorden nutriënt en farmaceutica). De bereiding van deze aminozuren door middel van traditionele organische synthese is tot op de dag van vandaag een enorme uitdaging. In een aantal gevallen kan de toepassing van een biokatalytische methode een belangrijk, milieuvriendelijk en competitief alternatief zijn. Aspartaat ammonia-lyases (aspartases) en methylaspartaat ammonia-lyases (MALs) zijn enzymen die onderzocht zijn, en worden, voor de productie van optisch zuiver L-asparaginezuur en derivaten daarvan. In de chemische industrie worden aspartases toegepast voor de productie van enantiomeerzuiver L-asparaginezuur, hetgeen een belangrijke bouwsteen is voor de kunstmatige zoetstof aspartaam. Helaas is het aantal substraten dat door aspartases wordt geaccepteerd voor omzetting tot asparaginezuurderivaten beperkt tot fumaarzuur en een aantal kleine, gesubstitueerde amines. Wij hebben in onze onderzoeksgroep geprobeerd om, door middel van het muteren van aspartases, het aantal substraten dat door dit enzym wordt omgezet uit te breiden. Deze pogingen zijn helaas op niets uitgelopen. Recentelijk is de driedimensionale structuur opgehelderd van een aspartase (AspB) in complexatie met het substraat L-aspartaat (i.e. het carboxylaatanion van asparaginezuur; Latijn: i.e., id est, dat wil zeggen). Deze driedimensionale structuur maakte duidelijk dat de binding van het substraat in het actieve centrum van het enzym een ingewikkelde beweging van een lus van het enzym teweeg brengt. De relatief grote beweging (10 Å) van deze lus is essentieel voor de katalyse die het enzym uitvoert aangezien de lus het actieve centrum niet alleen afdicht maar tevens completeert. Deze gegevens maken dat het muteren van aspartases, om zodoende het aantal substraten dat voor omzetting wordt geaccepteerd te verhogen, een enorme uitdaging is.

MAL katalyseert de reversibele additie van ammonia aan 2-methylfumaarzuur hetgeen de producten L-*threo*-(2*S*,3*S*)-3-methylasparaginezuur en L-*erythro*-(2*S*,3*R*)-3-methylasparaginezuur

oplevert. MAL is een homodimerisch enzym dat een rol speelt in de katabole route van glutamaat in anaerobe bacteriën en het heeft Mg^{2+} en K^{+} ionen nodig om maximale katalytische activiteit te bereiken. De MAL die voorkomt in de anaerobe bacterie *Clostridium tetanomorphum* is de best gekarakteriseerde MAL wat betreft substraatacceptatie en biochemische eigenschappen. Het enzym accepteert naast ammonia een beperkt aantal andere, kleine amines als nucleofiele substraten voor de additie aan 2-methylfumaarzuur hetgeen slechts een gelimiteerd aantal *N*-gesubstitueerde asparaginezuren als producten oplevert. MAL accepteert ook een klein aantal fumaarzuurderivaten met korte 2-alkylsubstituenten als alternatieve elektrofielen voor ammonia-additie hetgeen in slechts een beperkt aantal 3-gesubstitueerde asparaginezuurderivaten resulteert. Het gelimiteerd aantal nucleofiele als wel elektrofiele substraten dat door MAL wordt geaccepteerd voor enzymatische omzetting houdt in dat de biokatalytische toepassing van dit enzym beperkt is. Eens temeer omdat de producten met lage diastereomere overmaten worden verkregen. Het is interessant dat de kristalstructuur van MAL in complexatie met het natuurlijke substraat (i.e. L-*threo*-3-methylaspartaat) laat zien dat het actieve centrum van MAL conformationeel stabiel is en, in tegenstelling tot aspartases, géén grote conformationele verandering ondergaat als gevolg van substraatbinding. Dit houdt in dat het wellicht makkelijker is om MAL te muteren dan om aspartases te muteren zonder dat de werking van het actieve centrum wordt aangetast. In **hoofdstuk 1** zijn de eigenschappen, structuren, katalytische mechanismen en biokatalytische toepassingen van aspartases en methylaspartaat ammonia-lyases (MALs) op een rij gezet.

De doelen van de onderzoeken die in dit proefschrift zijn beschreven zijn om door middel van het muteren van MAL enerzijds het aantal substraten dat door MAL wordt geaccepteerd voor omzetting te verhogen en anderzijds de optische zuiverheid (i.e. diastereomere en enantiomere overmaten) waarmee de producten worden verkregen te verhogen. Het vervolgdoel is om te testen of deze nieuw ontworpen biokatalysatoren bruikbaar zijn voor de stereoselectieve synthese van een breed scala aan asparaginezuurderivaten. Een aanvullend doel is om een MAL uit een thermofiele bacterie te kloneren en te karakteriseren om zodoende een (thermo)stabiel MAL te verkrijgen dat

inzetbaar is voor grote-schaal-synthese van aminozuren en dat als een uitgangspunt kan dienen voor toekomstige mutatie-experimenten.

Mutaties van MAL om stereoselectiviteit en acceptatie van aantal substraten te verhogen

Wij hebben onze onderzoeken gefocust op MAL verkregen uit de anaerobe bacterie *Clostridium tetanomorphum,* de meest uitvoerig gekarakteriseerde MAL tot op dit moment, en het aangewend als uitgangspunt (*template*) voor onze mutatie-experimenten. De kristalstructuur van MAL uit *Citrobacter amalonaticus* in complexatie met L-*threo*-(2*S*,3*S*)-3-methylaspartaat gaf essentiële informatie over welke aminozuurresiduen interactie aangaan met het substraat (Figuur 1). Er is geopperd dat katalyse in MAL via een algemeen zuur-base-mechanisme werkt waarin Lys-331 het 3*S*-proton en His-194 het 3*R*-proton abstraheert van het betreffende isomeer van 3-methylasparaginezuur (Figuur 1a). In **hoofdstuk 2** is beschreven hoe het belang van de residuen Lys-331 en His-194 voor katalytische werking en stereoselectiviteit van MAL is onderzocht door middel van gerichte mutaties (*site-directed mutagenesis*) op posities 331 en 194. Kinetiek-experimenten hebben laten zien dat mutatie van zowel Lys-33 als His-194 een aanmerkelijk effect heeft op de k_{cat} en k_{cat}/K_m waarden van de natuurlijke activiteit hetgeen duidelijk maakt dat beide residuen een belangrijke rol spelen in het katalyse mechanisme. Productanalyse met behulp van ^{1}H NMR spectroscopie heeft aangetoond dat de K331A- en de H194A-mutant de diastereoselectiviteit van de aminering van 2-methylfumaarzuur hebben veranderd en zeer sterke voorkeur geven aan formatie van L-*threo*-3-methylasparaginezuur. Dit resultaat geeft aan dat de residuen op posities 331 en 194 een grote invloed hebben op de diastereoselectiviteit. Wellicht kan de hoge diastereoselectiviteit van de H194A-mutant benut worden voor de stereoselectieve synthese van de *threo*-isomeren van een reeks van 3-gesubstitueerde asparaginezuren.

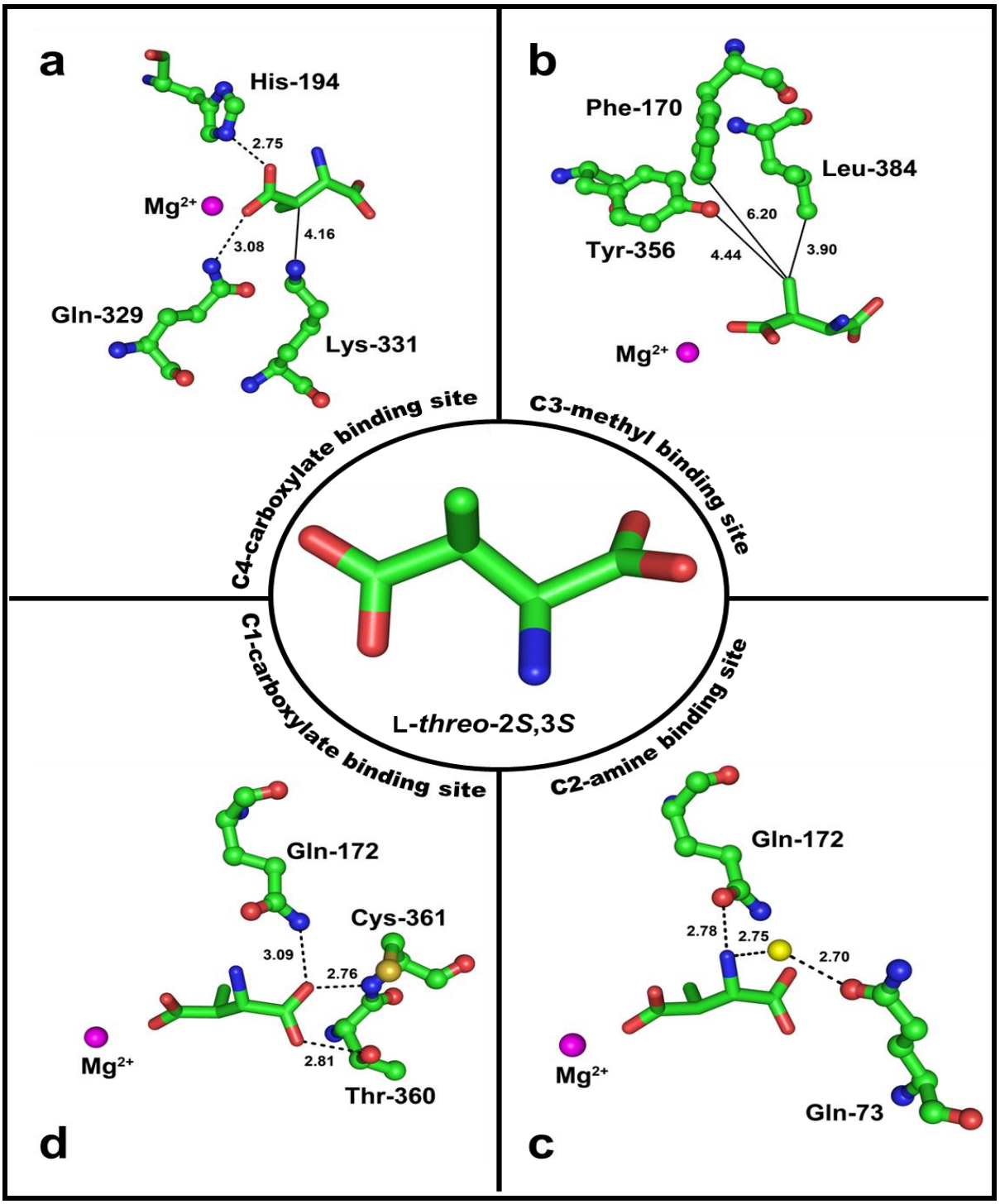

Binding site = bindingslocatie

Figuur 1. Kristalstructuur van MAL in complexatie met het natuurlijke substraat L-*threo*-(2*S*,3*S*)-3-methylaspartaat. Uitvergrotingen van het actieve centrum laten waterstofbruginteracties (stippellijnen) en atoomafstanden (ononderbroken lijnen) zien tussen (**a**) de C4-carboxylaatgroep van het substraat en de zijketens van de residuen His-194, Gln-329 en Lys-331; (**b**) de C3-methylgroep van het substraat met de zijketens van de residuen Phe-170, Tyr-356 en Leu-384; (**c**) de C2-aminogroep van het substraat met de zijketens van de residuen Gln-73 en Gln-172; en (**d**) de C1-carboxylaatgroep van het substraat en de

zijketens van de residuen Gln-172, Thr-360 en Cys-361. De koolstofatomen van de residuen in het actieve centrum en het substraat zijn groen gekleurd. Het magnesium ion en het watermolecuul zijn met, respectievelijk, magenta en geel gekleurde bollen afgebeeld. De afbeeldingen zijn gemaakt met behulp van het programma PyMOL (www.pymol.org).

In **hoofdstuk 3** staan de mutatie-experimenten met MAL beschreven met als doel de acceptatie van het aantal substraten te verhogen. Aan de hand van de kristalstructuur van MAL met het natuurlijke substraat zijn de residuen geselecteerd die verantwoordelijk zijn voor substraatbinding binnen het enzym (Figuur 1). Om het aantal substraten dat door MAL wordt geaccepteerd voor omzetting te vergroten zijn de residuen die verantwoordelijk zijn voor binding met de aminogroep van het substraat (residuen 73 en 172, Figuur 1c) onderworpen aan gerandomiseerde mutatie-experimenten (*saturation mutagenesis*). De op deze manier verkregen mutanten zijn vervolgens getest op hun vermogen om methylamine te adderen aan 2-methylfumaarzuur. Met deze aanpak is er een enkelvoudige mutant (Q73A) gevonden met een sterk verhoogde katalytische activiteit voor de additiereactie van methylamine. Bovendien accepteert de Q73A-mutant een breed scala van lineaire en cyclische alkylamines als nucleofiele substraten voor de additie aan 2-methylfumaarzuur. Het enzym katalyseert de amine-addities met hoge diastereoselectiviteit (*de* >95%) waarbij de *threo*-isomeren van de *N*-gesubstitueerde methylasparaginezuren in overmaat verkregen werden. Dezelfde strategie (*saturation mutagenesis*) is toegepast op de residuen die een rol spelen in de binding van de methylgroep van het substraat (Phe-170, Tyr-356 en Leu-384) om zodoende het aantal elektrofiele substraten te verhogen dat door MAL wordt geaccepteerd (Figuur 1b). De mutanten zijn onderzocht op hun vermogen om de additie van ammonia aan 2-hexylfumaraat te katalyseren. Er werd één enkelvoudige mutant gevonden (L384A) met een sterk verhoogde activiteit. Interessant genoeg accepteert deze mutant ook een ruime, aanvullende collectie van fumaarzuren met alkyl-, aryl-, alkoxy-, aryloxy-, alkylthio- en arylthiosubstituenten op de C2-positie, als elektrofiele substraten. Echter, ondanks dat de L384A-mutant de amine-addities met hoge regioselectiviteit uitvoert, variëren de diastereoselectiviteiten. Structuuranalyses van de Q73A- en de L384A-mutant

lieten zien dat beide mutanten een vergroot actief centrum hebben dat in staat is om de collectie van nieuwe, grotere substraten te accommoderen en te binden. Deze gemuteerde MALs hebben de aansprekende potentie om toegepast te worden in de asymmetrische synthese van *N*- en 3-gesubstitueerde asparaginezuren.

Biokatalytische toepassingen van de MAL-mutanten

In een volgende serie experimenten is de bruikbaarheid van de MAL-mutanten in preparatieve schaalexperimenten aangetoond. Het aanwenden van de Q73A-mutant voor de enantioselectieve synthese van een groot aantal *N*-gesubstitueerde asparaginezuren door middel van additie van verschillende amines aan fumaarzuur is beschreven in **hoofdstuk 4**. Het gezuiverde enzym werd geïncubeerd met fumaarzuur en de verschillende amines in afzonderlijke experimenten. Met slechts 0,05 mol% biokatalysator (i.e. Q73A) werden uitstekende conversies (91-100%) bereikt na reactietijden die variëren van 30 minuten tot 48 uur. In alle afzonderlijke experimenten werd slechts één aminozuurproduct gevonden. De producten werden gezuiverd en geïdentificeerd als *N*-gesubstitueerde asparaginezuren met behulp van ^{1}H NMR, ^{13}C NMR en HRMS spectroscopie. Om de absolute configuraties en de enantiomere zuiverheden van deze aminozuurproducten te achterhalen werden er referentiestoffen met bekende L- of D-configuratie gesynthetiseerd door middel van reductieve aminering. Analyses met HPLC, met een chirale vaste fase, van de aminozuurproducten en de referentieverbindingen toonden aan dat de enzym-gekatalyseerde amine-additions met hoge enantioselectiviteiten (*ee* >99%) plaatsvinden en dat de L-enantiomeren in overmaat worden verkregen.

In **Hoofdstuk 5** zijn de kinetische resoluties en asymmetrische syntheses van verschillende 3-gesubstitueerde asparaginezuren met behulp van de H194A- en de H194A/L384A-mutant beschreven. Ten eerste hebben we aangetoond dat L-*threo*-(2*S*,3*S*)-3-methylasparaginezuur op preparatieve schaal met hoge regio-, enantio- en diastereoselectiviteit verkregen kan worden door middel van katalyse met de H194A-mutant. Vervolgens zijn de hoge regio- en stereoselectiviteit

van de H194A-mutant benut voor kinetische resolutie-experimenten en asymmetrische synthese van meerdere 3-gesubstitueerde asparaginezuren. Onder andere van *threo*-3-methoxyasparaginezuur hetgeen een belangrijke inhibitor is van excitatorische glutamaattransporters (EAAT2 en EAAT5) in de hersenen. Er is tevens aangetoond dat de biokatalytische toepasbaarheid van de H194A-mutant uitgebreid kan worden wanneer de hoge stereoselectiviteit van H194A gecombineerd wordt met de brede substraatacceptatie van de L384A-mutant (i.e. de hoeveelheid aan substraten die door L384A wordt geaccepteerd). De dubbelmutant H194A/L384A kan inderdaad selectief de vorming van *threo*-3-butylasparaginezuur katalyseren en aan de hand hiervan kan geconcludeerd worden dat gemuteerde MALs de potentie hebben om toegepast te worden in de stereoselectieve synthese van een veelheid aan 3-gesubstitueerde asparaginezuren.

Gedetailleerd katalytisch mechanisme van MAL

In **hoofdstuk 6** worden de individuele rollen van de residuen in het actieve centrum van MAL beschreven in het katalytische mechanisme. Aan de hand van de kristalstructuur van MAL in complexatie met L-*threo*-(2*S*,3*S*)-3-methylaspartaat (Figuur 1) zijn er zeven residuen in het actieve centrum geselecteerd (Gln-73, Phe-170, Gln-172, Tyr-356, Thr-360, Cys-361 en Leu-384) en onderzocht op hun rol in de activiteit en diastereoselectiviteit van MAL. De geselecteerde residuen zijn onderworpen aan gerichte mutagenese (*site-directed mutagenesis*) en de mutanten zijn geïdentificeerd op basis van hun structuureigenschappen met behulp van CD-spectroscopie en *native PAGE* (PAGE met niet-gedenatureerd proteïne). De mutanten zijn tevens met een kinetisch onderzoek (*kinetic assay*) en met ^{1}H NMR spectroscopie getoetst op hun vermogen om de aminering van 2-methylfumaarzuur te katalyseren. Gebaseerd op de eigenschappen van de mutanten, eerder uitgevoerd kinetisch isotoop onderzoek, structuurstudies en enzymmutaties is er een gedetailleerd katalytisch mechanisme van MAL voorgesteld. In dit voorgestelde mechanisme acteert Lys-331 als een primaire base dat het 3*S*-proton van L-*threo*-3-methylaspartaat abstraheert hetgeen resulteert in een enolaatanion. Dit enolisch intermediair wordt gestabiliseerd door het

essentiële Mg^{2+} ion en het Gln-329 residu. Verval van dit intermediair resulteert in het vrijkomen van ammonia en de formatie van 2-methylfumaarzuur. Op eenzelfde wijze acteert His-194 als een secundaire base en abstraheert het het 3*R*-proton van de L-*erythro*-isomeer van 3-methylaspartaat eveneens resulterend in het enolisch intermediair. De zijketens van de residuen die tezamen in het actieve centrum de bindingslocatie vormen voor de C1-carboxylaatgroep (Gln-172, Thr-360 en Cys-361), de C2-aminefunctionaliteit (Gln-73 en Gln-172) en de C3-methylgroep (Phe-170, Tyr-356 en Leu-384) gaan bijkomende interacties aan die essentieel zijn voor substraatbinding en activering. Deze gedetailleerde informatie over het katalytische mechanisme van MAL geeft de richting aan voor toekomstige mutatie-experimenten.

Het kloneren en karakteriseren van een thermostabiel methylaspartaat ammonia-lyase

In **hoofdstuk 7** wordt het kloneren, de heterologische expressie en de zuivering beschreven van een methylaspartaat ammonia-lyase (genoteerd als *Ch*-MAL) die verkregen is uit de thermofiele bacterie *Carboxydothermus hydrogenoformans* Z-2901. *Ch*-MAL is een homodimeer in oplossing en heeft een optimale activiteit bij 70°C en een pH van 9.0. Hitte-inactivatie-studies hebben laten zien dat het gezuiverde enzym enkele uren stabiel is bij 50°C hetgeen betekent dat *Ch*-MAL de meest stabiele en hittebestendige is van alle bekend zijnde MALs. *Ch*-MAL accepteert fumaraat, 2-methylfumaraat, 2-ethylfumaraat en 2-propylfumaraat als substraten voor ammonia-additie. Het enzym accepteert bovendien methylamine, ethylamine, hydrazine, hydroxylamine en methoxylamine als alternatieve nucleofielen in plaats van ammonia voor de additie aan 2-methylfumaarzuur. De corresponderende *N*-gesubstitueerde methylasparaginezuurproducten werden met zeer hoge diastereomere overmaten verkregen. De hoge thermostabiliteit en stereoselectiviteit tezamen met de uitgebreide substraatacceptatie maken dat *Ch*-MAL een aantrekkelijke biokatalysator is voor asymmetrische grote-schaal-synthese van asparaginezuurderivaten. Tevens is het een veelbelovend uitgangspunt voor toekomstige mutatie-experimenten.

Conclusies en toekomstperspectief

Gedurende het onderzoek dat in dit proefschrift beschreven wordt is het enzym MAL zodanig gemuteerd dat zowel de stereoselectiviteit als wel het aantal substraten dat geaccepteerd wordt voor omzetting zijn verhoogd. Op basis van kristalstructuren zijn mutaties van verschillende residuen in het actieve centrum van MAL doorgevoerd. Deze hebben geleid tot de identificatie van drie enkelvoudige mutanten: één met een sterk verbeterde diastereoselectiviteit (H194A), één die een uitgebreide hoeveelheid aanvullende nucleofiele substraten accepteert voor omzetting (Q73A) en ten slotte één die een significante hoeveelheid aanvullende elektrofiele substraten accepteert voor omzetting (L384A). De bruikbaarheid van deze MAL-mutanten voor de selectieve synthese van diverse gesubstitueerde asparaginezuren is overtuigend aangetoond. Dit wordt wellicht het best geïllustreerd met de door de L384A-mutant gekatalyseerde synthese van L-*threo*-(2*S*,3*S*)-3-benzyloxyasparaginezuur (L-TBOA in Figuur 2), een belangrijke inhibitor van excitatorische glutamaattransporters in de hersenen. Vergeleken met de moeilijke en tijdrovende 15-staps chemische synthese van L-TBOA is onze 3-staps chemo-enzymatische synthese van L-TBOA (*de* >98% en *ee* >99%) een simpele en milieuvriendelijke methode voor het vervaardigen van deze stof.

Op basis van de resultaten beschreven in de voorgaande alinea ontstond er de behoefte om een tweede generatie op MAL gebaseerde biokatalysatoren te ontwikkelen die een nóg grotere hoeveelheid substraten accepteert voor omzetting en tevens meer robuust is dan de eerste generatie MAL-afgeleide biokatalysatoren. De L384A-mutant accepteert bijvoorbeeld een grote hoeveelheid substraten voor omzetting maar heeft een lage diastereoselectiviteit. Om de stereoselectiviteit van deze mutant te verhogen werd de dubbelmutant L384A\H194A geconstrueerd. Op deze manier werd een poging gedaan om de uitgebreide substraatacceptatie van de L384A-mutant te combineren met de hoge diastereoselectiviteit van de H194A-mutant. Helaas bleek de dubbelmutant een lage amineringsactiviteit te hebben. Vanwege dit resultaat zijn we met een onderzoek begonnen om de katalytische activiteit van de dubbelmutant te verbeteren. Wanneer dit succesvol verloopt zou deze

tweede generatie biokatalysatoren, met nieuwe mutaties, bruikbaar kunnen zijn voor de stereoselectieve synthese van een brede variëteit van 3-gesubstitueerde asparaginezuren.

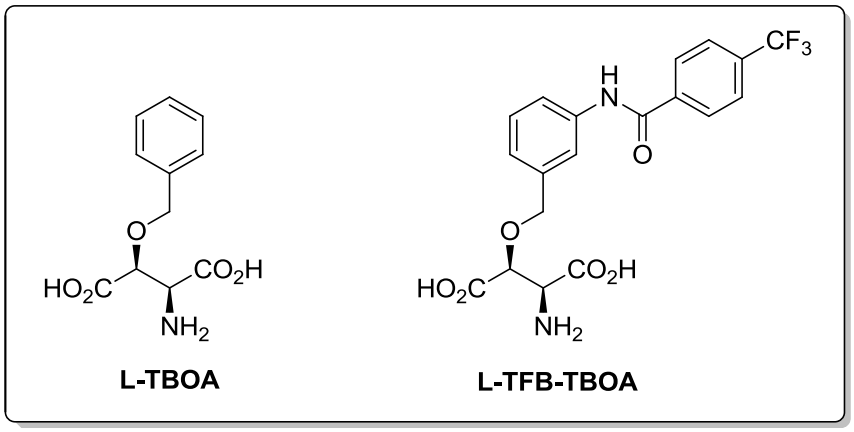

Figuur 2. Structuren van L-TBOA en L-TFB-TBOA.

Op vergelijkbare wijze beperkt zich het aantal nucleofielen dat door de Q73A-mutant wordt geaccepteerd tot een aantal relatief kleine (C1-C7) primaire amines. Om grote en complexe *N*-gesubstitueerde asparaginezuren te synthetiseren, die kunnen dienen als bouwstenen voor lage-calorie zoetstoffen zoals de aspartaamderivaten advantaam en neotaam (Figuur 3), zal het palet aan nucleofielen dat door MAL-Q73A geaccepteerd wordt voor omzetting uitgebreid moeten worden met grotere en vertakte amines. Vergelijkbaar hiermee zal MAL-L384A op zodanige wijze gemuteerd moeten worden dat het relatief grote 2-aryloxyfumaraten accepteert als substraten om zodoende grote L-TBOA-derivaten te synthetiseren zoals L-TFB-TBOA (Figuur 2), de meest potente inhibitor van excitatorische glutamaattransporters in de hersenen. De combinatie van *in silico* mutagenese en substraat-accommodatie (*substrate docking*) is wellicht een aantrekkelijke strategie om de essentiële mutaties te vinden die *in vitro* doorgevoerd moeten worden om het aantal nucleofiele als wel elektrofiele substraten te verhogen dat door MAL wordt geaccepteerd én om er voor te zorgen dat het aantal mutanten dat *in vitro* gescreend moet worden (*sequence space*), om een verbeterde mutant te vinden, niet te hoog wordt. Vervolgens kan gepoogd worden om de

katalytische activiteit van de op deze manier ontworpen mutanten verder te verbeteren met gerandomiseerde mutagenese (i.e. *error-prone PCR*) en activiteitsonderzoeken.

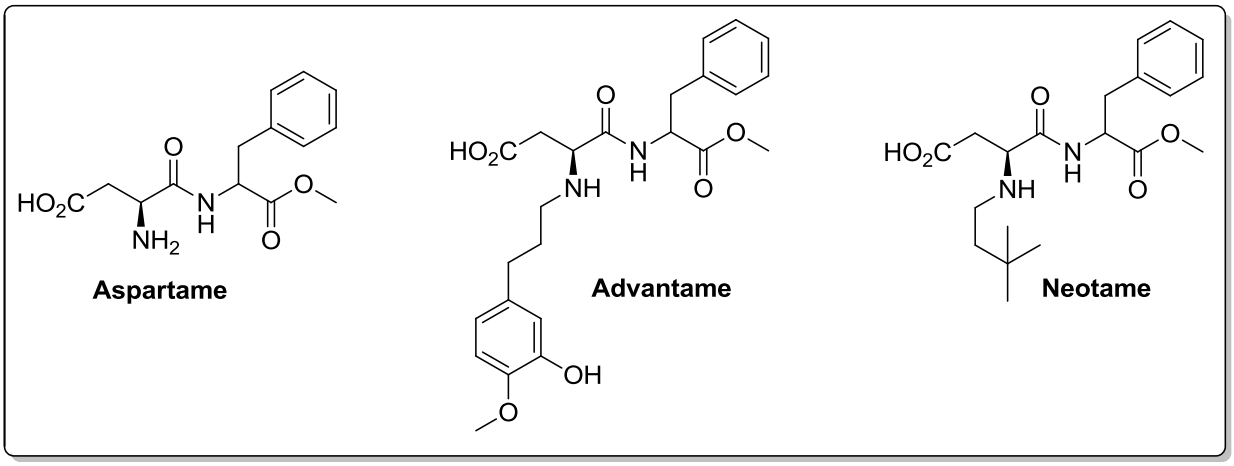

Figuur 3. Structuren van aspartaam, advantaam en neotaam.

De resultaten die in dit proefschrift gepresenteerd worden suggereren dat de combinatie van het gevarieerd aantal nucleofielen dat door de Q73A-mutant wordt geaccepteerd en de collectie elektrofielen die door de L384A-mutant wordt geaccepteerd een nieuw enzym (Q73A/L384A) kan opleveren dat in staat is om vele verschillende combinaties van amines en fumaraten om te zetten. Echter, de MAL-dubbelmutant Q73A/L384A is vrijwel inactief en daarom ongeschikt voor de synthese van aminozuren. Met toekomstig onderzoek zullen we daarom door middel van *saturation mutagenesis* een doelgerichte bibliotheek construeren van dubbelmutanten die gemuteerd zijn op posities 73 en 384. Het onderzoeken van deze bibliotheek levert hopelijk verschillende biokatalysatoren op die ieder een optimale activiteit hebben voor omzetting van een unieke combinatie van een nucleofiel en een elektrofiel substraat. Het is belangrijk om te beseffen dat hoogstwaarschijnlijk niet alle nucleofiel-elektrofiel-combinaties succesvol zullen worden omgezet aangezien grote substituenten op zowel het amine- als het fumaarzuursubstraat de additiereactie sterisch kunnen hinderen.

Op dit moment hebben we MAL succesvol gemuteerd zodat de stereoselectiviteit en de hoeveelheid substraten die geaccepteerd worden, voor de synthese van een grote collectie α-aminozuren, zijn verhoogd. De volgende grote uitdaging zal zijn om MAL zodanig te muteren dat het de synthese van β-aminozuren kan katalyseren. Helaas heeft een herontwerp van de bindingslocatie van de C1-carboxylaatgroep van het substraat door middel van *saturation mutagenesis* van posities Gln-172, Thr-360 en Cys-361 (Figuur 1d) niet tot mutanten geleid die de amine-additie aan onverzadigde monocarbonzuren kunnen katalyseren. Dit is de reden dat we zijn begonnen om verschillende groepen van residuen van MAL tegelijkertijd te muteren om zodoende één of meerdere mutanten te verkrijgen die de asymmetrische synthese van β-aminozuren kunnen katalyseren. De achterliggende gedachte is dat er wellicht een synergistisch effect optreedt wanneer er verschillende groepen residuen tegelijkertijd worden gemuteerd. Deze onderzoeksopzet vereist een pragmatische, en ook gevoelige, manier van detectie van de gewenste activiteit, bijvoorbeeld het meten van de activiteit van clusters van 100 tot 500 kloons met behulp van HPLC (i.e. *cluster screening*).

Appendix

Acknowledgements

List of Publications

ACKNOWLEDGEMENTS

Here it ends! I hope that from now on I don't have to answer the question when I will be finished with my studies. Many people have contributed to this journey in different ways, and now I would like to take this opportunity to thank every one of them.

First and foremost, I offer my earnest gratitude to my supervisor and promotor Prof. Dr. **Gerrit J. Poelarends**. Gerrit, your support, motivation, guidance and unflinching encouragements was instrumental towards the completion of this thesis. I admire your passion and enthusiasm for science and research. I respect your caring, friendly and easy going attitude towards your students. Last but not the least; I admire your meticulousness in describing science in words. Gerrit, thank you very much for providing me an opportunity to work as your student, truly I learned a lot from you.

I am deeply grateful to my second promotor Prof. Dr. **Wim J. Quax** for giving me the opportunity to carry out my PhD work at the Department of Pharmaceutical Biology. Wim, I have always appreciated your views. The way you connect science from lab bench to its commercial aspect, which scientists often least care about, is very inspiring. Thanks for teaching the basics of sailing without knowing that I have poor swimming skills.

I would also like to thank the members of the reading committee, Prof. Dr. **A. S. S. Dömling**, Prof. Dr. ir. **M. W. Fraaije** and Prof. Dr. ir. **A. J. Minnaard**.

My heartfelt thanks to Prof. Dr. **Dick B. Janssen** for his valuable critical remarks and suggestions during various meetings. Your comments on our manuscripts were always of great help and compelled me to look at my data differently. Besides science I also appreciate your knowledge about Dutch history, geography and honey bees.

I would like to thank Prof. Dr. **Ben L. Feringa** for his very enthusiastic and inspiring remarks on our manuscripts. I would also like to thank Dr. **Barbara Weiner**, with whom we initiated our first

collaboration on the MAL project at the Organic Chemistry Lab. I offer my special thanks to Dr. **Wiktor Szymański**, a very positive, enthusiastic and friendly chemist (an occasional biochemist). Wiktor, thanks for teaching me the organic synthesis and purifications of amino acids. Your support and prompt replies to my e-mails and queries were very helpful.

I would like to offer my sincere thanks to B-Basic group members from Zernike (**Wu Bian**, **Ciprian**, **Gjalt**, **Jan** and **Alja**) and people from DSM Geleen (Dr. **Oliver May** and Dr. **Stefaan de Wildeman**) for the fruitful collaboration over the years.

My sincere thanks to **Andre** and Prof Dr. **Frank J. Dekker** for their support, help and discussions in chemistry lab in the Pharmacy building.

My warm thanks to **Henriëtte J. Rozeboom** and Dr. **A.M.W.H. Thunnissen** for crystallizing the MAL mutants in a rather short time. I really appreciate the assistance provided by the staff at the NMR facility at Zernike (**Pieter van der Meulen**), at the Mass Spectroscopy facility at Pharmacy building (**Annie van Dam** and **C.M. Jeronimus-Stratingh**) and at the CD spectroscopy facility at Zernike (**Gea K. Schuurman-Wolters**).

A big thanks to my colleagues at the department of Pharmaceutical Biology for their help and support during work, and providing a very friendly working environment. They have all contributed in one way or the other to this thesis. Especially, **Janita** and **Yvonne** for taking care of all the paper work. Janita, thanks for answering my queries and taking care of the promotion formalities. **Rita**, **Ronald** and **Pieter** for their assistance in taking care of all lab related matters. Rita, I admire your super friendly nature and "always ready to help other's" attitude. Pieter, thanks for all the (bad) jokes and for your help in the chemistry lab.

My special thanks go to all my colleagues in the room 905 for making it the loudest, noisiest and funniest room on 9th floor. **Vinod**, thanks for your "ever ready to help" attitude, naive jokes (since,

you left Groningen I miss those sometimes) and friendship over the years. **Anna** for keeping our office loud, funny and full of energy. **Bert-Jan** for various discussions over the years ranging from enzyme kinetics to social issues. Also, thanks for always reminding me that I need to clean my lab bench before I start working there (because you always used it but never cleaned it). **Ellen** for all the discussions and help with tax related issues.

I would like to thank **Marianne** and **Jandre**, new additions to MAL team, for their very friendly and helping nature. Marianne, for your help and discussions on MAL project, and keeping our office's (905) gender in balance. Jandre, thanks for teaching me squash tricks, for cooperation in the lab and for the great time at the conference in Sicily.

Since, the last female colleague left 905, it was just like a "sausage fest". I would like to pass my sincere thanks to Dr. **Edzard M. Geertsema** for all the nice conversations (scientific and non-scientific) and for translating the summary in Dutch. I wish to thanks to **Yufeng**, **Mehran**, **Jan-Ytzen** and **Harsh** for keeping the office atmosphere loud, funny, workable and achieving new lows with their good jokes. Apart from their jokes, I am also benefitted by your unreserved suggestions and constructive criticisms during various discussions. **Harsh**, thanks for all the desi-discussions and being my paranymph. To Harsh, Mehran, Jan-Ytzen and Yufeng I wish you all the best for your PhD.

A big thanks to my other colleagues and good friends in/outside lab with whom I had a great time in Groningen. Special thanks to **Elena** (for a constant supply of Italian cookies. Occasionally I miss your loud laugh); **Gudrun** (for all the Austrian chocolates and Rum, and for the fun and jokes whether it was October fest, squash or lunch talks); **Polito** (for constant supply of nasty jokes, for telling me about different comedy shows and occasional hangouts); **Remco** (for odd long smoky talks); **Carlos** (for helping with molecular docking studies and providing beautiful colorful pictures for the manuscripts, and tips for career related matters); **Evelina** (for all coffee breaks and bringing me to

Salsa dance lessons); and **Robbert** (for all the friendly conversations. I admire your very positive and always smiling replies). I would like to extend my gratitude to my friends **Chiara** and **Arno** for their friendship, fun and parties over the years in Groningen. I am glad to have company of friends like you.

I would like to offer my sincere thanks to **Oliver**, **Mariette**, **Ingrid**, **Torsten**, **Anna-Margarita**, **Octavia**, **Mariana**, **Aart**, **Matthieu**, **Luis**, **Magda**, **Nizar**, **Dan**, **Mark**, **Putri**, **Christel**, **Emanuele**, **Ilse**, **Roeland**, **Thai**, **Ya-Wang** and others whose names are not mentioned here for their help and support in lab.

Outside the lab, I know a big Indian community which made my stay in Groningen memorable and pleasant with different festival celebrations, dance nights and dinners. My special thanks to Puri (**Pranav** and **Vaishali**) and Mehta families (**Naveen bhaiya**, **Anu bhabhi** and **Palak**) for their help, support, food (whenever I was single in Goningen), fun (whether it is Uno or Squash), travels and discussions over the years. Pranav and Vaishali, I wish you both good luck for finishing your PhD's. Naveen bhaiya, thanks for being my paranymph, and I still cannot believe that you people have moved to Eindhoven.

I would also like to offer my heartfelt thanks to my "buren" **Fokko** and **Dia** for their help, care, jokes, and discussions that made my stay at the Fultsemaheerd very pleasant.

Many thanks to my other Indian friends **Anant**, **Prashant-Aradhana**, **Anil**, **Vinay-Chetna**, **Raaj-Shirisha**, **Samta-Ilija**, **Gopi**, **Yamini**, **Vinod-Kalyani**, **Ratna-Kalyani**, **Vikram-Ritika**, **Bala**, **Aneesh**, **Ranjeet-Kavita**, **Anjali** and **Mehul-Kanchan**. Big thanks to members of Philips gang (**Kekin**, **Pawan**, **Arun**, **Imran**, **Bhupinder** and **Ajit**) and their family members.

I would like to express my sincere gratitude to people who have helped me in many ways to become what I am today. My foremost thanks to my primary school teacher Mr. **Davinder Brar**. I admire your honest and sincere efforts in teaching. I am very grateful to my school time friends **Dalbir**

and **Rajender** (and their better half's) for their enormous support and help over the years. I offer my sincere thanks to my Panjab University teachers; especially Prof. Dr. **F. S. Nandel** and Prof. Dr. **M.P. Bansal** for their hard work in teaching and motivation.

The best part of University life is the time you spend with your friends and do all sorts of stupid things, which you remember for rest of your life. I am very fortunate that I met a bunch of such guy's during my stay at University in Chandigarh. My special thanks to **Rakesh-Tanzeer** (for being my best buddies over the years and for all the joyful time we had whether it was School or University. Thanks for everything), **Parvinder-Mini** (for your friendship and keeping the relation alive), **Diwya-Sonika** (for all the cheerful days that we had at University. Sorry girls, it is difficult for me to separate these names!), **Sapna** (for all the canteen or stucy talks), **Navjot** (for being the best stucy friend), **Gaurav** (for all the bad jokes we used to crack at Hostel and late night paranthas), **Yash** (for all the laughter's and being a gentlemen), **Harry** (for the great time at PU Hostel), **Gandhi** (for being a good dark side of the force!), **Gurdarshan** (for your help, company, friendship, motivations and discussions over the years. I learned a lot from you) and **Manoj** (for your constant positive outlook towards life and help in preparing for the interview). I am very happy to have friends like you.

I would also like to extend my sincere gratitude to my extended family members including my cousins, uncles, aunts, elders, and my in-laws for their unconditional love, affection and support. My special thanks to **Sukhvir** uncle for his constant support and motivation, and without which it would not have been possible to attain this level of education. My gratitude to my uncles and friends **Sitaram-Dataram** (Your home was my second home. You are amazing personalities and I learned a lot from you), **Subhash** and **Mahavir** for their constant support and motivations over the years. I am very thankful to my **Mama Ji** for their motivation and reminders, told in a very friendly and easy going way, that hard work and positive thinking are the only ways to succeed in life.

I wouldn't have reached this far without the constant support, love, affection and motivation from my family. I would like to express my deepest gratitude to my family. Especially my **Mom**, **Dad** and my brother **Ram**. I wish that my grandfather was alive today to witness this achievement. Last but not least, I would like to thank my better half **Sangeeta** for her perseverance, support, friendship and love. I am very pleased with the unique combination of a scientist and an accountant. This gives us the opportunity to talk non-scientifically and unaccountably, which I enjoy a lot. I consider myself very fortunate to have you all as part of my life. I couldn't have asked for a better family.

In the end, I would like to dedicate my thesis to my uncle and a very good friend **Het Ram**, who passed away last year. The whole family misses you.

Hans Raj

LIST OF PUBLICATIONS

From this thesis

1) **H. Raj** and G.J. Poelarends. The roles of active site residues in the catalytic mechanism of methylaspartate ammonia lyase. ***FEBS Open Bio*****.** 2013; 3: 285-290.
2) **H. Raj**, W. Szymański, J. de Villiers, V. Puthan Veetil, W.J. Quax, K. Shimamoto, D.B. Janssen, B.L. Feringa and G.J. Poelarends. Kinetic resolution and stereoselective synthesis of 3-substituted aspartic acids using engineered methylaspartate ammonia lyases. ***Chem. Eur. J.*** 2013;19: 11148-11152.
3) V. Puthan Veetil,[*] **H. Raj**,[*] M. de Villiers, P.G. Tepper, F.J. Dekker, W.J. Quax and G.J. Poelarends. Enantioselective synthesis of N-substituted aspartic acids using an engineered variant of methylaspartate ammonia lyase. ***ChemCatChem.*** 2013; 5: 1325-1327. (*Both authors contributed equally)
4) M. de Villiers, V. Puthan Veetil, **H. Raj**, J. de Villiers and G.J. Poelarends. Catalytic mechanisms and biocatalytic applications of aspartate and methylaspartate ammonia lyases. ***ACS Chem. Biol.*** 2012; 7: 1618-1628.
5) **H. Raj**, W. Szymański, J. de Villiers, H.J. Rozeboom, V. Puthan Veetil, C.R. Reis, M. de Villiers, F.J. Dekker, S. de Wildeman, W.J. Quax, A.M.W.H. Thunnissen, B.L. Feringa, D.B. Janssen and G.J. Poelarends. Engineering methylaspartate ammonia lyase for the asymmetric synthesis of unnatural amino acids. ***Nature Chemistry*** 2012*;* 4: 478-484.
6) **H. Raj**, V. Puthan Veetil, W. Szymański, F.J. Dekker, W.J. Quax, B.L. Feringa, D.B. Janssen and G.J. Poelarends. Characterization of a thermostable methylaspartate ammonia lyase from *Carboxydothermus hydrogenoformans*. ***Appl. Microbiol. Biotechnol*****.** 2012; 94: 385-397.

7) **H. Raj**, B. Weiner, V. Puthan Veetil, C.R. Reis, W.J. Quax, D.B. Janssen, B.L. Feringa and G.J. Poelarends. Alteration of the diastereoselectivity of 3-methylaspartate ammonia lyase by using structure-based mutagenesis. ***ChemBioChem*****.** 2009; 10: 2236-2245.

Other publications related to this work

1) **H. Raj**, J. de Villiers, V. Puthan Veetil and G.J. Poelarends. Structure-function relationship of methylaspartate ammonia lyase. ***Manuscript in preparation***.
2) J. de Villiers, M. de Villiers, **H. Raj** and G.J. Poelarends. Chemo-enzymatic synthesis of *ortho-*, *meta-* and *para*-substituted derivatives of L-*threo*-3-benzyloxyaspartate (L-TBOA), an important glutamate transporter blocker. ***Manuscript in preparation***.

Other publications

1) P. Nadal-Jimenez, G. Koch, C.R. Reis, R. Muntendam, **H. Raj**, C.J. Jeronimus-Stratingh, R.H. Cool and W.J. Quax. PvdP is a tyrosinase that drives maturation of the pyoverdine chromophore in *Pseudomonas aeruginosa*. ***Submitted***.
2) V. Puthan Veetil, G. Fibriansah, **H. Raj**, A.M.W.H. Thunnissen and G.J. Poelarends. Aspartase/fumarase superfamily: a common catalytic strategy involving general base-catalyzed formation of a highly stabilized *aci*-carboxylate intermediate. ***Biochemistry*** 2012; 51: 4237-4243.
3) V. Puthan Veetil, **H. Raj**, W.J. Quax, D.B. Janssen and G.J. Poelarends. (2009) Site-directed mutagenesis, kinetic, and inhibition studies of aspartate ammonia lyase from *Bacillus* sp. YM55-1. ***FEBS J***. 2009; 276: 2994-3007.